DESIGN, PROCESS DEVELOPMENT, MANUFACTURE, TEST AND EVALUATION OF BORON-ALUMINUM FOR SPACE SHUTTLE COMPONENTS

FINAL REPORT

MCDONNELL DOUGLAS ASTRONAUTICS COMPANY - EAST

MCDONNELL DOUGLAS

CORPORATION

DESIGN, PROCESS DEVELOPMENT, MANUFACTURE, TEST AND EVALUATION OF BORON-ALUMINUM FOR SPACE SHUTTLE COMPONENTS

30 JULY 1973	MDC E0825

FINAL REPORT

Prepared for
George C. Marshall Space Flight Center
Marshall Space Flight Center, Alabama 35812
under
Contract NAS 8-27735
by
R. A. Garrett, et al

FOREWORD

This Final Report covers the work accomplished by the McDonnell Douglas
Astronautics Company - East (MDAC-E), St. Louis, Missouri, during the period
from 29 June 1971 thru 31 July 1973 in the evaluation of boron-aluminum for
Space Shuttle components. This work was conducted under sponsorship of the
Research and Process Technology Division, Product Engineering and Process
Technology Laboratory of the George C. Marshall Space Flight Center (MSFC),
National Aeronautics and Space Administration (NASA). The contract identifica-
tion is NAS 8-27735, "Design, Process Development, Manufacture, Test and Evalua-
tion of Boron-Aluminum for Space Shuttle Components", dated 29 June 1971.
Mr. R. L. Nichols, S&E-PT-MXS, is the NASA MSFC Contracting Officer Representa-
tive (COR) under supervision of Mr. Edwin L. Brown; their help and guidance in
this program have been most appreciated.

The program was performed by the Advanced Composites Group, MDAC-E, with
Mr. R. A. Garrett serving as Program Manager. Significant contributions to this
program have been made by the following MDAC-E personnel:

Mr. John T. Niemann, Materials and Processes Development
    Mr. W. J. Lewis
    Mr. D. C. Ruhmann
Mr. Owen R. Otto, Strength Analysis
    Mr. R. E. Bohlmann
    Dr. R. A. Melliere
    Mr. F. J. Vyzral
Mr. Nick M. Brown, Structural Design and Fabrication Coordination
    Mr. R. A. Benjamin
    Mr. F. Pacotti
Mr. Robert E. Heinrich, Manufacturing
    Mr. P. R. Arzt
    Mr. F. S. Pogorzelski

Their contributions to the report and the completed program are gratefully
acknowledged.

ABSTRACT

A multi-phase boron-aluminum design and evaluation program for Space Shuttle Components was conducted, culminating in the fabrication of a 1.22 m (48 inch) x 1.83 m (72 inch) boron-aluminum compression panel capable of distributing a point load of 1555 kN (350,000 lbs) into a uniform running load at a temperature of 589°K (600°F). This panel was of the skin-stringer construction with two intermediate frame supports; seven unidirectional stringers varied in thickness from 5 plies to 52 plies and the $\pm \frac{\pi}{4}$ rad ($\pm 45°$) skin was contoured to thicknesses ranging from 10 plies to 62 plies. Both the stringers and the skin incorporated Ti-6Al-4V titanium interleaves to increase bearing and in-plane shear strength. The strength and load redistribution characteristics of this panel design were verified by extensive mechanical property testing, a full length 1.83 m (72 inch) stringer element test at room temperature to 100% design ultimate load, and a test of a 1.22 m (48 inch) x 0.61 m (24 inch) component panel to 1780 kN (400,000 lbs, 115% design ultimate) at 589°K. (600°F). These test results have established full confidence in the Compression Panel design.

The five discrete program phases were Materials Evaluation, Design Studies, Process Technology Development, Fabrication and Assembly, and Test and Evaluation. In the Materials Evaluation phase, incoming material quality and mechanical property test results were generally better and more consistent than those previously obtained. During the Process Technology Phase, production processes were optimized and the results expressed as Process Specifications which governed the manufacture of the compression panel and test components. Design Studies of several structures were conducted as well as trade-off studies of the Compression Panel configuration to determine the best structural approach; standard analysis techniques suitably modified for the particular composite characteristics were used. Fabrication and Assembly of the three test structures utilized mechanical forming of flat packs prior to bonding for stringer fabrication and several improved lay-up machining and drilling techniques. Under Test and Evaluation, an elastic foundation structure was used successfully in the Component Panel test set-up to simulate full size panel stiffness.

The full size Compression Panel test assembly has been completed and delivered to MSFC.

TABLE OF CONTENTS

TABLE OF CONTENTS (continued)

TABLE OF CONTENTS (continued)

MCDONNELL DOUGLAS ASTRONAUTICS COMPANY - EAST

1.0 INTRODUCTION AND PROGRAM SUMMARY

This Final Report describes the work accomplished on the design, process technology development, manufacture, test and evaluation of boron-aluminum for Space Shuttle components under NASA Contract NAS 8-27735. The objective of this program was the development of sufficient technology to permit application of boron-aluminum to Space Shuttle components with high confidence. In addition to the acquisition of a significant quantity of mechanical property and process technology data, the realization of this objective was further demonstrated by fabrication and test of a 1.22m (48 inch) x 1.83m (72 inch) boron-aluminum compression panel capable of distribution a point load of 1555 kN (350,000 lbs) into a uniform running load, within a peaking factor of 1.3, at a temperature of 589°K (600°F). Small component testing has been successfully performed by MDAC-E at room temperature and 589°K (600°F) to verify the compression panel design; however, testing of the delivered full size Compression Panel Assembly will be accomplished by MSFC. The Compression Panel, shown in Figure 1-1, has been completed and delivered to MSFC for such structural testing.

A total of 21 monthly progress reports and 4 Quarterly Reports (References 1, 2, 3, and 4) have been submitted to date which provide a detailed development history of this program. This Final Report is intended to summarize these developments, present all pertinent data, draw conclusions relating to program progress and to recommend future work which in our opinion should be initiated or continued.

The contracted effort included the following five program phases:

        Phase I   — Materials Evaluation

        Phase II   — Design Studies

        Phase III — Process Technology Development

        Phase IV   — Fabrication Assembly

        Phase V   — Test and Evaluation

The Phase I, Materials Evaluation, work took place principally during the first three quarters of the program and included both review and characterization of incoming material and the generation of sufficient mechanical property data (1100 series aluminum alloy matrix and 5.6 mil boron filament) for compression Panel design purposes. Data were determined for both multilayer unidirectional laminates and crossply laminates.
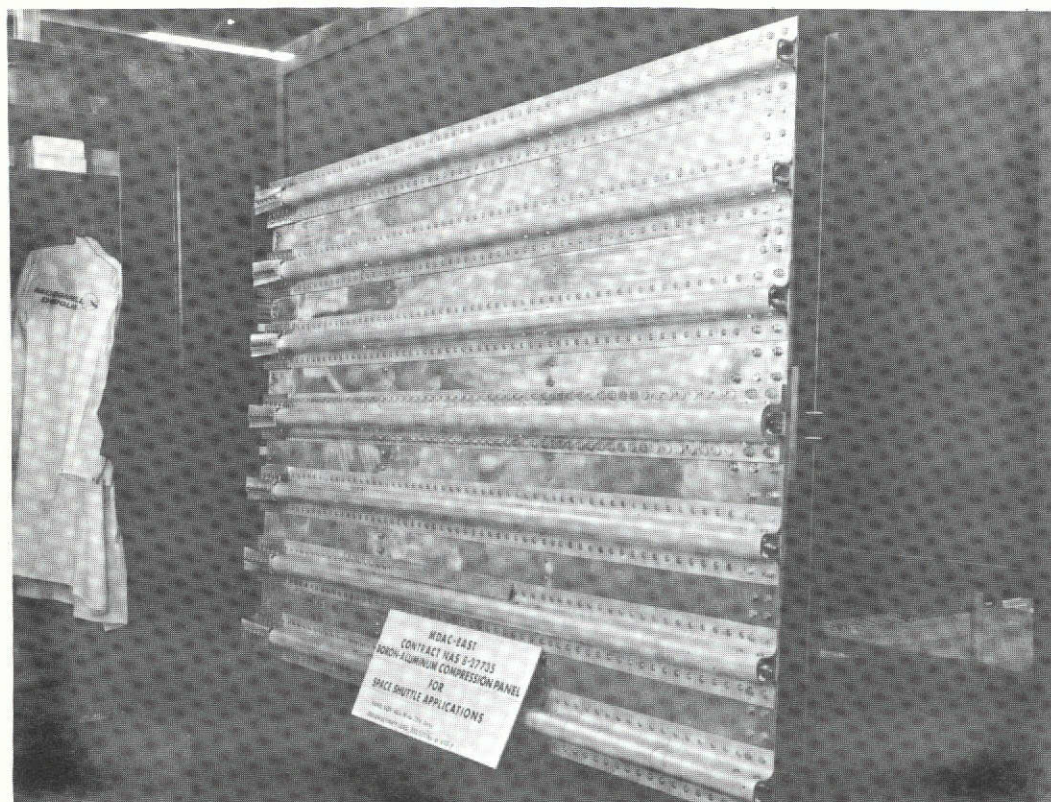
Stringer Side
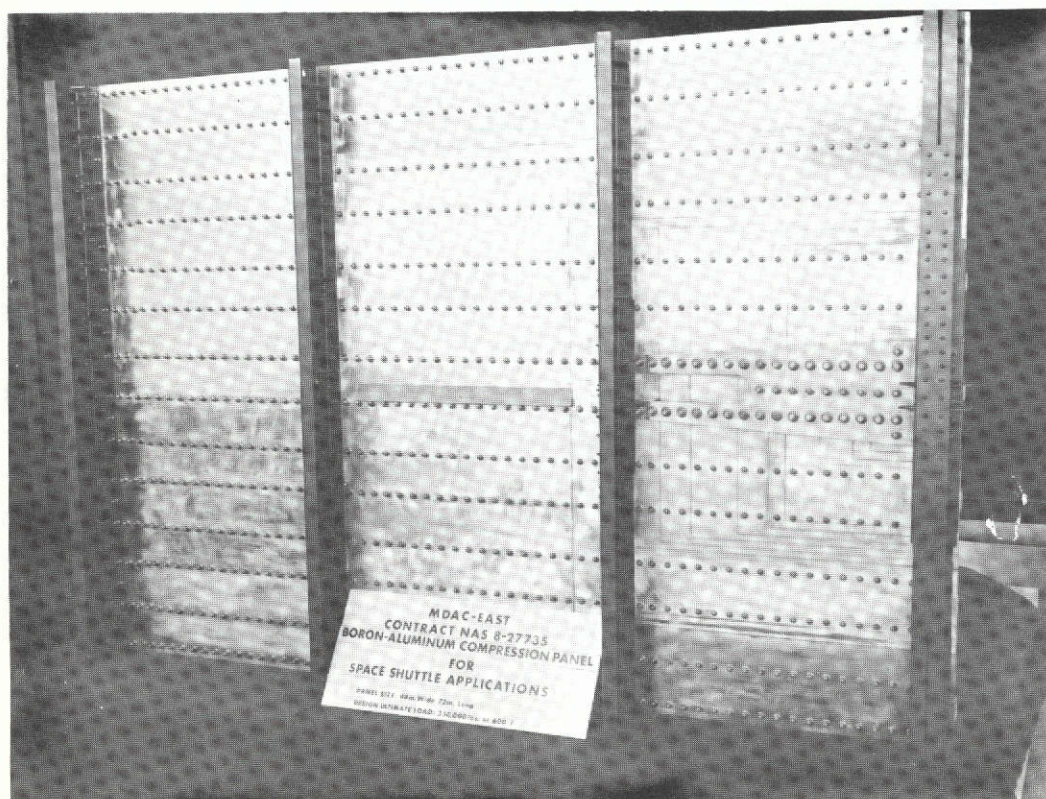
Skin Side
COMPLETED COMPRESSION PANEL ASSEMBLY

Figure 1-1

1-2

In Phase I, Amercom Inc. was selected as a boron-aluminum monolayer and bi-
layer material supplier on the basis of a review of material from both Harvey
Aluminum and Amercom Inc. Over 250 kg (550 lbs) of material was purchased from
Amercom for purposes of this program. Approximately 12.1% of all material supplied
(45.7 pounds) was rejected for a variety of reasons; the most serious defect was
poor diffusion bonds in bilayer material. The frequency and type of various
material defects experienced during the program required 100% inspection of all
material received. Over 1000 coupon tension tests were performed to verify mono-
layer and bilayer strength - of which 1.2% (4.5 lbs) fell below minimum specifica-
tion filament strength requirements (400 ksi, minimum). However, it should be
noted that the material supplied by Amercom for this program was judged to be of
significantly better quality than previously available material.

Phase I mechanical property element tests performed totaled over 500,
and included tests at both room temperature and 589°K (600°F). These tests were
intended primarily to verify initially established panel design allowables; the
test results indicated that the design allowables used for panel design were con-
servative (from 0 to 30%, depending on type loading and temperature) and that the
results exceeded (and were more consistent than) previously obtained data. Signi-
ficant areas of improvement include crippling (compression) strength of boron-
aluminum hat section elements and the development of meaningful rail shear test
techniques and allowables.

In Phase II, Design Studies, components and assemblies representative of
full scale hardware were designed and analyzed and included a 1.22 m x 1.83 m
(48 inch x 72 inch) compression panel, a thrust structure beam of truss design, a
thrust structure beam of shear web design, representative joint designs and panel
components and element designs. Three of these structures designed under Phase II
were also fabricated for structural testing; i.e., the Stringer Test Assembly shown
in Figure 1-2, the Component Panel Test Assembly shown in Figure 1-3 and finally
the full size Compression Panel Test Assembly shown in Figure 1-1. Of the re-
maining designs, the truss beam and shear web beam thrust structure configurations
shown in Figures 1-4 and 1-5 were carried far enough to determine an overall
structural arrangement, size all elements and calculate structural weights for
comparison purposes. For the loading cases considered, the shear web beam design was
37.5 kg (82.8 lbs), or about 8%, lighter than the truss beam design (929.4 lbs vs
1012.2 lbs). For all design studies, specific analysis techniques tailored for

metal matrix composites were developed, based in part on techniques already developed for resin matrix composites and in part on conventional metals structures techniques. These techniques were fully verified by successful testing of the Stringer Test Assembly and the Component Panel Test Assembly conducted at room temperature and 600°F respectively - both in achieved ultimate strength and demonstrated load distribution.
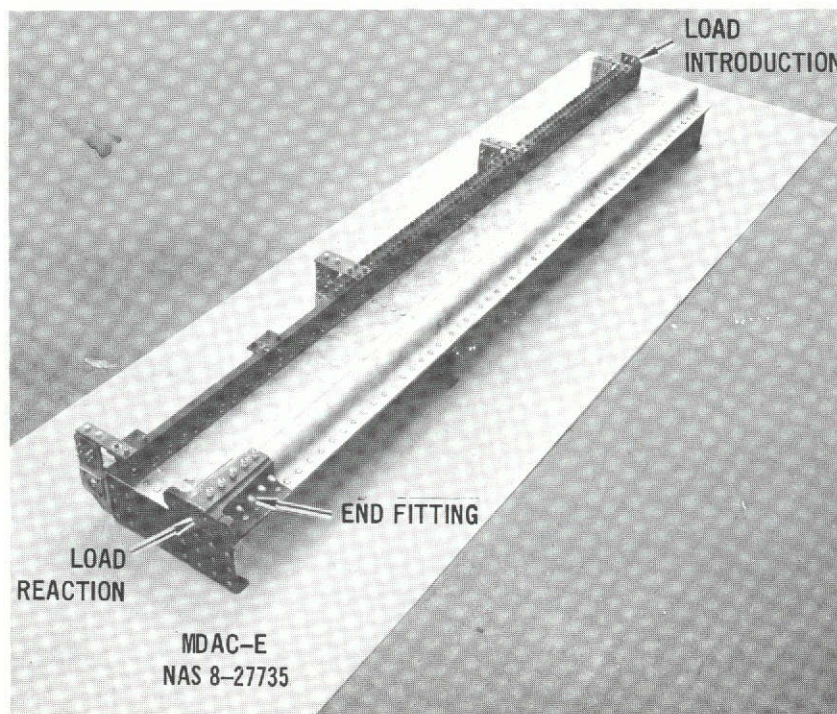
COMPLETED ASSEMBLY - STRINGER TEST COMPONENT

Figure 1-2

Phase III, Process Technology Development, was concerned with improving the procedures and techniques used to fabricate boron-aluminum structures from monolayer foils. The primary emphasis was placed on the cleaning, coating and bonding thermal cycles associated with the eutectic bonding process and on improving lay-up procedures to reduce fabrication costs. As a result of these studies, the quality and reliability of eutectic bonded parts were improved significantly at the same time that processing costs were reduced. Process specifications were prepared on the basis of Phase III study results and these documents governed the successful fabrication of test components and the full size compression panel.
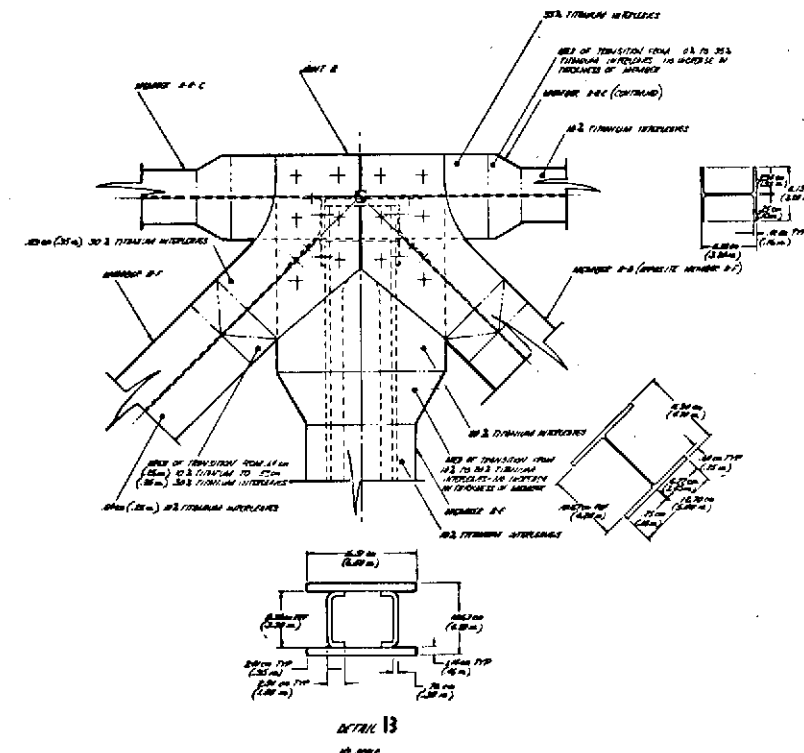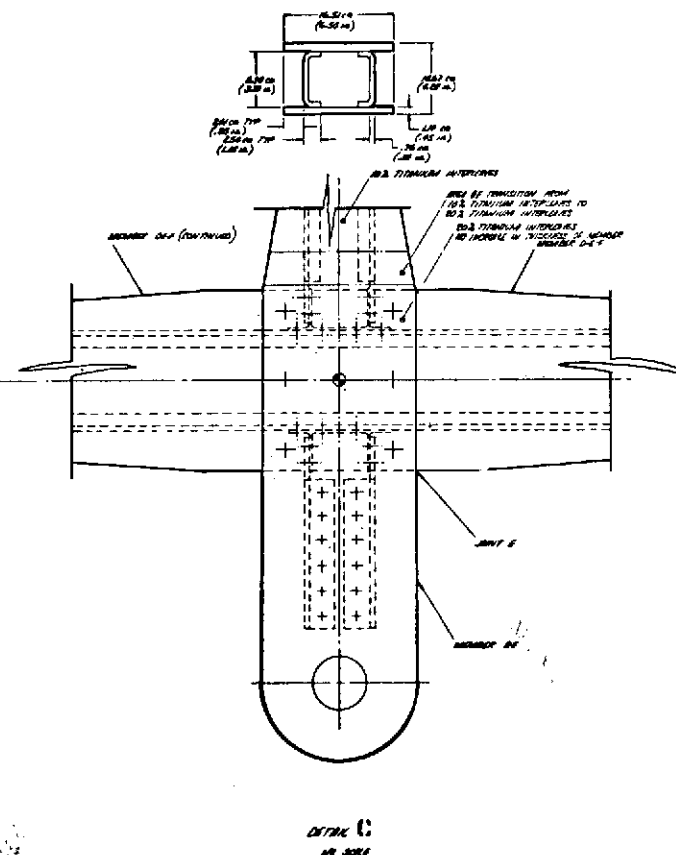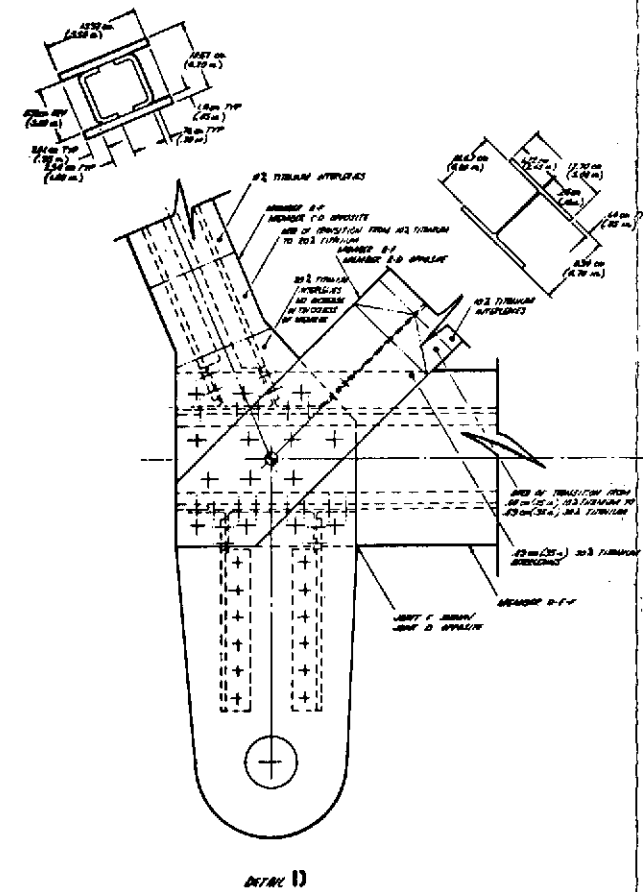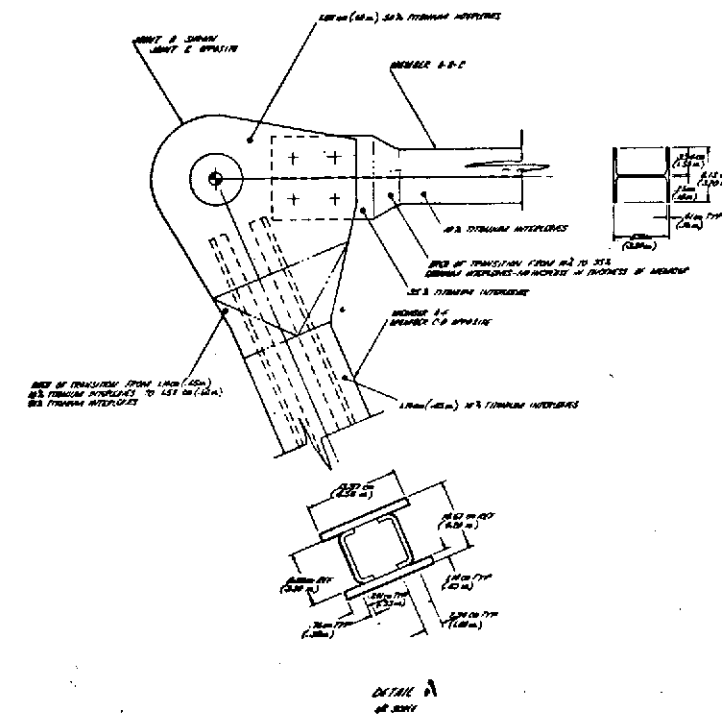
Figure 1-4

FOLDOUT FRAME

FOLDOUT FRAME

Stringer Side

Skin Side

COMPLETED COMPONENT PANEL ASSEMBLY

Figure 1-5 (Continued)

Figure 1-5

Fabrication and assembly under Phase IV included manufacture of selected joint configurations, the Component test specimen, the Stringer element test specimen and the complete 1.22 m (48 inch) x 1.83 m (72 inch) Compression Panel. These units were successfully fabricated and delivered to the responsible test agencies. Notable in the fabrication achievements were the development of a mechanical forming technique which enabled producing the variable cross section stringers comprised of between 52 to 5 plies with "hard to form" titanium inter- leaves and the fabrication of the large 1.22 m by 1.83 m (4 x 6 ft.) variable thickness complex skin of 62 to 10 plies, also with titanium interleaves. The successful fabrication of these test articles has demonstrated the present day capability to produce complex boron-aluminum composite assemblies of consistent sound quality.

Work performed by MDAC-E under Phase V, Test and Evaluation, included performance of joint tests and the component and stringer element tests. Further, a Test plan was prepared by MDAC-E for the Compression Panel test by MSFC to be followed by an evaluation by MDAC-E of all program testing. Under Phase V testing, two significant milestones in panel design verification were achieved: successful testing to ultimate design load (or equivalent) of the 1.83 m (72 inch) Stringer Test Assembly at room temperature and the .61 m (24 inch) x 1.22 m (48 inch) Component Panel Test Assembly at 589°K (600°F). In the test of the Stringer Test Assembly, a maximum load of 100,000 pounds was applied to the test assembly at room temperature; this is equivalent to the Stringer Design Ultimate Load (DUL) of 50,000 pounds (22,680 Kg) at 589°K (600°F). In the Component Panel test at (600°F), a maximum load of 400,000 pounds (181,440 Kg) (> 1.15 times DUL) was achieved at 589°K; subsequent panel inspection revealed only minor structural damage. The results of these tests, coupled with the evaluation of associated test strain and deflection data, fully verified the full size Compression Panel design. A test Plan for MSFC testing of the Compression Panel has also been completed and is included as Appendix B of this report.

From the results of this program it may be concluded that the program objec- tive has been met; that is, sufficient technology and test data have been developed to permit application of boron-aluminum to Space Shuttle components with high con- fidence. Mechanical property data and raw material quality have now stabilized to the point where rational and attractive design allowable data have been developed. The processing required for boron-aluminum fabrication has been clearly transformed from a laboratory operation status to a production shop status with appropriate

process specifications developed to provide part quality assurance. The design and fabrication technology have also been significantly advanced. Complex, tapered and contoured structures utilizing sophisticated re-inforcement techniques have been successfully designed, fabricated and tested to excess of design ultimate loads at temperatures up to 589°K (600°F) to provide confirmation of the developed technology. In summary, the boron-aluminum material system has been developed to the point where its use can provide significant weight savings, system performance improvements and increased payload capabilities for the Space Shuttle or other vehicle systems.

2.0 SUMMARY OF WORK ACCOMPLISHED BY PROGRAM PHASE

Work accomplished under this contract was in each of five distinct program phases; namely:

        Phase I   – Materials Evaluation

        Phase II   – Design Studies

        Phase III – Process Technology Development

        Phase IV   – Fabrication and Assembly

        Phase V   – Test and Evaluation

The results in each phase are discussed separately below.

2.1 Phase I - Materials Evaluation

The work to be accomplished under Phase I included both review and characterization of incoming material and generation of sufficient mechanical property data using 1100 series aluminum alloy matrix and 5.6 mil boron filament for compression panel design purposes.

In terms of tests, they included longitudinal tensile, transverse tensile, compression, rail shear, diagonal tension, crippling and interlaminar shear at room temperature and 589°K (600°F). Data were determined for both multilayer unidirectional laminates and crossply laminates.

The data derived from incoming material evaluation and from mechanical property testing are described separately below.

2.1.1 Boron-Aluminum Supplier and Monolayer Evaluation - The materials evaluation phase of this program had two objectives. The first was to select a material supplier from the two available boron-aluminum fabricators who were Amercom, Inc. and Harvey Aluminum Co. This selection was based on an assessment of 13.6 kg (30 lbs) of material submitted for evaluation by each company. The second objective was to assess the quality of the material being received for use on the program to assure conformance to procurement specification requirements.

2.1.1.1 Selection of Material Supplier - Areas of special interest in the selection of the supplier included the surface quality, bond quality, and filament characteristics of each supplier's material. A summary of the quality assessment of the material from each supplier is presented below; a more detailed

discussion is given in Reference 1.

Surface quality characteristics including surface roughness, surface flaws such as laps and cracks, cleanliness, and thermal wrinkles were of prime concern because of their effect on the eutectic bonding processes. Longitudinal surface flaws resembling laps were observed in both the Harvey and Amercom material. These defects occurred at the midpoint between filaments and were the result of flow of aluminum around the boron during the diffusion bond cycle. In general, the frequency of these defects was greater in Amercom material, but the severity was more pronounced in Harvey foils. The Amercom material was determined to be adequate for use with respect to these defects whereas the Harvey material was not acceptable due to the severity of the laps and the large number of resulting splits observed.

Initial shipments of Harvey material had the best surface finish of any material tested; however, later shipments were of considerably lower quality due to many crossovers, laps and residual parting compound. Amercom, on the other hand, showed quality improvement with time, and their last shipment in the 13.6 kg evaluation order was considered acceptable for eutectic bonding. Material supplied by Amercom was consistently cleaner than Harvey supplied material which was covered with an oil film and much residual parting compound.

To evaluate monolayer bond quality, visual examination, in conjunction with hand peel testing, and three types of nondestructive testing (radiographic examination, ultrasonic inspection, and infrared testing) were utilized. Of the various methods of bond quality evaluation, the hand-peel test proved to be the most reliable and expedient method. It was possible to detect complete disbonds but not weak bonds with ultrasonic C-scan inspection techniques; however, such complete disbonds were also observable visually prior to ultrasonic inspection. After an assessment of the bond quality of the 13.6 kg (30 lbs) of material from each supplier, the Amercom material was judged to be acceptable in this regard whereas Harvey Aluminum material was unacceptable. It should be noted that the best diffusion bond quality was rated as acceptable only, and was found to be in general need of further improvement.

Filament defects such as broken filaments, poor filament spacing, and filament crossovers were also evaluated in this program. Representative sheets of Amercom and Harvey monolayer were radiographed to detect filament defects. The most serious defects found by radiography were filament crossovers and uneven

filament spacings. Very few broken filaments were observed. The severe cross-over regions observed in the Harvey material were judged unacceptable. Amercom also experienced some difficulty with crossovers but their material, on the average, was judged acceptable.

The presence of fiber defects observed by radiographic examination usually were also detected visually, especially the cases of crossovers and poor spacing. Therefore, the value of radiographic examination as a quality control method was only to document defects already observed visually.

Based on the above monolayer evaluation, Amercom, Inc. was selected as the supplier of the remainder of the boron-aluminum material required for the program, and was used as the source for all composite material used during the program.

2.1.1.2 <u>Evaluation of Incoming Production Material</u> - Approximately 172 kg (380 lbs) of boron-aluminum monolayer and bilayer tape were received and inspected for use on this program. A flow chart of the receiving inspection quality assurance program is shown in Figure 2-1. The controlling documents on which acceptances or rejections were based were the two material procurement specifications which cover the basic filaments and the monolayer foil. These are McDonnell Douglas - St. Louis Specification MMS-583 - "Boron Mono-filament" and MMS-584 - "Composite Foil, Boron Filament - Aluminum Matrix - Diffusion Bonded." These specifications are appended to Reference 1.

After review of the Certificate of Conformance, all material was evaluated with respect to surface quality. This step involved determinations of cleanliness, surface finish, and surface flaws. Associated with the surface quality evaluation was an assessment of filament spacing, filament crossovers, and broken filaments. Surface finish was not found to be a problem, but other surface irregularities which resulted from poor filament spacing and crossovers and general cleanliness did result in some rejection of material. Approximately 11 kg (24.2 lbs) or 6.4% of the total purchased material was rejected for the reasons discussed above.

The next sequential inspection step was that of a diffusion bond quality evaluation which was accomplished by hand peel tests. In the early days of the program, both monolayer and bilayer material showed occasional evidence of poor bond quality, and approximately 7.7 kg (17 lbs) or 4.5% of material were rejected for this reason. <u>Monolayer</u> bond quality improved markedly during the program and was not a serious problem during fabrication of the panel; however, poor diffusion
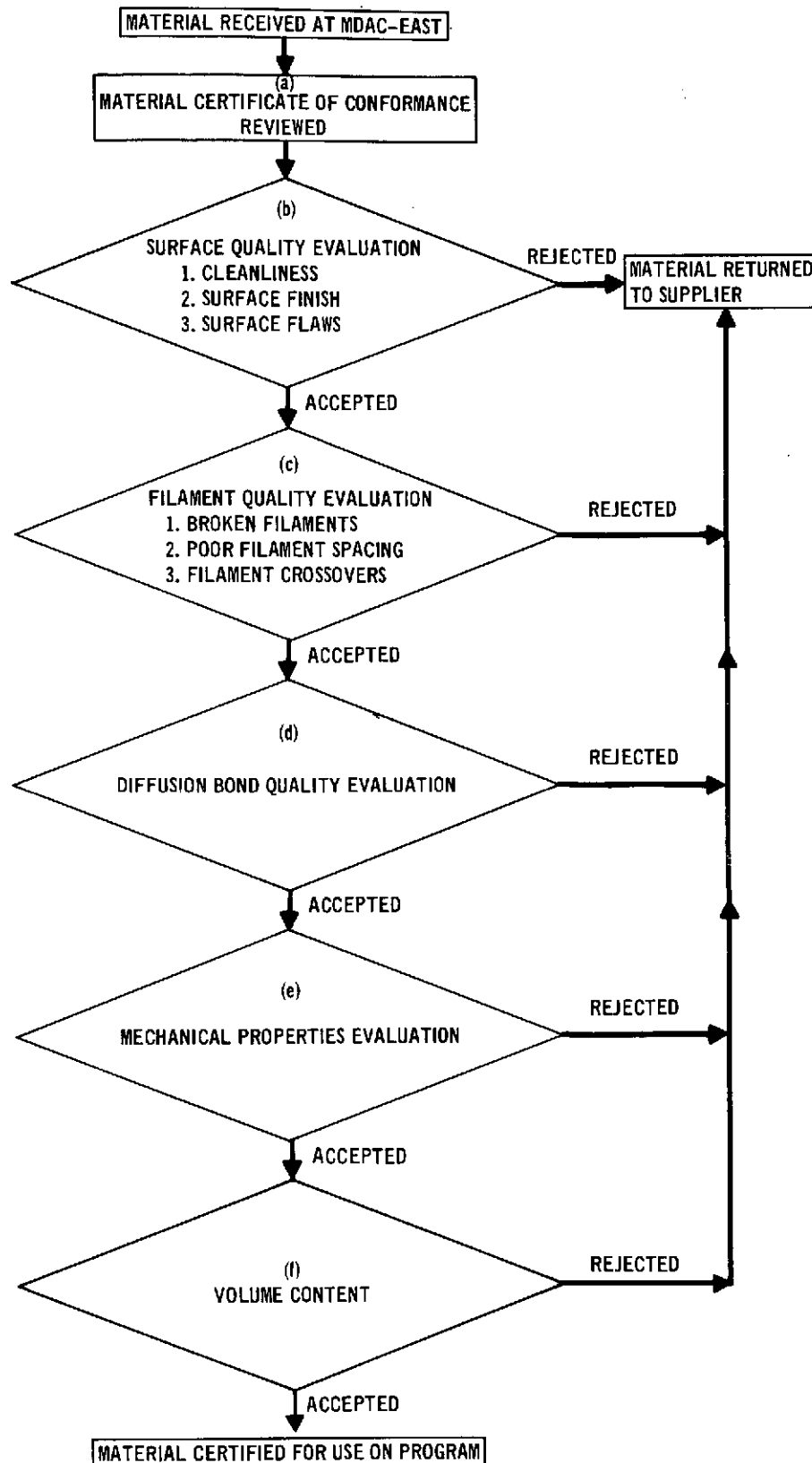
FLOW CHART FOR RECEIVING INSPECTION QUALITY
ASSURANCE PROGRAM

Figure 2–1

bonds in the <u>bilayer</u> material resulted in localized areas of delaminations in com-
pleted test specimens and structures. These defective foils had previously passed
the hand peel tests; however detection of weak diffusion bonds in this bilayer
material by peel testing or by any other technique is unreliable. Figure 2-2
shows a cross-section of bilayer which illustrates fiber touching and weak bond
lines. Additional work must be conducted to establish reliable NDE techniques for
multiply material.
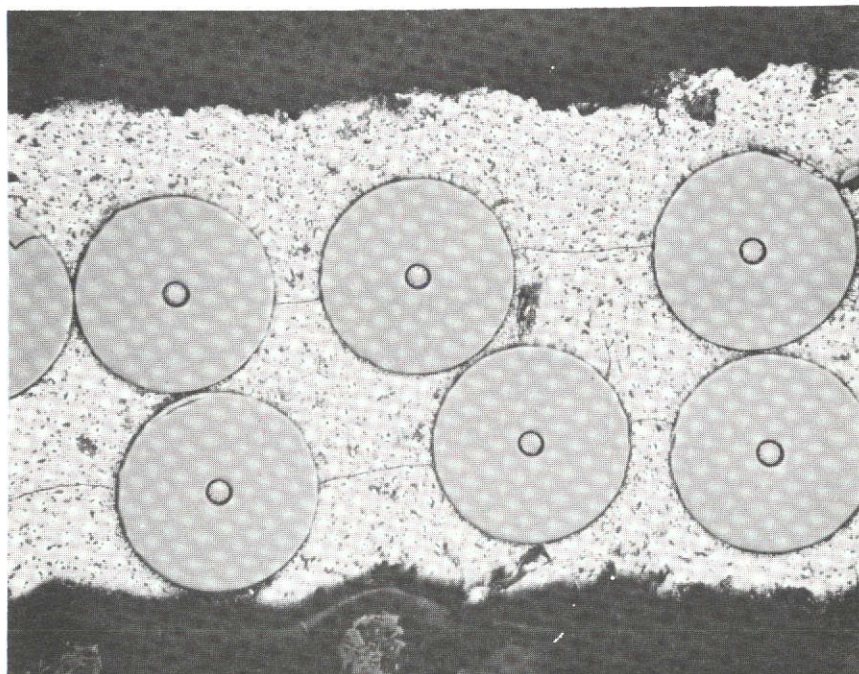
175X

BILAYER FOIL

Figure 2-2

The mechanical properties evaluation consisted of a verification through
strength testing of incoming material. These tests served as a check on the
initial filament strength and ensured that processing parameters were controlled
adequately to prevent significant filament degradation. Approximately 2 kg
(4.5 lbs) or 1.2% of the total was rejected because of low strength. Though the
low rejection rate showed the material to be generally acceptable, significant
variation was noted in the results of the strength determination tests. The cu-
mulative frequency distribution of the filament bundle strength for all monolayer
and bilayer material received on the program is presented in Figure 2-3. These
data are based on 706 monolayer tests and 407 bilayer tests. The method used to
calculate the filament bundle strength has been previously reported in Reference

2. It should be noted that the variation in strengths occurred randomly through-
out the duration of the program.
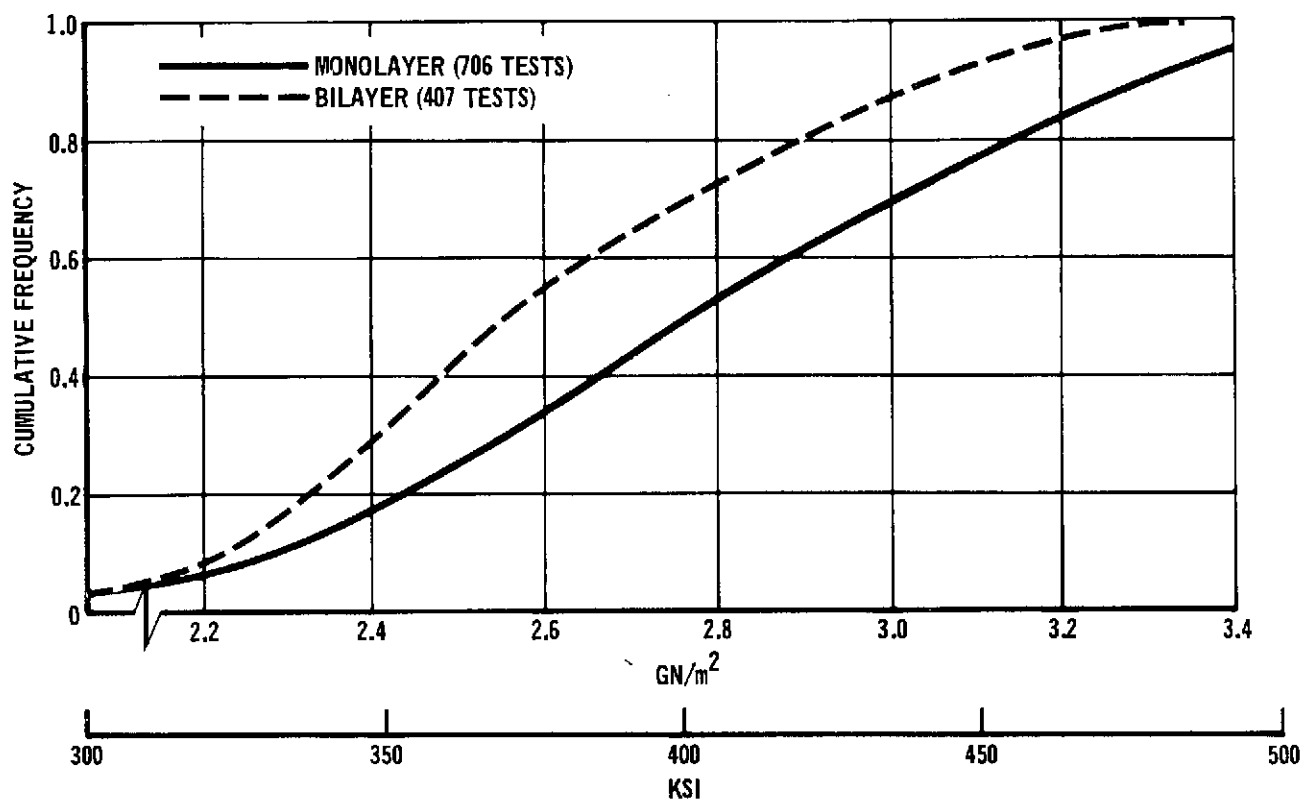
FILAMENT BUNDLE STRENGTH

Figure 2–3

In summary, the following quantities of monolayer and bilayer boron-aluminum
were rejected for the reasons shown:

DEFECT	kg (lbs) REJECTED	% OF TOTAL QUANTITY (= 172 kg or 380 lbs)
Surface Quality (Visual)	11 kg (24.2 lbs)	6.4%
Poor Diffusion Bond (Hand Peel)	7.7 kg (17 lbs)	4.5%
Low Filament Strength (Below Ave F_{tu} = 400 ksi)	2 kg (4.5 lbs)	1.2%
TOTAL	20.7 kg (45.7 lbs)	12.1%

The quanitites and percentages are significantly lower than data for early boron-
aluminum material but still indicate areas where further improvement is needed.
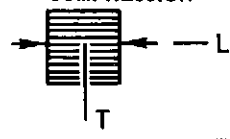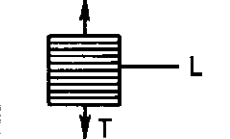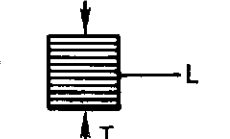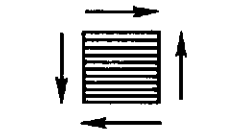
2.1.2 <u>Mechanical Property Test Results</u> - Element tests of boron-aluminum speci-
mens were conducted to verify predicted mechanical properties essential for the
analysis of the compression panel. These test specimens were fabricated from
both monolayer and bilayer material containing 5.6 mil boron filaments. In
general, it was found that essentially the same strength properties were obtained
from the two material configurations when the filament volume fraction was the
same and the "as-received" material was of good quality.

Strength and stiffness properties of boron-aluminum laminates are derived
from the fundamental mechanical properties of a unidirectional laminate. Average
unidirectional laminate properties determined in the element test program are
summarized in Figure 2-4. These properties and other design data employed in the
compression panel analysis are discussed in detail in subsequent sections.

2.1.2.1 <u>Longitudinal Tension</u> - Determination of stress-strain response,
ultimate strength (F_L^{tu}) and strina (ε_L^{tu}), and initial values of tangent modulus
(E_L^t) and major Poisson's ratio (μ_{LT}^t), at both room temperature and 589°K (600°F)
were primary test objectives. Average tensile properties are shown in Figure 2-5.
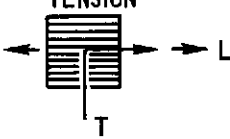
Ten tensile coupons and five sandwich beam specimens were tested at room
temperature, and ten tensile coupons were tested at 589°K (600°F). In each group,
five tensile coupons were made from monolayer material and five from bilayer
material. The average failure strength of tensile coupons fabricated from mono-
layer was 1110.0 MN/m^2 (161 KSI) at room temperature and 1068.0 MN/m^2 (155 KSI) at
589°K (600°F). The respective values for bilayer material specimens were 1116.0
MN/m^2 (162 KSI) and 992.0 MN/m^2 (144 KSI), indicating that use of bilayer material
results in an 8% greater reduction in strength at elevated temperature than speci-
mens fabricated from monolayer material. However, this apparent difference between
monolayer and bilayer material is considered inconclusive. As expected, sandwich
beam specimens produce a somewhat higher average ultimate strength (1336.0 MN/m^2)
than the tensile coupons.

The longitudinal tensile coupons shown in Figure 2-6 are 22.9 cm (9.0 in.)
long and 2.54 cm (1.0 in.) wide with a 7.62 cm (3.0 in.) gage length and 7.62 cm
(3.0 in.) end tabs. Each end tab has a six mil aluminum ply adhesively bonded to
both sides to prevent the serrated Instron jaws from penetrating the outer boron-
aluminum ply and damaging the boron filaments. THe coupon configuration including
the location of strain gages is presented in Figure 2-7. Back to back strain
gages were used to check for the presence of bending during test although self-
aligning Instron grips are used to minimize bending of the specimen. Room

PROPERTY	TEMPERATURE °K	ULTIMATE STRENGTH		ULTIMATE STRAIN	INITIAL MODULUS		POISSON'S RATIO	TEST METHOD
		MN/m^2	KSI	μm/m	GN/m^2	10^6 PSI		
LONGITUDINAL TENSION	R.T. 589	1110.0 1068.0	161.0 155.0	5740 6440	207.0 186.0	30.0 27.0	0.25 0.30	COUPON COUPON
LONGITUDINAL COMPRESSION	R.T.	2360.0	343.0	10600	243.0	35.3	0.28	BEAM
TRANSVERSE TENSION	R.T. 589	101.2 26.9	14.7 3.9	3290 6480	126.0 80.5	18.3 11.7	0.18 0.095	COUPON COUPON
TRANSVERSE COMPRESSION	R.T. 589	258.0 66.1	37.5 9.6	24000 10700	97.2 109.5	14.1 15.9	0.16 0.17	BEAM BEAM
SHEAR	R.T. 589	46.2 15.8	6.7 2.3	>20000 >20000	58.6 27.6	8.5 4.0	– –	RAIL SHEAR RAIL SHEAR

UNIDIRECTIONAL LAMINATE MECHANICAL PROPERTY SUMMARY
(Average Values)

Figure 2–4

TYPE TEST	TEST TEMPERATURE		PLY MATERIAL	ULTIMATE STRENGTH		ULTIMATE STRAIN	INITIAL MODULUS		INITIAL POSSON'S RATIO	FILAMENT VOLUME %
	^0K	^0F		MN/m^2	KSI	$\mu m/m$	GN/m^2	10^6 PSI		
COUPON	R.T.	R.T.	MONOLAYER	1110.0	161.2	5740	207.0	30.0	0.25	46.3
COUPON	R.T.	R.T.	BILAYER	1118.0	162.2	6350	207.0	30.0	0.24	42.3
COUPON	589	600	MONOLAYER	1068.0	155.0	6440	186.0	27.0	0.30	44.8
COUPON	589	600	BILAYER	992.0	143.8	6640	159.8	23.2	0.36	44.7
BEAM	R.T.	R.T.	BILAYER	1332.0	193.6	7255	197.0	28.6	0.38	—

NOTE: RESULTS ARE AVERAGE VALUES BASED ON TESTS OF FIVE SPECIMEN MINIMUM IN EACH GROUP.

AVERAGE LONGITUDINAL TENSILE PROPERTIES OF BORON ALUMINUM
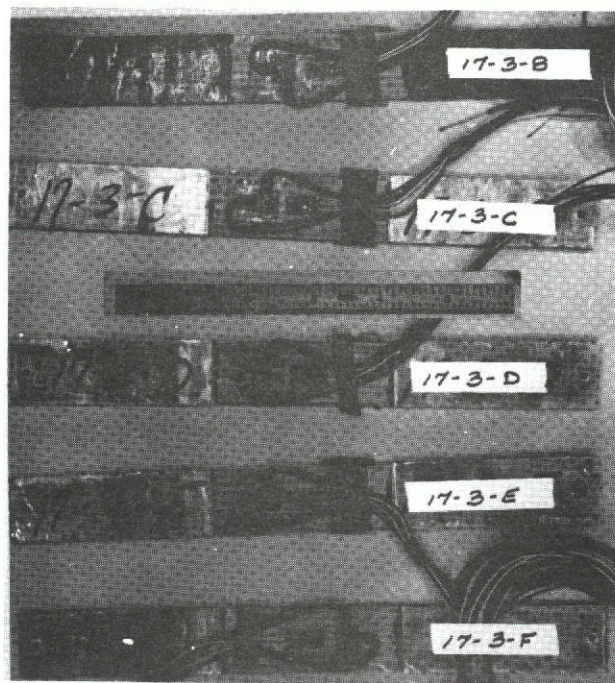
Figure 2-5

BEFORE TEST
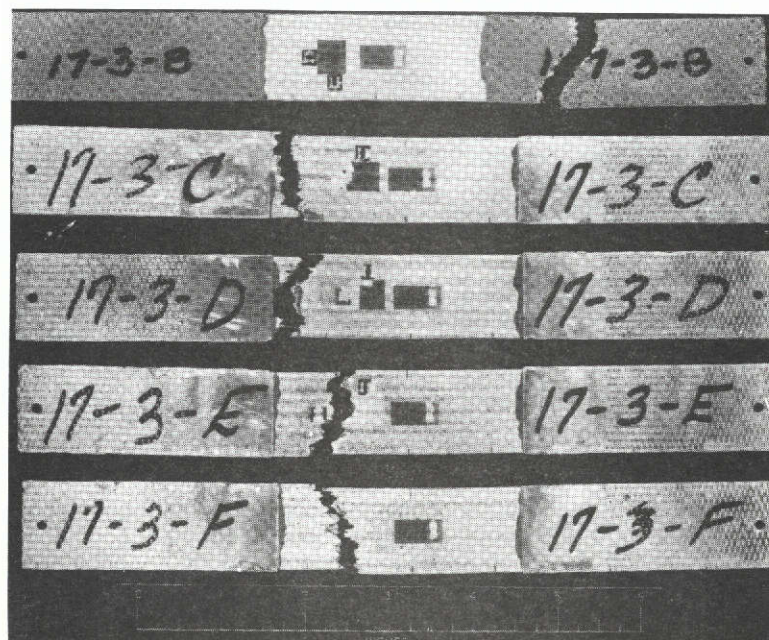
AFTER TEST AT ROOM TEMPERATURE

BORON ALUMINUM LONGITUDINAL TENSILE COUPONS

Figure 2-6
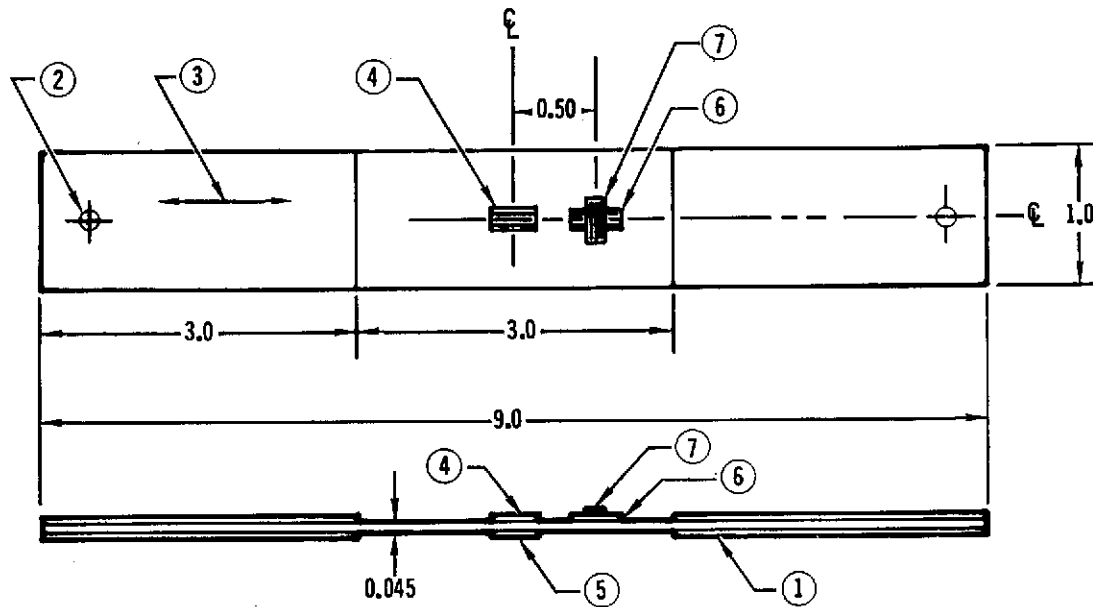
(1) 6 MIL, 1100 ALUMINUM TAB ADHESIVE BONDED TO SPECIMEN (TYP 4 PLACES)

(2) 0.095 INCH DIA ALIGNMENT PIN HOLE

(3) BORON FILAMENT DIRECTION

(4) UNIAXIAL LONGITUDINAL GAGE, L_1

(5) UNIAXIAL LONGITUDINAL GAGE, L_2

(6) ROSETTE LONGITUDINAL GAGE, L_3

(7) ROSETTE TRANSVERSE GAGE, T_3

TENSILE COUPON FOR LONGITUDINAL TENSION TESTS

Figure 2-7

temperature coupons were loaded to failure at a loading rate of .0762 cm/min (.030 in./min.). Elevated temperature coupons were soaked at 589°K (600°F) for at least 30 min. before being loaded to failure at a rate of .127 cm/min. (.050 in./min.). Continuous load-strain curves were recorded for each specimen.

Sandwich beam specimens shown in Figure 2-8 are 55.9 cm (22.0 in.) long and 2.54 cm (1.0 in.) wide. Faceplates are adhesively bonded to an aluminum honeycomb core which is 3.81 cm (1.50 in.) thick. In a 7.62 cm (3.0 in.) section at the center of the specimen, bonding is prevented by inserting teflon tape between the core and faceplate. This technique minimizes the influence of core on faceplate and allows the faceplate to respond in a manner similar to a tensile coupon. The specimen configuration was tested with a four point load application as il-

lustrated in Figure 2-9. Specimens were loaded to failure at room temperature
with a loading rate of .127 cm/min. (.050 in./min.). Continuous load-strain curves
were recorded for each specimen. No elevated temperature tests were planned using
sandwich beams, since adhesive bond failures were anticipated at 589°K (600°F)
test temperature.

Typical tensile coupons and sandwich beam specimens after test are shown in
Figures 2-6 and 2-8. The failure mode in all specimens was a tensile failure
with no evidence of bending or delamination.

Average stress-strain curves for coupons and sandwich beam specimen are shown
in Figures 2-12, 2-13 and 2-14. All curves are essentially linear to failure.
Initial modulus obtained from tensile coupons is slightly higher than that from
sandwich beam specimen.

2.1.2.2 Transverse Tension - Determination of stress-strain response, ulti-
mate transverse tensile strength (F_T^{tu}) and strain (ε_T^{tu}), initial values of elastic
modulus (E_T^t), and minor Poisson's ratio (μ_{TL}^t); at both room temperature and 589°K
(600°F) were primary test objectives of transverse testing performed under this
contract. Average transverse tensile properties from these tests are shown in
Figure 2-15.

Five tensile coupons and five sandwich beams were tested at room temperature,
and six tensile coupons and five sandwich beams were tested at 589°K (600°F). All
tensile coupons were made from bilayer material which was of good quality. The
sandwich beam specimens also were made using bilayer material obtained early in
the program and it was of poor quality. As a result, values of ultimate strength
obtained from sandwich beam tests were significantly less than those determined
using tensile coupons and were not considered to be representative of well bonded
boron-aluminum composite.

The transverse tensile coupons, shown in Figure 2-17, are 22.9 cm (9.0 in.)
long and 2.54 cm (1.0 in.) wide with a 7.62 cm (3.0 in.) gage length and 7.62 cm
(3.0 in.) end tabs. Each end tab has a six mil 1100 aluminum ply adhesively
bonded to both sides to prevent damage from the serrated Instron jaws. The cou-
pon configuration including the location of strain gages is illustrated in Figure
2-17. Back to back gages are used to check for the presence of bending during test.

All coupons were loaded to failure at a loading rate of .023 cm/min. (.009 in./
min.). Typical failed specimens are shown in Figure 2-18. Elevated temperature
specimens were soaked at 589°K (600°F) for at least 30 min. before loading. Con-
tinuous load-strain curves were recorded for each specimen.

2-12
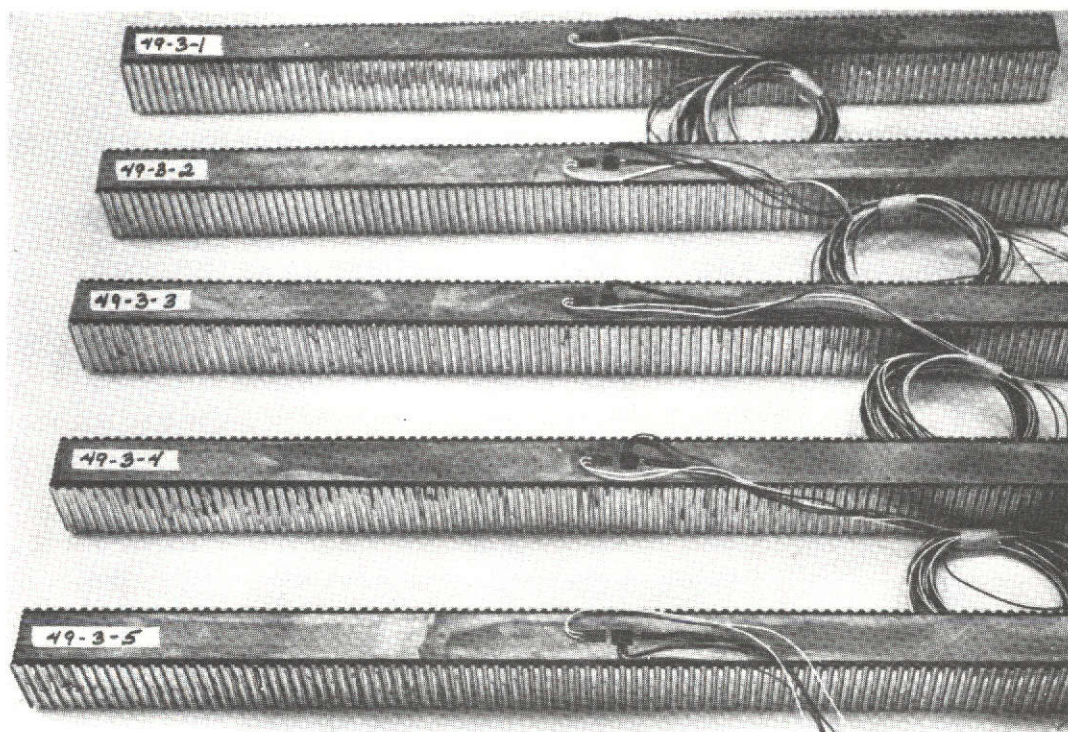
BEFORE TEST
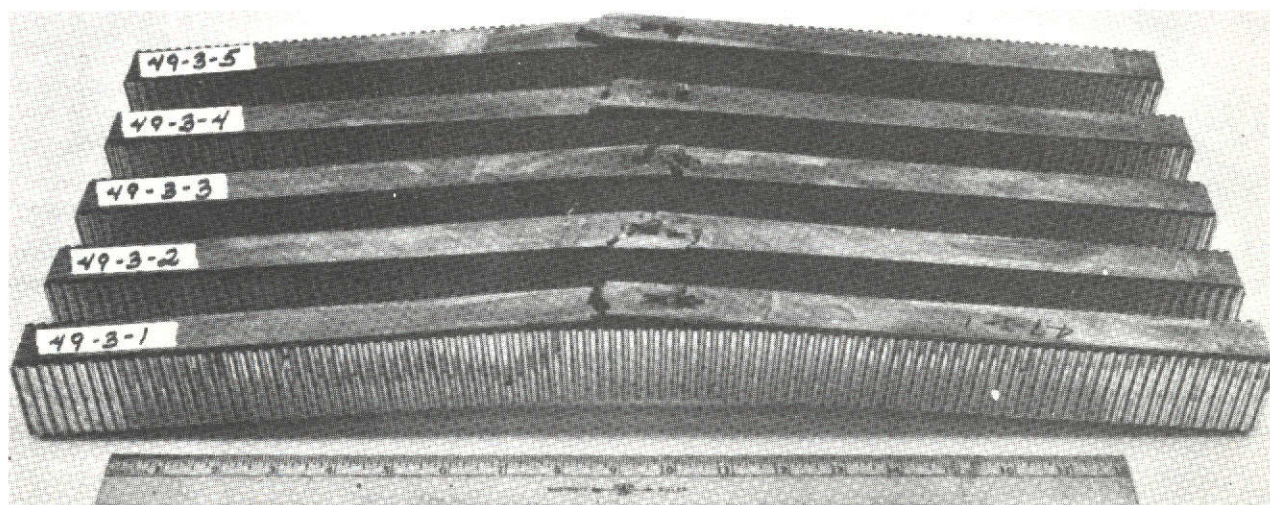
AFTER TEST AT ROOM TEMPERATURE

BORON ALUMINUM SANDWICH BEAM SPECIMENS FOR LONGITUDINAL TENSILE TESTS

Figure 2–8
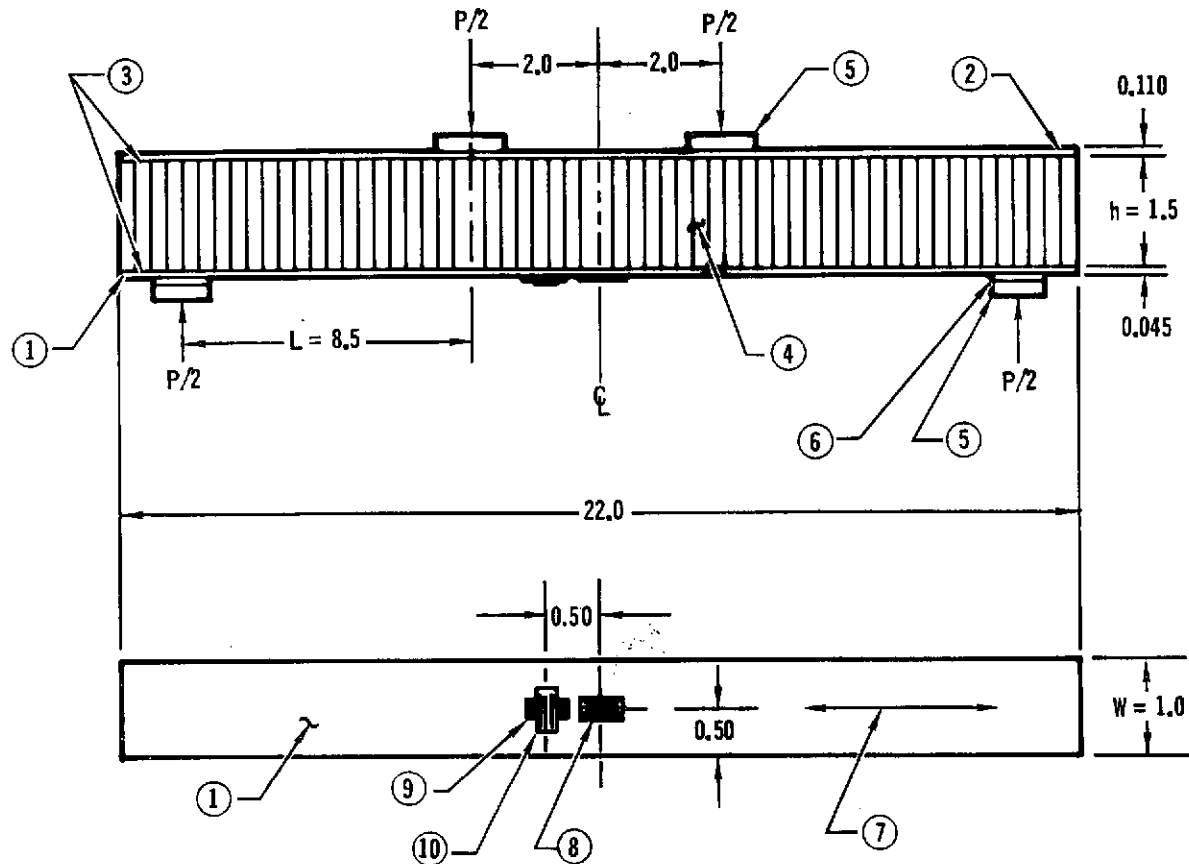
1. 6 PLY BORON (5.6 MIL)/ALUMINUM SKIN
2. TITANIUM – 6AL–4V SHEET
3. HT–424 ADHESIVE
4. ALUMINUM HONEYCOMB CORE
5. STEEL LOAD BEARING PLATE
6. SILICONE RUBBER PAD
7. BORON FILAMENT AND CORE RIBBON DIRECTION
8. UNIAXIAL LONGITUDINAL GAGE, L_2
9. ROSETTE LONGITUDINAL GAGE, L_1
10. ROSETTE TRANSVERSE GAGE, T_1

SANDWICH BEAM SPECIMEN USED FOR LONGITUDINAL TENSILE TESTING

Figure 2–9
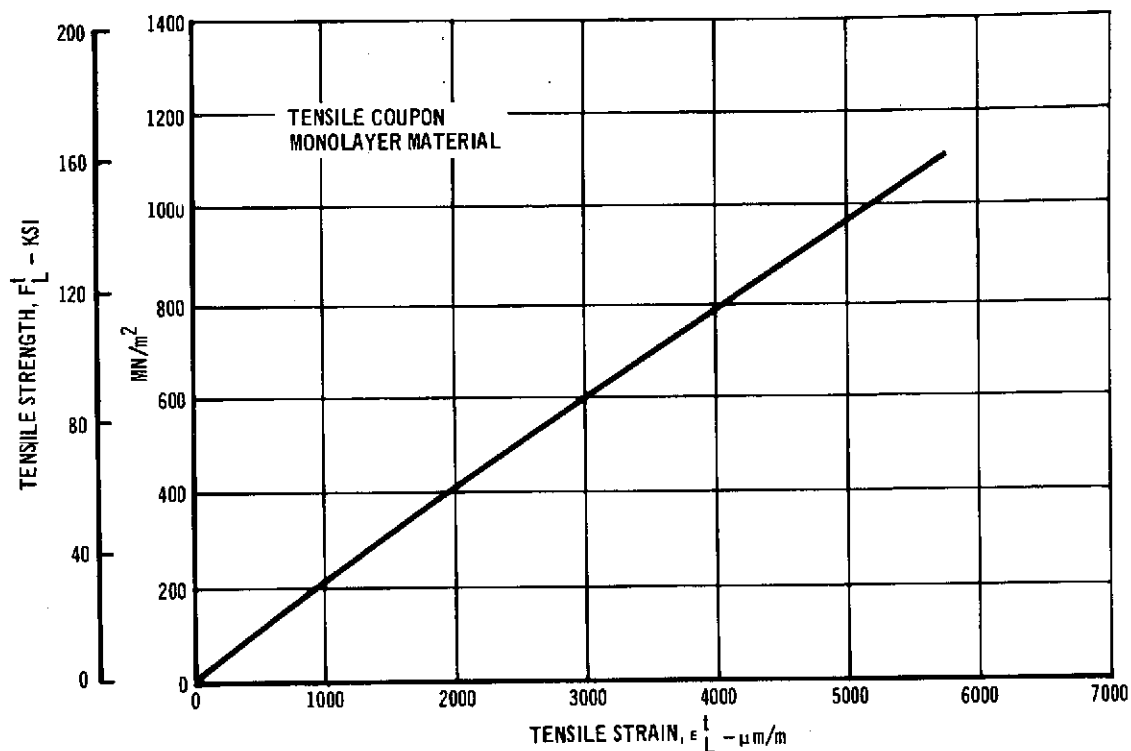
**LONGITUDINAL TENSION AVERAGE STRESS–STRAIN RESPONSE
AT ROOM AT ROOM TEMPERATURE**

Figure 2–12
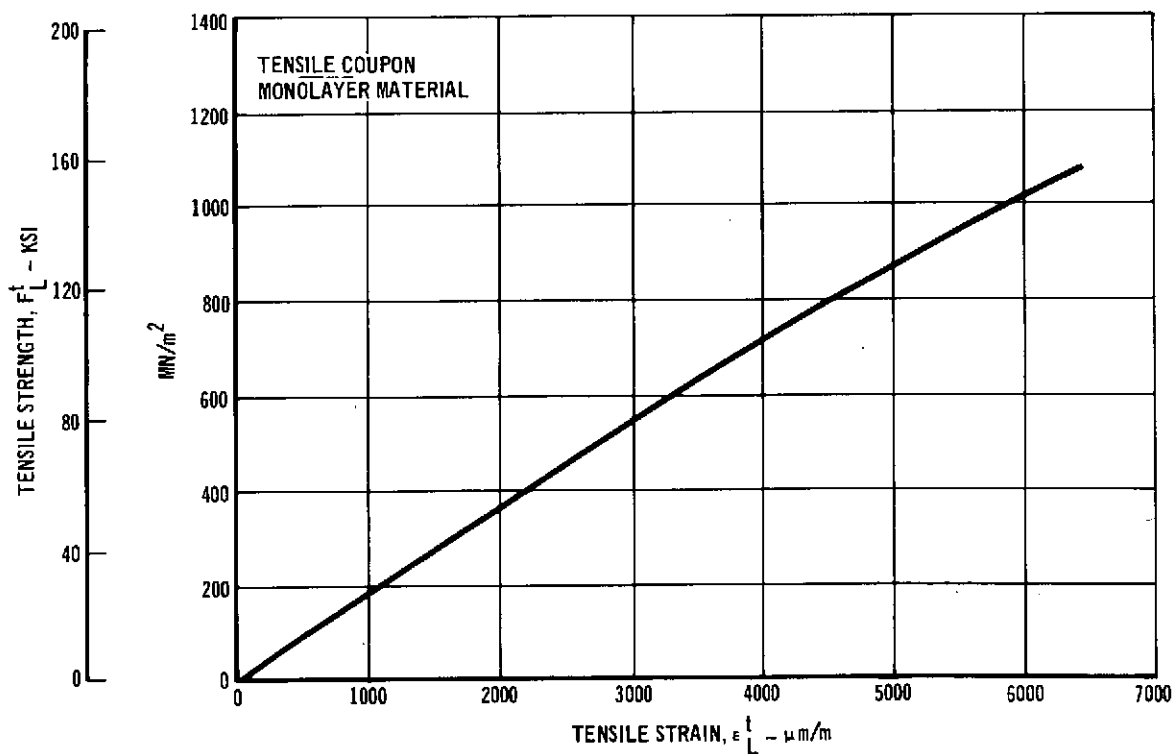
LONGITUDINAL TENSION AVERAGE STRESS–STRAIN RESPONSE AT 589°K

Figure 2–13
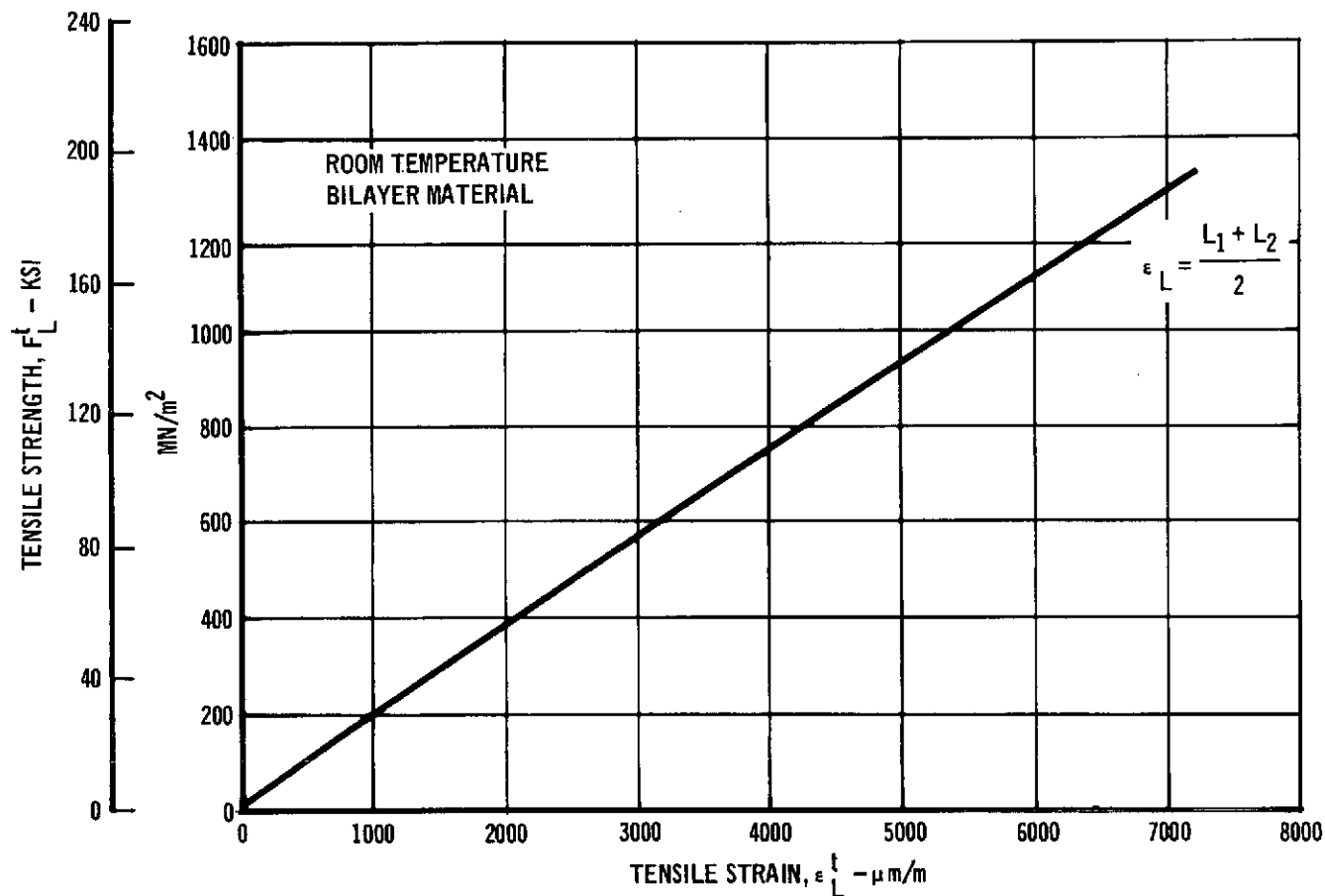
LONGITUDINAL TENSION AVERAGE STRESS–STRAIN RESPONSE
FROM SANDWICH BEAM SPECIMEN

Figure 2–14

TEST METHOD	TEST TEMPERATURE		ULTIMATE STRENGTH		ULTIMATE STRAIN	INITIAL MODULUS		INITIAL POISSON'S RATIO	FILAMENT VOLUME %
	°K	°F	MN/m²	KSI	μm/m	GN/m²	10⁶ PSI		
COUPON	R.T.	R.T.	101.2	14.7	3290	126.0	18.3	0.180	–
COUPON	589	600	26.9	3.9	6480	80.5	11.7	0.095	46.3

NOTES: 1. RESULTS ARE AVERAGE VALUES BASED ON TESTS OF FIVE SPECIMEN MINIMUM IN EACH GROUP.
2. BILAYER PLY MATERIAL

AVERAGE TRANSVERSE TENSILE PROPERTIES OF BORON ALUMINUM

Figure 2–15
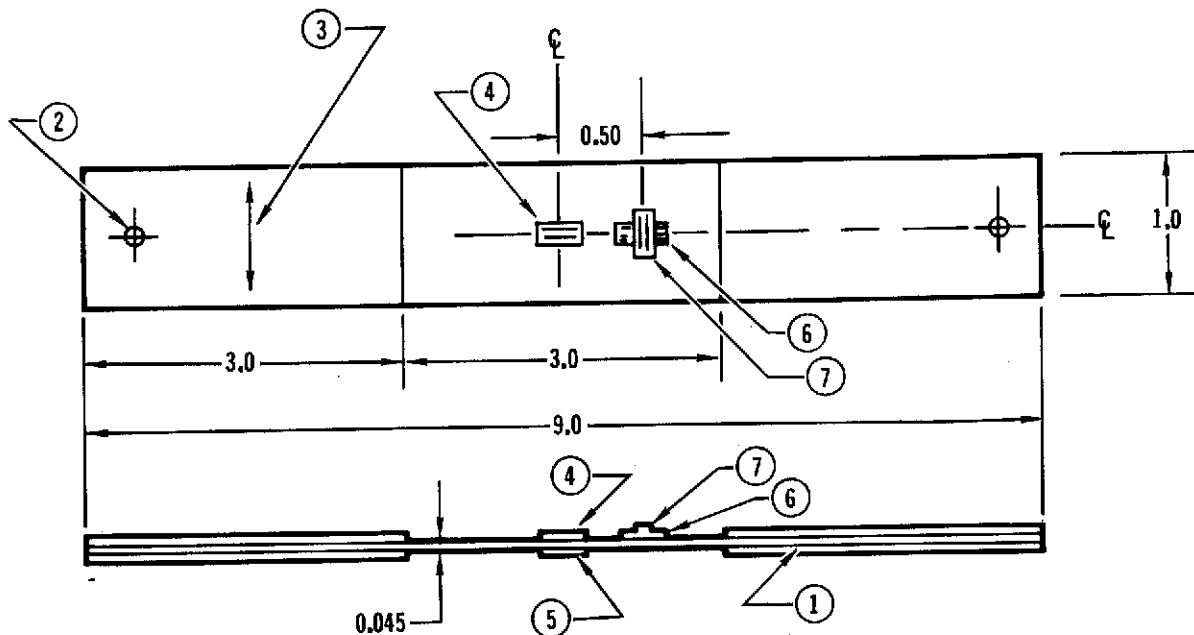
1. 6 MIL, 1100 ALUMINUM TAB ADHESIVE BONDED TO SPECIMEN (TYP 4 PLACES)
2. 0.095 INCH DIA ALIGNMENT PIN HOLE
3. BORON FILAMENT DIRECTION
4. LONGITUDINAL GAGE, L_1
5. LONGITUDINAL GAGE, L_2
6. ROSETTE LONGITUDINAL GAGE, L_3
7. ROSETTE TRANSVERSE GAGE, T_3

TENSILE COUPON USED FOR TRANSVERSE TENSION TEST

Figure 2—17
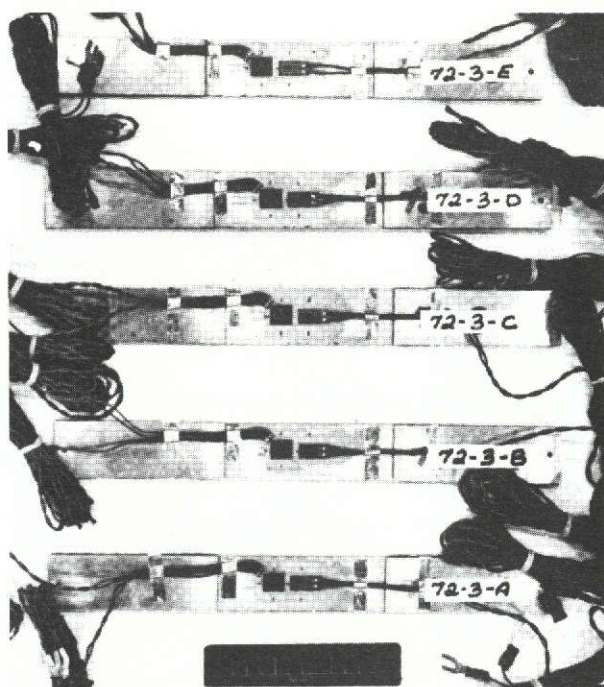
BEFORE TEST

AFTER TEST AT ROOM TEMPERATURE

BORON ALUMINUM TRANSVERSE TENSILE COUPONS

Figure 2–18

Average transverse tensile stress-strain response at room temperature and 589°K (600°F) are shown in Figures 2-19 and 2-20. Since transverse tensile properties are highly matrix dependent, nearly the entire stress-strain curve is nonlinear.
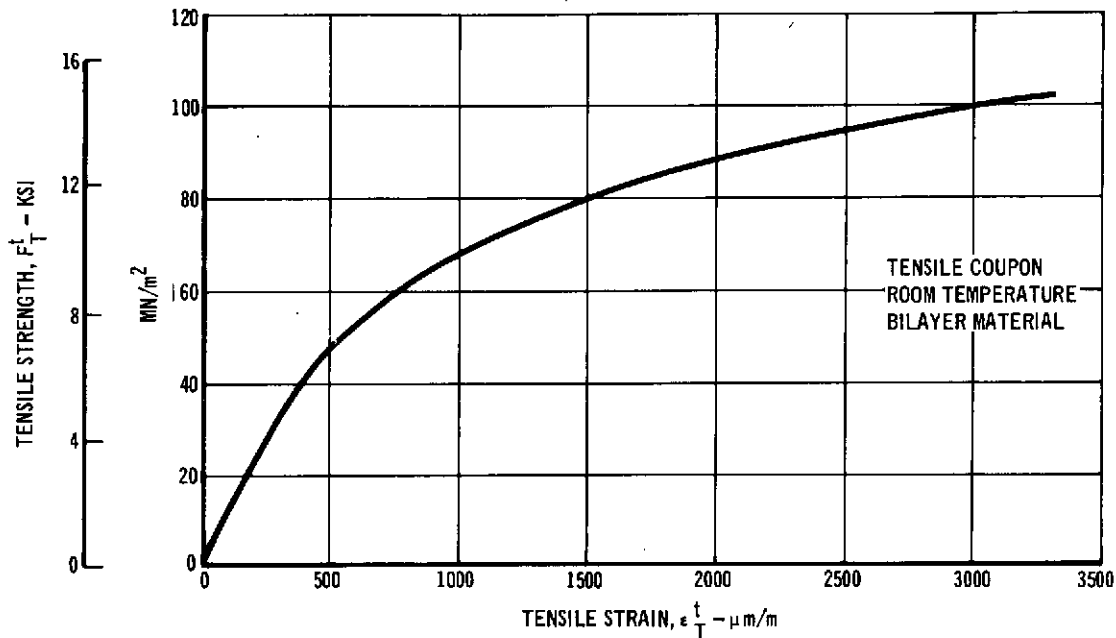
**TRANSVERSE TENSION AVERAGE STRESS-STRAIN RESPONSE
AT ROOM TEMPERATURE**

Figure 2-19
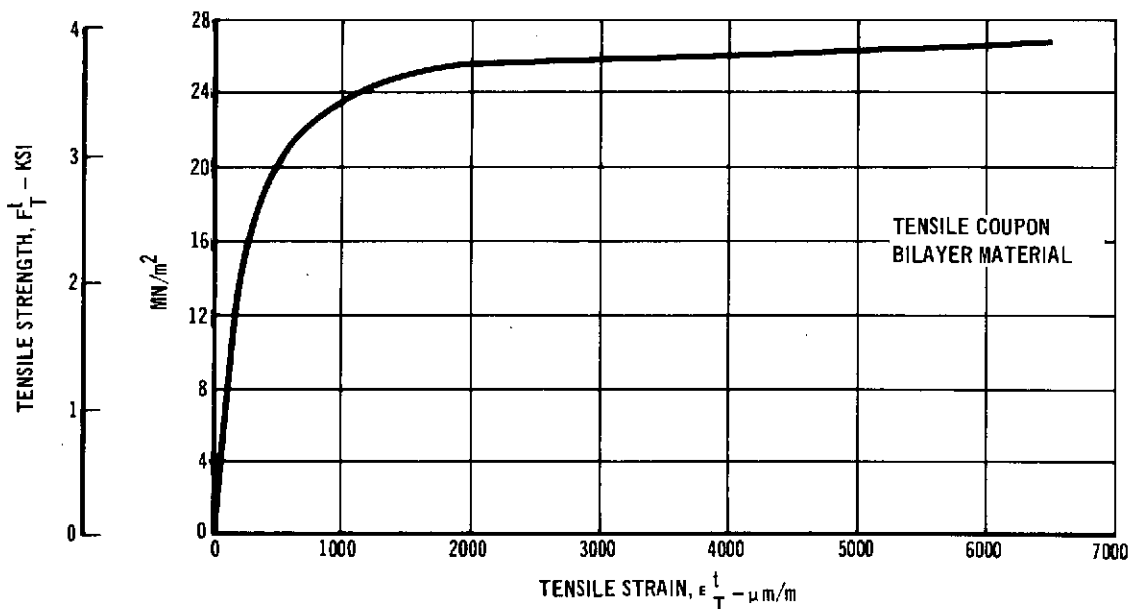
**TRANSVERSE TENSION AVERAGE STRESS-STRAIN RESPONSE
AT 589°K**

Figure 2-20

2.1.2.3 <u>Longitudinal and Transverse Compression</u> -- Determination of stress-strain response, ultimate longitudinal (F_L^{cu}) and transverse (F_T^{cu}) compressive strengths, initial values of elastic moduli $(E_L^c$ and $E_T^c)$, and initial values of major (μ_{LT}^c) and minor (μ_{TL}^c) Poisson's ratio, at both room temperature and 589°K (600°F) were primary test objectives. Average mechanical properties obtained from these tests are shown in Figure 2-21.

TYPE TEST	TEST TEMPERATURE		PLY MATERIAL	ULTIMATE STRENGTH		ULTIMATE STRAIN	INITIAL MODULUS		POISSON'S RATIO	FILAMENT VOLUME %
	°K	°F		MN/m^2	KSI	$\mu m/m$	GN/m^2	10^6 PSI		
LONGITUDINAL COMPRESSION	R.T.	R.T.	BILAYER	2360.0	343.0	10600	243.0	35.3	0.284	43.6
TRANSVERSE COMPRESSION	R.T.	R.T.	BILAYER	258.0	37.5	24000	97.2	14.1	0.165	43.5
TRANSVERSE COMPRESSION	589	600	MONOLAYER	66.1	9.6	10700	109.5	15.9	0.166	--

NOTE: 1. SANDWICH BEAM TEST METHOD
2. RESULTS ARE AVERAGE VALUES BASED ON TESTS OF FIVE SPECIMENS MINIMUM IN EACH GROUP.

AVERAGE LONGITUDINAL AND TRANSVERSE COMPRESSIVE PROPERTIES OF BORON ALUMINUM

Figure 2-21

Longitudinal specimens for tests at room temperature consisted of five sandwich beams and six edge-loaded panels. Sandwich beams were used in all transverse loading tests with five specimens tested at room temperature and five specimens tested at 589°K (600°F).

Edge-loaded panel specimens were planned for longitudinal compressive tests at 589°K (600°F) since adhesive bond failures were anticipated if sandwich beams were used at elevated temperature. To evaluate the test method, six room temperature tests were conducted. Results from these tests indicated that the edge-loaded panel method was unacceptable because premature low failure strengths were obtained. The low failure strengths were caused by facesheet brooming at the ends of the specimen. Potting the specimen ends to prevent brooming was not successful. Consequently, longitudinal compressive strength at elevated temperature was not obtained. However, longitudinal compressive strength properties were of litt:

importance in the compression panel analysis because failure modes lower than block compression, such as crippling, always prevailed. The longitudinal modulus at 589°K is estimated to be 26.0×10^6 psi, based on data from instrumented crippling specimens.

Sandwich beam specimens used for longitudinal compressive tests were identical to those used in longitudinal tensile tests. Typical failures in longitudinal beam specimens are shown in Figure 2-22.
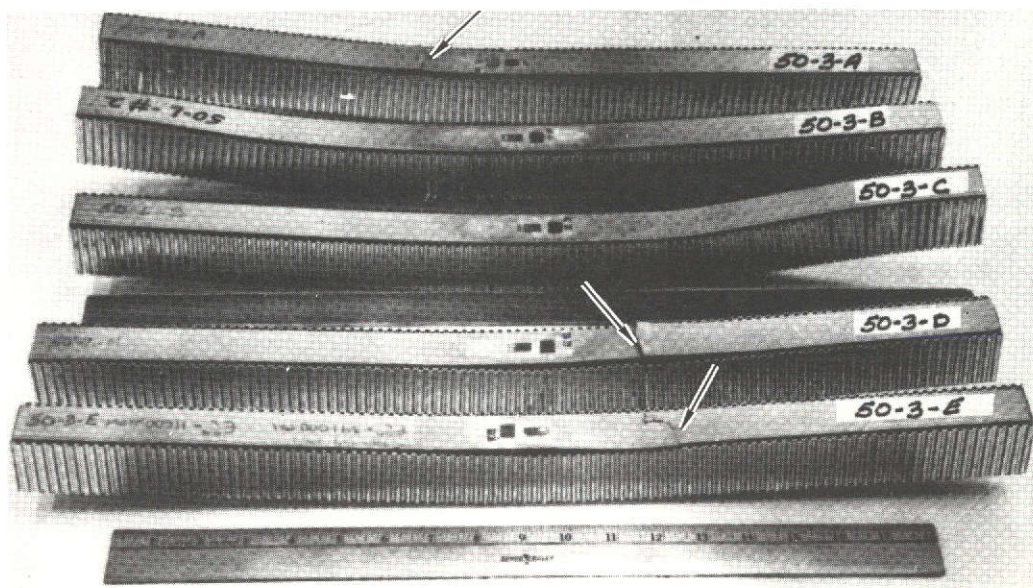
*ARROWS DENOTE LOCATION OF FAILURE

ROOM TEMPERATURE TESTS

BORON ALUMINUM SANDWICH BEAM SPECIMENS
AFTER LONGITUDINAL COMPRESSIVE TESTS

Figure 2-22

Sandwich beam specimens used for transverse compressive tests are similar to the longitudinal beam specimen except that the length is reduced from 55.9 cm (22 in.) to 40.7 cm (16 in.). Typical transverse beam specimens before and after test are shown in Figures 2-23 and 2-24.

Average longitudinal and transverse compressive stress strain curves are shown in Figures 2-25, 2-26, and 2-27. The longitudinal curve is essentially linear to failure; however, the transverse curves at both room and elevated temperature are non-linear over a majority of loading range.

2.1.2.4 <u>Rail Shear</u> - The purpose of this test was to determine the in-plane shear stress-strain response and ultimate shear strength of unidirectional and $\pm \frac{\pi}{4}$ rad laminates. Tests were conducted at both room temperature and 589°K

2-21

(600°F) with a 30 minute soak at temperature prior to test. Average rail shear test results are shown in Figure 2-28. Typical rail shear test specimens before test are shown in Figure 2-29.
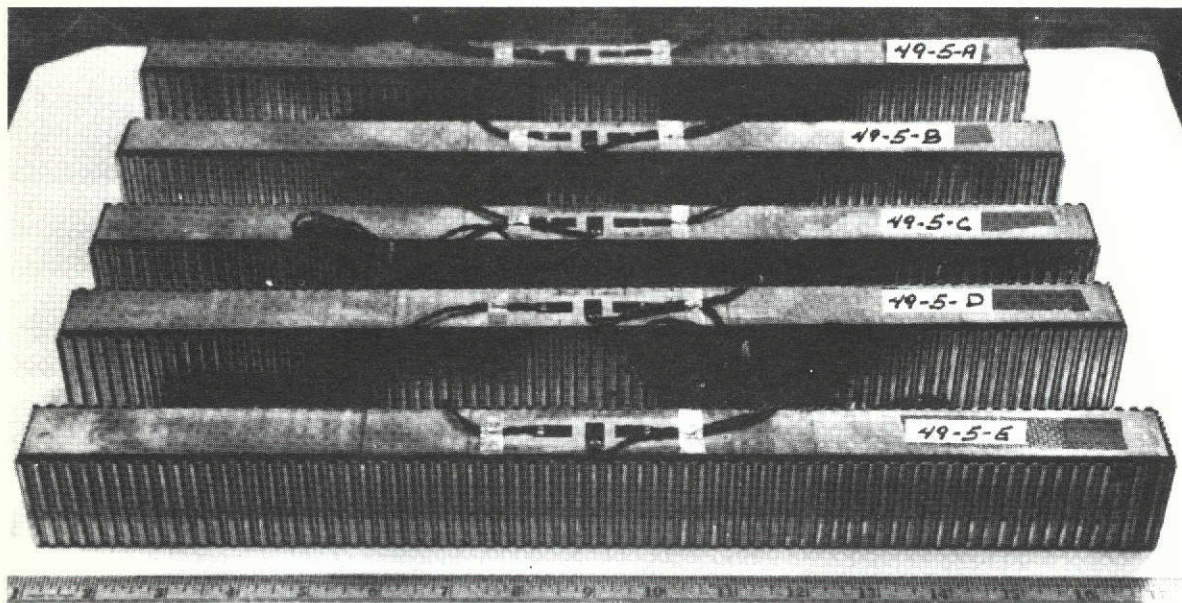
BEFORE TEST

BORON ALUMINUM SANDWICH BEAM SPECIMENS FOR TRANSVERSE COMPRESSIVE TESTS

Figure 2-23
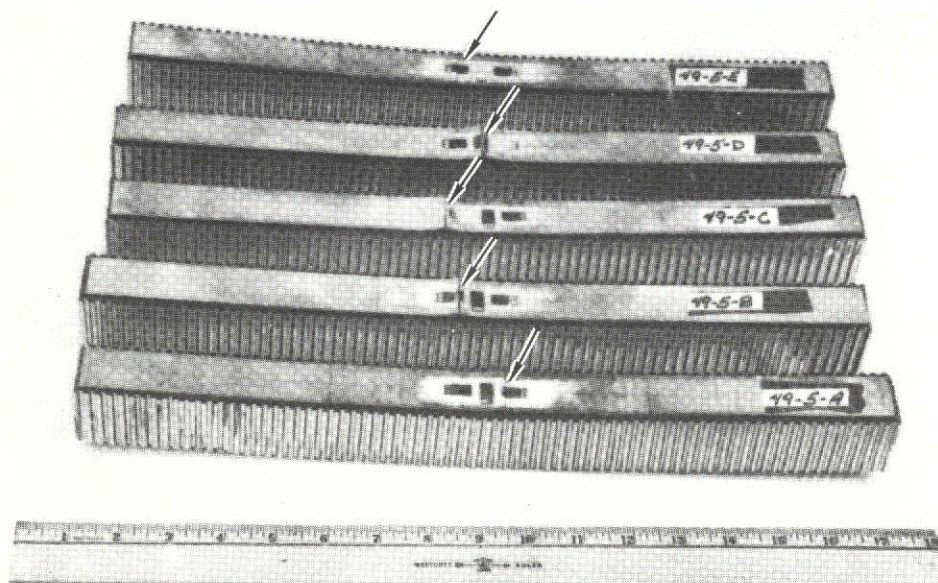
*ARROWS DENOTE LOCATION OF FAILURE

AFTER TEST AT ROOM TEMPERATURE

BORON ALUMINUM SANDWICH BEAM SPECIMENS FOR TRANSVERSE COMPRESSIVE TESTS

Figure 2-24
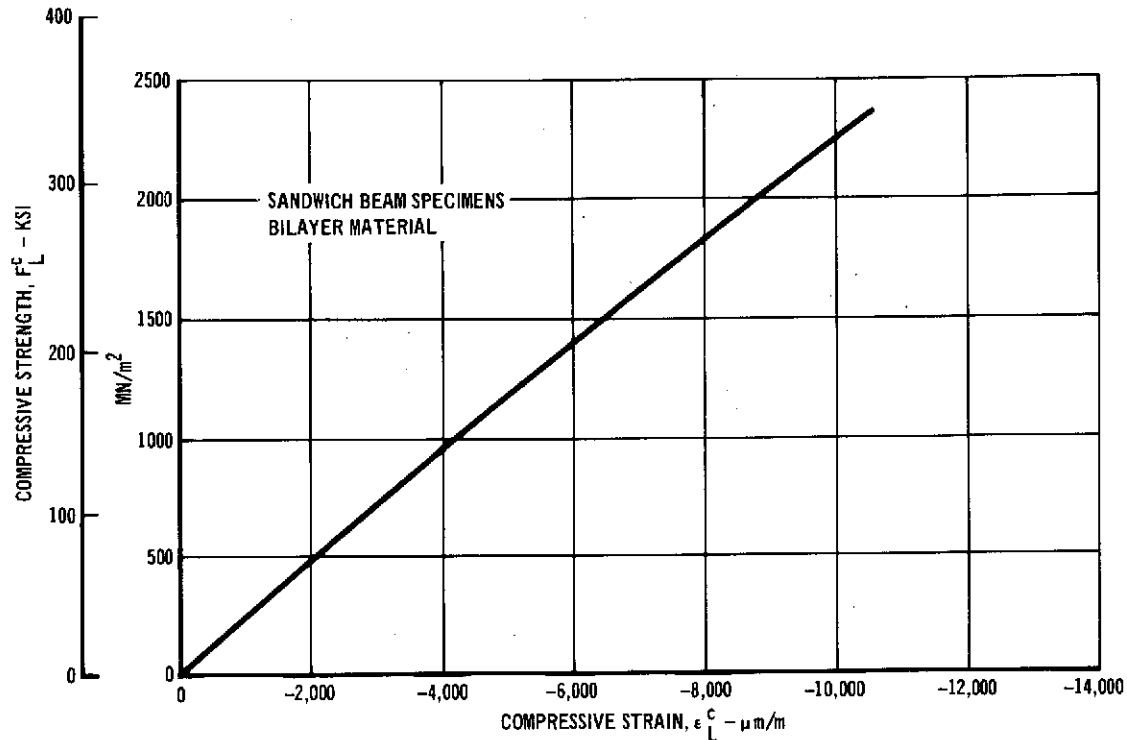
LONGITUDINAL COMPRESSION AVERAGE STRESS–STRAIN RESPONSE
AT ROOM TEMPERATURE

Figure 2–25
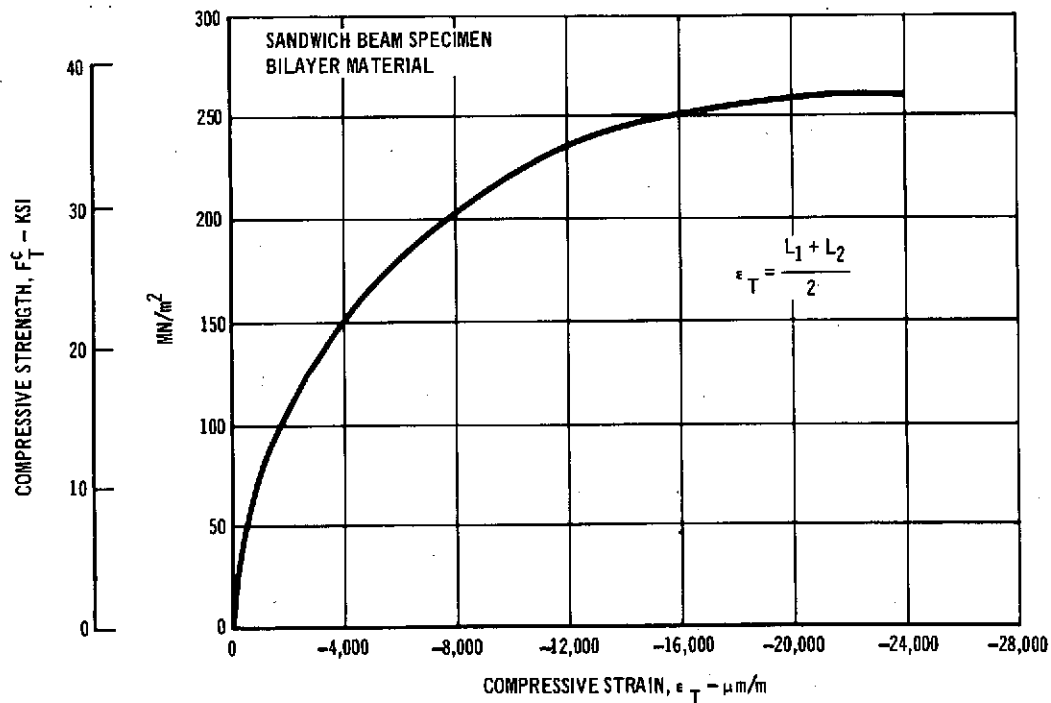
TRANSVERSE COMPRESSION AVERAGE STRESS–STRAIN RESPONSE
AT ROOM TEMPERATURE

Figure 2–26

2–23
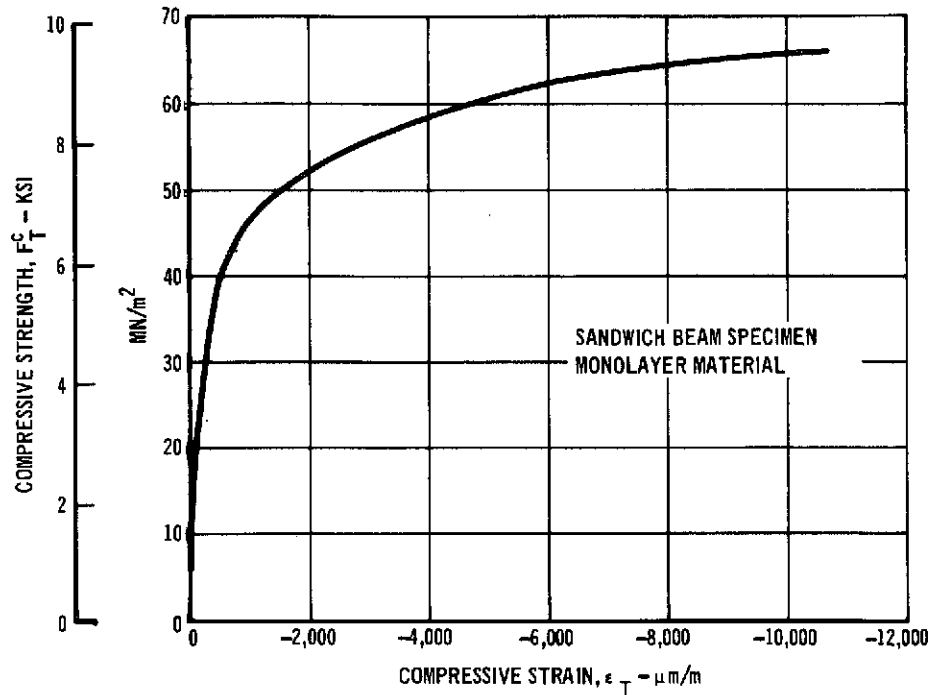
TRANSVERSE COMPRESSION AVERAGE STRESS–STRAIN RESPONSE AT 589ºK

Figure 2–27

FILAMENT ORIENTATION Θ	NUMBER OF SPECIMEN TESTED /2\	PLY MATERIAL	TEST TEMPERATURE		ULTIMATE SHEAR STRENGTH		ULTIMATE SHEAR STRAIN	SHEAR MODULUS		FILAMENT VOLUME
			ºK	ºF	MN/m^2	KSI	μm/m	GN/m^2	10^6 PSI	%
0 rad	3	MONOLAYER	R.T.	R.T.	55.2 /1\	8.0	15,700	66.2	9.6	50.3
	3	MONOLAYER	589	600	23.4 /1\	3.4	> 10,000	29.6	4.3	50.3
	3	BILAYER	R.T.	R.T.	46.2 /1\	6.7	> 18,000	55.2	8.0	43.9
	3	BILAYER	589	600	15.8 /1\	2.3	18,200	22.7	3.3	43.9
π/2 rad (90º)	7	BILAYER	R.T.	R.T.	46.2 /1\	6.7	> 20,000	62.0	9.0	44.5
	3	BILAYER	589	600	15.8 /1\	2.3	> 32,000	34.5	5.0	44.5
±π/4 rad (±45º)	7	MONOLAYER	R.T.	R.T.	297.0	43.1	4,200	86.1	12.5	39.7
	5	MONOLAYER	589	600	151.0	21.9	> 1,500	68.2	9.9	39.7

/1\ SHEAR STRENGTH DETERMINED AT STRAIN OF 10,000 μm/m.

/2\ RAIL SHEAR TEST METHOD

AVERAGE IN–PLANE SHEAR PROPERTIES OF BORON ALUMINUM

Figure 2–28
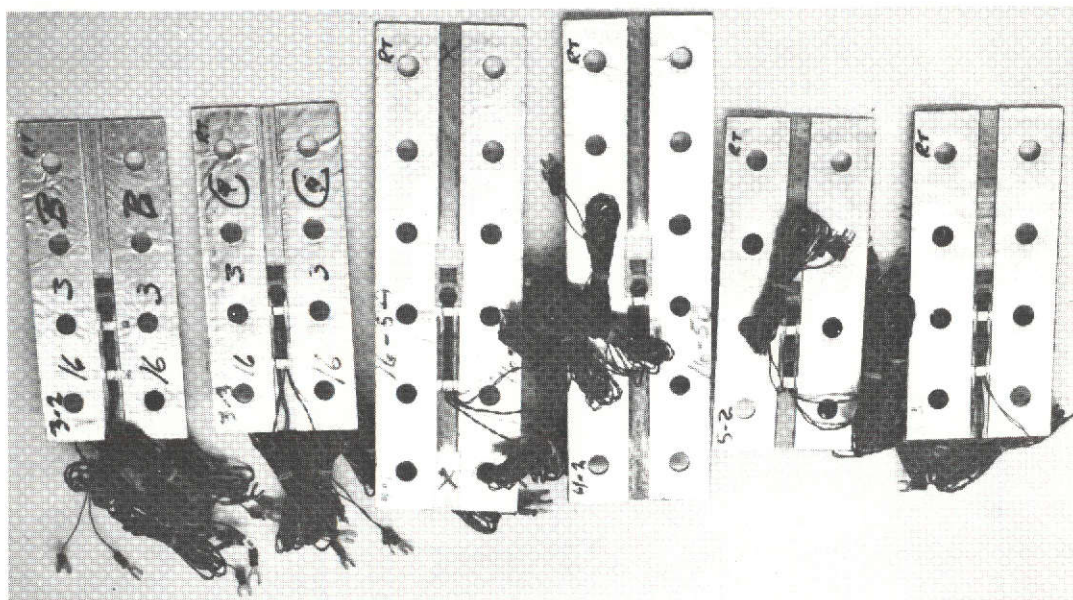
0 rad
MONOLAYER

0 rad
BILAYER

π/2 rad
BILAYER

TYPICAL BORON ALUMINUM RAIL SHEAR SPECIMENS BEFORE TEST
Room Temperature

Figure 2–29

Both monolayer and bilayer material were used to fabricate unidirectional laminates where the boron filaments are aligned parallel to the rail test fixture (filament orientation = 0 rad, Figure 2-28). Although the monolayer specimens possessed higher strength and stiffness properties, most of this difference is attributed to the higher filament volume fraction for monolayer material. Shear stress-strain response of monolayer and bilayer material are shown in Figures 2-30 and 2-31 respectively. Failure modes of unidirectional, 0-rad laminates made from monolayer material are shown in Figure 2-32. Laminates tested at 589°K (600°F) experienced more shear deformation than laminates tested at room temperature and failure initiated at the specimen ends.

Specimens with lengths of 20.3 cm (8 in.) and 30.5 cm (12 in.) were tested to determine if length affected rail shear strength. Results showed that specimen length had little effect on either shear strength or stiffness; therefore, test results were not separated by specimen length.

In-plane shear properties of unidirectional laminates were determined using specimen with filaments oriented both parallel (0 rad) and perpendicular ($\frac{\pi}{2}$ rad) to rails of test fixture. Over the useable loading range of interest, strength

and stiffness properties determined by the two methods at both room and elevated temperature are nearly the same (Figure 2-28). Also, stress-strain response from the two laminates are similar as shown in Figures 2-31 and 2-33. Differences in the two curves are within the scatter of test data.
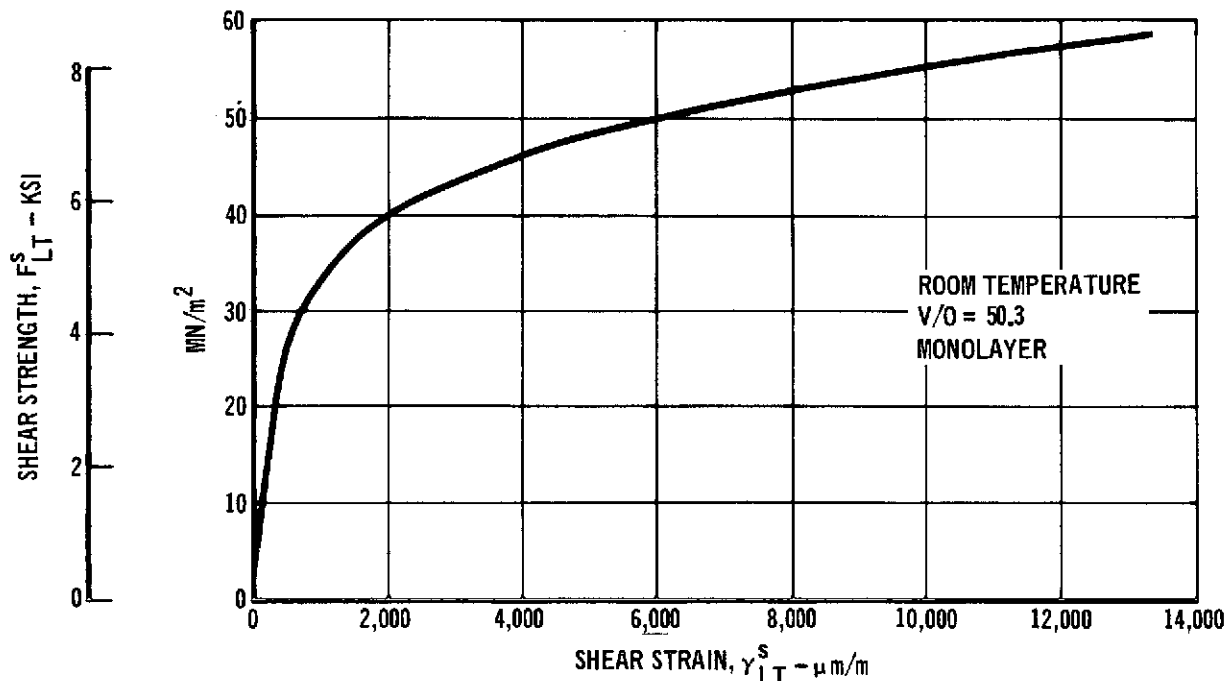
AVERAGE SHEAR STRESS–STRAIN RESPONSE OF 0-rad BORON ALUMINUM

Figure 2–30
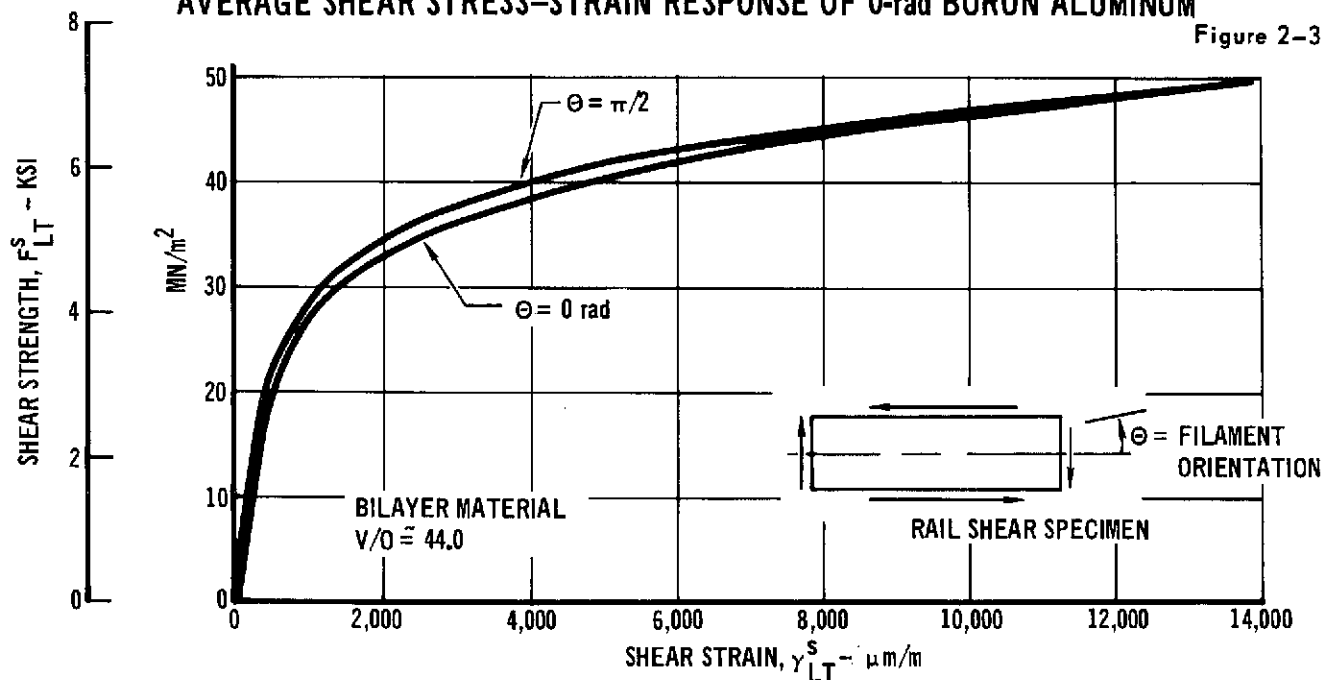
**AVERAGE SHEAR STRESS–STRAIN RESPONSE OF UNIDIRECTIONAL
BORON ALUMINUM AT ROOM TEMPERATURE**

Figure 2–31

2-26

ROOM TEMPERATURE TEST   589°K (600°F) TEST
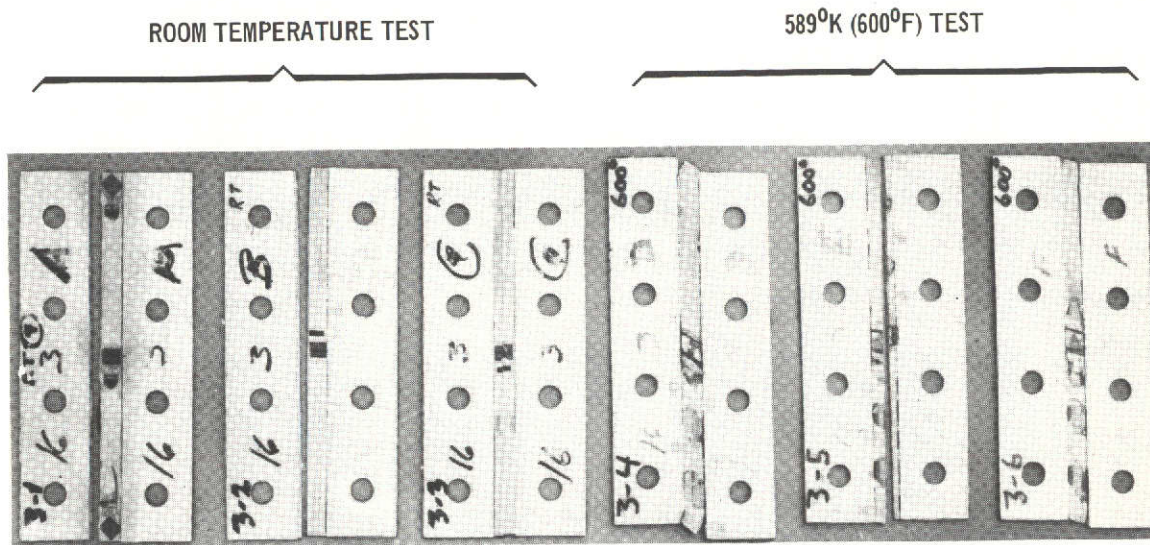
FILAMENT ORIENTATION = 0 rad

BORON ALUMINUM RAIL SHEAR SPECIMENS AFTER TEST

Figure 2–32
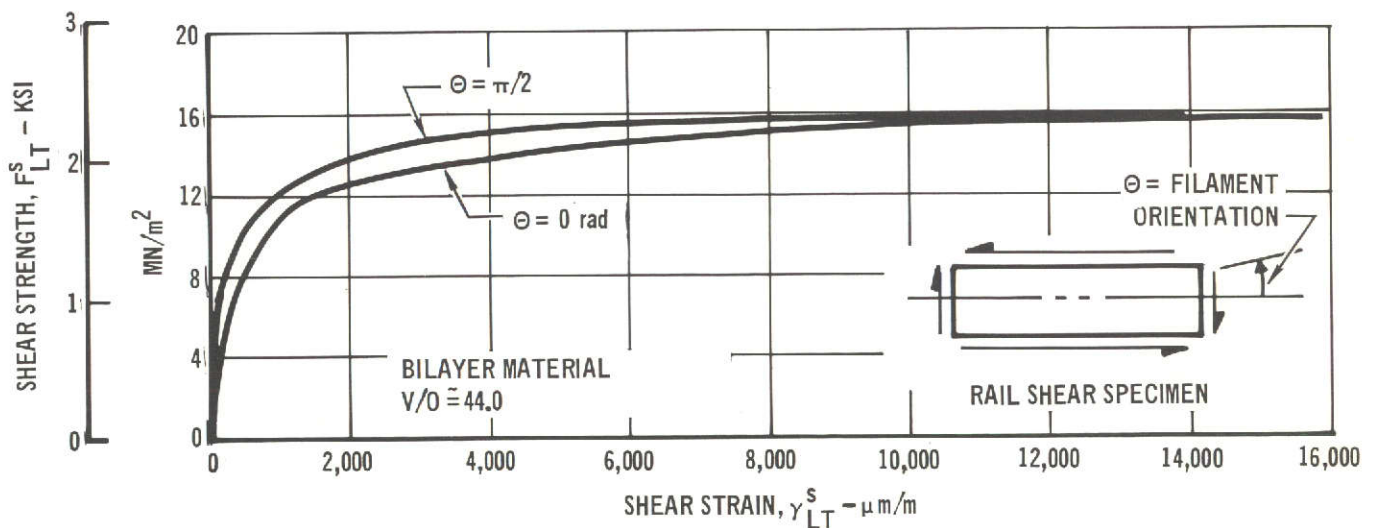
AVERAGE SHEAR STRESS–STRAIN RESPONSE OF UNIDIRECTIONAL BORON ALUMINUM AT 589°K

Figure 2–33

Shear strains at failure of $\frac{\pi}{2}$ rad laminates are associated with excessive deformation of the test specimen as shown in Figure 2-34. At shear strains above about 10,000 µm/m, loads applied to the rails are no longer resisted entirely by shear in the matrix because of the high strain deformation. Instead, loads are carried primarily by the filaments which can lead to exaggerated reports of shear strengths at failure. These values at specimen failure are not representative of true shear strength of unidirectional boron-aluminum laminates. For this

reason, shear strengths of 0 and $\frac{\pi}{2}$ rad laminates are reported in Figure 2-28 for shear strain levels of 10,000 μm/m.

Both room and elevated temperature tests were conducted on $\pm\frac{\pi}{4}$ rad laminates. Photographs of these specimen after test are shown in Figure 2-35. Shear stress-strain response of this laminate is shown in Figure 2-36. Because shear characteristics of this laminate are controlled primarily by the filaments, the stress-strain curve is nearly linear.
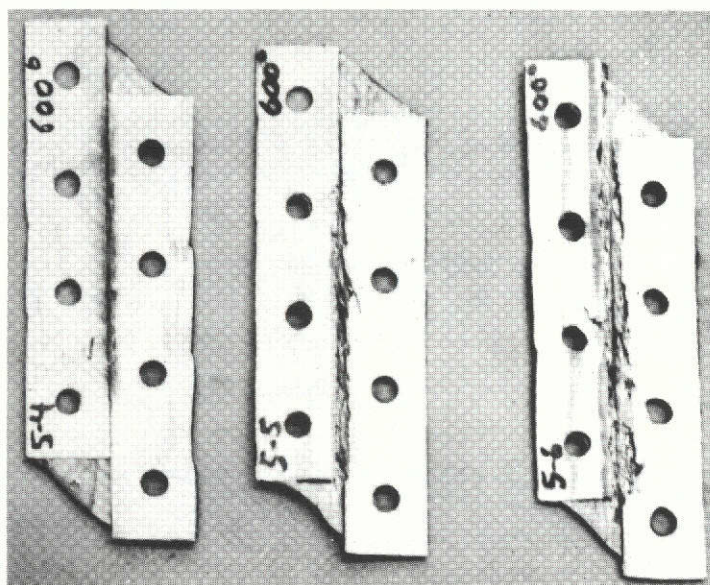
FILAMENT ORIENTATION = π/2 rad
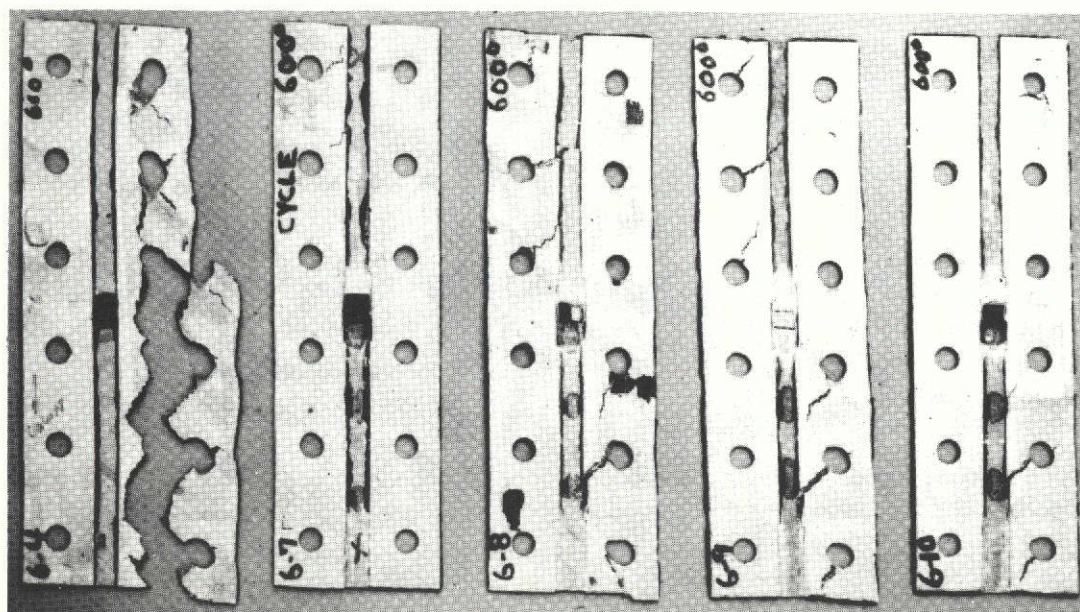
FILAMENT ORIENTATION = ± π/4 rad

BORON ALUMINUM RAIL SHEAR SPECIMENS AFTER TEST AT 589°K

Figure 2-35

2-28
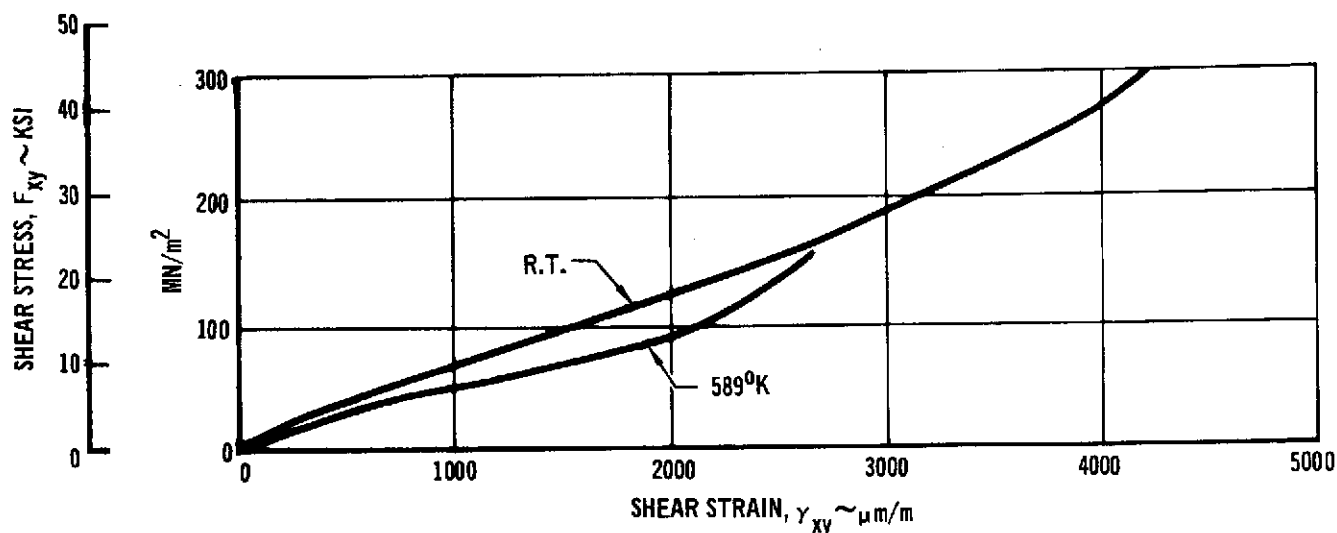
AVERAGE SHEAR STRESS – STRAIN PROPERTIES OF ± π/4 rad LAMINATES AT ROOM TEMPERATURE AND 589°K

Figure 2–36

2.1.2.5 Diagonal Tension - The purpose of this test was to determine the effect of outer ply filament orientation and bending stresses caused by buckling on the shear strength and stiffness of $\pm \frac{\pi}{4}$ rad symmetric, boron-aluminum laminates. Results from these tests are summarized in Figure 2-37. As shown, filament orientation affects shear strength but has little effect on stiffness. Also, bending stresses appear to reduce ultimate shear strength; this can be observed by comparing results from these tests with rail shear tests of Section 2.1.2.4.

SPECIMEN NO.	TEST TEMPERATURE		NUMBER OF PLIES	ULTIMATE SHEAR STRENGTH		ULTIMATE SHEAR STRAIN	INITIAL SHEAR MODULUS		OUTER PLY FILAMENT ORIENTATION
	°K	°F		MN/m²	KSI	um/m	GN/m²	10⁶ PSI	
1	R.T	R.T	4	228.0	33.1	3940	75.8	11.0	①
2	R.T	R.T	4	289.0	42.0	4220	74.5	10.8	②
3	R.T	R.T	8	250.0	36.3	3190	75.8	11.0	①
4	589	600	4	154.3	22.4	>2830	51.6	7.5	①

① PARALLEL TO LOAD
② PERPENDICULAR TO LOAD

SHEAR PROPERTIES OF ± π/4 rad BORON ALUMINUM LAMINATES DIAGONAL TENSION TEST METHOD

Figure 2-37

Typical diagonal tension test specimens, shown in Figure 2-38, are 17.8 cm
(7.0 in.) square including tabs for joining to picture frame test fixture. The
test zone inside end tabs is approximately 10 cm (4.0 in.) square. A six mil
aluminum ply is adhesively bonded to each side of the end tabs to prevent damage
from test fixture. Back-to-back strain rosettes were bonded to the specimen in two
locations as shown in Figure 2-38. In addition, deflectometers were attached to the
specimen adjacent to the strain gages for purposes of recording lateral deflection
due to buckling.

SPECIMEN 1   SPECIMEN 2
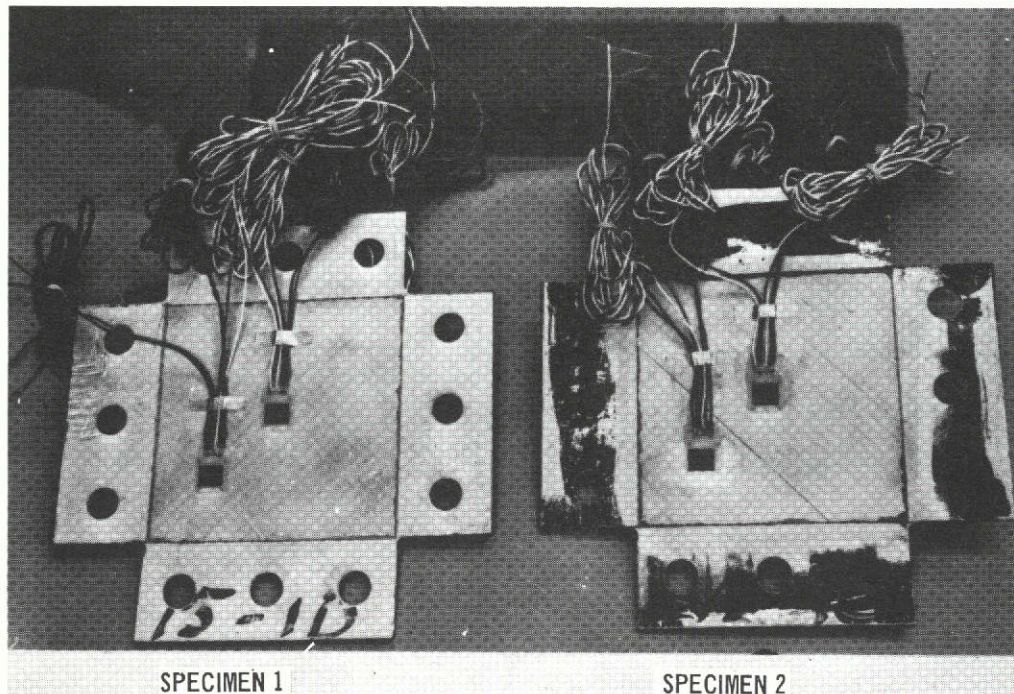
ROOM TEMPERATURE
BORON ALUMINUM DIAGONAL TENSION SPECIMENS PRIOR TO TEST

Figure 2-38

Two types of failure modes are possible depending on outer ply filament ori-
entation as shown in Figures 2-39 and 2-40. In Figure 2-39, outer ply filaments
are oriented parallel to applied load. This specimen failed in shear along the
edges of specimen. Outer ply filaments are oriented perpendicular to load for
specimen shown in Figure 2-40. This is the preferred orientation because the
specimen possesses maximum flexural stiffness to resist buckling caused by internal
compressive loads acting perpendicular to applied loads. Deflectometer readings
showed that the preferred orientation specimen (Figure 2-40) experienced smaller
lateral deflections than the specimen shown in Figure 2-39. As a result, bending
stresses were lower which permitted that specimen to carry higher shear loads
before failure (Reference Figure 2-37).
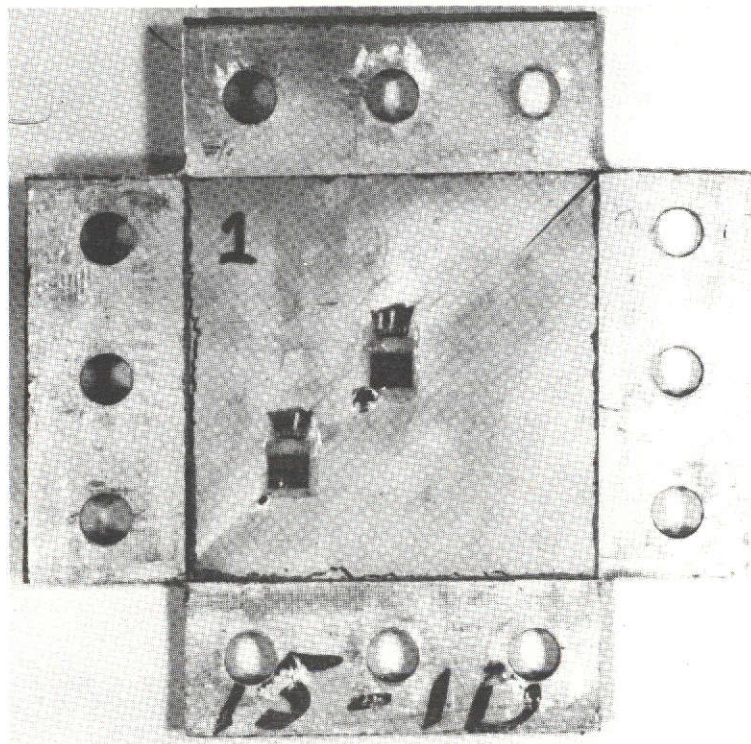
FILAMENT ORIENTATION PARALLEL TO LOAD

BORON ALUMINUM DIAGONAL TENSION SPECIMENS AFTER TEST AT ROOM TEMPERATURE

Figure 2–39
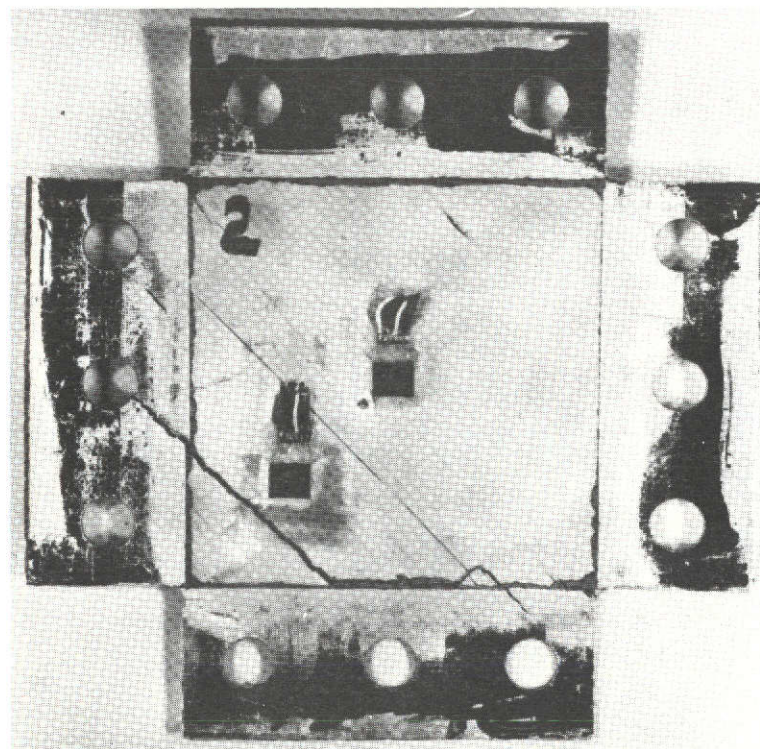
FILAMENT ORIENTATION PERPENDICULAR TO LOAD

BORON ALUMINUM DIAGONAL TENSION SPECIMENS AFTER TEST AT ROOM TEMPERATURE

Figure 2–40

In the compression panel, both preferred and unpreferred filament orientations are present in the skin at opposite sides of the centerline stringer. For this reason, ultimate shear strengths obtained from diagonal tension tests are conservatively based on unpreferred filament orientation.

A typical shear stress-strain curve for a diagonal tension specimen is shown in Figure 2-41. Although this curve was obtained from a specimen having preferred outer ply filament orientation, the response is similar over a majority of the curve to specimen with unpreferred outer ply filament orientation.
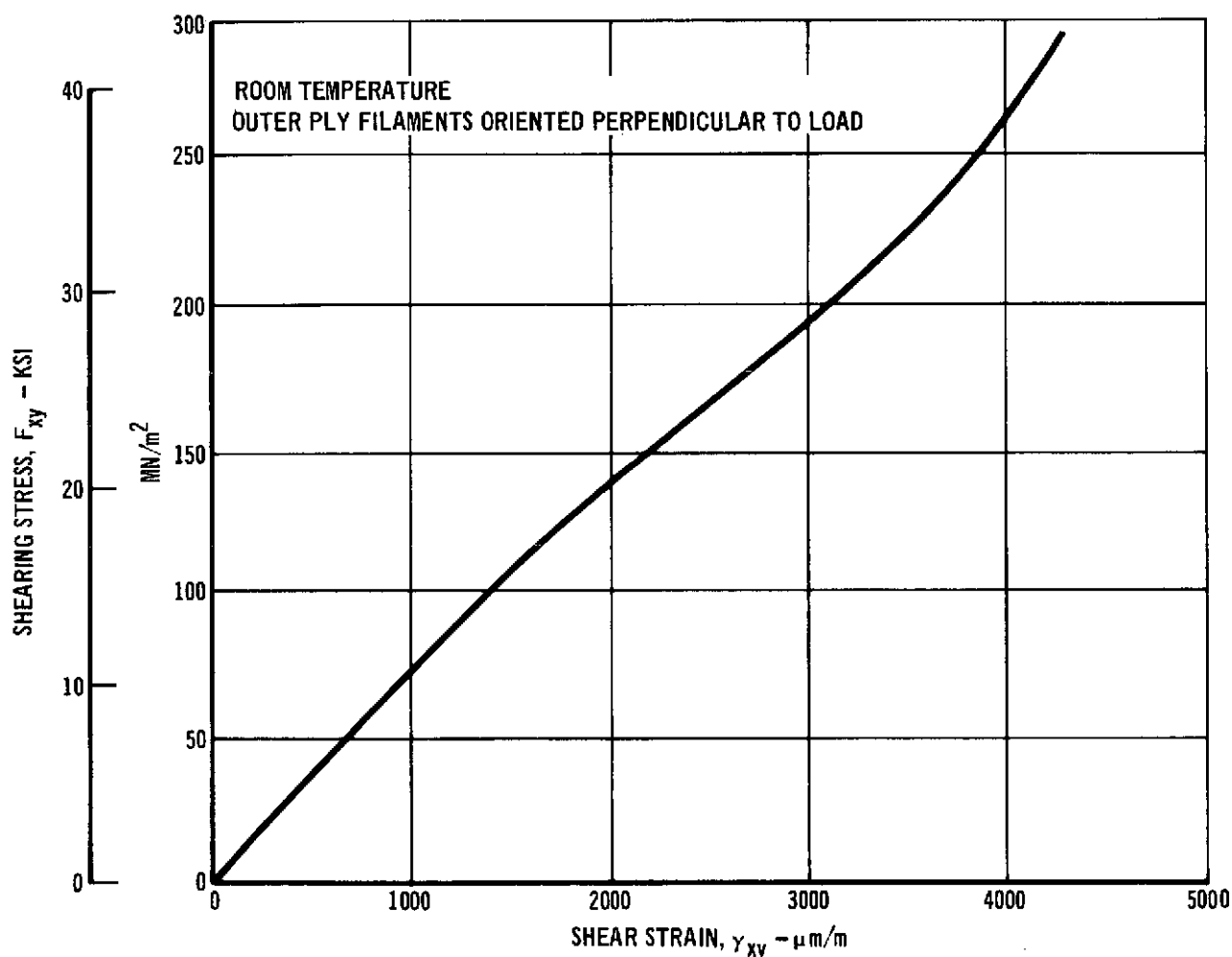
TYPICAL SHEAR STRESS-STRAIN RESPONSE OF ± π/4 rad LAMINATE FROM
DIAGONAL TENSION SPECIMEN

Figure 2-41

2.1.2.6 Crippling - Crippling strength of a unidirectional boron-aluminum stringer having several different thicknesses was determined by test at room temperature and 589°K (600°F). The stringer hat shape selected, shown in Figure

2-42, was used on all stringers of the 1.83 m (72 inch) long by 1.22 m (48 inch) wide compression panel. These stringers have constant shape but are tapered in thickness by adding or removing plies to carry the variable load along their length. The range of stringer thicknesses tested (6 ply to 19 ply) was chosen to cover the range in thickness required for loads expected in the seven stringers on the compression panel.

NUMBER PLIES	T (cm)	A (cm)	B (cm)	C (cm)	R_1 (cm)	R_2 (cm)
6	.117	1.98	.81	.97	1.27	1.90
10	.190	2.11	1.01	1.07	1.37	1.90
14	.267	2.16	1.40	1.14	1.27	1.42
19	.361	2.19	1.40	1.14	1.27	1.14
5	.097	2.42	.97	1.07	1.27	1.50
17	.328	2.49	1.14	1.01	1.27	1.12
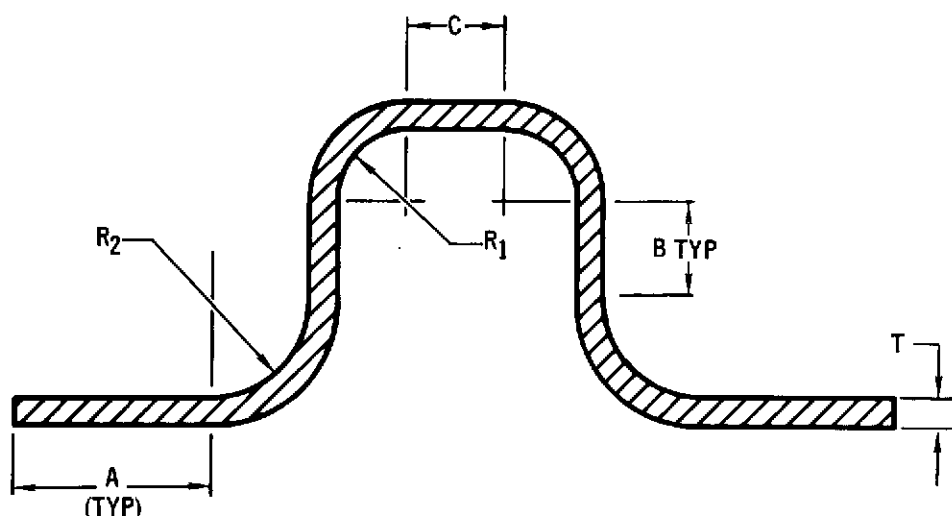
CRIPPLING SPECIMEN CONFIGURATION
FOR 5.6 MIL BORON/ALUMINUM HAT SECTION STRINGERS

Figure 2-42

Results from crippling tests are summarized in Figure 2-43 and graphically presented in Figure 2-44. Crippling strengths defined by curves shown in Figure 2-44 are considered to be average values. The 10 ply specimens contained defective

2-33

areas prior to testing and the results are treated accordingly. Crippling
strength at 589°K (600°F) is about 55 percent of the room temperature strength.

NUMBER OF PLIES	TEST TEMPERATURE		INITIAL BUCKLING LOAD		CRIPPLING LOAD		CRIPPLING STRESS		FILAMENT VOLUME %
	°K	°F	kN	KIPSI	kN	KIPS	MN/m²	KSI	
6	R T	R T	21.8	4.9	84.1	18.9	427.0	62.0	45.3
6	589	600	①	①	38.2	8.6	194.3	28.2	45.3
10	R T	R T	81.9	18.4	147.2	33.1	408.0	59.3	44.6
10	589	600	1	1	64.1	14.4	184.5	26.8	44.6
14	R.T	R.T	242.0	54.5	266.5	59.9	571.0	82.8	45.0
14	589	600	113.0	25.4	181.0	40.7	385.0	55.9	45.0
19	R.T	R.T	①	①	489.0	110.0	800.0	116.0	44.9
19	589	600	254.5	57.2	267.0	60.0	433.0	62.9	44.9
5②	R T	R T	18.2	4.1	72.1	16.2	442.0	64.1	
17③	R T	R T	①	①	468.0	105.3	855.0	124.0	

① INITIAL BUCKLING LOAD NOT DETECTED

② FOUR, 0 rad B/AL PLIES AND ONE TITANIUM PLY AT MIDPLANE

③ SIXTEEN, 0 rad B/AL PLIES AND ONE TITANIUM PLY AT MIDPLANE

CRIPPLING STRENGTH OF UNIDIRECTIONAL BORON ALUMINUM
Hat Section Stringers

Figure 2—43
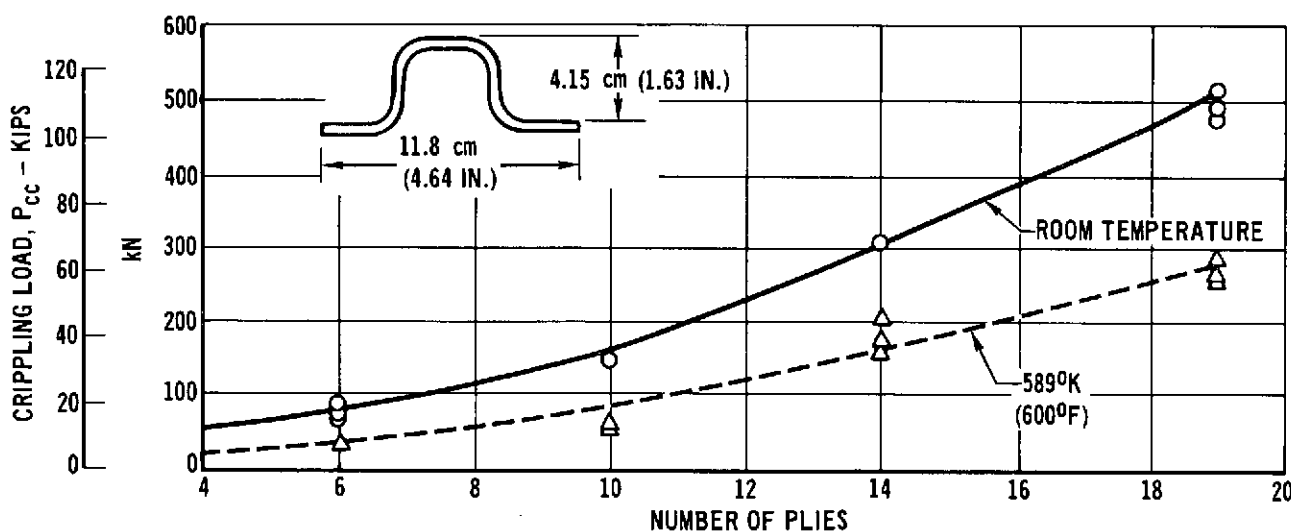
SELECTED HAT STRINGER CRIPPLING LOAD CAPABILITY
AT ROOM TEMPERATURE AND 589°K (600°F)

Figure 2—44

A typical crippling specimen with ends potted ready for test is shown in Figure 2-45. Potting was required particularly for the thick specimens to prevent brooming of specimen ends. Glasrock castable ceramic was the potting material used for some room temperature specimens and all 589°K (600°F) specimens. The potting material was retained by a steel frame as shown in Figure 2-45.
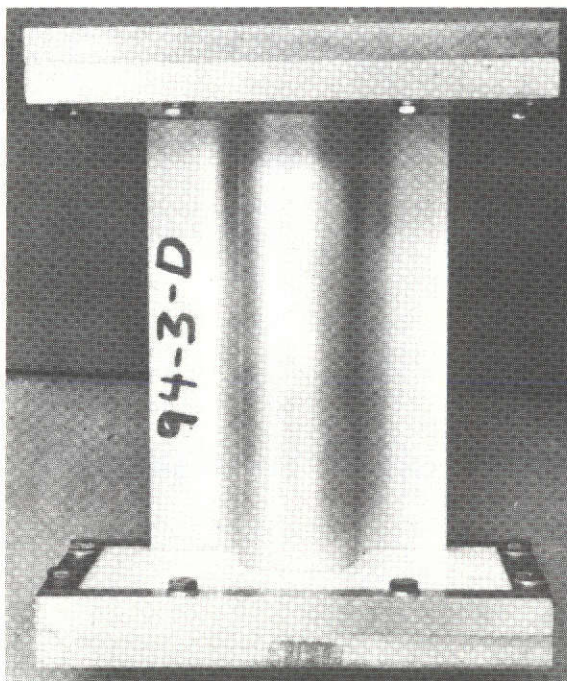
**TYPICAL BORON ALUMINUM CRIPPLING SPECIMEN POTTED
WITHIN RETAINING FIXTURE**

Figure 2-45

Failure modes typical of six and 19 ply specimens are shown in Figures 2-46 and 2-47 respectively. It was noted before testing that some specimens had no eutectic bonds in free flange radii probably due to insufficient early processing hand-forming pressure or bonding pressure in these areas. Evidence of these poor bonds is shown by type of failure revealed in Figure 2-47. Stringers used in the compression panel were formed by a mechanical process which provides much higher forming pressures to insure inter-ply contact for bonding; therefore, it is expected that compression panel stringers have higher crippling strengths than those determined in the element test program.

The compression panel stringers contain titanium interleaves to improve in-plane shear and bearing strengths of the stringers. To determine the effect of titanium interleaves on crippling strength, a five ply and a seventeen ply crippling specimen were tested at room temperature. Both specimens contained only one
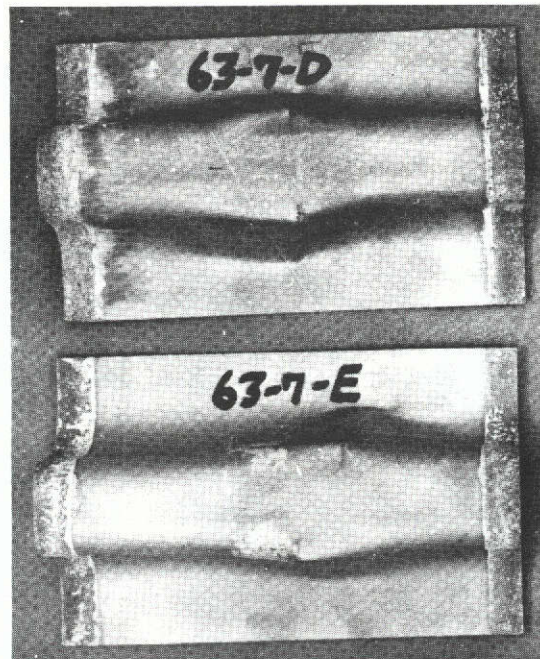
TEMPERATURE = 589°K (600°F)

TYPICAL 6 PLY CRIPPLING SPECIMEN AFTER TEST

Figure 2–46

EUTECTIC
BONDLINE
DELAMINATION

EUTECTIC
BONDLINE
DELAMINATION
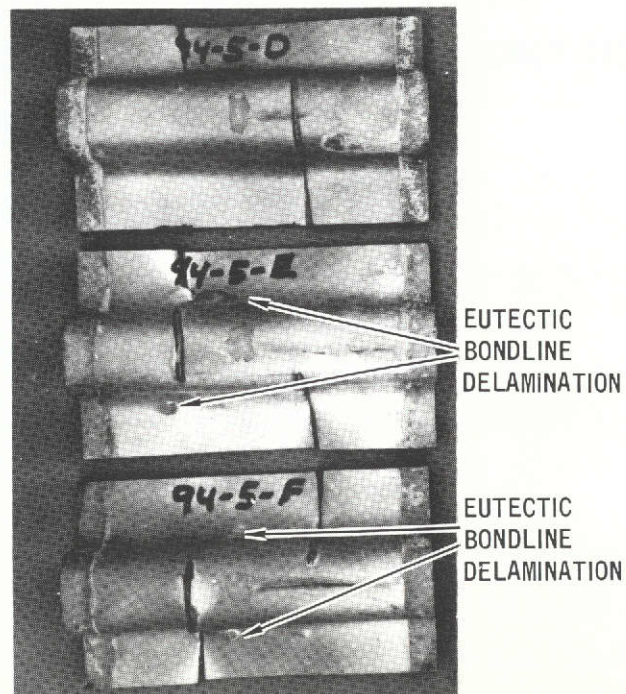
TEMPERATURE = 589°K (600°F)

TYPICAL 19 PLY CRIPPLING SPECIMEN AFTER TEST

Figure 2–47

titanium ply located at the midplane. Results show that the titanium ply had little affect on room temperature crippling strength. At elevated temperatures (589°K), titanium interleaves are expected to significantly improve crippling strength because strength and stiffness of titanium is not affected by temperature to the same extent as the matrix dependent transverse properties of boron-aluminum. Transverse properties of boron-aluminum influence crippling strength as evidenced by longitudinal splitting in failed specimens (Figures 2-46 and 2-47). These longitudinal splits are significantly reduced in the five ply specimen containing a titanium interleaf as shown in Figure 2-48.
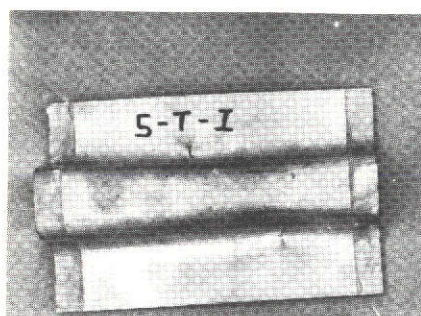
2 PLY 0° B/AL,Ti, 2 PLY 0° B/AL AT R.T.
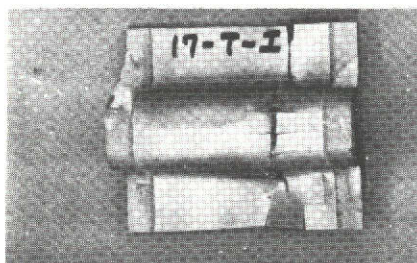
8 PLY 0° B/AL, Ti, 8 PLY 0° B/AL AT R.T.
ROOM TEMPERATURE

BORON ALUMINUM CRIPPLING SPECIMENS WITH TITANIUM INTERLEAF AFTER TEST

Figure 2-48

A few specimens were instrumented with strain gages to record distribution of load within the specimen and to determine onset of free flange buckling. A 6 ply unidirectional boron-aluminum crippling specimen containing several strain gages was tested at room temperature. Results are shown in Figure 2-49. The free flange was observed to buckle at 38.2 kN (8600 lbs) which agrees well with divergence of back to back strain gages 1 and 2. These two gages also indicate that after free flange buckling, no additional load is carried by that portion of flange. Gages 3 and 4 show that the corner radii region has not buckled and continues to accept additional load until overall crippling occurs.

STRAIN GAGE PLACEMENT
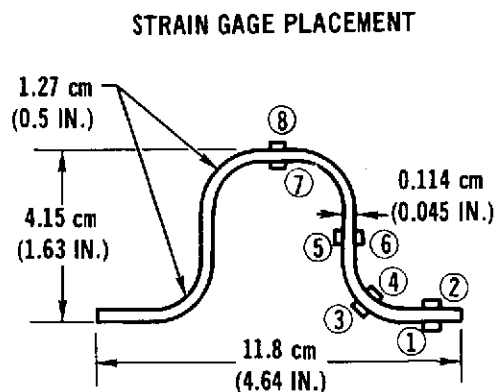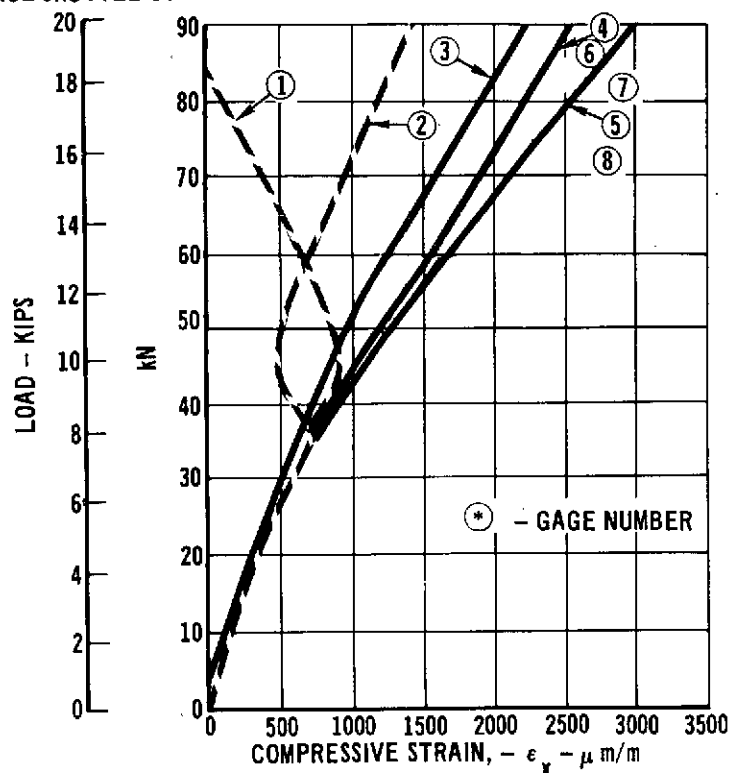
STRINGER HAT SECTION POSSESSES GOOD POST BUCKLING STRENGTH

Figure 2-49

A 19 ply crippling specimen containing strain gages was tested at 589°K (600°F) and stress-strain response is shown in Figure 2-50. These results show that the specimen was uniformly loaded. The initial modulus obtained from this specimen is about 179 GN/m^2 (26.0 x 10^6 PSI) which is about 80% of the room temperature stiffness.
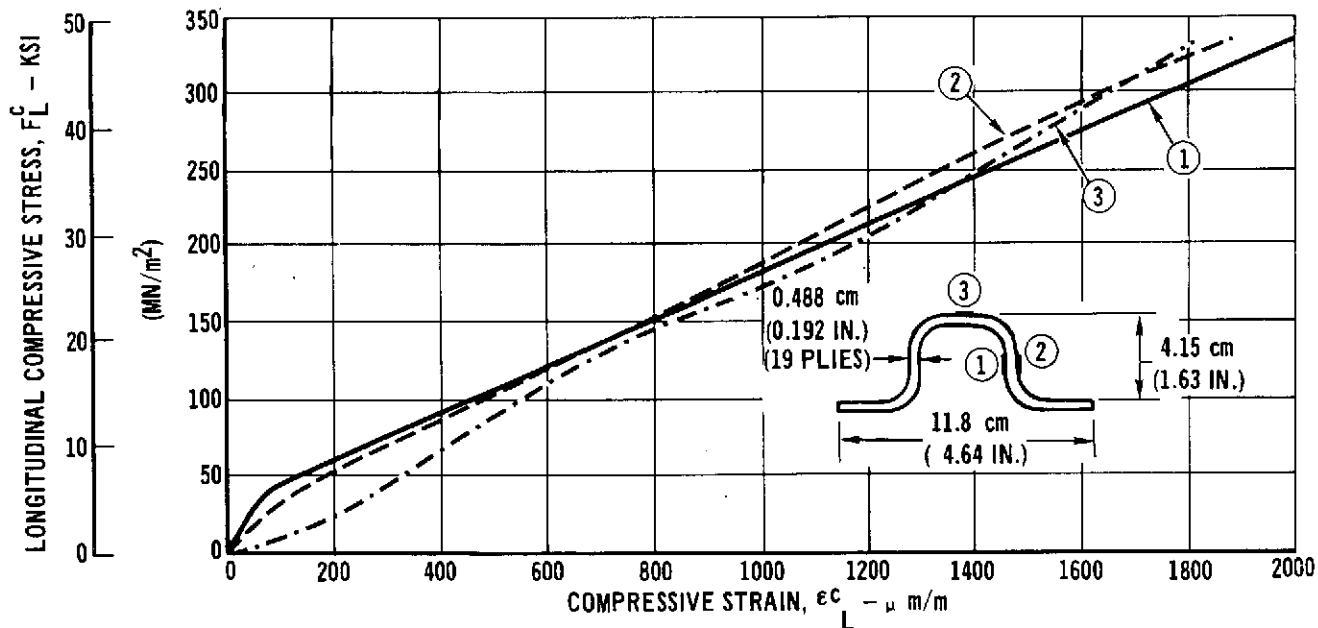
HAT STRINGER COMPRESSIVE STRESS-STRAIN RESPONSE AT 589°K (600°F)

Figure 2-50

2.1.2.7 Interlaminar Shear - The objective of this test was to determine
interlaminar shear strength of eutectic bonded, unidirectional boron-aluminum
laminates at room and elevated temperature. Five specimens were tested at room
temperature and five were tested at 589°K (600°F) after a 30 minute exposure to
temperature. Results from these tests are summarized in Figure 2-51.

TEST TEMPERATURE		INCIPIENT ⚠ SHEAR STRENGTH		SHEAR STRENGTH AT ULTIMATE LOAD		DEFLECTION AT ULTIMATE LOAD	
°K	°F	MN/m²	KSI	MN/m²	KSI	mm	in
R.T	R.T	32.7	4.75	69.6	10.1	1.64	.0645
589	600	13.1	1.90	21.4	3.1 ⚠	⚠	⚠

⚠ DETERMINED AT POINT WHERE LOAD – DEFLECTION CURVE BECOMES NON–LINEAR

⚠ SHEAR STRENGTH AT DEFLECTION OF 1.64 mm

⚠ TEST DISCONTINUED PRIOR TO SPECIMEN FAILURE

AVERAGE INTERLAMINAR SHEAR STRENGTH OF BORON ALUMINUM

Figure 2-51

Each specimen was 2.54 cm long, .762 cm wide and 24 plies thick. Three-
point loading was used to bend the specimens and cause interlaminar shear stresses.
A deflectometer recorded deflection as a function of applied load for each specimen.
Typical load-deflection curves obtained at room temperature and 589°K (600°F) are
shown in Figures 2-52 and 2-53 respectively. Incipient shear strength is deter-
mined at the load where the load-deflection curve becomes non-linear.

Specimens tested at room temperature experienced predominantly tensile
failures rather than shear failures as shown in Figure 2-54. The maximum load
carried by these specimen was used to calculate shear strength at specimen failure
reported in Figure 2-51. The average deflection at failure for room temperature
specimen was .164 cm (.0645 in.).

Specimens tested at 589°K (600°F) experienced large deflections without
failure as shown in Figure 2-54. Shear strength at specimen failure, therefore,
was recorded at the same deflection used for room temperature specimen (.164 cm).
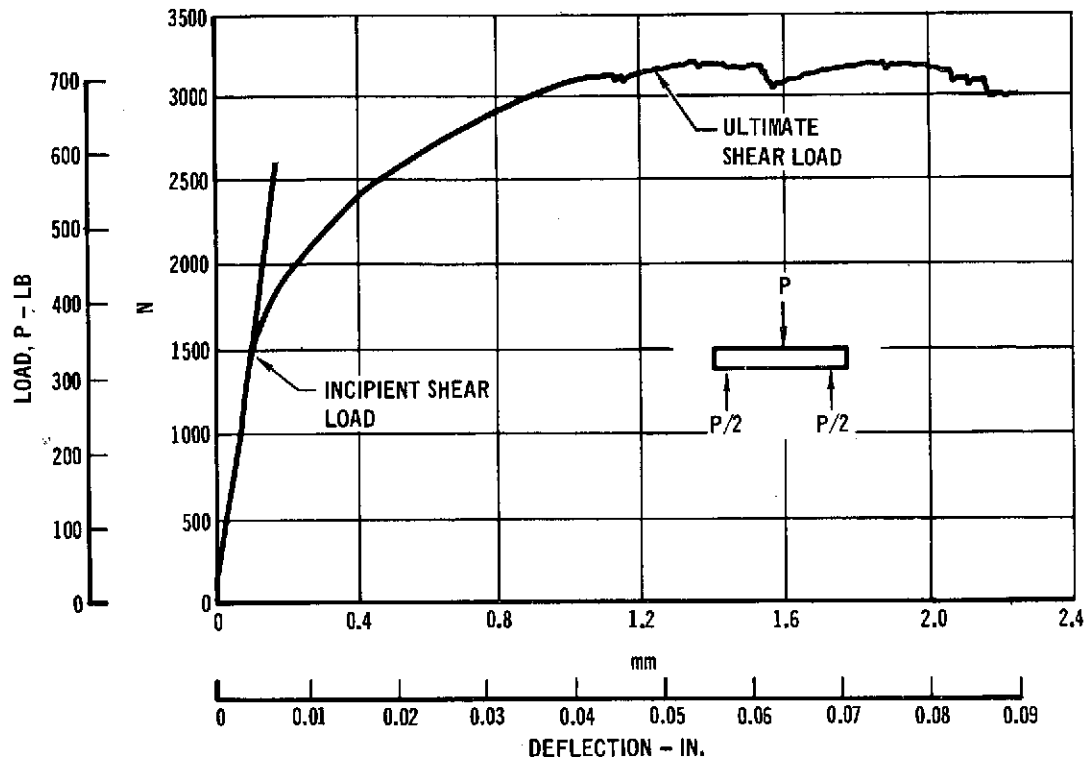
TYPICAL LOAD-DEFLECTION OF INTERLAMINAR SHEAR SPECIMEN
AT ROOM TEMPERATURE

Figure 2—52
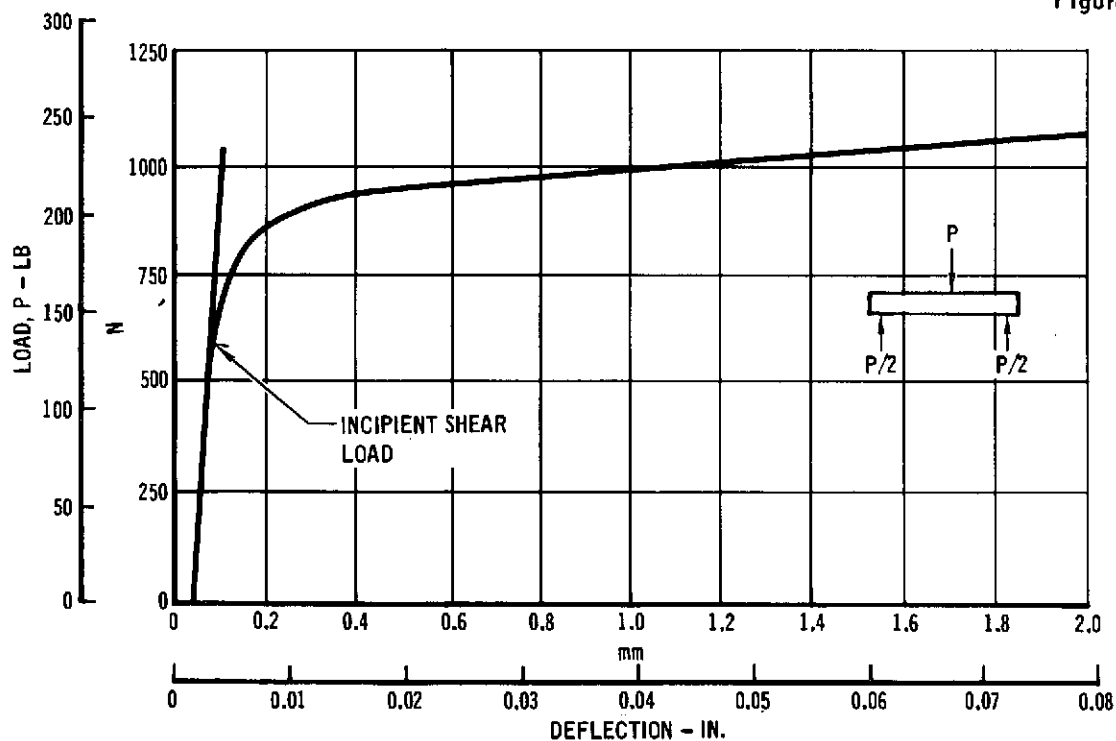
TYPICAL LOAD – DEFLECTION OF INTERLAMINAR SHEAR SPECIMEN AT 589°K

Figure 2—53

TENSILE
FAILURE
PREDOMINATE

3X

ROOM TEMPERATURE

NO VISIBLE
FRACTURE

3X
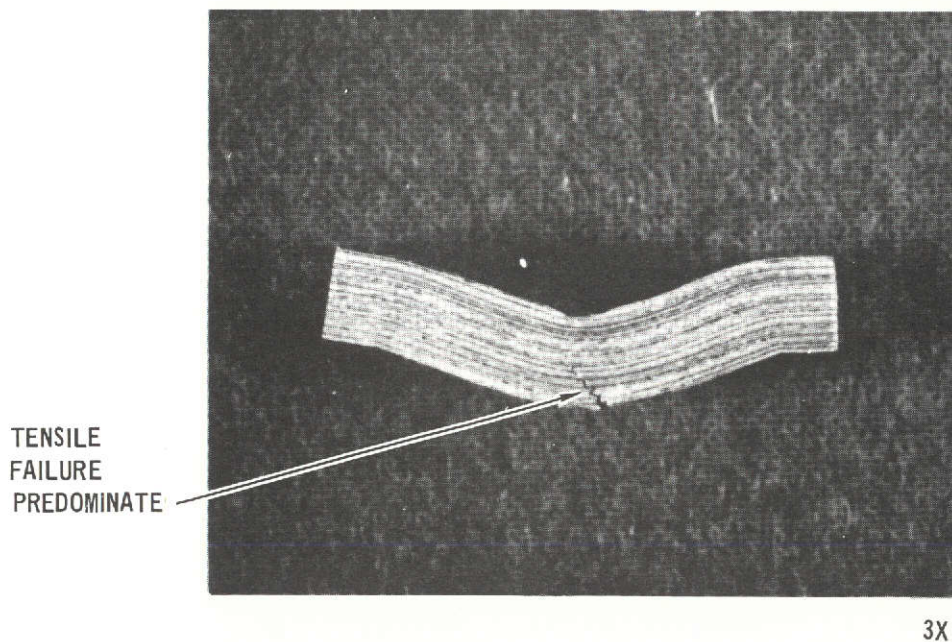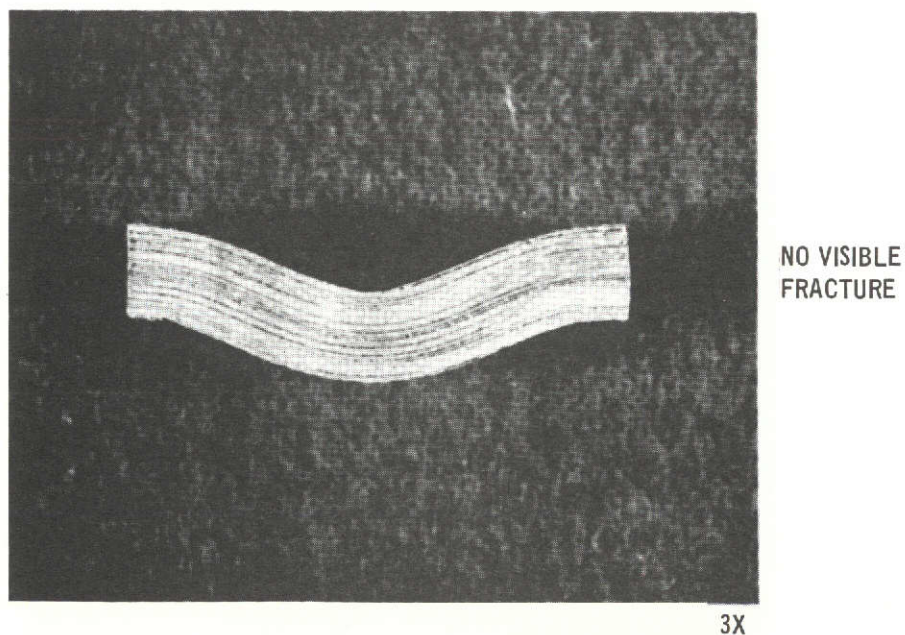
TEMPERATURE = 589°K (600°F)

TYPICAL BORON ALUMINUM INTERLAMINAR SHEAR SPECIMEN AFTER TEST

Figure 2-54

2-41

2.1.2.8 Compression and Tension of $\pm \frac{\pi}{4}$ rad Laminates – The objective of this

test was to determine ultimate strength and stress-strain response of $\pm \frac{\pi}{4}$ rad

laminates subjected to both compressive and tensile loads. Sandwich beam specimens

were used for compressive tests and both sandwich beam and tensile coupons were

used for tensile tests. Results are summarized in Figure 2-55. Strength and

stiffness values shown using sandwich beam specimens are the average of five tests

while values shown for tensile coupon are the average of three tests.

TYPE TEST	TEST MATCHED	TEST TEMPERATURE		ULTIMATE STRENGTH		ULTIMATE STRAIN	INITIAL MODULUS		FILAMENT VOLUME
		^0K	^0F	MN/m^2	KSI	$\mu m/m$	GN/m^2	10^6 PSI	%
COMPRESSION	BEAM	R.T.	R.T.	214.5	31.1	17,200	108.3	15.7	47.1
COMPRESSION	BEAM	589	600	60.0	8.7 △1	△2	85.5	12.4	37.0
TENSION	BEAM	R.T.	R.T.	237.5	34.5	17,700	92.4	13.4	46.8
TENSION	COUPON	R.T.	R.T.	180.5	26.2	27,000	91.0	13.2	–

△1 FAILURE OCCURRED IN B/AL LAMINATE TO CORE BONDLINE

△2 STRAIN GAGES FAILED PRIOR TO SPECIMEN FAILURES.

**AVERAGE TENSILE AND COMPRESSIVE PROPERTIES OF $\pm \pi/4$ rad
BORON ALUMINUM LAMINATES**

Figure 2-55

Sandwich beam specimens used for compressive tests, shown in Figure 2-56,

are 40.7 cm long, 2.54 cm wide, and 3.81 cm high. The compressive faceplate is

and eight ply, $\pm \frac{\pi}{4}$ rad laminate. Sandwich beam specimens used for tensile tests

were identical to those used for compressive tests with the exception that the

tensile faceplate was a four ply, $\pm \frac{\pi}{4}$ rad laminate. The four ply tensile coupon

was 2.54 cm wide and 20.3 cm long. They were made from the same laminate used to

make the tensile faceplate on sandwich beam specimens.

Typical compressive stress-strain curves at room temperature and 589°K

(600°F) are shown in Figures 2-57 and 2-58 respectively. Because these curves

are nonlinear over a majority of the range of interest, initial modulus values

shown in Figure 2-55 are applicable only for a very small portion of the curve.

Two sandwich beam specmines for obtaining tensile properties were cyclically

loaded and a typical stress-strain response is shown in Figure 2-59. The material

2-42

displayed limited hysteresis and the stress-strain curve was not affected by the cyclic load.

At $\pm \frac{\pi}{4}$ rad laminate loaded in either tension or compression experiences large deformations due to shear forces acting on the matrix material. As a result, Poisson's ratio is large and continually changes as shown in Figure 2-60. Evidence of this effect is visible in sandwich beam test specimens shown in Figure 2-61.
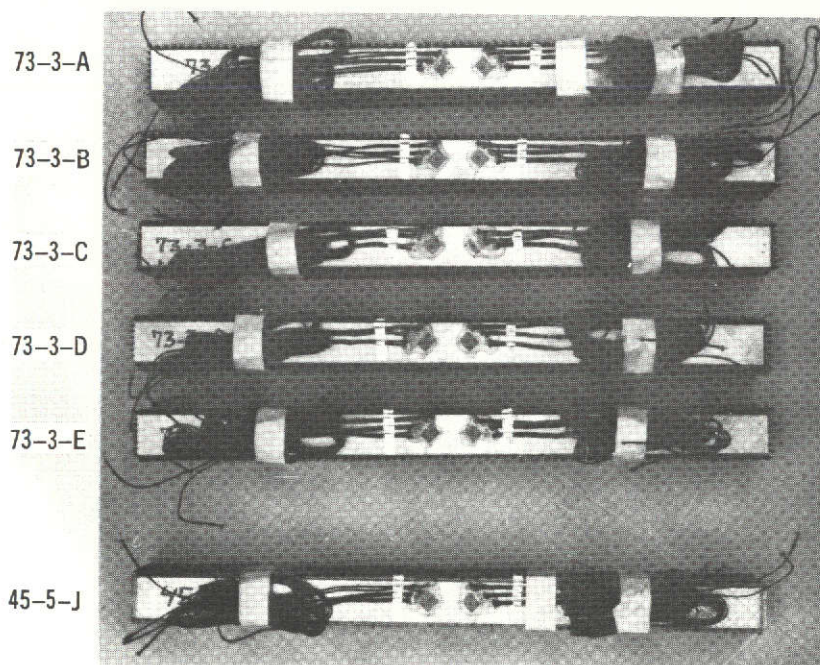
$\pm \pi/4$ rad LAMINATES

TEMPERATURE = 589^{0}K (600^{0}F)

TYPICAL BORON ALUMINUM SANDWICH BEAM SPECIMEN BEFORE TEST

Figure 2-56
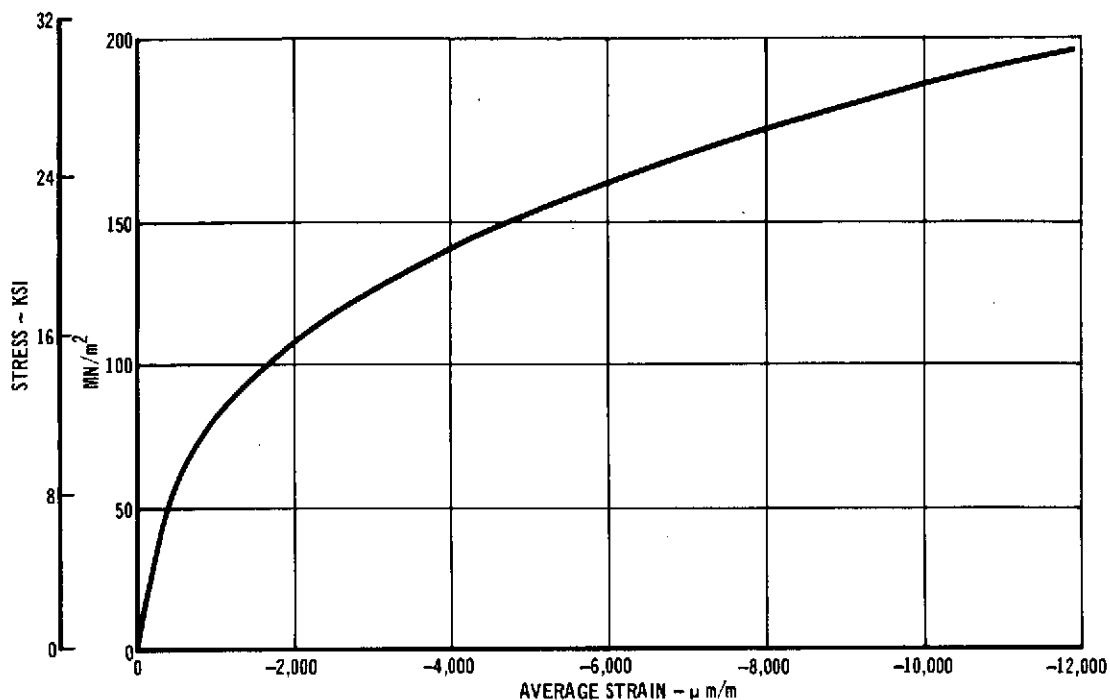
TYPICAL COMPRESSIVE STRESS–STRAIN RESPONSE OF ± π/4 rad LAMINATES AT ROOM TEMPERATURE

Figure 2– 57
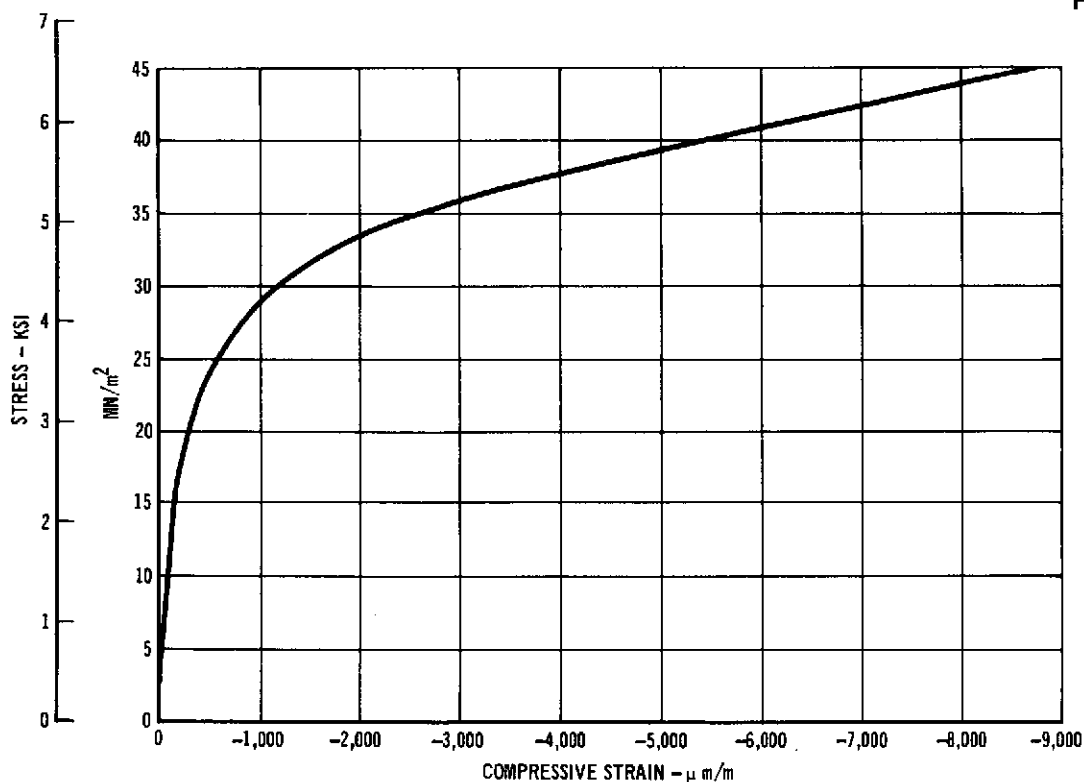
TYPICAL COMPRESSIVE STRESS–STRAIN RESPONSE OF ± π/4 rad LAMINATES AT 589°K (600°F)

Figure 2– 58
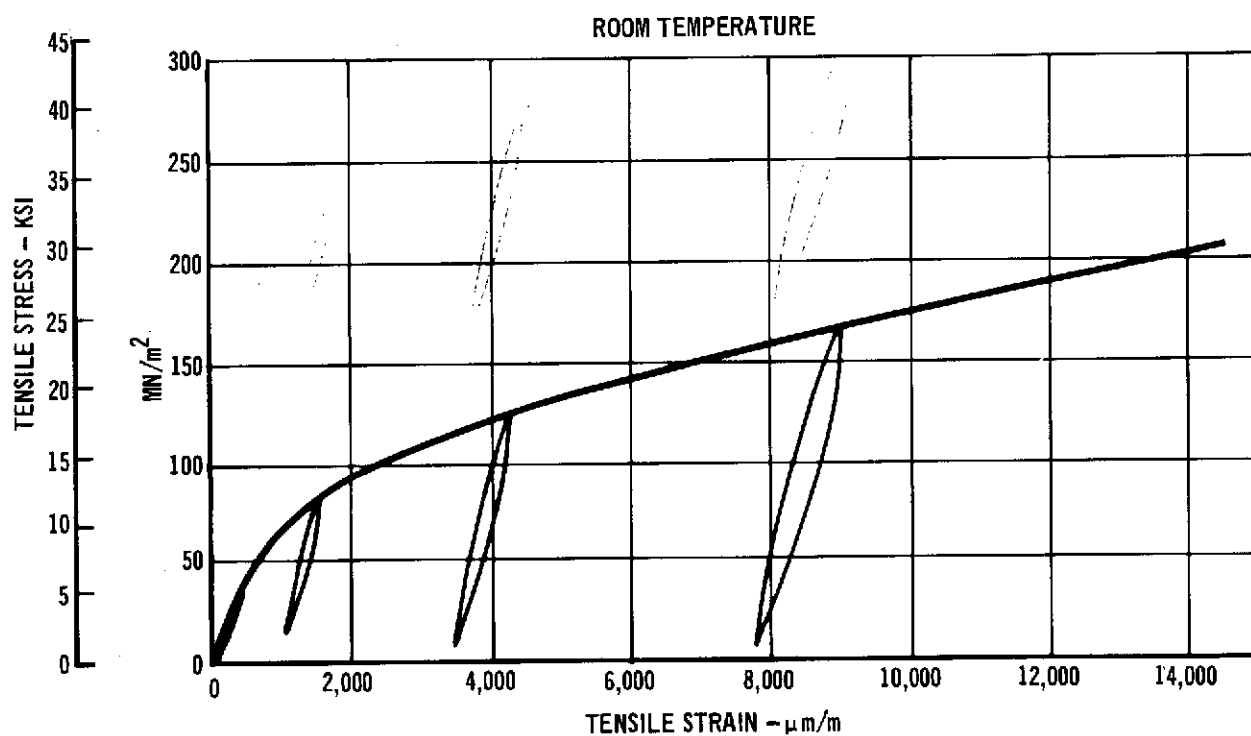
TYPICAL TENSILE STRESS–STRAIN RESPONSE OF ± π/4 rad LAMINATES
SUBJECTED TO CYCLIC LOADING

Figure 2–59

MCDONNELL DOUGLAS ASTRONAUTICS COMPANY - EAST
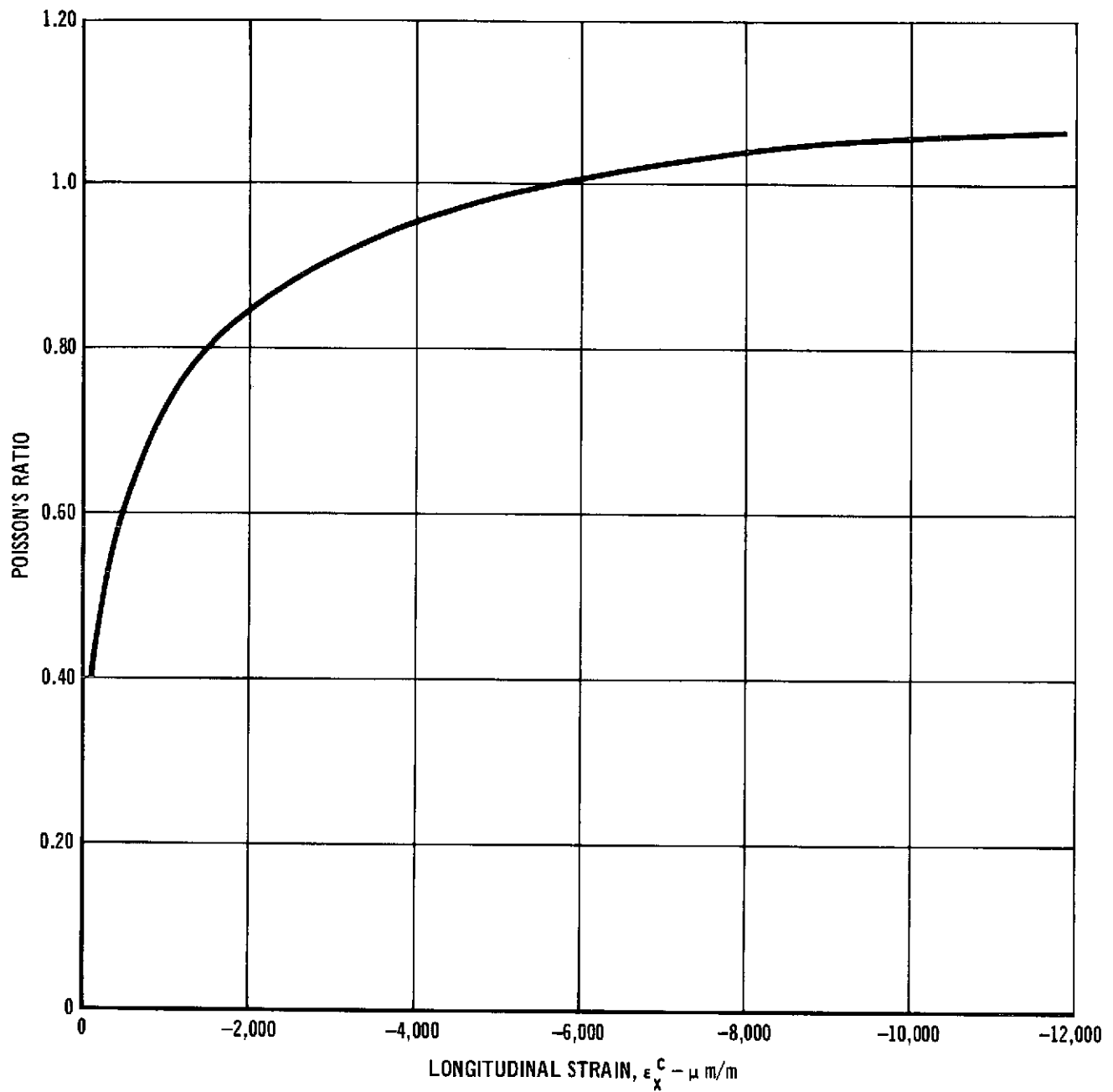
TYPICAL POISSON'S RATIO FOR $\pm\,\pi/4$ rad LAMINATES IN COMPRESSION
ROOM TEMPERATURE

Figure 2– 60
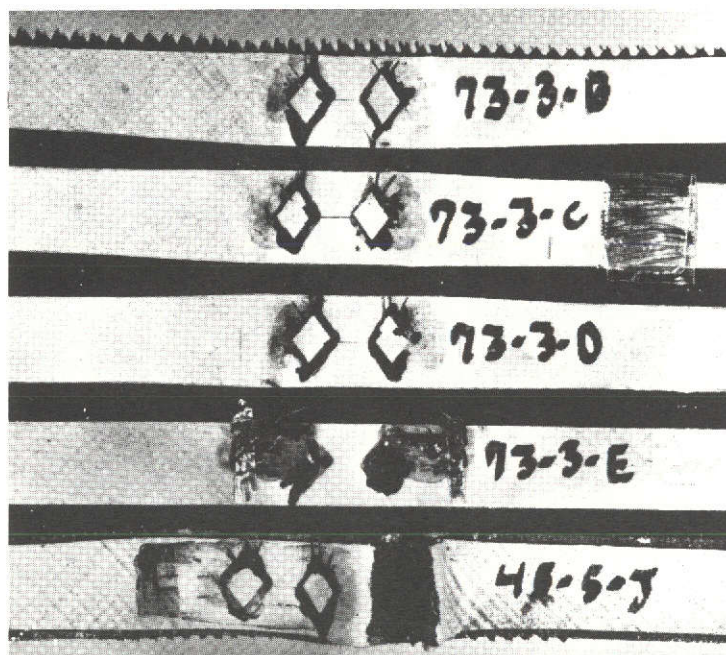
TEMPERATURE = 589°K (600°F)
COMPRESSIVE LOAD IN LAMINATE

EFFECTS OF HIGH POISSON'S RATIO FOR + π/4 rad LAMINATES SHOWN IN
SPECIMEN AFTER TEST

Figure 2– 61

2.2 Phase II Design Studies

In Phase II, components and assemblies representing full scale hardware were designed and analyzed. These included a 1.22 m x 1.83 m (48 inch x 72 inch) Compression Panel, a thrust structure beam of truss design, a thrust structure beam of shear web design, a Component Panel Test Assembly and a Stringer Test Assembly. Detail production drawings were prepared for fabrication of the Compression Panel, including supports for testing and a splice joint fitting design at the load reaction end representative of a typical production splice joint. In addition, two structural assemblies were selected for fabrication and testing; a stringer assembly identical to outboard stringer on compression panel and a component panel representative of the first bay of the full scale Compression Panel. Design details and test results of the Stringer Assembly and Component Panel are given in Section 2.5; design and analysis of the Compression Panel, thrust structure truss beam and shear web beam are presented in the following sections.

2.2.1 Compression Panel Design and Strength Analysis – The selected compression panel design, shown in Figure 2-62 resulted from conceptual studies of several candidate designs as discussed in Appendix A. The selected panel configuration consists of seven unidirectional tapered stringers and a $\pm \frac{\pi}{4}$ rad ($\pm 45°$) tapered skin supported laterally by four steel frames. The panel was designed to carry a concentrated ultimate compression load of 1555 kN (350,000 lbs) applied at one end reacted by a distributed load at the opposite end while at a temperature of 589°K (600°F). Peaking at the distributed load end must not exceed a uniformly distributed load by more than 30% as illustrated in Figure 2-63.

The structural adequacy of the boron-aluminum panel structure to sustain the design ultimate conditions was analytically verified during Phase II; in addition, the predicted external load distribution which is well within the 30% peaking requirement was verified by the component panel test (Section 2.5.2). Minimum calculated margins of safety for primary stringer and skin components are given below.

ITEM	DESIGN CONDITION	DESIGN TEMP.	CRITICAL LOCATION	FAILURE MODE	M.S.
Boron-Alumimum Hat Stringer (0°, 11 Ply)	Ultimate Load	589°K	X=61.0 cm Y=54.8 cm	Bending and Axial Load	.02
Boron-Aluminum Skin (±45°, 48 Ply)	Ultimate Load	589°K	X=9.6 cm Y=9.9 cm	In-Plane Shear Strength	.26

PRECEDING PAGE BLANK NOT FILMED

COMPRESSION PANEL ASSY
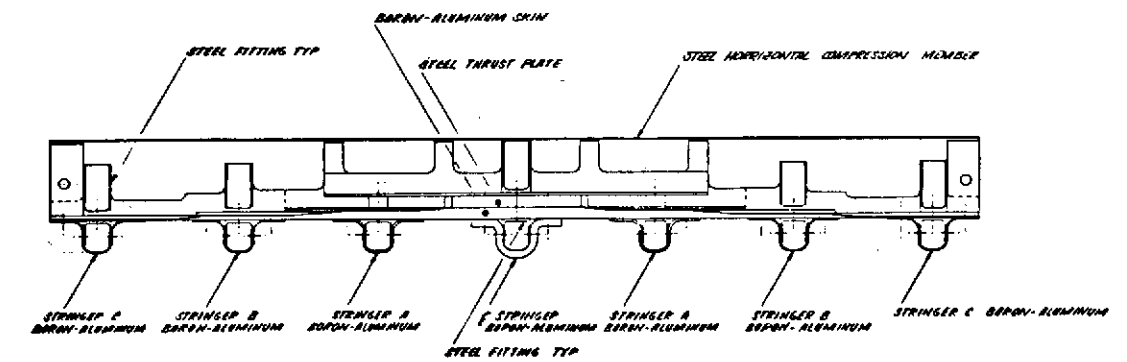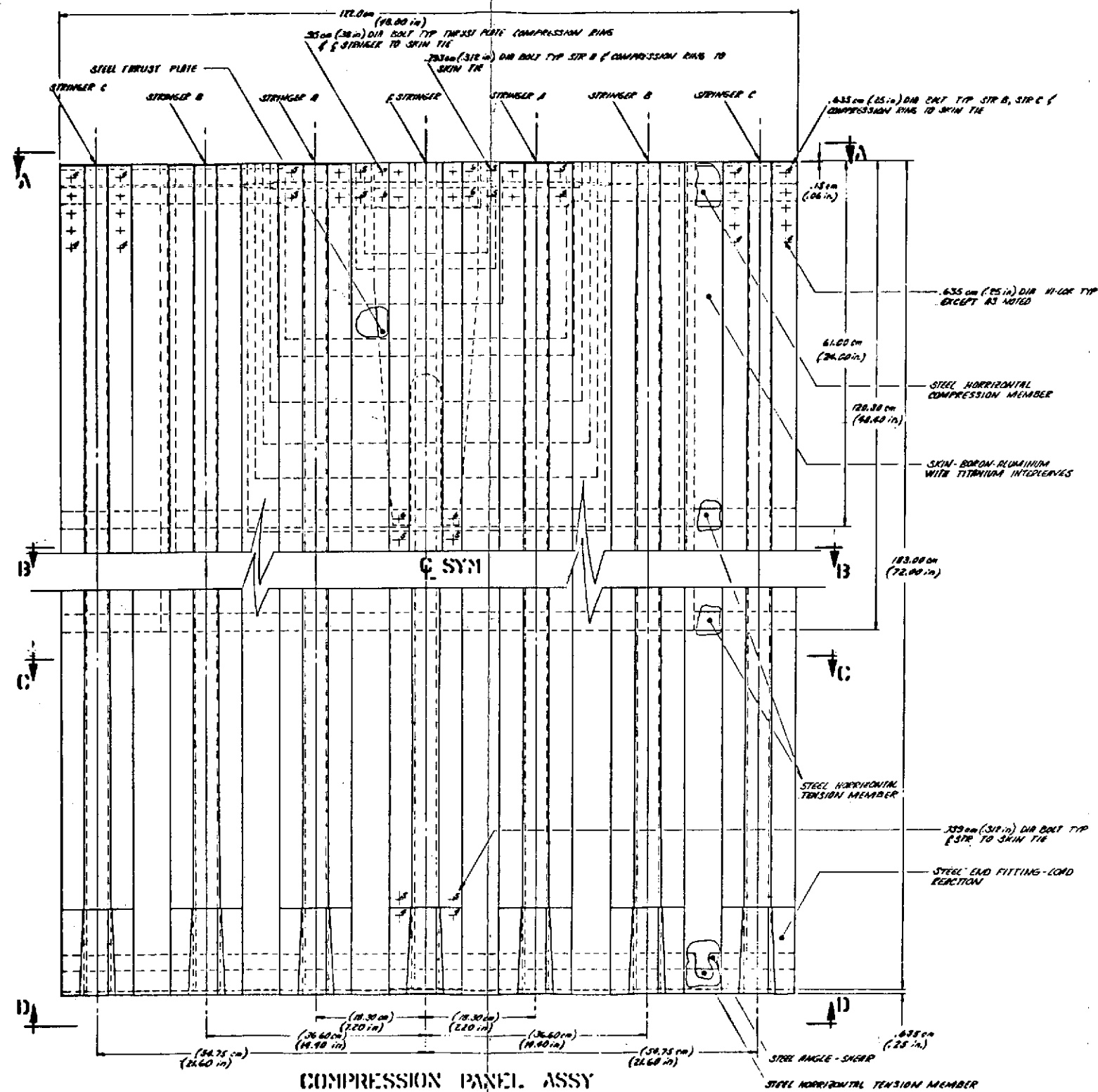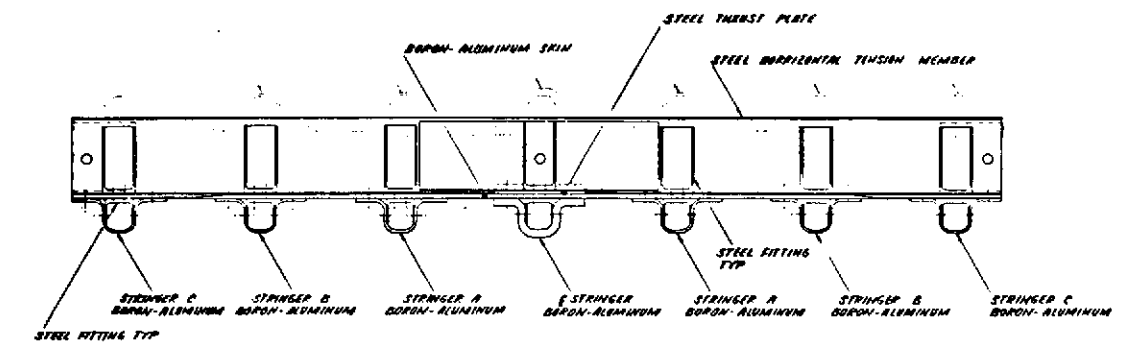
SECTION VIEW A-A
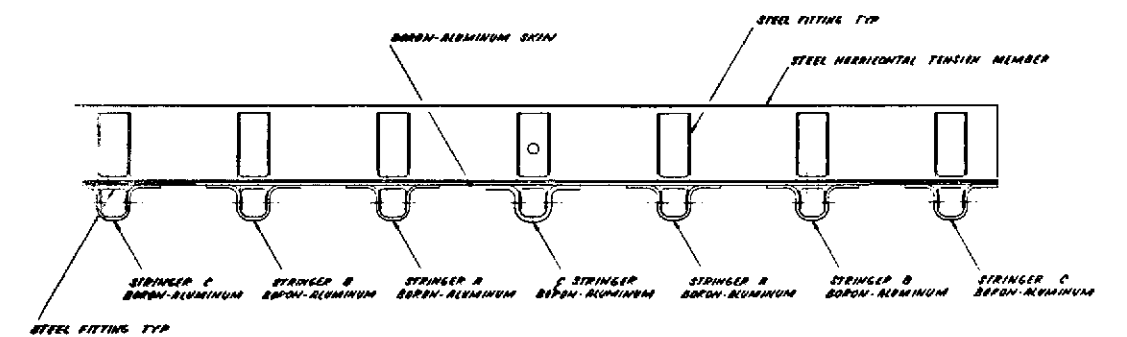
SECTION B-B

SECTION C-C

SECTION VIEW D-D

FOLDOUT FRAME

P = 1555 kN (350,000 LBS)

b = 0.61m (24 IN.)

w_x; WHERE: $2\int_0^b w_x dy = 1555$ kN (350,000 LBS)

AND $w_{x_{MAX}} \leq 1.3 \left(\dfrac{P}{2b}\right)$
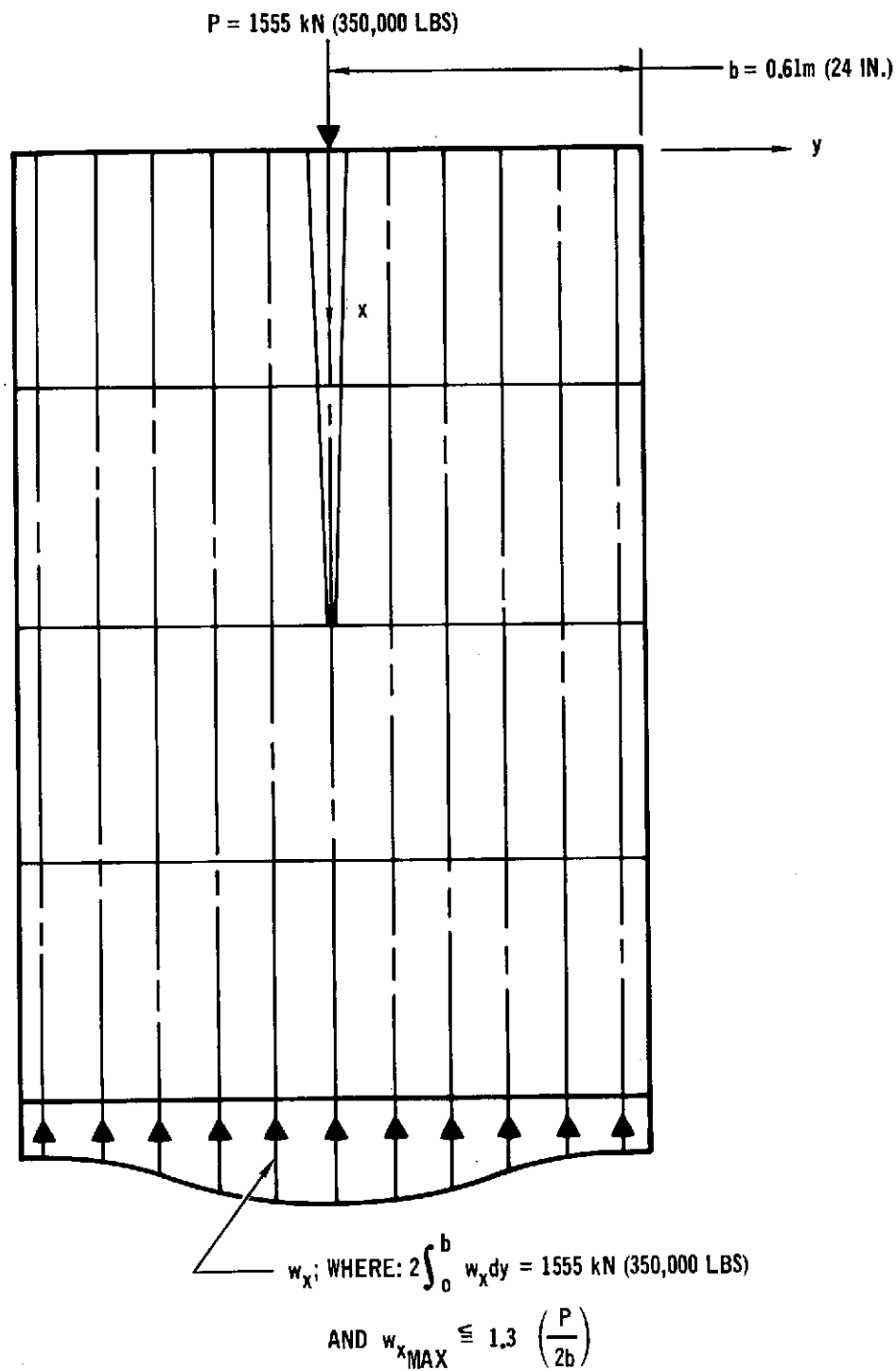
COMPRESSION PANEL EXTERNAL LOADS

Figure 2– 63

Further design details, internal loads distribution, methods of analysis, selected strength analysis and compression panel weights are presented in the following sections.

2.2.1.1 Compression Panel Structural Description – The selected configuration (Figure 2-62) consists of seven unidirectional tapered thickness stringers, a $\pm \frac{\pi}{4}$ rad (+45°) tapered skin, a steel thrust plate, and four steel frames to provide lateral support. Titanium interleaves are incorporated in both the skin and stringers to increase bearing allowables and improve transverse tension and shear properties.

The unidirectional stringers are designed primarily to carry uniaxial compressive loads. Stringer thickness and titanium interleaf requirements are tailored to meet the predicted axial loads and shear loads given in Section 2.2.1.2.4. Unidirectional boron-aluminum monolayer and titanium interleaf stacking sequence for the stringers is shown in Figure 2-64.

The $\pm \frac{\pi}{4}$ rad (+45°) skin is designed primarily for shear resulting from the distribution of the concentrated compressive load applied to center line stringer to seven approximately equal stringer reaction loads over a 3 bay length. The $\pm \frac{\pi}{4}$ rad (+45°) laminate orientation was chosen to achieve maximum skin shear strength. Skin thickness tapering is based on internal predicted shear flows (see Section 2.2.1.3.4) and allowable laminate shear strength. All changes in skin thickness are accomplished in 4 ply increments to maintain laminate symmetry. Skin design is resistant to shear buckling at ultimate loads in all areas. Ply layup for $\pm \frac{\pi}{4}$ rad (+45°) skin with titanium interleaves is shown in Figure 2-65.

For design purposes, the central concentrated load was assumed to be applied over an area 11.42 cm (4.5 in.) x 19.7 cm (7.75 in.) in which all load is transferred in bearing to the center line stringer, thrust plate and local skin area. Figure 2-66 illustrates the load introduction end of the compression panel. This load introduction design was verified by the component panel test article (Section 2.5.2) which was loaded to 115% of design ultimate load at 589°K (600°F) without failure.

Steel fittings at the load reaction end of panel simulate an actual design of a production splice joint with capability for transition from composite to conventional materials. The joint and panel end design are shown in Figure 2-67. Stringers contain additional titanium interleaves to provide bearing strength for load transfer by mechanical fasteners. These fittings extend beyond the panel skin and stringer to positively react the compression load at the fittings. Each
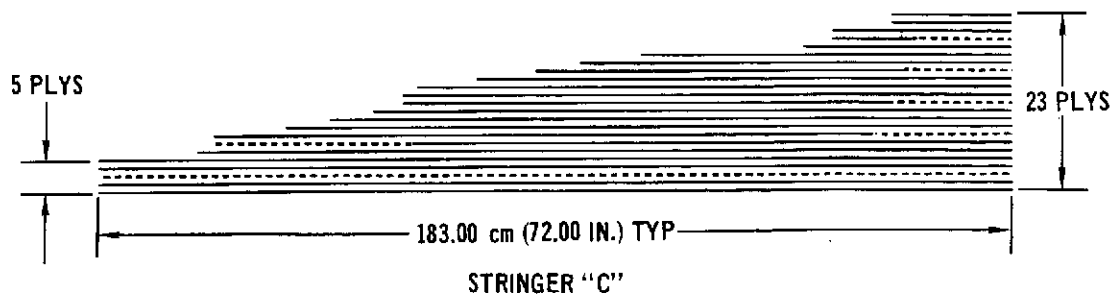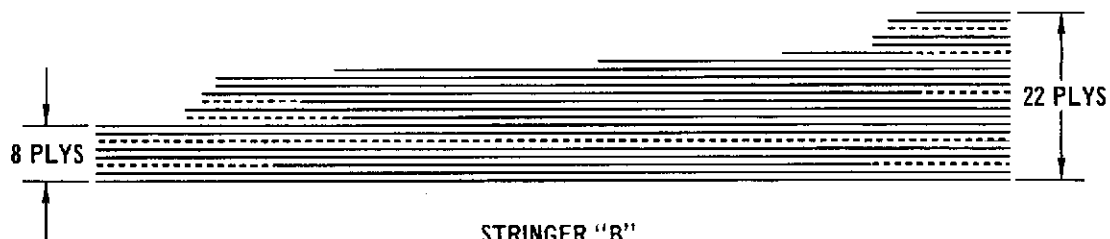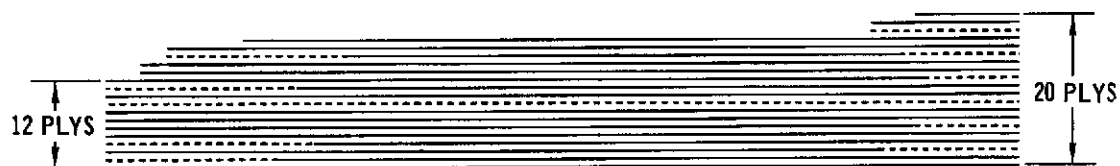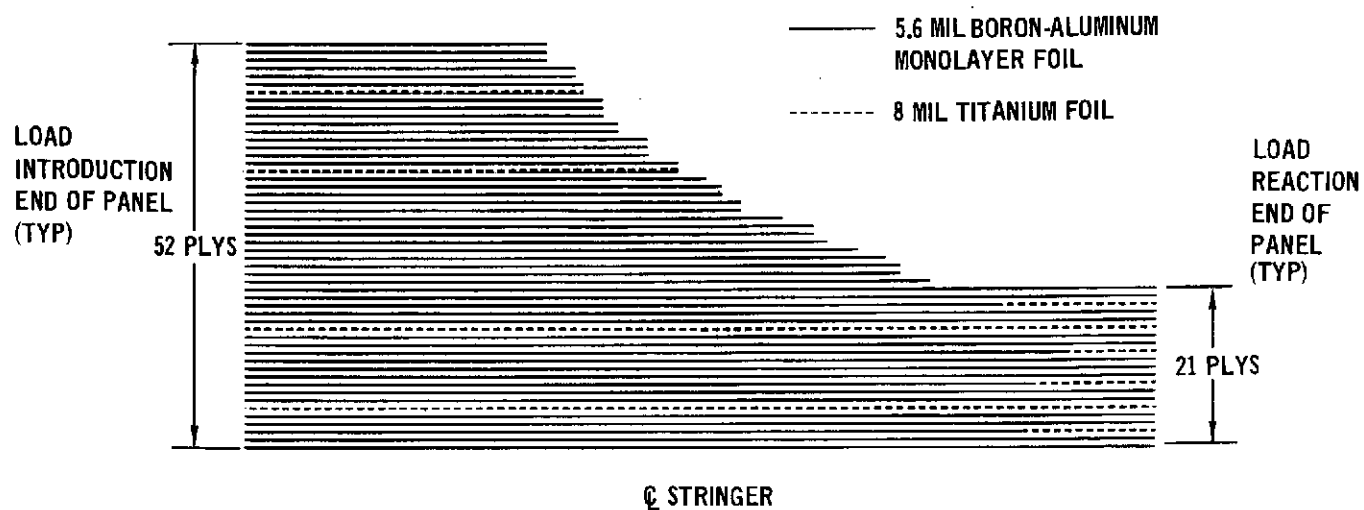
STRINGER PLY STACKING SEQUENCE

Figure 2- 64

± π/4 rad B/AL PLIES	TITANIUM PLIES	TOTAL NO. PLIES
58	4	62
54	4	58
50	4	54
46	4	50
42	4	46
40	3	43
36	3	39
32	3	35
28	3	31
24	3	27
20	2	22
16	2	18
12	2	14
8	2	10
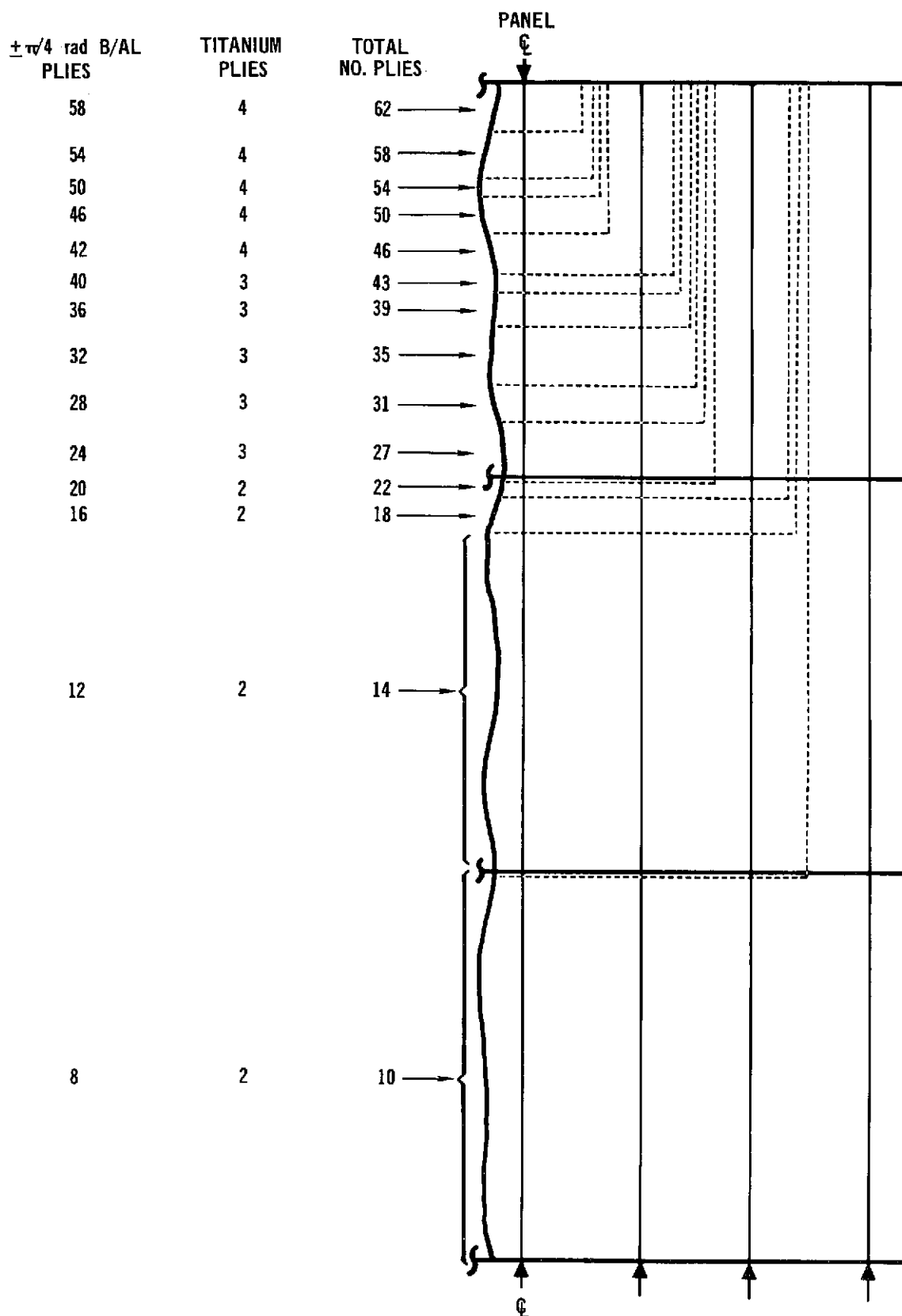
SKIN THICKNESS IS MAXIMUM AT CONCENTRATED LOAD END OF PANEL

Figure 2-65
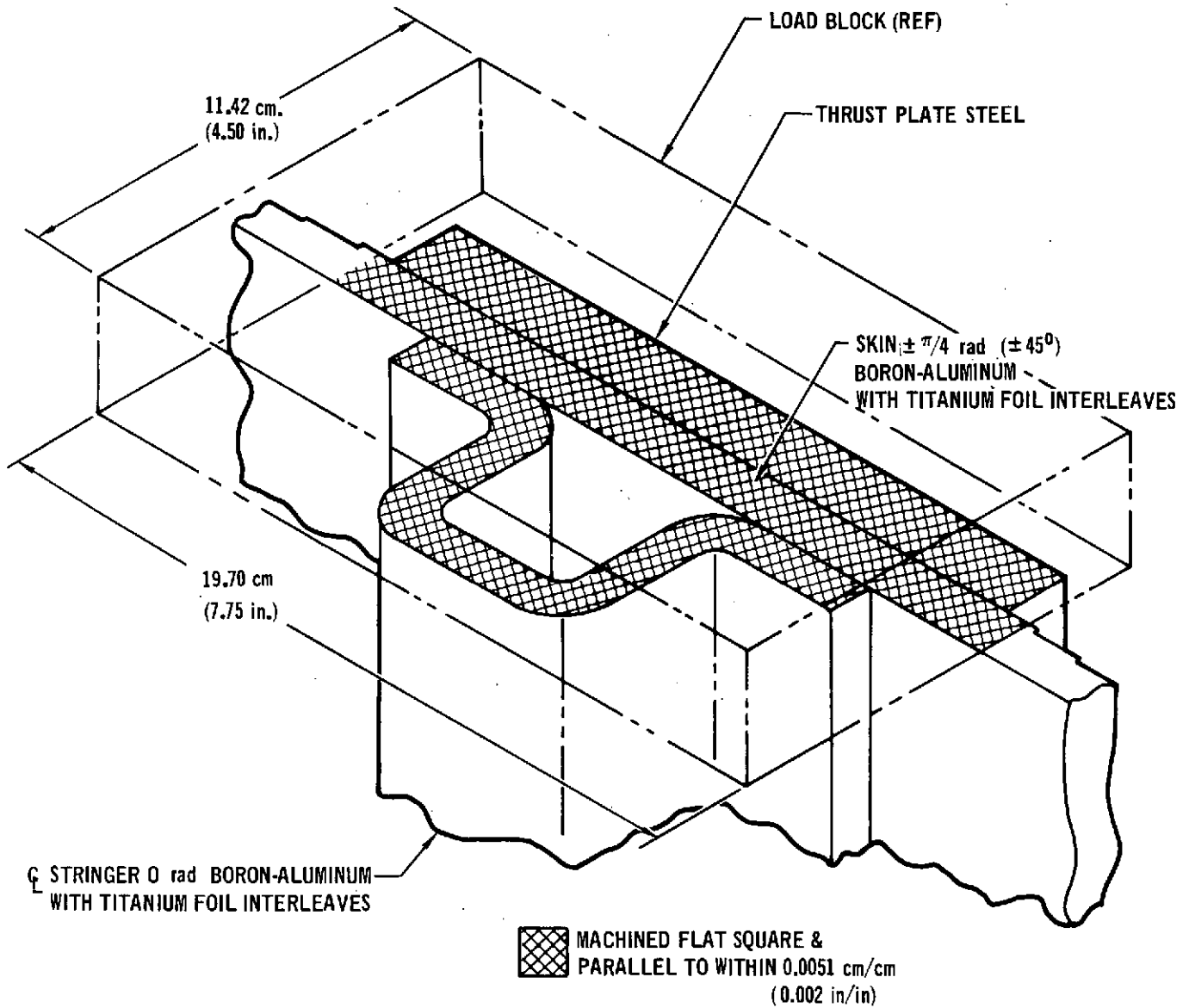
LOAD INTRODUCTION END OF BORON – ALUMINUM COMPRESSION PANEL
(Frame Omitted for Clarity)

Figure 2–66

STRINGER 0 rad BORON-ALUMINUM
WITH TITANIUM FOIL INTERLEAVES

BEARING SURFACE(TYP)
MACHINED FLAT SQUARE &
PARALLEL TO WITHIN
0.0051 cm/cm

CLOSEOUT FITTING
STEEL(TYP)

FRAME
STEEL

SKIN $\pm\pi/4$ rad
BORON-ALUMINUM
WITH TITANIUM FOIL
INTERLEAVES

$\mathbb{C}$ SYM
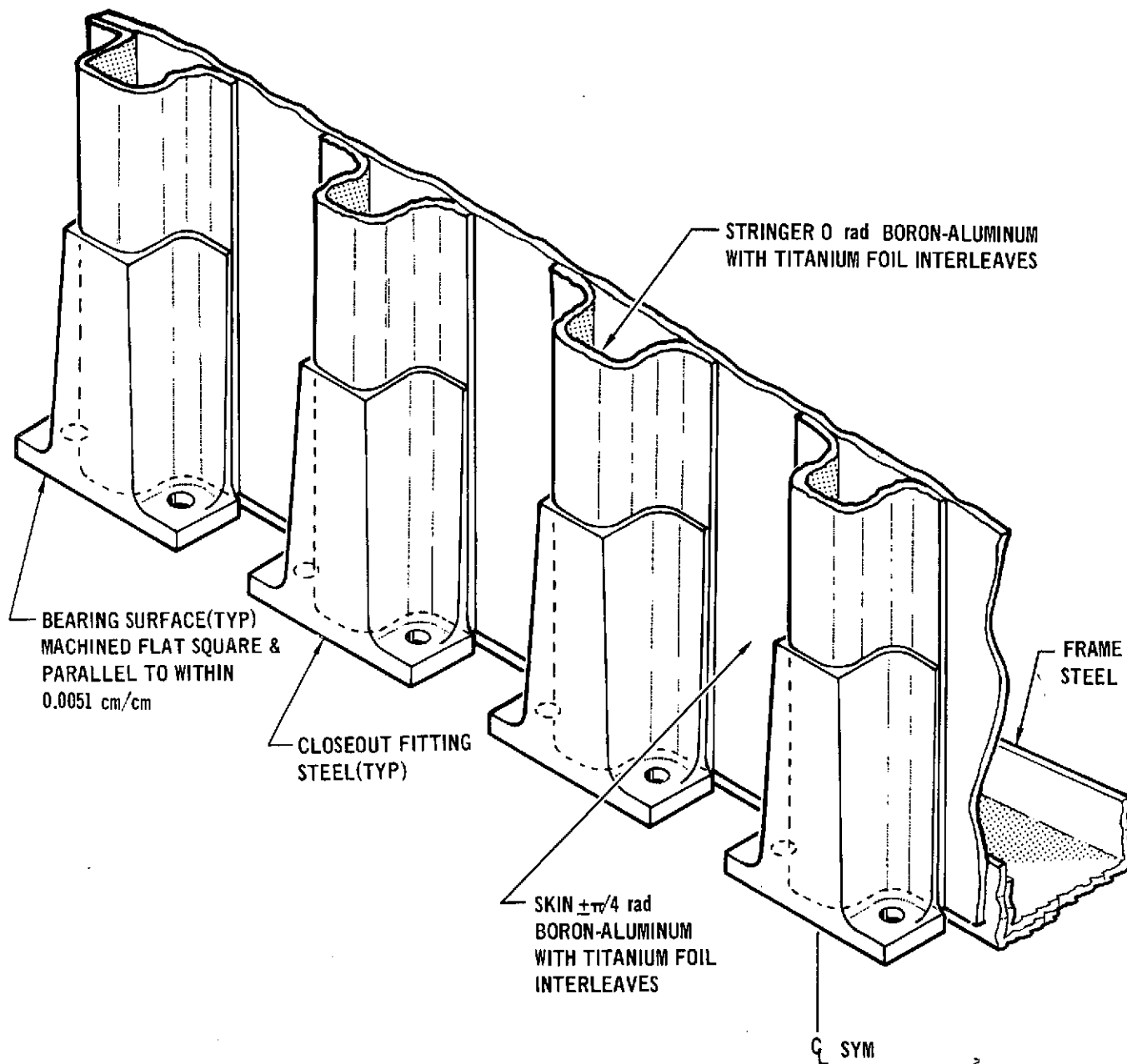
LOAD REACTION END OF BORON-ALUMINUM COMPRESSION PANEL

Figure 2–67

fitting was designed with two lugs providing tension capability across the joint equal to 50% of compression capability. Since the compression panel will not be tested in tension, lugs were not machined on fittings to reduce costs.

2.2.1.2 <u>Methods and Approaches Used for Compression Panel Analysis and Joint Strengths</u> – This section discusses the methods of analysis incorporated in computer programs which were employed in the analysis and evaluation of various thrust structure concepts, the Stringer Test Assembly, the Component Panel Assembly and the Compression Panel. In addition, the analytical procedure developed for predicting mechanical joint strength of boron-aluminum containing titanium interleaves is discussed.

2.2.1.2.1 <u>Applicable Computer Programs</u> – Due to the internal and external redundancy of the compression panel, the use of tapered stringers and skin, and the analytical complexity of laminated composites, four computer programs were used extensively:

> Computer Aided Structural Design (CASD)
> Laminate Strength and Stiffness Properties
> Ultimate Strength of Laminated Composites
> Orthotropic Plate Buckling

<u>Computer Aided Structural Design (CASD) Program</u> – CASD was used to determine internal loads distribution in each of the structures investigated and to size stringers and skin used in component and compression panel. The step by step sizing process is discussed in Section 2.2.1.3.1. This linear finite element program provides the capability to rapidly size and analyze complex structures subjected to multiple design constraints. The member sizing process can consider multiple conditions of ultimate strength and stiffness requirements. Member gages are computed which satisfy these conditions. However, the program can be used to determine loads based on given section properties and to check if allowable stresses are exceeded. Structure is modeled with single or two element bar members and shear panels interconnected at nodal points. Support conditions can be either fully fixed, pinned, or combinations thereof. Applied loading can be in the form of concentrated forces and moments or distributed pressures and temperatures.

A powerful design analysis feature is the ability to define many individual structural modules which can then be assembled into a single structure. Changes can be made to a module without affecting the entire structural model.

Laminate Strength and Stiffness Properties Program - This program was used in trade studies to evaluate candidate compression panel skin configurations for maximum strength and to obtain laminate stiffness properties for use in buckling analyses. Using elastic moduli for unidirectional lamina defined in terms of the principal lamina axes, stiffness properties of the midplane symmetric laminate are developed using lamination theory as illustrated below:

$$[A_{ij}] = \sum_{k=1}^{n} (\overline{Q}_{ij})_k (h_k - h_{k-1})$$

$$[D_{ij}] = \frac{1}{3} \sum_{k=1}^{n} (\overline{Q}_{ij})_k (h_k^3 - h_{k-1}^3)$$

where $[A_{ij}]$ = laminate in-plane stiffness matrix

$[D_{ij}]$ = laminate flexural stiffness matrix

n = total number of plies in laminate

k = lamina number

h = distance from reference surface to ply surface

$[\overline{Q}_{ij}]$ = stiffness of the individual lamina referenced to the laminate axes system

Using the above laminate in-plane stiffness matrix and a particular applied state of stress, the program calculates the corresponding laminate strains. These strain values are then transformed into individual lamina strains and compared to allowable lamina strains based on ultimate strain failure criteria.

The laminate flexural stiffness matrix is used in determining compression and shear buckling strength of flat composite plates.

Ultimate Strength of Laminated Composites Program - The ultimate strength program was used to determine the nonlinear strength and stiffness response of the $\pm \frac{\pi}{4}$ rad ($\pm 45°$) compression panel skin under various combinations of biaxial loading and shear. Complex states of stress in skin vary from biaxial compression and shear at the load introduction region to biaxial tension, compression and shear at the load reaction end. Strength and stiffness data obtained from this program were used in the finite element analysis of compression panel employing CASD.

The program uses basic lamina and laminate constitutive relations as well as lamina stress-strain curves to determine stress-strain response of the laminate under biaxial in-plane loading. Nonlinear lamina material behavior is included by incrementally applying average laminate stresses and utilizing a simple Euler-type

· 2-58

integration procedure.

Initially, a stress state is applied to the laminate, and using the intial
laminate compliance matrix, $[A_{ij}]^{-1}$. The first increment of laminate strains is
calculated assuming the laminate behaves linearly over the applied stress incre-
ment. This statement expressed mathematically in matrix form becomes:

$$[\Delta\epsilon]_{n+1} = [A_{ij}]^{-1}_n [\Delta\sigma]_{n+1} \text{ ---------------------------(a)}$$

The increment of laminate strains, $\Delta\epsilon$, is then added to any previous strains
to determine the current total laminate strain:

$$[\epsilon]_{n+1} = [\epsilon]_n + [\Delta\epsilon]_{n+1}$$

For the first increment $[\epsilon]_1 = 0$.

Using basic strain transformation equations, lamina strains in the principal
lamina axis system are then calculated and corresponding lamina stiffnesses
$[Q_{ij}]_n$ are obtained using the tangent moduli obtained from the empirical stress-
strain data at the nth value of lamina strain.

The laminate stiffness matrix $[A_{ij}]$ for the $(n+1)^{th}$ stress increment is then
calculated using the nth values of the $\overline{Q}$'s. The laminate compliance matrix
$[A_{ij}]^{-1}$ is utilized in Equation (a) to determine the laminate strains which result
from the next load increment of $\Delta\sigma_x$, $\Delta\sigma_y$, and/or $\Delta\tau_{xy}$. In this manner, the total
laminate stress-strain curve to ultimate strain is determined by the successive
solution of a number of linear problems. Failure was assumed to occur when any of
the ultimate lamina strain allowables are exceeded.

Orthotropic Plate Buckling Program - This computer program provides an ac-
curate, fast and useful method for determining the elastic buckling strength of
orthotropic rectangular laminated composite plates. It computes the critical
elastic buckling strength of orthotropic rectangular plates subjected to combined
in-plane axial and shear loads. Edge conditions can be fully fixed, simply
supported, or combinations thereof. The method of analysis is applicable to
orthotropic flat plates with uniform thickness and arbitrary ply orientations.
It was used to determine the buckling strength of compression panel skin under
biaxial compression and shear as shown in Figure 2-68. The margin of safety in
buckling for this loading condition is,

$$M. S. = \frac{\overline{F_x}_{cr}}{F_x} - 1$$

and,

$$\overline{Fx}_{cr} = \frac{Fx_{cr}}{2}\left(\frac{Fxy_{cr}}{Fx_{cr}} \times \frac{Fx}{Fxy}\right)^2 \left[-1 + \sqrt{1 + 4\left[\left(\frac{Fx_{cr}}{Fxy_{cr}}\right)\left(\frac{Fxy}{Fx}\right)\right]^2}\right] \text{(Ref. 5)}$$

where:

Fx = applied compressive stress in x direction

Fy = applied compressive stress in y direction

Fxy = applied shear stress

Fx_{cr} = allowable biaxial compressive buckling stress

Fxy_{cr} = allowable shear buckling stress

$\overline{Fx}_{cr}$ = allowable compressive buckling stress under the combined applied stresses

Allowable shear buckling stress for a simply supported plate with large aspect ratio is defined by,

$$Fxy_{cr} = \frac{1}{t}\left(\frac{2}{b}\right)^2 \sqrt{D_{22}\ (D_{12} + 2D_{66})}\ \left[11.7 + .532\theta + .938\theta\right]$$

where:

t = plate thickness

a = plate length

b = plate width

D_{ij} = plate flexural stiffnesses

$$\theta = \frac{\sqrt{D_{11}D_{22}}}{D_{12} + 2D_{66}} < 1$$

Allowable biaxial compressive buckling stress for a simply supported plate with large aspect ratio is defined by,

$$Fx_{cr} = \frac{\pi^2}{tb^2}\left[\frac{D_{11}m^4\ (\frac{b}{a}) + 2\ (D_{12} + 2D_{66})\ m^2n^2\ (\frac{b}{a})^2 + D_{22}n^4}{m^2\ (\frac{b}{a})^2 + (\frac{Fy}{Fx})\ n^2}\right]_{\text{min.}} \text{(Ref. 5)}$$

where:

m = number of half sine waves in x direction

n = number of half sine waves in y direction

Buckling equation to be minimized with respect to

$$m, n, = 1, 2, \text{----------}$$

2.2.1.2.2 Joint Allowables for Stringers with Titanium Interleaves - The
unidirectional, hat-section stringer is attached to the skin at the free flanges
by a single row of mechanical fasteners in each flange. Shear load from the skin
is introduced to the stringer by bearing at the fasteners and then distributed to

2-60
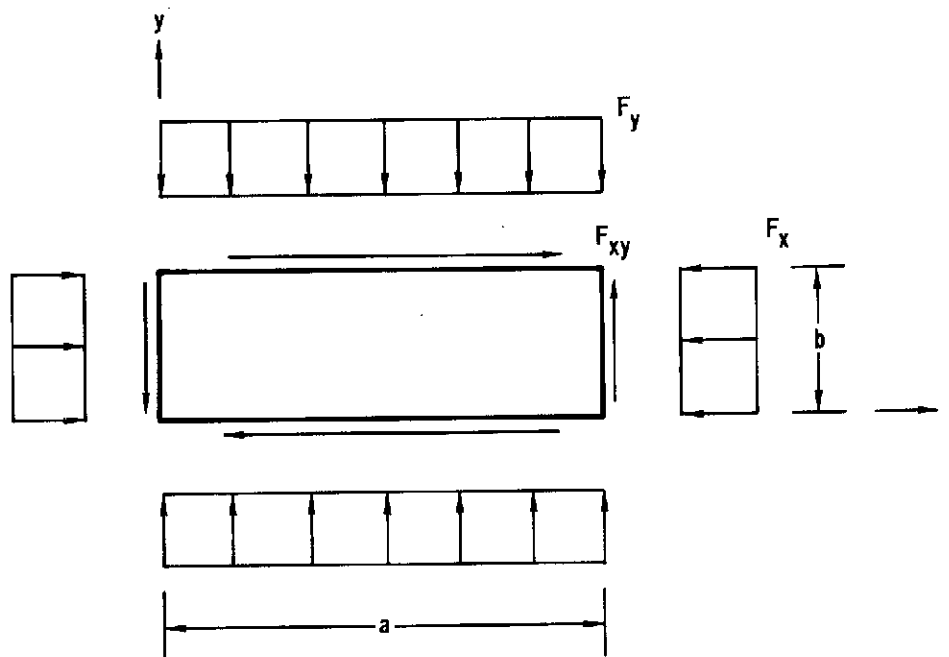
STATE OF STRESS IN SKIN FOR BUCKLING ANALYSIS

Figure 2-68

the stringer cross section through shear as shown in Figure 2-69 . To provide adequate shear and bearing strength, titanium interleaves were added to the unidirectional boron-aluminum plies.

The method of analysis developed for the boron-aluminum with titanium inter-leaves is a combination of two methods presented in the literature for resin matrix composites with metallic plies. The method of analysis presented in Reference 5 assumes that the full bearing strength of the metallic ply may be combined with the full joint allowable of the composite material. However, a second method of analysis discussed in References 6 and 7 reduces the bearing allowable of the metallic ply to account for buckling of these plies at the fastener.

The method developed for boron-aluminum with titanium interleaves employs a compromise between the two methods for resin matrix composites. Accordingly, a bearing allowable of 862 MN/m^2 (125,000 psi) at 589°K was chosen for the titanium plies. This value is midway between the full titanium bearing strength of 1310 MN/m^2 (190,000 psi) and a ply buckling strength of 414 MN/m^2 (60,000 psi) predicted on the basis that the boron-aluminum plies provide an elastic foundation to the titanium ply.
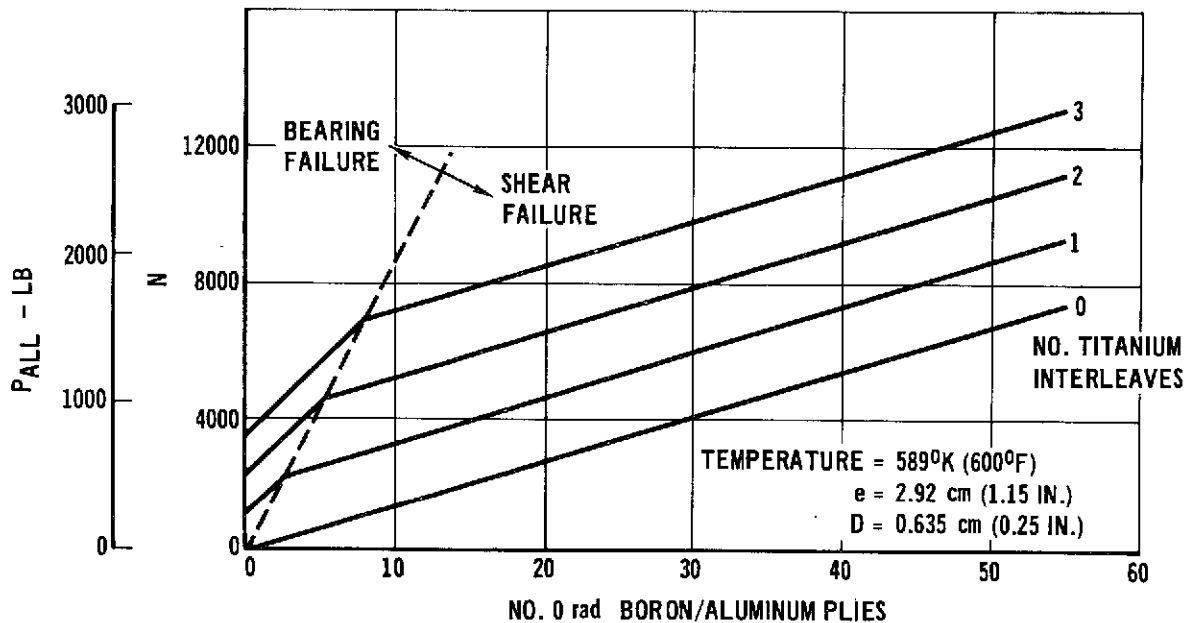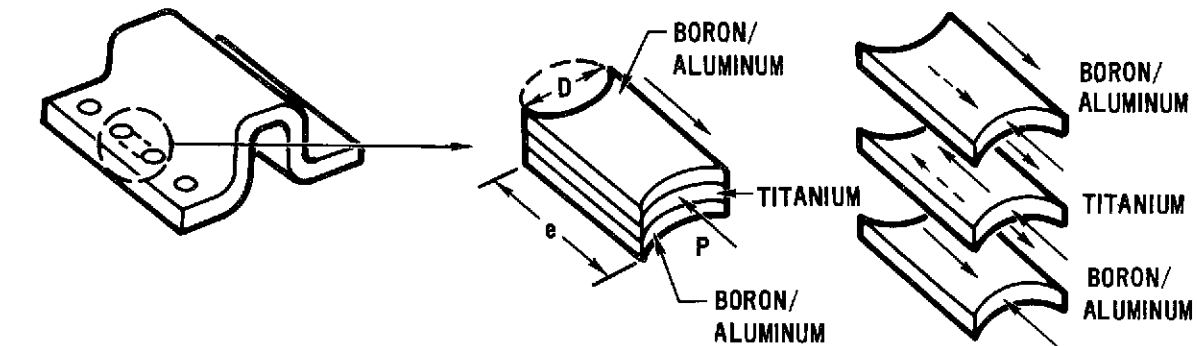
TITANIUM INTERLEAVES ARE ADDED TO STRINGERS
TO PROVIDE NECESSARY FASTENER STRENGTH

Figure 2-69

Bearing strength of the joint (P_{BR}) is the sum of the bearing strength of the boron-aluminum plies and the modified bearing strength of the titanium interleaves.

$$P_{BR} = F_{BR_{ti}} (D) (N) t_{ti} + F_{BR_0} (D) (M) t_0$$

where : $F_{BR_{ti}}$ = Modified bearing strength of titanium interleaf

$= 862$ MN/m^2 (125000 PSI) at 589°K (600°F)

F_{BR_0} = Bearing strength of 0° boron-aluminum

$= 386$ MN/m^2 (56000 PSI) at 589°K (600°F)

N   = Number of titanium interleaves

t_{ti} = Thickness of individual titanium interleaf

t_o = Thickness of individual 0° boron-aluminum ply

         = 0.0183 cm (0.0072 in.)

D   = Fastener hole diameter, cm (in)

M   = Number of boron-aluminum plies

Joint strength is a function of both bearing and shear strength of the stringer flange. Shear strength (P_{su}) is the sum of the individual shear strengths of the boron-aluminum plies and the titanium interleaves as defined by the following equation:

$$P_{su} = [F_{su_{ti}} \ (e-D) \ (N) \ (t_{ti}) + F_{su_o} \ (e-D) \ (M) \ (T_o)]$$

where: $F_{su_{ti}}$ = Ultimate shear strength of titanium

                    = 414 MN/m^2 (60000 PSI) at 589°K (600°F)

           F_{su_o} = Ultimate shear strength of 0° boron-aluminum

                    = 32.3 MN/m^2 (4680 PSI) at 589°K (600°F)

           e   = Center-line spacing of fasteners, cm (in)

The ultimate shear strength of 0° boron-aluminum employed in this equation was obtained by reducing average test values at 589°K (600°F) by 10 percent.

The joint allowable (Pall) is the minimum of the single shear strength (P_{su}) and the bearing strength (P_{BR}).

         Pall = Min (P_{su}, P_{BR})

This formulation was employed to develop the design curve shown in Figure 2-69 where the joint allowable for .635 cm (.25 in.) fasteners spaced at 2.92 cm (1.15 in.) is expressed as a function of number of boron-aluminum plies and titanium interleaves. A significant improvement in joint strength is provided by the addition of one or more titanium interleaves.

2.2.1.3 Compression Panel Internal and External Loads Analysis - Analysis of the B/Al skin-stringer Compression Panel required adapting a linear, finite element method of analysis to a structure exhibiting, in part, highly nonlinear material behavior. A sizing procedure was developed to obtain the minimum weight

2-63

structure capable of transforming a concentrated 1555 kN (350,000 lb) load at one end into a distributed reaction which peaks less than 30% at the other end. Predicted loads distribution for the panel sized by this technique is given in Section 2.2.1.3.4. Verification of the method of analysis for predicting loads was accomplished by comparing test data and predicted loads for the component panel as discussed in Section 2.2.1.3.5.

Distribution of shear flow between legs of hat section stringers was determined through a detailed finite element model of a portion of the panel using the NASTRAN program. Details of this investigation are discussed in Section 2.2.1.3.6.

2.2.1.3.1 Finite Element Model – A linear finite element model was used to idealize the skin-stringer panel shown in Figure 2-62. Unidirectional boron-aluminum stringers and titanium frames were assumed to carry axial loads only, and were modeled by axial bar elements. The $\pm \frac{\pi}{4}$ rad ($\pm 45°$) boron-aluminum skin was modeled by axial bar elements and shear panel elements. Axial bar elements represented the longitudinal and transverse tensile and compressive capability of the skin while shear panel elements simulated shear behavior. Axial bar and shear panel elements were also used to idealize the thrust plate.

A fine grid of elements was required in the model to determine the state of combined shear and biaxial tensile and compressive stresses in the skin. Also, a fine grid of both bar and shear panel elements was necessary to determine the variation of this complex state of stress in a given bay. Similarly, a fine grid of elements was required to accurately predict load variation in stringers, thrust plate, and frames.

The resulting finite element model is illustrated in Figure 2-70. Shown are typical element grids modeling portions of the panel bounded by two adjacent frames and two adjacent stringers. The model of the entire panel utilizes 625 joints, 1200 bars, and 576 shear panels. Grid spacing was chosen to provide an accurate description of expected variation in internal loads, with the smallest spacing occurring near the concentrated load end.

2.2.1.3.2 Material Properties – Material properties assumed for the frames, stringers, thrust plate, and skin are given in Figure 2-71. Estimated mechanical properties at 589°K (600°F) were employed because analysis of the compression panel occurred before results from element test program were available. In Figure 2-72, the allowable column stress, as a function of cross sectional area, is presented for hat section unidirectional boron-aluminum stringers, and includes the interaction of crippling and column failure modes. Estimated 589°K (600°F) lower bound crippling curves were employed to develop these data.

2-64
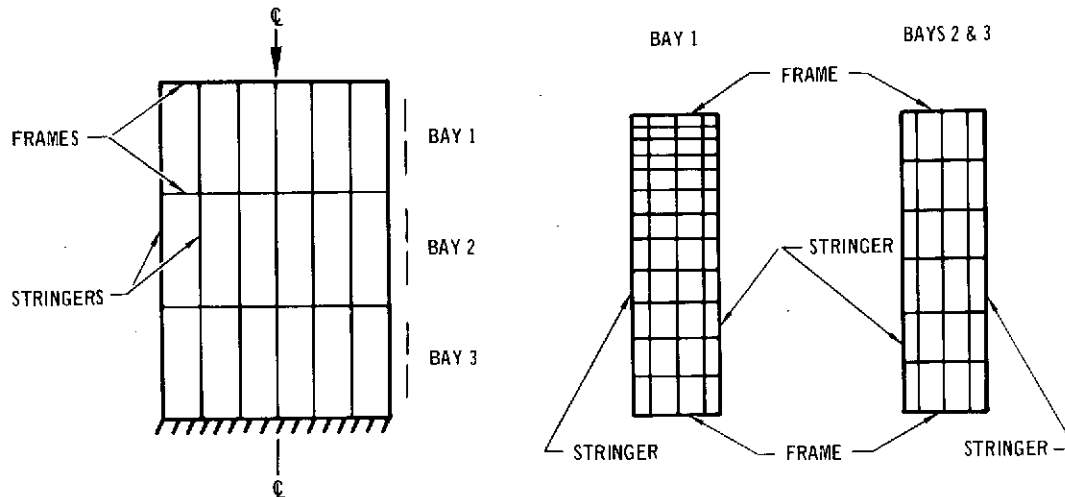
FINITE ELEMENT DISTRIBUTION				
EACH SHEAR WEB (18 TOTAL)		EACH STRINGER (7 TOTAL)	EACH FRAME (4 TOTAL)	GRAND TOTAL (ENTIRE PANEL)
BAY 1	BAY 2 OR 3			
BARS 80	38	24	24	1200
PANELS 48	24	–	–	576
JOINTS –	–	–	–	625

MANY ELEMENTS REQUIRED FOR ACCURATE STRUCTURAL IDEALIZATION OF COMPRESSION PANEL

Figure 2–70

FRAMES   – TITANIUM 6 AL–4V

E = 93.8 GN/m^2 (13.6 x 10^6 PSI)

F^{tu} = 0.815 GN/m^2 (118 KSI)

ρ = 4.42 g/cm^3 (0.160 LB/IN.^{3})

STRINGERS AND THRUST PLATE –
UD BORON–ALUMINUM

E_L^C = 151.7 GN/m^2 (22 x 10^6 PSI)

F_L^{tu} = 0.930 GN/m^2 (135 KSI)

F_L^{cu} = F_L^{tu} FOR THRUST RATE

       = SEE FIGURE 2–72 FOR STRINGERS

ρ = 2.63 g/cm^3 (0.095 LB/IN.^{3})

SKIN – ·π/4 rad (· 45^0) BORON–ALUMINUM

G_{XY} = 41.4 GN/m^2 (6.0 x 10^6 PSI)

F^{su}_{xy} = 0.110 GN/m^2 (16.0 KSI)

ρ = 2.63 g/cm^3 (0.095 LB/IN.^{3})

**MATERIAL PROPERTIES EMPLOYED IN SIZING PANEL
Temperature: 589^{0}K (600^{0}F)**

Figure 2–71

2–65
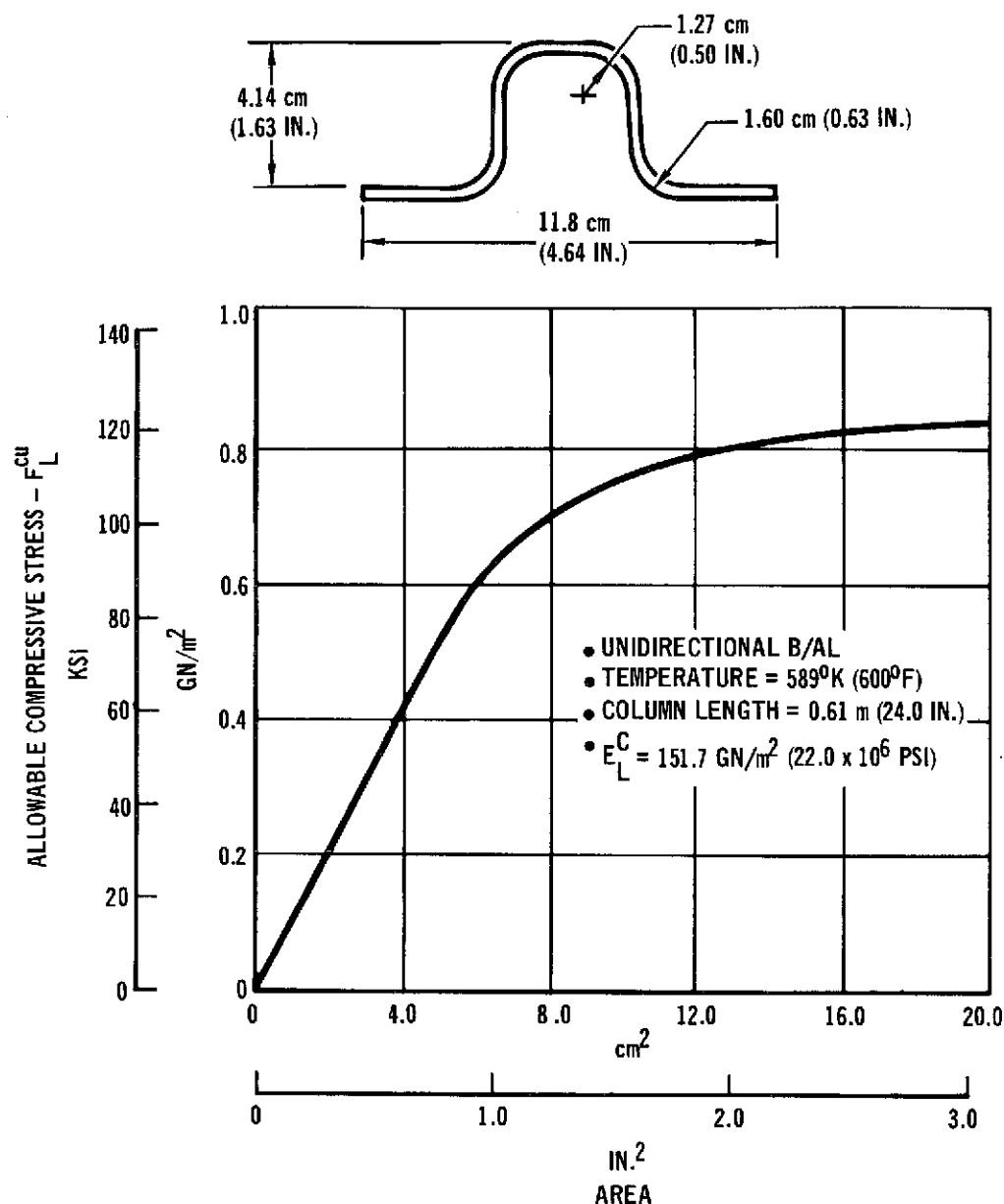
COLUMN ALLOWABLES FOR BORON ALUMINUM STRINGERS

Figure 2-72

Interaction of biaxial tensile and compressive stresses with shear stresses for $\pm45°$ boron aluminum skin is shown in Figure 2-73 . Allowable shear strength of 0.110 GN/m^2 (16.0 ksi) was chosen for the skin since for shear stresses below this value, Figure 2-73 indicates little or no interaction with axial stresses. However, Figure 2-73 does indicate that the ratio of biaxial stresses has an important influence on the tensile and compressive behavior of the skin. Treatment of this nonlinear biaxial behavior requires special consideration and is described in the following section.

SHEAR STRESS
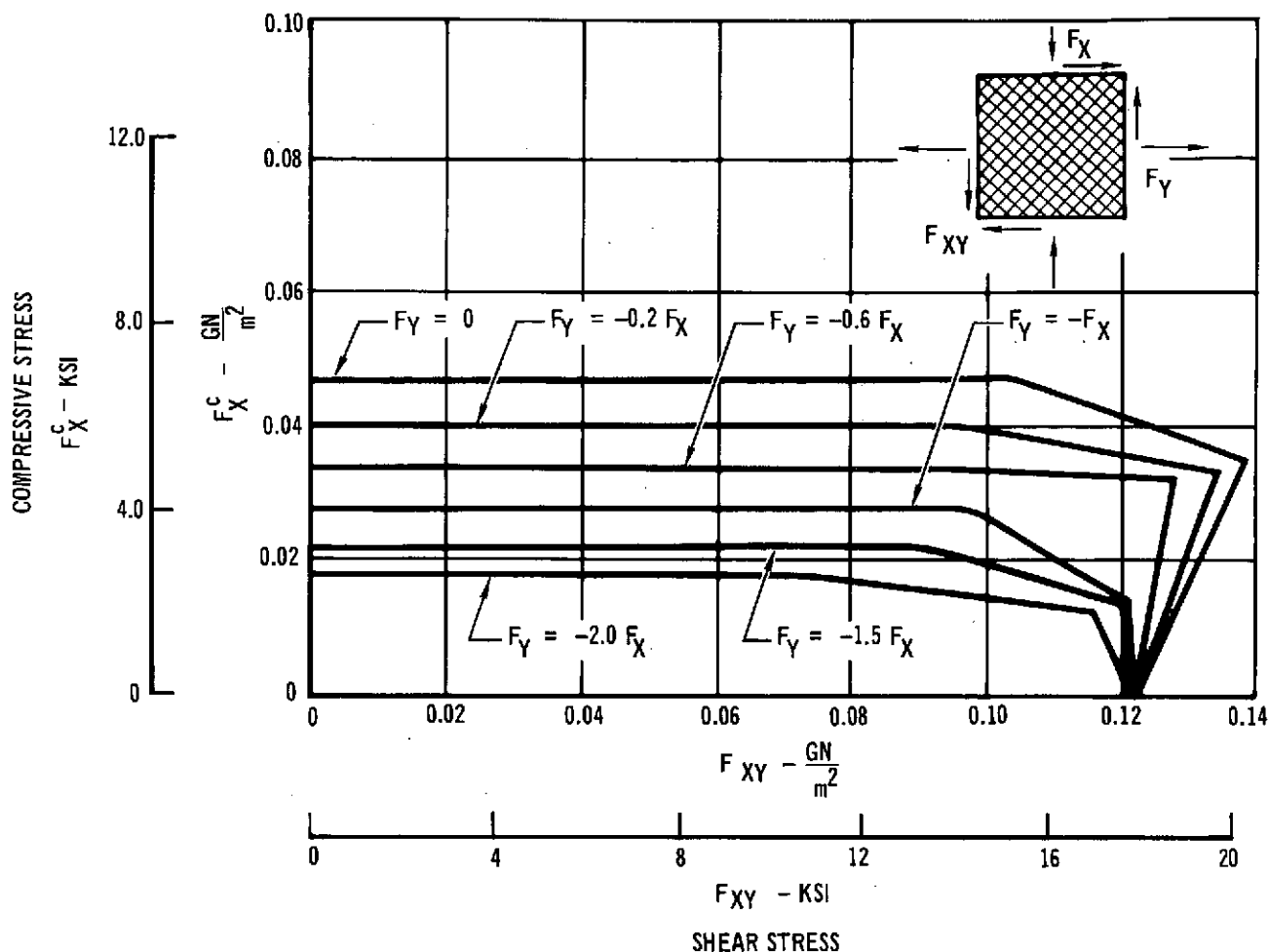
PREDICTED ULTIMATE STRENGTH OF ± 45° LAMINATE AT 589°K (600°F)

Figure 2-73

2.2.1.3.3 Sizing Procedure - The finite element model described in Section 2.2.1.3.1 was used to size the skin, stringers, and frames. Use of the MDAC-E computer program CASD allowed a rapid determination of member sizes in a minimum weight structure for the design conditions. A four step sizing procedure was used in the concept selection studies described in Appendix A. Because results from that study could be applied to the final sizing operation for the panel, a three step sizing procedure was only required as outlined in Figure 2-74. This procedure incorporated strength and stiffness constraints, minimum gage considerations, and nonlinear material behavior. In each step, the panel was supported at the applied load end and a uniform load imposed at the distributed load end to force compliance with the 30% peaking constraint. The actual support condition of zero deflection at the distributed load end was simulated by imposing a stiffness constraint requiring each stringer to deflect an equal amount.
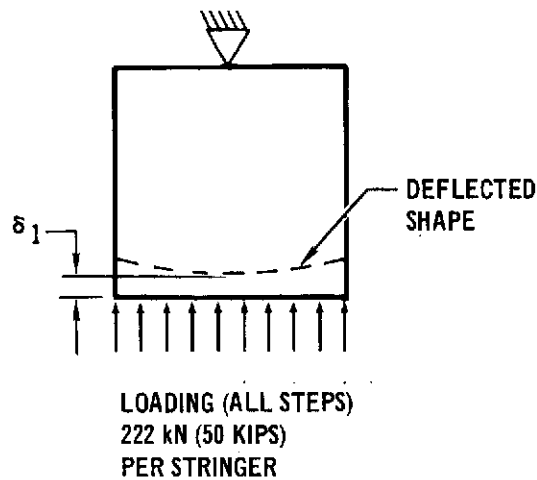
STEP I
- STRUCTURE SIZED FOR STRENGTH
  (MARGIN OF SAFETY = 0)
- MEMBER STRENGTHS AND STIFFNESSES
  BASED ON ESTIMATED INTERNAL LOADS

LOADING (ALL STEPS)
222 kN (50 KIPS)
PER STRINGER
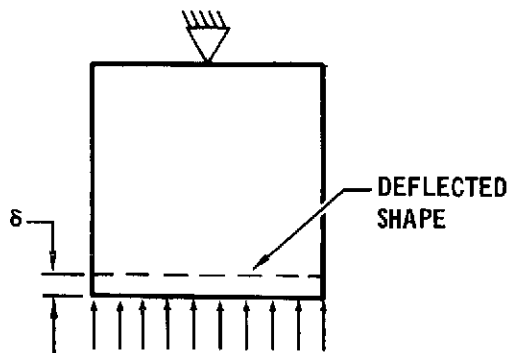
STEP II
- STRUCTURE RESIZED FOR STRENGTH
- STIFFNESS CONSTRAINT IMPOSED
  $$\delta = \delta_1$$
- MEMBER STRENGTHS AND STIFFNESSES
  BASED ON RESULTS OF STEP I
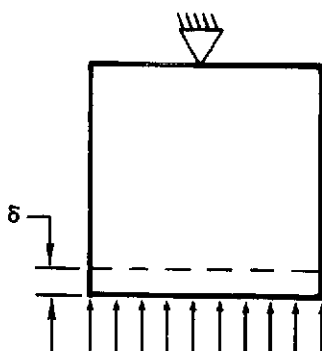
STEP III
- STRUCTURE RESIZED FOR STRENGTH
- STIFFNESS CONSTRAINT IMPOSED
  $$\delta = \delta_1$$
- MEMBER STRENGTHS AND STIFFNESSES
  BASED ON RESULTS OF STEP II
- MINIMUM SKIN THICKNESS IMPOSED (12 PLIES)
- SKIN GAGES FORCED TO REFLECT MULTIPLES
  OF 4 PLIES

STEPS LEADING TO SKIN, STRINGER, AND FRAME SIZES FOR INTERNAL LOADS ANALYSIS

Figure 2–74

In step one, the panel was sized for strength only to obtain the minimum weight structure for the condition of uniform loading at the distributed load end. Member strengths and stiffnesses employed in the model were based on estimated internal loads distribution obtained from concept selection studies (Appendix A). The centerline deflection of the panel obtained in this manner became the deflection constraint which was imposed on all stringers in subsequent sizing steps.

Step two involved resizing the panel to determine the minimum weight structure for the conditions of uniform loading and uniform deflection at the distributed load end. The deflection constraint imposed was the centerline deflection from step one. Revised allowables and moduli were employed for each element in the model based on internal loads and member gages determined in step one. The allowable compressive stress for each stringer element was revised using Figure 2-72 and resized stringer areas from step one. The method illustrated in Figure 2-75 was used to incorporate the nonlinear biaxial response of the $\pm 45°$ skin. Modulus and allowable strength were estimated for each skin bar element in step one based on predicted strain using a stress-strain curve derived for a specific predicted stress ratio as shown in Figure 2-75. In step two, this process was repeated using strains and stress ratios determined in step one to update properties for each skin bar element.
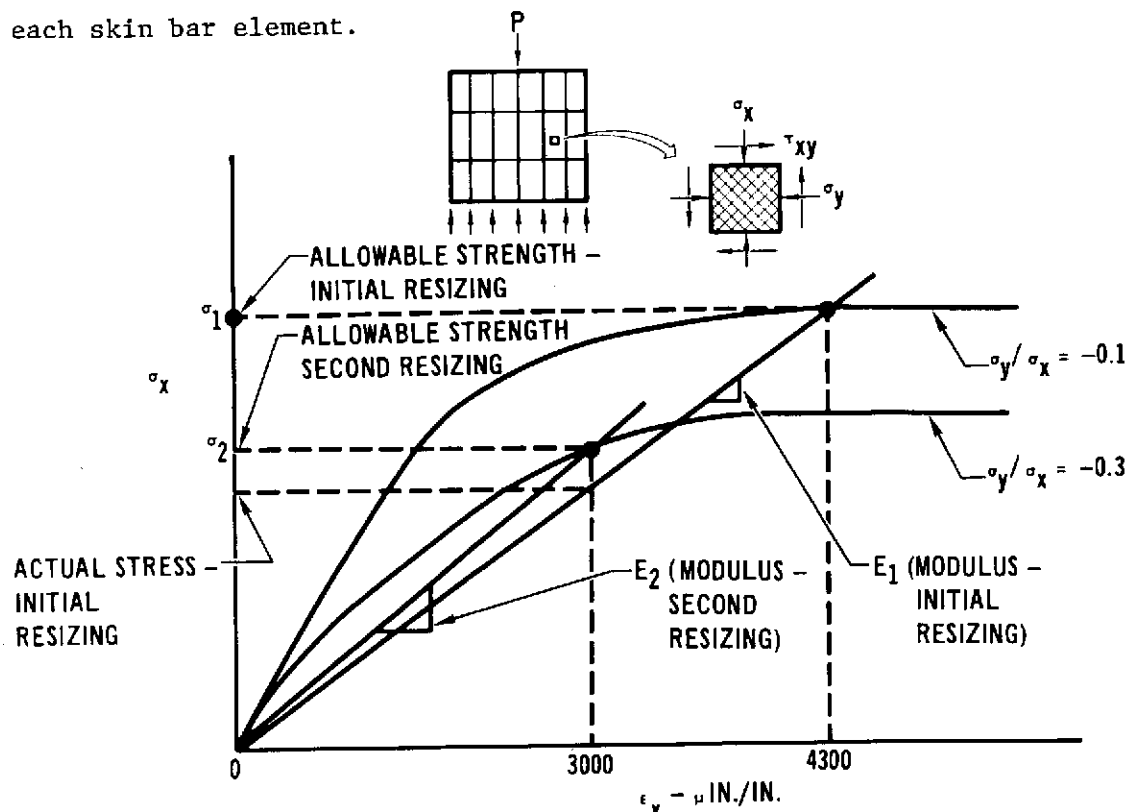
PANEL RESIZING INFLUENCED BY NONLINEAR RESPONSE OF SKIN

Figure 2-75

2-69

In the third and final step, the panel was again resized for the conditions of uniform loading and uniform deflection at the distributed load end. Strength and stiffness of each element was based on internal stresses and strains from step two. Additional constraints employed were that minimum $\pm \frac{\pi}{4}$ rad ($\pm 45°$) skin panel thickness was 0.22 cm (.0865 in.) corresponding to 12 plies, and skin laminate thicknesses should reflect multiples of four plies to maintain midplane symmetry.

2.2.1.3.4 <u>Predicted Loads Distribution</u> - Stringer, thrust plate, and frame area requirements as well as skin gages determined from the sizing procedure were adjusted to reflect manufacturing considerations and are shown in Figures 2-76 through 2-78. These member gages, as well as material properties consistent with internal stresses and strains from step three of the sizing procedure, were incorporated in the finite element model. The 1555 kN (350,000 lb) concentrated load was applied to this resized structure with the distributed load end of the panel supported at a rigid boundary. Resulting load distribution at supported end of panel has a 6.8% peaking factor as shown in Figure 2-79. Internal loads in stringers, thrust plate, skin, and frames are shown in Figures 2-80 through 2-84.

Stringer, thrust plate, and frame areas as well as skin thicknesses shown in Figures 2-76 through 2-78 represent a near minimum weight panel having both sufficient strength and stiffness to meet the uniform load constraint at the supported end. In addition to adjustments in areas and gages due to manufacturing considerations, titanium interleaves also were added locally to stringers and skin to provide necessary shear and bearing strengths. A sensitivity study employing the finite element model was made to determine the effect of these perturbations in member sizes on loads distribution. No effect on internal and external loads could be determined.

Other modifications, in addition to those mentioned above, were necessary due to economic considerations. First, steel frames were selected to replace the titanium frames assumed in the original analysis. This substitution was made on an equivalent stiffness basis wherever possible. Adequate strength was provided in every case. Second, the all boron-aluminum thrust post concept was replaced with one made up of a full length boron-aluminum stringer plus a steel thrust plate extending over the first bay. This substitution was made on an equivalent stiffness basis while providing adequate strength.

DISTANCE FROM CONCENTRATED LOAD END – X
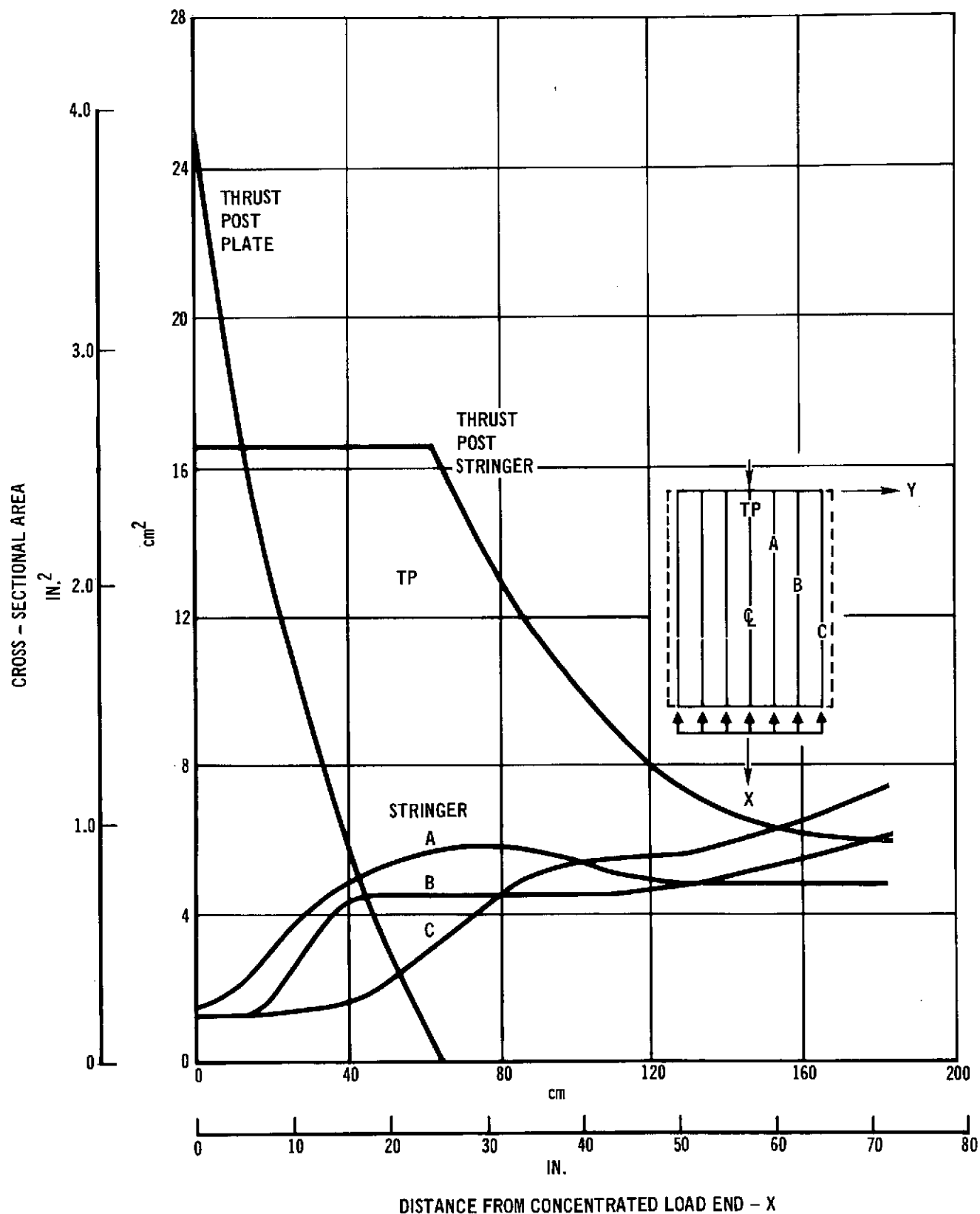
STRINGER AND THRUST POST AREA REQUIREMENTS DETERMINED BY SIZING PROCEDURE

Figure 2–76

2-71

DISTANCE FROM CENTERLINE OF PANEL – Y
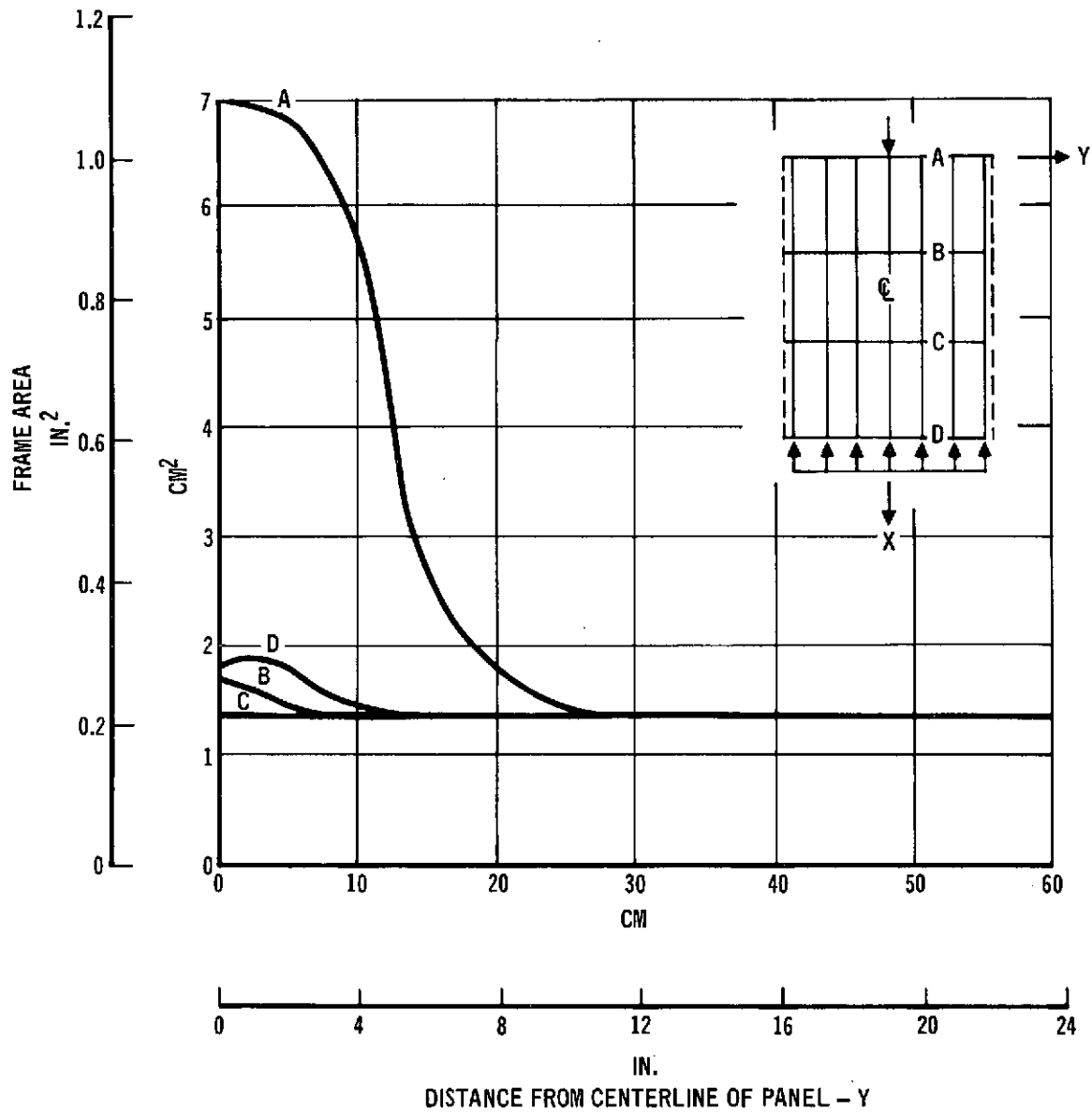
TITANIUM FRAME AREA REQUIREMENTS DETERMINED BY SIZING PROCEDURE

Figure 2–77
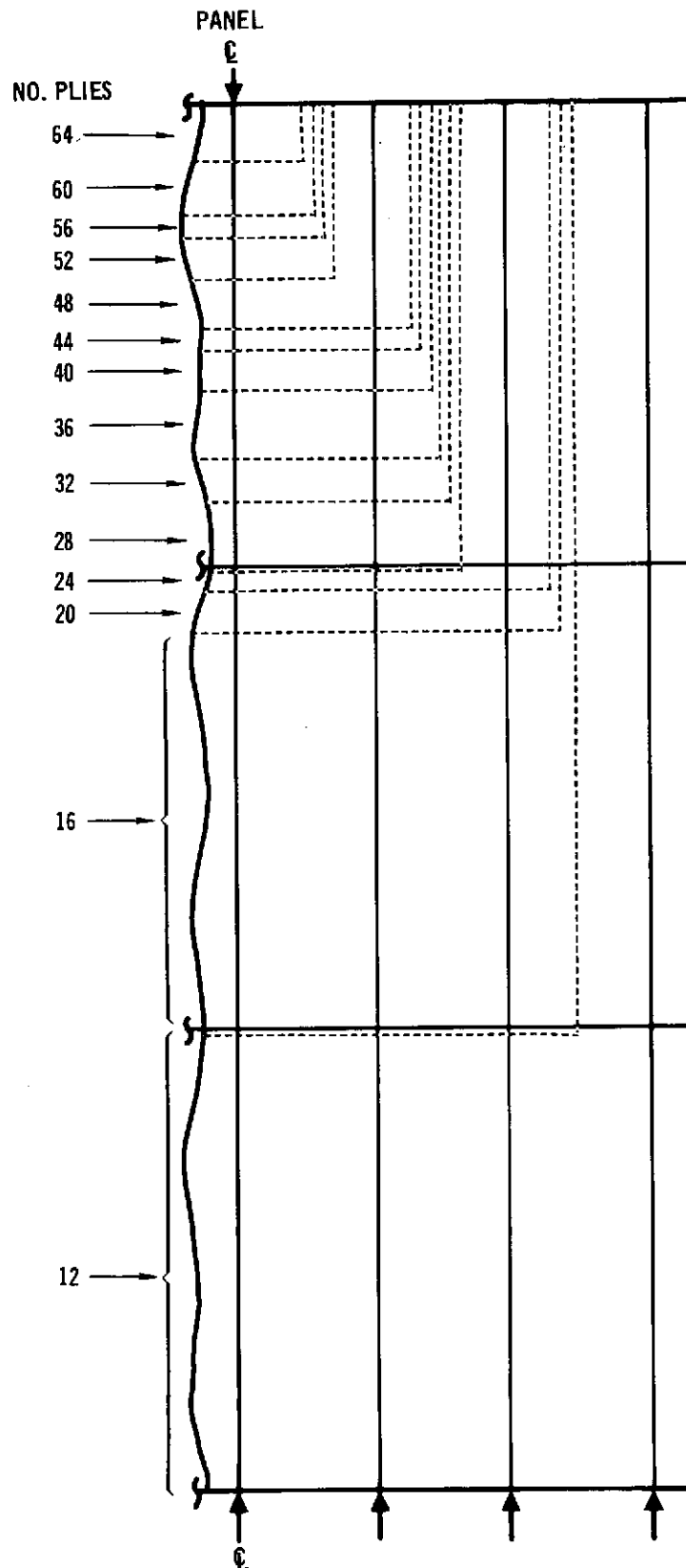
SKIN THICKNESS REQUIREMENTS DETERMINED BY SIZING PROCEDURE

Figure 2-78

1555 kN (350 KIPS)

225	214	220	237	220	214	225	kN
50.6	48.1	49.6	53.4	49.6	48.1	50.6	KIPS

6.8% MAXIMUM DEVIATION
FROM UNIFORM DISTRIBUTION
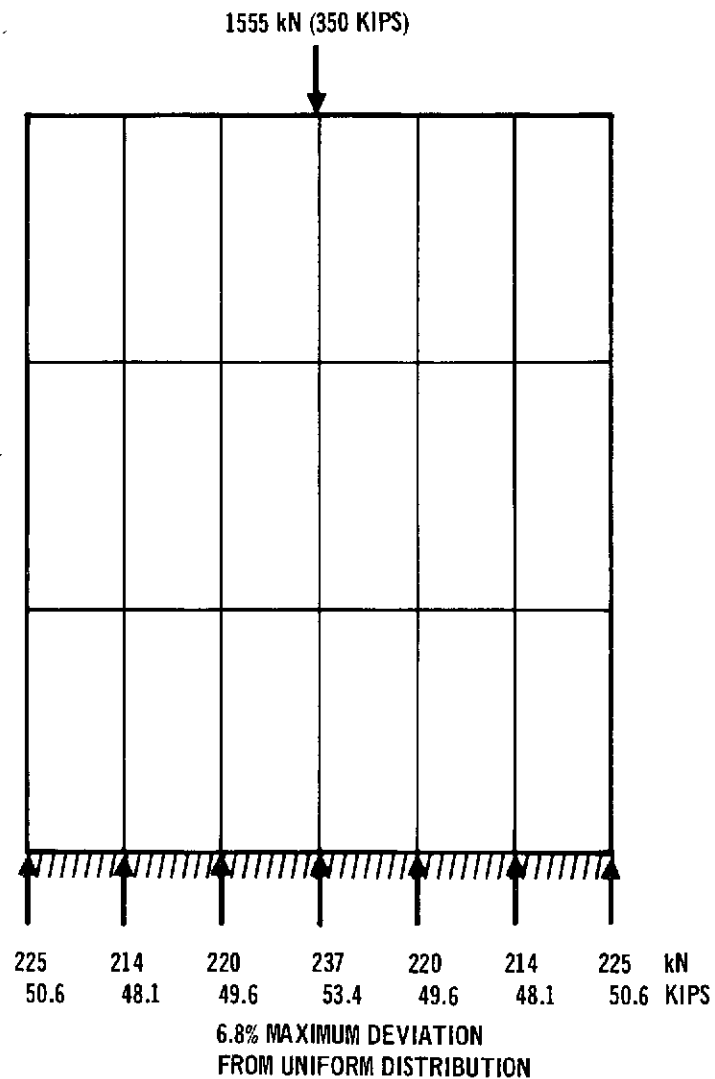
LOAD DISTRIBUTION AT DISTRIBUTED LOAD END
OF PANEL IS NEARLY UNIFORM

Figure 2-79
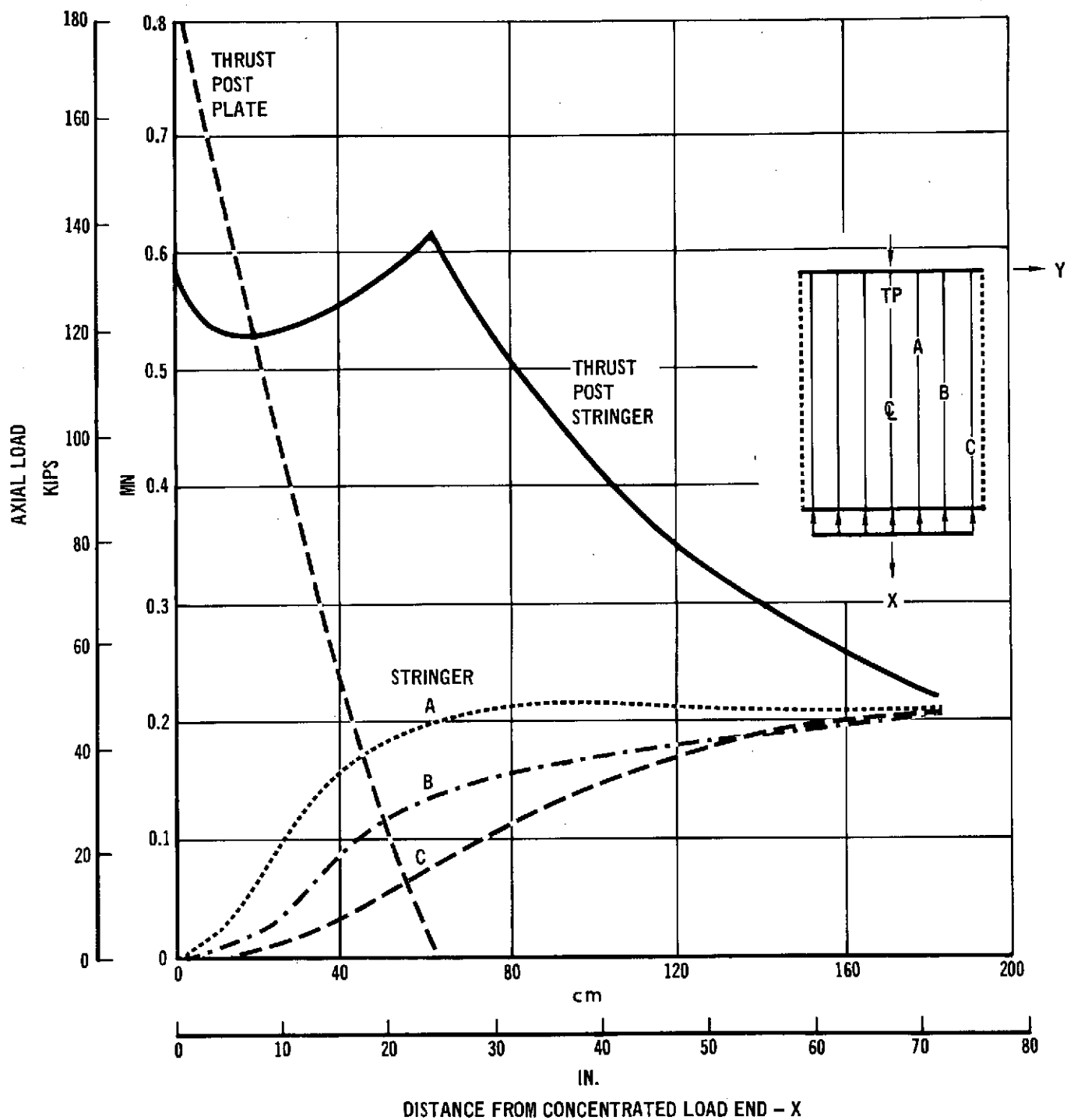
STRINGER AND THRUST POST AXIAL LOAD DISTRIBUTION

Figure 2-80
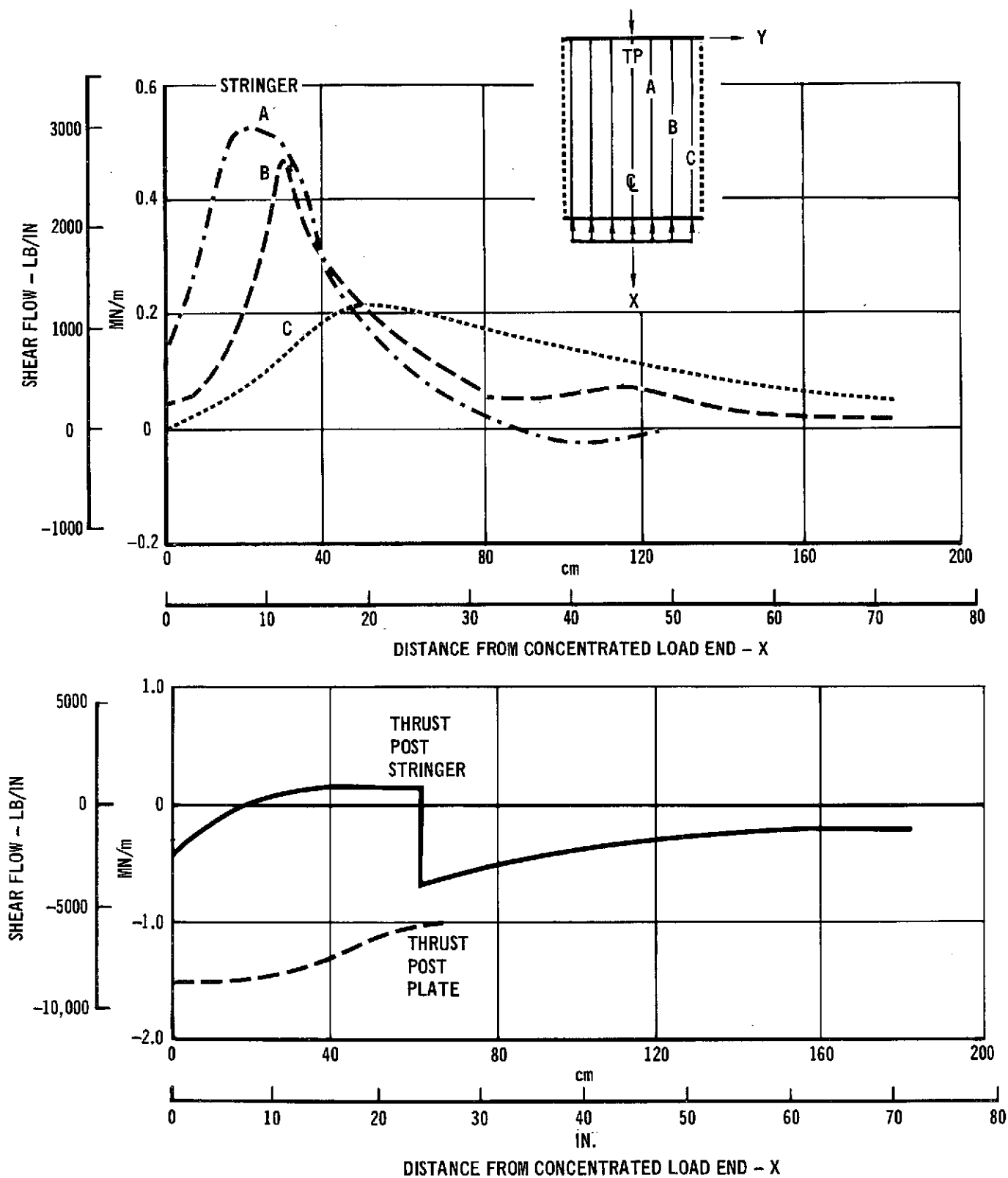
STRINGER AND THRUST POST SHEAR FLOW DISTRIBUTION

Figure 2-81
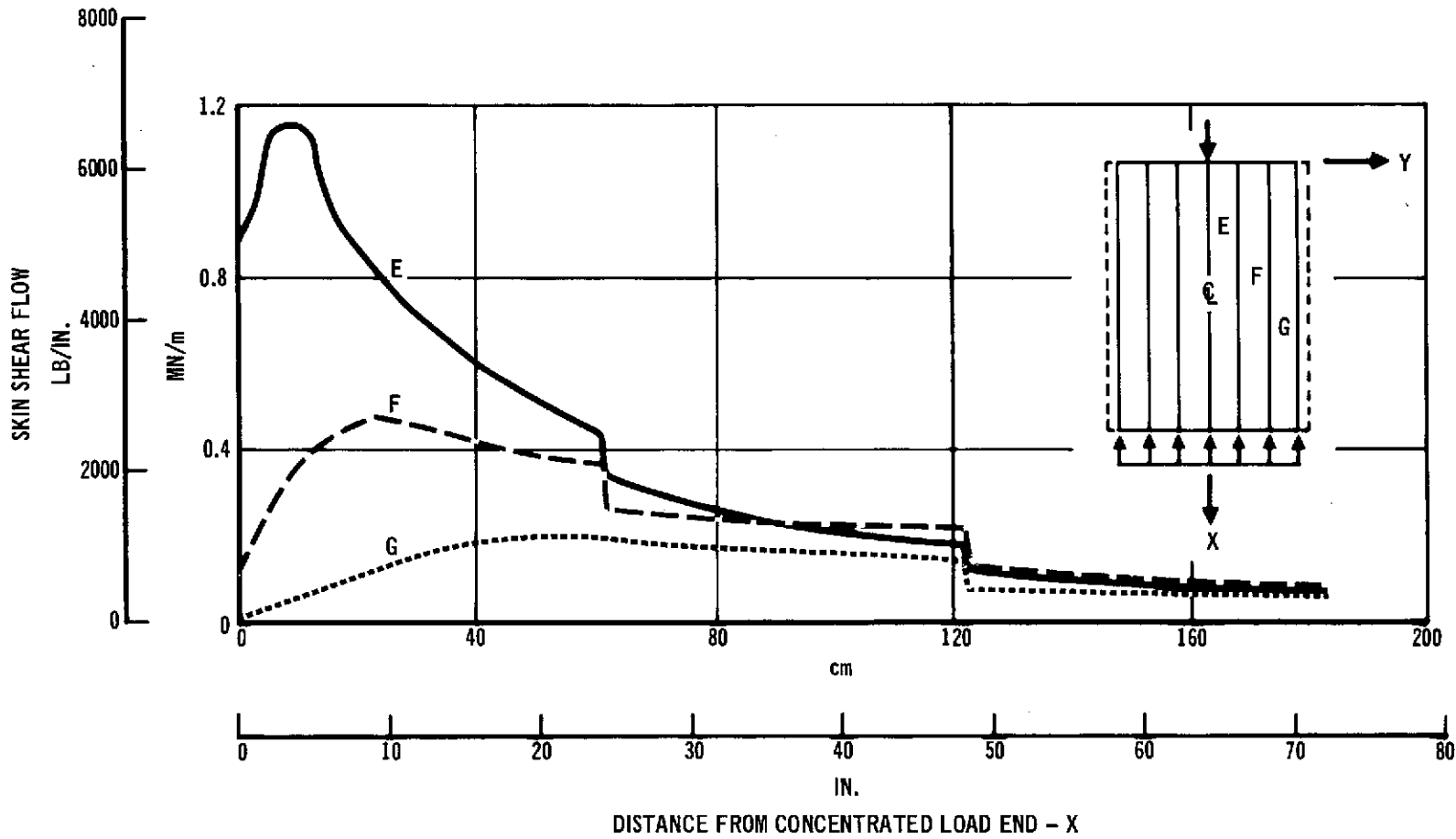
SHEAR FLOW IN SKIN IS MAXIMUM AT CONCENTRATED LOAD END OF PANEL
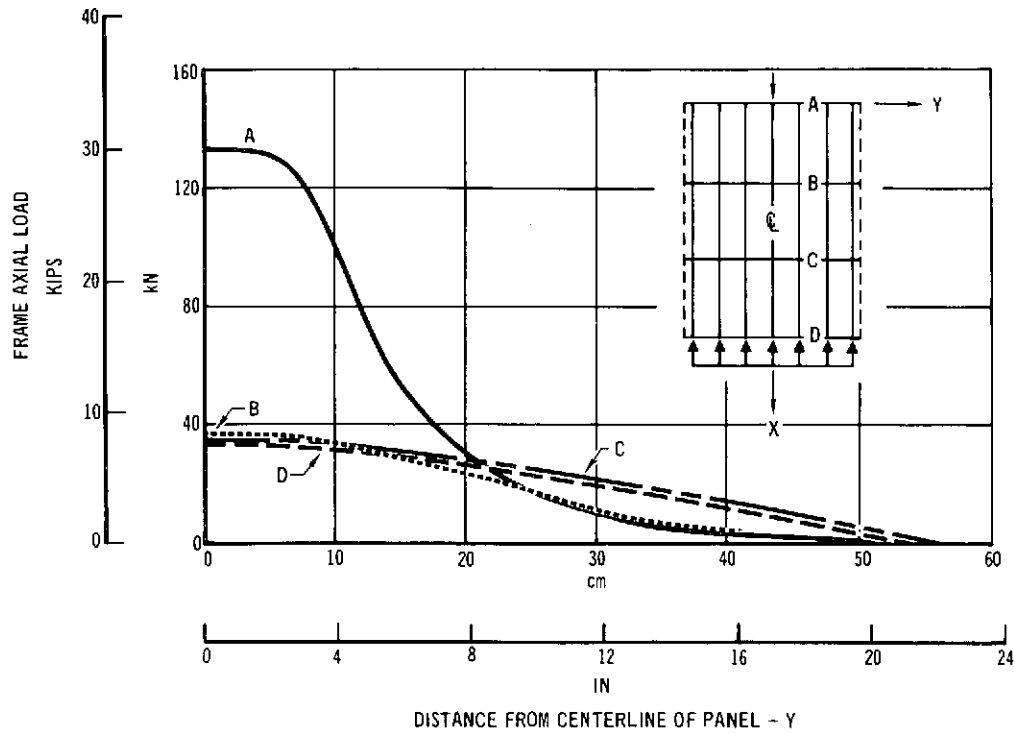
FRAME AXIAL LOADS ARE MAXIMUM ADJACENT TO PANEL ₵

Figure 2-83
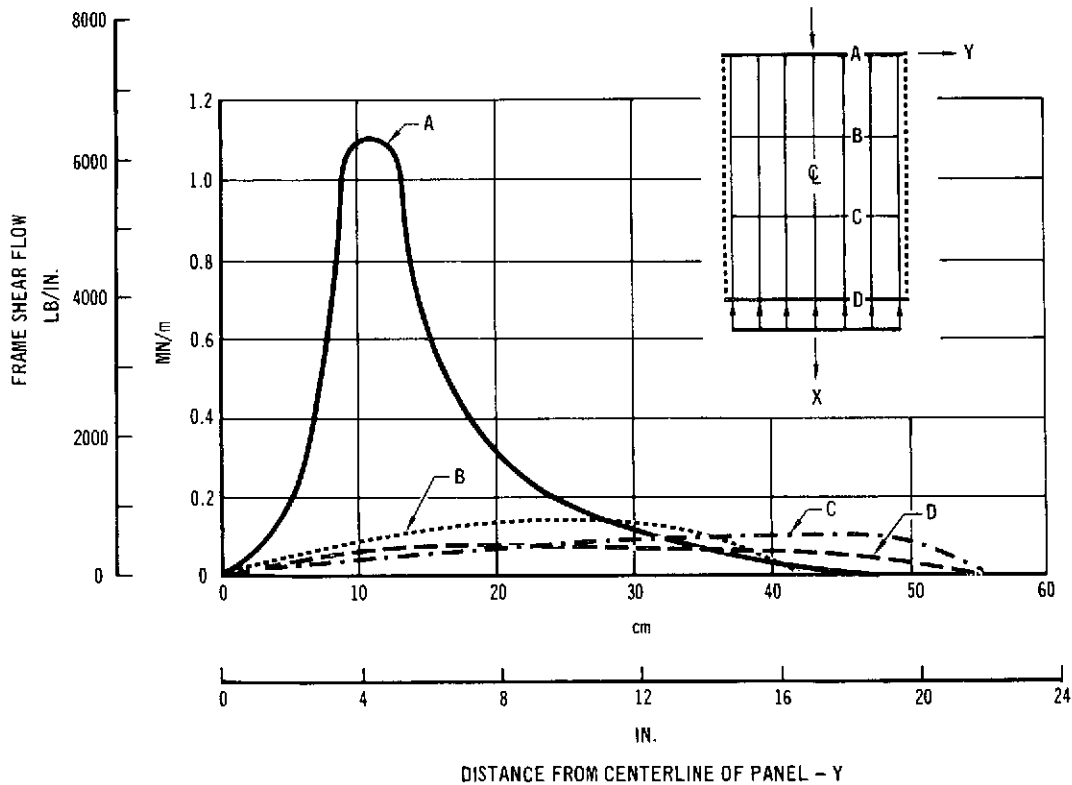
FRAME SHEAR FLOWS ARE MAXIMUM ADJACENT TO PANEL ₵

Figure 2-84

2.2.1.3.5 <u>Verification of Method for Predicting Loads</u> - The finite element
technique employed to obtain compression panel internal loads distribution
described in Section 2.2.1.3.4 was used also to predict loads distribution for
the component panel whose structural arrangement is described in Section 2.5.
While at 589°K (600°F), the component panel was subjected to a 1555 kN (350,000 lb)
concentrated load at one end and supported on an elastic foundation at the other.
Loads distribution predicted by the finite element model for this same condition
are compared in Figure 2-85 to loads obtained by test. The good agreement between
predicted and measured loads for the component panel verifies the procedure used for
design and analysis of the compression panel.

LOADS DISTRIBUTION
(600°F)

P = 350 (KIPS)

PREDICTED – COMPONENT PANEL(KIPS) 23.0	37.2	48.0	133.5	48.0	37.2	23.0
MEASURED – COMPONENT PANEL(KIPS) 23.6	–	–	135.0	45.0	40.0	21.2

SI UNITS OMITTED FOR CLARITY
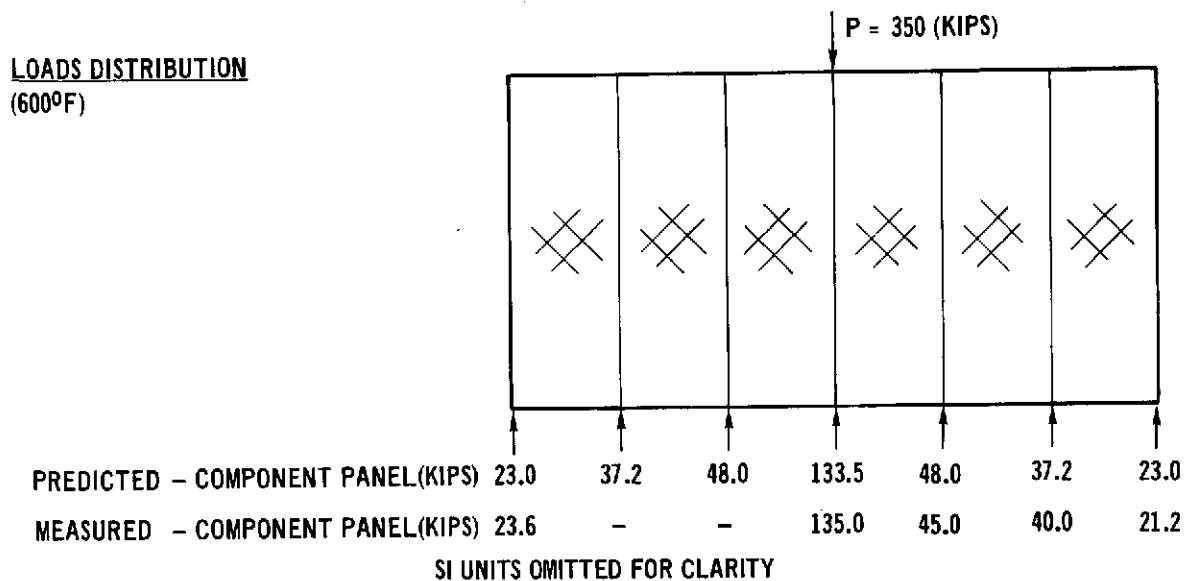
**PREDICTED LOADS DISTRIBUTION OF COMPONENT
PANEL VERIFIED BY TEST AT 600°F**

Figure 2-85

2.2.1.3.6 <u>Distribution of Shear Flow to Stringer Legs</u> - The shear flow
distribution to the hat section stringers described in Figure 2-81 is transmitted
by mechanical fasteners to the two legs of the hat section stringer. Distribution
of this shear flow to each leg of the hat is important for local shear and bearing
strength considerations. Therefore, a finite element model of a portion of the
compression panel was created using the NASTRAN program. Five stringers and one
bay of the compression panel were modeled as shown in Figure 2-86 using ortho-
tropic plate elements and bar elements. Each hat section stringer was modeled with
multiple plate elements to obtain distribution of load in the cross section. The
thrust post and frames were modeled with bar elements. Orthotropic plate elements

were used to model the $\pm 45°$ skin. Member gages and material properties were chosen to reflect those in the compression panel at 589°K (600°F). Internal skin and stringer loads at the first intermediate frame, obtained from the finite element model of the compression panel, were used as applied loads in the NASTRAN model.

PORTION OF COMPRESSION
PANEL MODELED WITH
NASTRAN ORTHOTROPIC
PLATE ELEMENTS

183.CM(72 IN.)

122.CM(48. IN.)

61.CM(24.IN.)

0.00 CM(0.IN.)

P_1

TYPICAL GRID
OF PLATE ELEMENTS
MODELING STRINGERS

q_2

P_2

q_1

$P_1 > P_2$
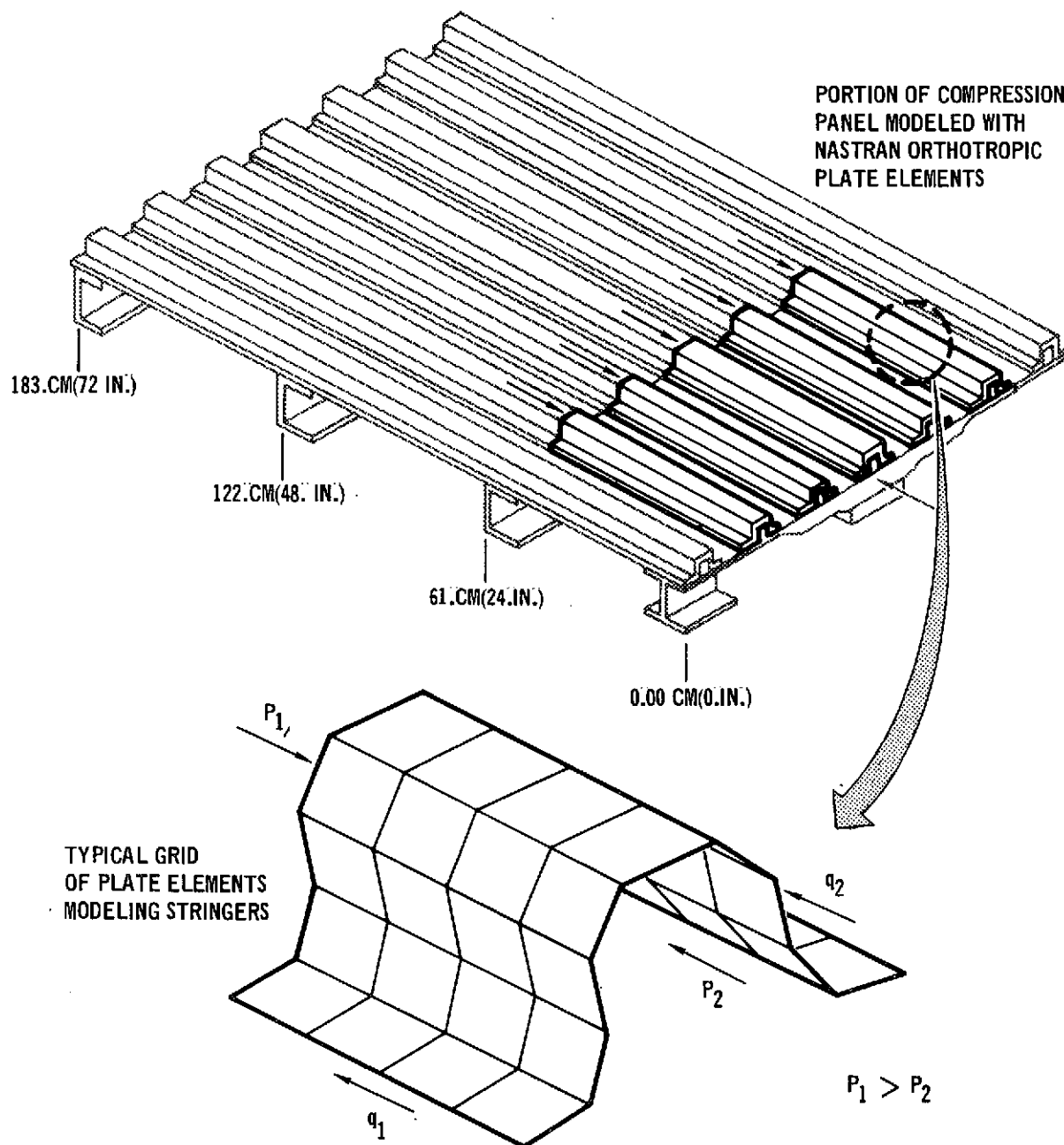
NASTRAN MODEL TO DETERMINE DISTRIBUTION OF SHEAR
FLOW BETWEEN LEGS OF HAT SECTION STRINGERS

Figure 2–86

The maximum ratio of shear flows (q_1/q_2 in Figure 2-86) introduced to the legs of the hat was found to be 1.36 corresponding to 42.5% of the shear introduced to one leg and 57.5% introduced to the other. Based on these results, detail analysis of the skin/stringer joints in the compression panel assumed that 60% of the shear in Figure 2-81 could be introduced through either leg of the hat.

2.2.1.4 Detailed Strength Analysis – This section contains strength analysis of the compression panel in specific areas as defined in Figure 2-87.

a) strength analysis of outboard stringer (Section A-A)

b) shear and bearing analysis of stringer for loads introduced through mechanical fasteners (Section B-B)

c) ultimate strength analysis of skin for biaxial loading and shear (View C)

d) buckling analysis of skin (View D)
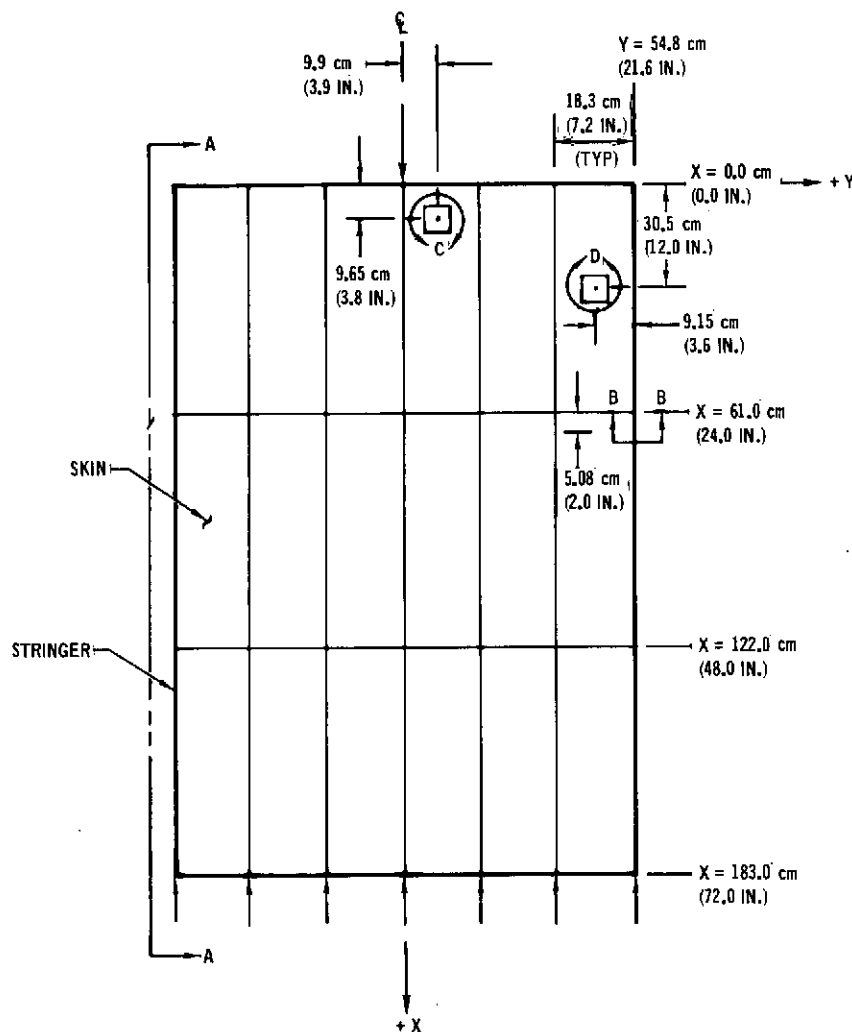
STRENGTH CHECK LOCATIONS ON COMPRESSION PANEL

Figure 2-87

Stringer Analysis - Based on shear and bending moment distributions shown
in Figure 2-88, the critical section occurs at Section E-E (X = 61 cm, 24 in.).
This section is shown in Figure 2-89. The maximum applied bending moment of 406 M-N
(3600 in.-lbs) was obtained from a beam column solution. Maximum applied stress
due to axial load and bending is:

$$F = \frac{P}{A} + \frac{MC}{I}$$

$$= \frac{-82.3}{3.68} + \frac{40.7\ (-1.57)}{9.37}$$

$$= -22.36 - 6.82 = -29.2\ kN/_{cm}2\ (-43200\ psi)$$

The allowable compressive load of a 11 ply unidirectional stringer is 110 kN
(24,500 lbs) (Ref. Figure 2-44) which results in an average allowable stress of

$$F_{ALL} = \frac{P}{A} = \frac{-110}{3.68} = -29.9\ kN/_{cm}2\ (-43300\ psi)$$

The resulting margin of safety is slightly conservative since effective skin was not
included.

$$M.S. = \frac{F_{ALL}}{F} - 1 = \frac{-29.9}{-29.2} - 1 = .02$$

Stringer Bearing and Shear Analysis - The section to be analyzed (Section B-B)
is located 66 cm (26 in.) from the thin end of the outboard stringer as shown in
Figure 2-90. The applied shear flow on stringer at X = 66 cm (26 in.) is
q = 193.0 kN/m (1100 lbs/in.) (Ref. Figure 2-81). The inboard leg of stringer is
designed to withstand 60 percent of this shear as described in Section 2.2.1.3.6.
Load applied to stringer per fastener is:

$$P_{APPLIED} = .60\ qe$$

$$= .6\ (193.0)\ (.0292) = 3380N\ (760\ lbs)$$

An allowable load of 3560N (800 lbs) per fastener at 589°K (600°F) is determined
from Figure 2-69 for a layup having 13 0 rad (0°) B/Al plies and 1 titanium ply.
Of the two potential failure modes (bearing and shear), shear is predominant at
this location. Margin of safety is:

$$M.S. = \frac{P_{ALL}}{P_{APP}} - 1 = \frac{3560}{3380} - 1 = +.05$$

Based on a comparison of applied and allowable loads shown in Figure 2-91, the
margin of safety is larger at all other stations for in-plane shear strength.
This figure also indicates that shear strength would be unacceptable without
titanium interleaves.

SECTION A-A ROTATED $\pi/2$ rad· CCW.│(REF. FIG. 2–87)

X

E

E

q (SHEAR FLOW)

61 cm (24 in) (TYP)

1739 N (391 LBS)

2090 N (470 LBS)

2046 N (460 LBS)

1823 N (410 LBS)

E–E

210 kN/m (1200 LB/IN.)

APPLIED SHEAR FLOW – q

4.22 kN (950 LB)

SHEAR DIAGRAM

BENDING MOMENT DIAGRAM

407 m–N (3600 IN-LB)

CRITICAL LOCATION

222 kN (50000 LBS)

AXIAL LOAD DIAGRAM
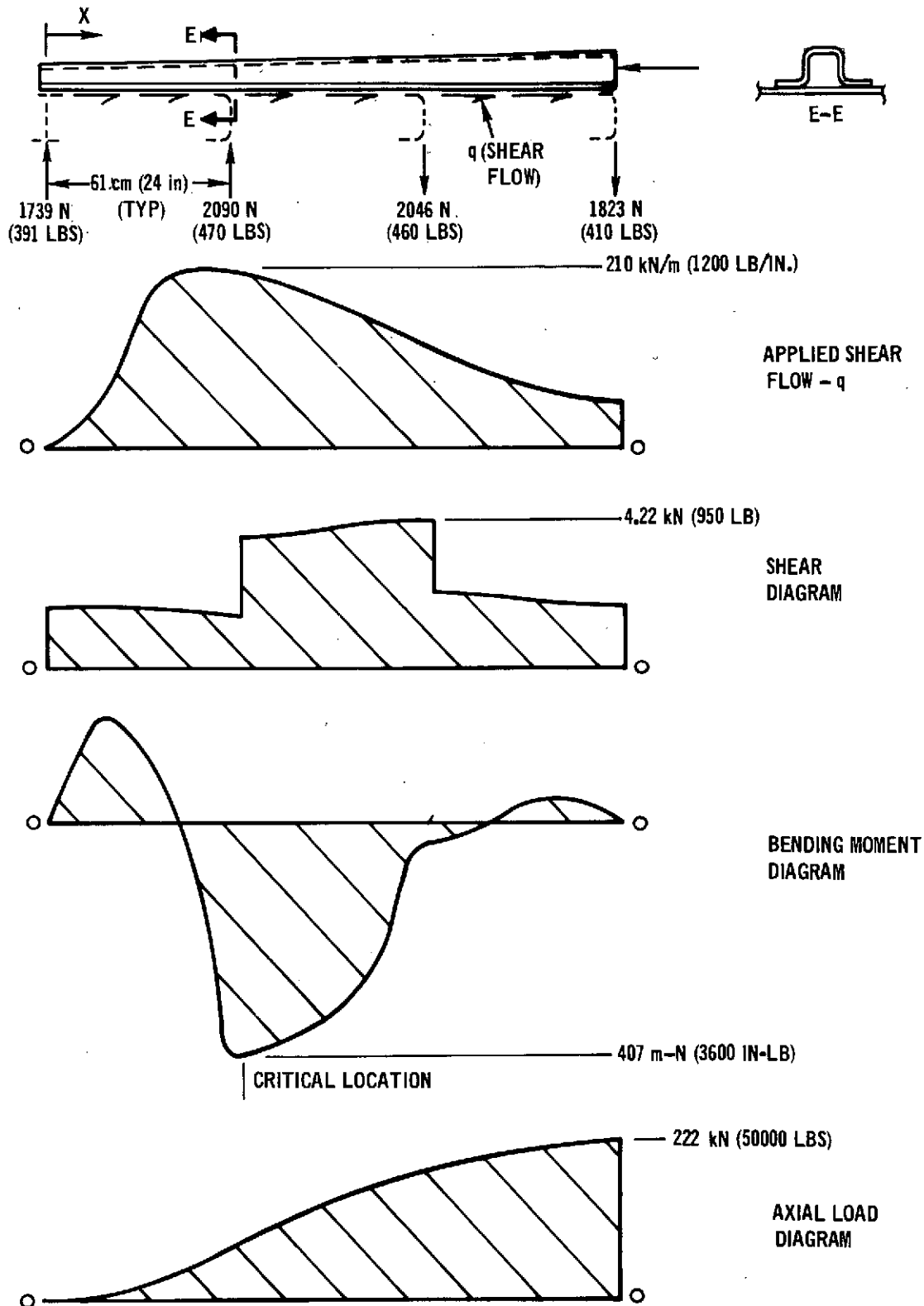
STRINGER "C" EXTERNAL AND INTERNAL LOADS

Figure 2–88

2–83

ULTIMATE LOADS AT 589°K (600°F)

$P = -82.2$ kN $(-18500$ LB)

$M = 406$ m-N (3600 IN-LB)

$A = 3.68$ cm^2 (0.570 IN.^{2})

$I = 93.5$ cm (0.225 IN.^{4})

$\bar{y} = 1.68$ cm (0.66 IN.)

$C = -(\bar{y} - t/2) = -1.57$ cm (-0.619 IN.)

t = 0.21 cm (0.0825 IN.)
11 PLIES UNIDIRECTIONAL B/AL

4.34 cm (1.71 IN.)

$\pi/4$ rad ($\pm$ 45°) SKIN

20.15 cm (4.64 IN.)
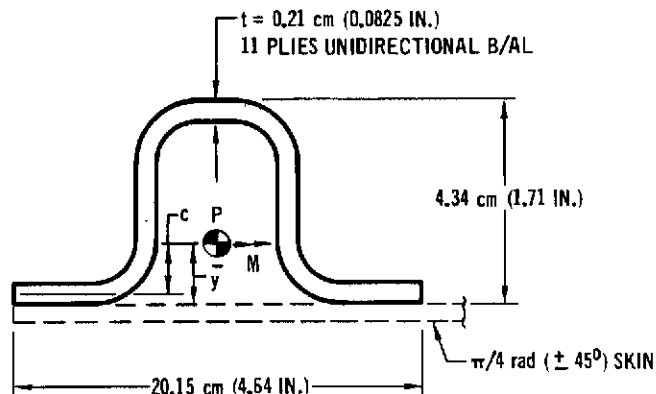
SECTION E–E OF FIGURE 2–88

STRINGER "C" CROSS SECTION AT X = 61 cm

Figure 2–89

UNIDIRECTIONAL STRINGER
WITH TITANIUM INTERLEAVES

.635 cm (.25 IN.) DIA.
HI–LOKS

$\pm \frac{\pi}{4}$ rad SKIN

SECTION B–B

13 PLIES 0 rad B/AL
1 PLY 6 AL–4V TITANIUM

2.92 cm (1.15 IN.)

$P_{APPLIED}$

P_{ALL}

SECTION D–D
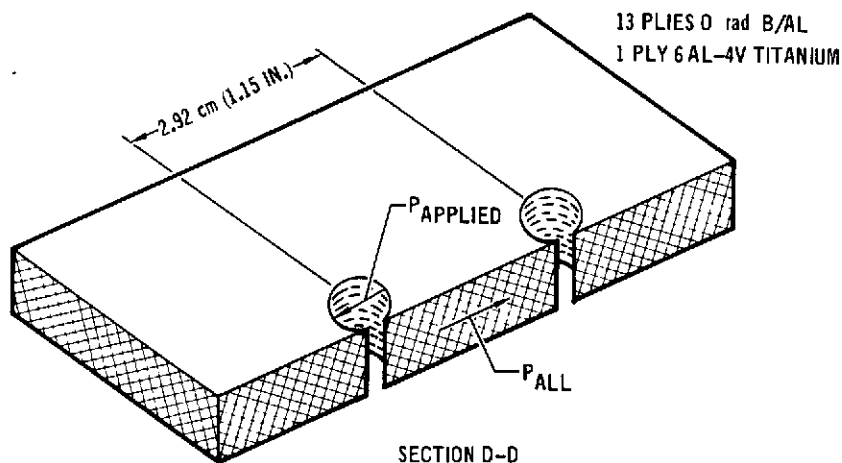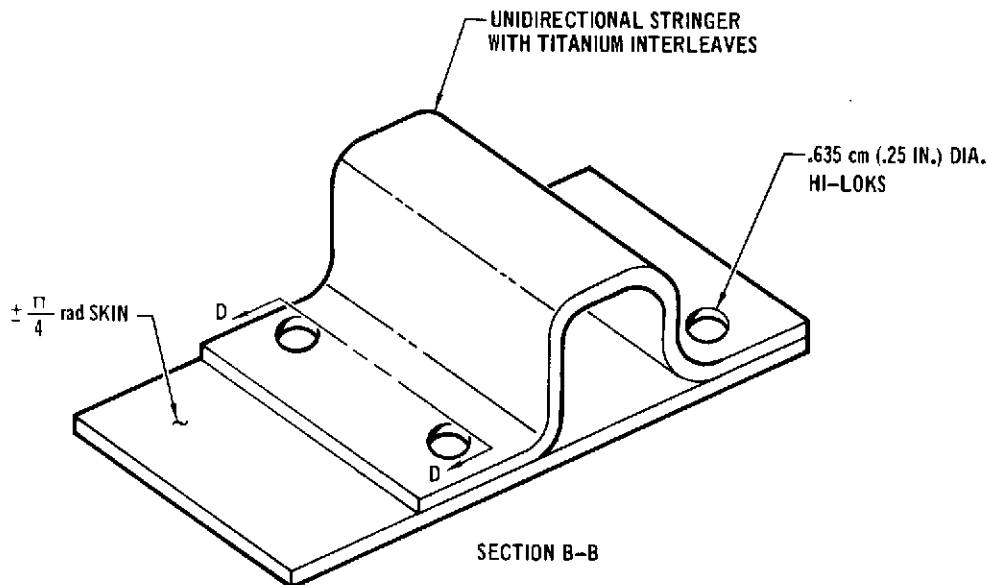
STRINGER "C" SINGLE SHEAR FAILURE PLANE

Figure 2–90
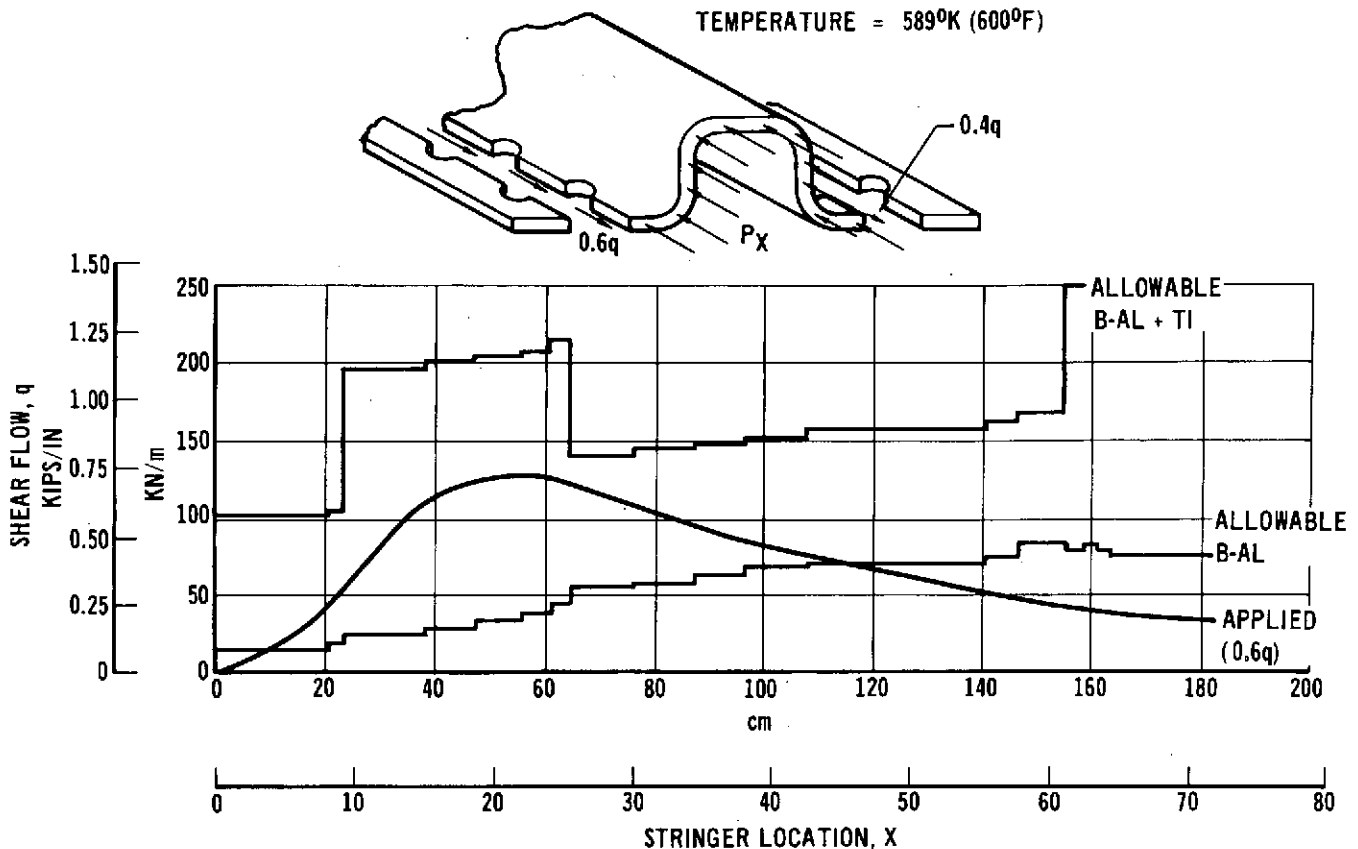
OUTBOARD STRINGER "C" IS CRITICAL AT X = 66 cm (26 IN.)
FOR IN PLANE SHEAR STRENGTH

Figure 2-91

Ultimate Strength Analysis of Skin at 589°K – Shear and biaxial stresses
acting on skin at location "C" (Figure 2-87) are shown in Figure 2-92. Shear
strength allowable of a $\pm \frac{\pi}{4}$ rad ($\pm$45°) midplane symmetric laminate is limited
by the transverse tensile strain allowable of the individual lamina. As
illustrated in Figure 2-93, adding compressive stresses to a $\pm \frac{\pi}{4}$ rad ($\pm$45°) laminate
loaded in shear reduces the transverse tensile strain. This condition allows the
application of additional shear loading to arrive at the same allowable transverse
tensile strain as the pure shear condition. Therefore, for the condition of shear
and biaxial compression, the margin of safety is conservative when the applied
shear stress is compared to a pure shear stress allowable for a laminate. Shear
strength allowable determined from tests at 589°K (600°F) is $F_{xy}^{s\mu} = 151$ MN/m^2
(21,900 psi), reference Figure 2-28.

$$M.S. = \frac{F_{xy}^{s\mu}}{F_{xy}^{s}} - 1 = \frac{151}{120} - 1 = .26$$

2-85

π/4 rad (45°)

F_x^c

F_{xy}^s

F_y^c

VIEW C
(REF FIG 2–87)
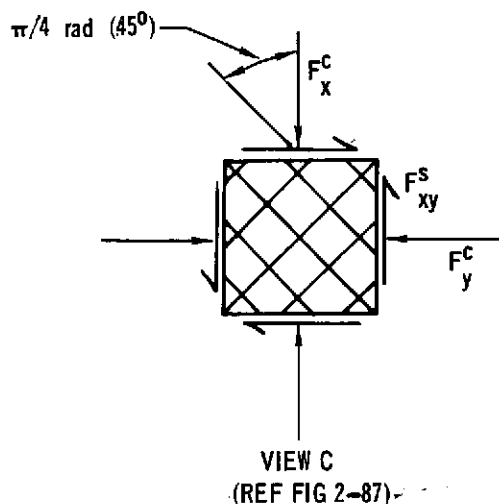
APPLIED ULTIMATE STRESSES

$F_x^c = 38.9$ MN/m^2 (5650 PSI)

$F_y^c = 36.8$ MN/m^2 (5350 PSI)

$F_{xy}^s = 120$ MN/m^2 (17400 PSI)

SKIN LAYUP

• ± π/4 rad (± 45°) B/AL WITH TITANIUM INTERLEAVES
• 44 B/AL PLIES – 0.819 cm (0.330 IN.)
• 4 TITANIUM PLIES – 0.076 cm (0.030 IN.) 6AL–4V ANNEALED

ULTIMATE STRENGTH ANALYSIS OF SKIN (589°K)

Figure 2–92

F_C

F_C

SHEAR COMPONENT   COMPRESSION COMPONENT

F_S

F_C

F_C

LONGITUDINAL AND TRANSVERSE TENSION
AND COMPRESSION ON THE LAMINA.

LONGITUDINAL AND TRANSVERSE COMPRESSION
AND SHEAR ON THE LAMINA.
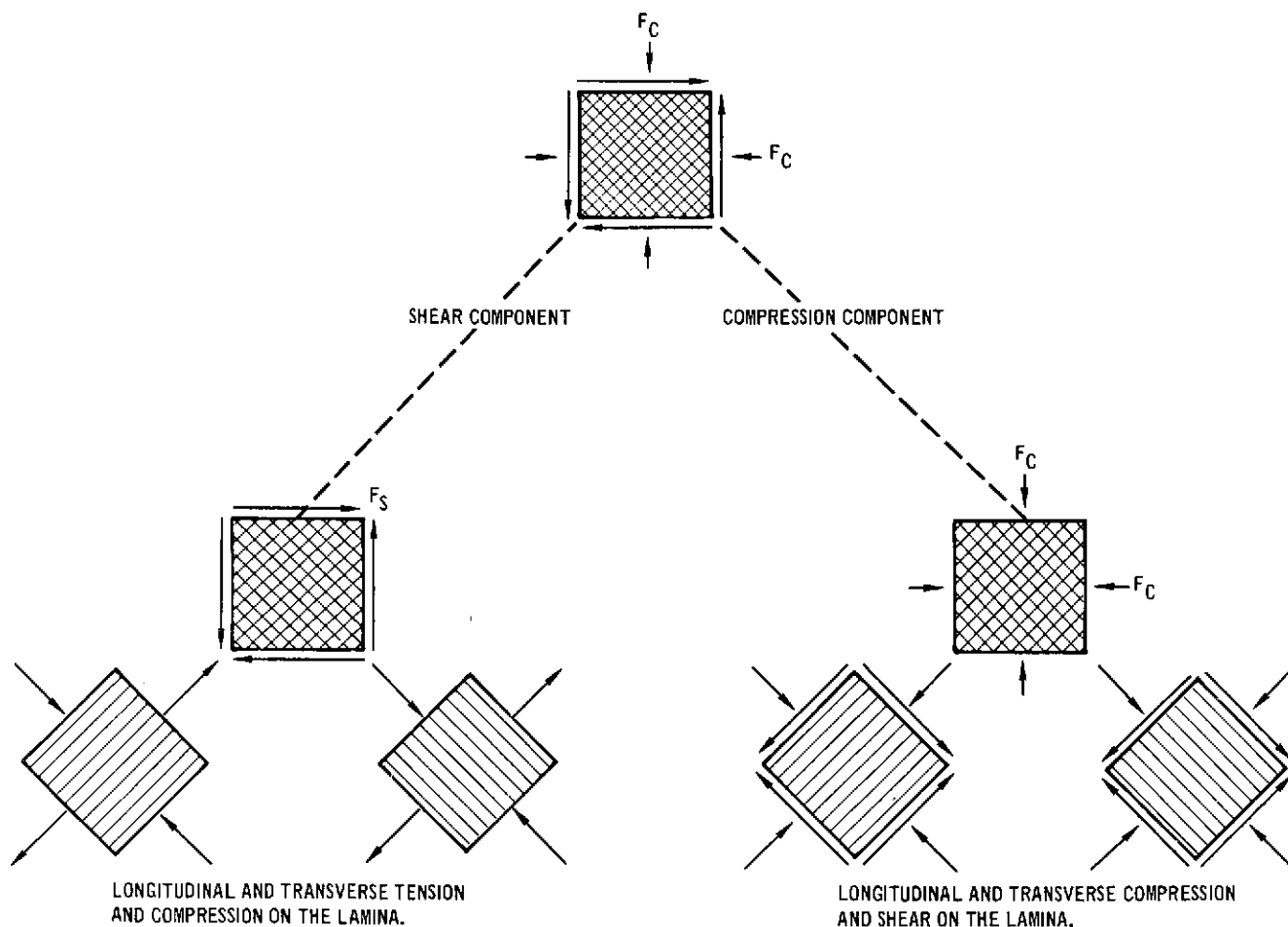
COMPRESSIVE STRESSES ON ± π/4 rad LAMINATE LOADED IN SHEAR
REDUCE LAMINA TRANSVERSE TENSILE STRESSES

Figure 2–93

Skin Buckling Analysis – Shear and biaxial stresses acting on the skin at location "D" (Figure 2-87) are shown in Figure 2-94. The allowable compressive buckling stress under the combined applied stresses is F_{xcr} = 73.8 MN/m^2 (10,700 psi) and was obtained utilizing the method of analysis given in Section 2.2.1.2. Margin of safety for buckling is

$$M.S. = \frac{F_{xcr}}{F_x^c} - 1 = \frac{73.8}{25.6} - 1 = 1.88$$

F_x^c = 25.6 MN/m^2 (3710 PSI)

F_y^c = 12.7 MN/m^2 (1850 PSI)

F_{xy}^s = 63.8 MN/m^2 (9270 PSI)

b = 8.29 cm (3.29 IN.)

a = 61 cm (24 IN.)

VIEW B
(REF FIG 2-87)
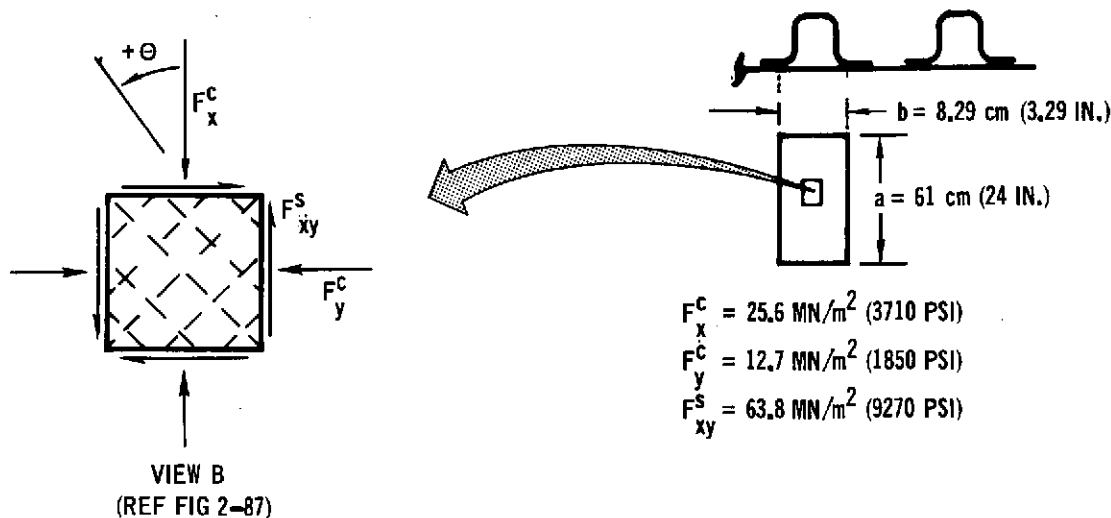
Applied Ultimate Stresses at 589°K (600°F)

0.019 cm
(0.0075 IN.
TYP)

TITANIUM
+ 45
- 45
- 45
+ 45

B/AL

₵ SYM
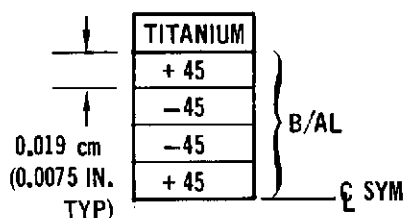
2 SURFACE PLIES
  6AL-4V TITANIUM (ANNEALED)
    E = 90.3 GN/m^2 (13.1 x 10^6 PSI)
    G = 35.2 GN/m^2 (5.1 x 10^6 PSI)   REF 8
    μ = 0.31

BORON ALUMINUM PLIES
  E_L = 185 GN/m^2 (26.9 x 10^6 PSI
  E_T = 37.5 GN/m^2 (5.45 x 10^6 PSI)   △1
  G_{LT} = 29.2 GN/m^2 (4.25 x 10^6 PSI)
  $μ_{LT}$ = 0.30

△1 BORON ALUMINUM PROPERTIES REPRESENT LAMINA SECANT STIFFNESS VALUES AT THE LAMINA STRESSES CORRESPONDING TO THE APPLIED STRESSES.

Skin Stacking Sequence and Properties

PROPERTIES FOR SKIN BUCKLING ANALYSIS

Figure 2-94

2.2.1.5 Compression Panel Weights – A weight summary of the 1.22m (48 in.)
wide by 1.83m (72 in.) long skin-stringer Compression Panel is shown in Figure
2-95. Total panel calculated weight is 95.51 kg (210.63 lbs) of which 43.67 kg
(96.34 lbs) is boron-aluminum structural elements including weight of all
titanium interleaves. As described earlier, frames and fittings were not optimiz-
ed for minimum weight and comprise a significant percentage (40%) of the total
panel weight.

MATERIAL	ITEM	NUMBER REQUIRED	WEIGHT (1)	
			kg	(LB)
BORON-ALUMINUM WITH TITANIUM INTERLEAVES	STRINGER ℄	1	6.39	14.10
	STRINGER A	2	6.17	13.62
	STRINGER B	2	5.02	11.08
	STRINGER C	2	5.24	11.56
	SKIN	1	20.85	45.98
STEEL	THRUST PLATE	1	2.32	5.12
	FRAMES	4	16.14	35.58
	FITTINGS	80	20.78	45.83
ALUMINUM	SHIMS	–	0.52	1.15
STEEL & TITANIUM	MECHANICAL ATTACHMENTS	–	12.08	26.64
		$\sum$	95,51	210.63

(Stringers through Skin bracketed: 43.67 kg / 96.34 LB)

(1) CALCULATED WEIGHTS

COMPRESSION PANEL WEIGHT SUMMARY

Figure 2-95

(Note: In the following two sections, Section 2.2.2 and Section 2.2.3, is
described work performed on the Truss Beam design and Shear Web Beam design
respectively. These designs represent two possible approaches to beam or transfer
primary Shuttle engine thrust loads from engine support points to the Shuttle
sidewall structure – of which the Compression Panel fabricated under this program
is a simulated part. The evaluation of these possible approaches under Phase II
was done to permit optimization or selection of the appropriate configuration
for this thrust support structure; hence, it is included under Phase II in this
report although unrelated the Compression Panel design itself).

2.2.2 <u>Truss Beam Design and Analysis</u> - Requirements for minimum weight and feasible
joint and lug design dictated the truss beam concept shown in Figure 2-96. Tubular
members with both circular and rectangular cross sections were evaluated. Although
a circular tube loaded in compression is lighter, this weight savings is more than
offset by the weight penalties of the complex and heavy fittings required for
joining circular tubes. Further, bending moments can be more efficiently carried
by rectangular members. Consequently, a rectangular member with variable cap width
is an efficient compromise when axial load, bending, joint requirements, and lug
design are all considered.

The truss beam compression members are rectangular tubes formed by braze
bonding two flat plate caps of variable width and thickness to two channel sections.
Tension members are integrally-constructed "I" sections which also have caps of
variable width and thickness. All members were designed to fit together with
only minimum use of shims.

Members are joined by mechanical fasteners through the caps where cap width
is increased locally to accomodate sufficient mechanical fasteners. This technique
eliminates heavy gusset members at joints and minimizes the number of mechanical
fasteners because selected highly loaded members are continuous through the joint.
Titanium interleaves are added in the joint areas to provide necessary bearing
strength. Lugs are formed by extending the cap members.

2.2.2.1 <u>Truss Beam Internal Loads Distribution</u> - Basic geometry and applied
loads for the truss structure are shown in Figure 2-97. Although the structure
is externally statically determinate, it is internally redundant because of fixed
joints, continuous members, and side loads applied at lugs 45.7 cm (18 in.) below
truss cap member. Initial member sizes were obtained assuming pinned joints and
an estimated internal moment distribution. These initial member sizes were used
in a finite element analysis of the structure to obtain final loads distribution.

A finite element model of the truss, Figure 2-98, was constructed using
bending bars connected by rigid joints for solution with CASD (Reference Section
2.2.1.2). External loads and moments were applied to the model as indicated in
Figure 2-98 and the resulting deflected shape and internal loads distribution
are shown in Figures 2-99 and 2-100. These internal loads were used to resize the
members in the final analysis. In addition, a reversed loading condition was
assumed for design of tensile members. Members AB and BC were designed for a
compressive load of 78.4 kN while members BD and BF were designed for 209 kN in
compression.
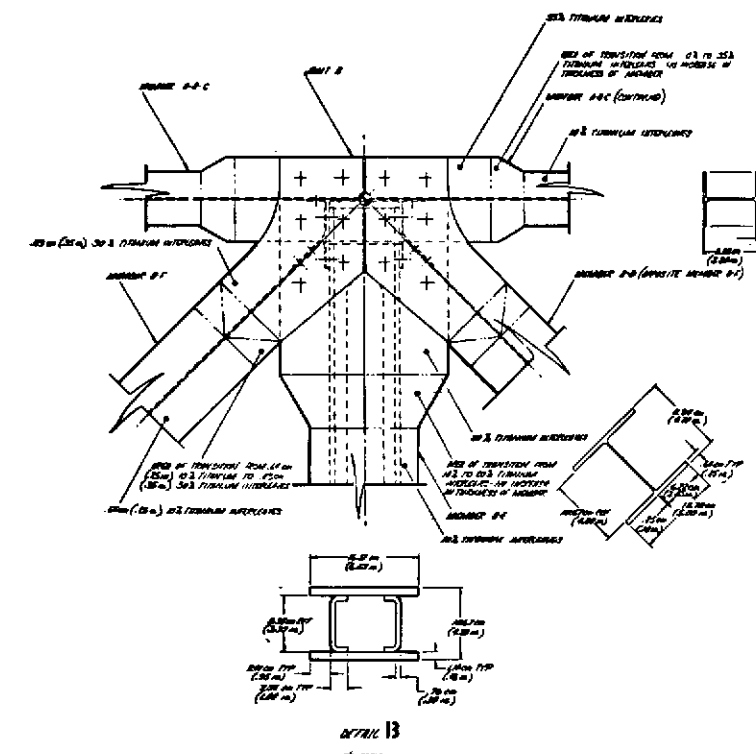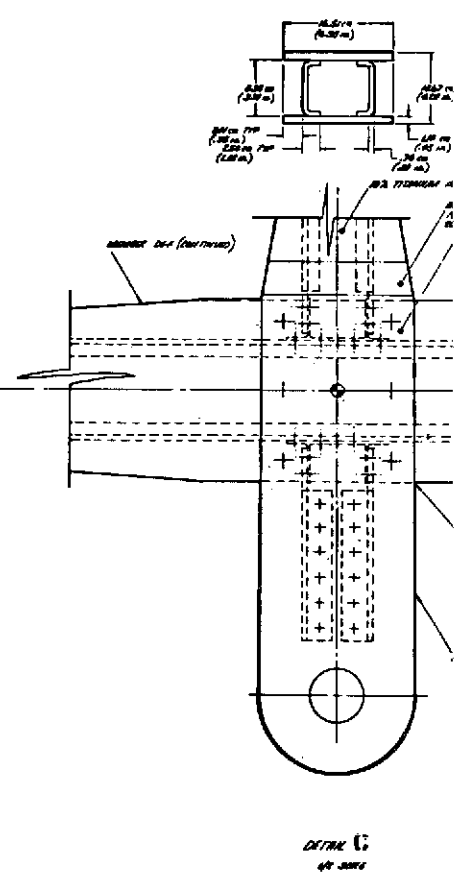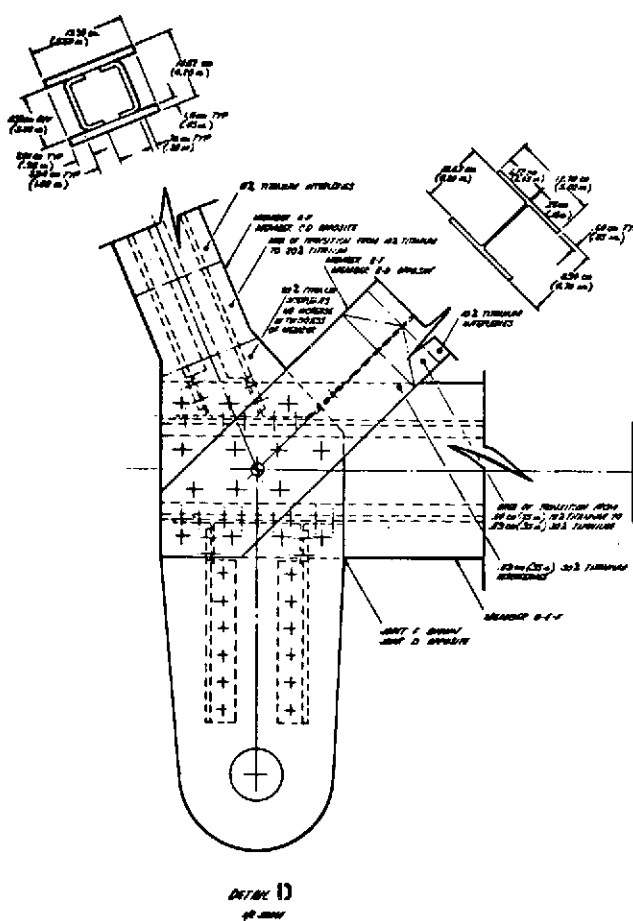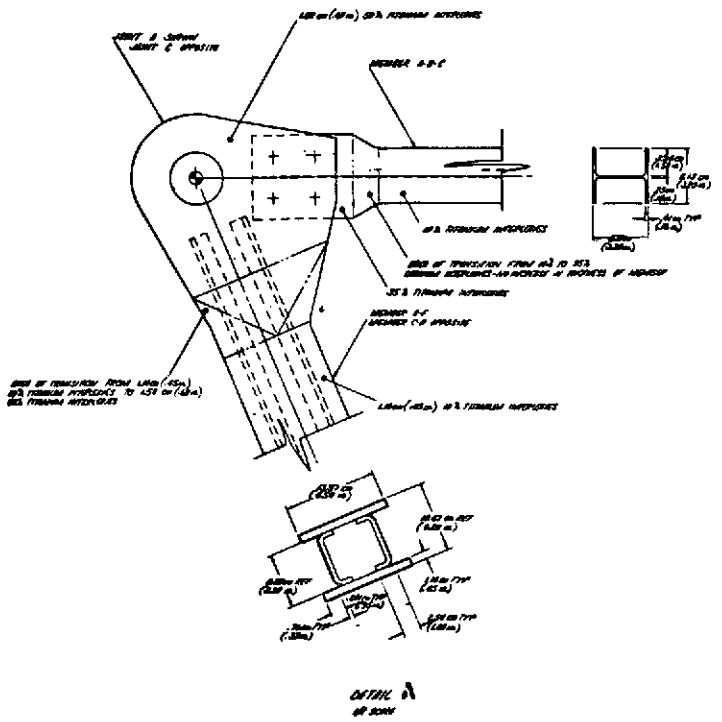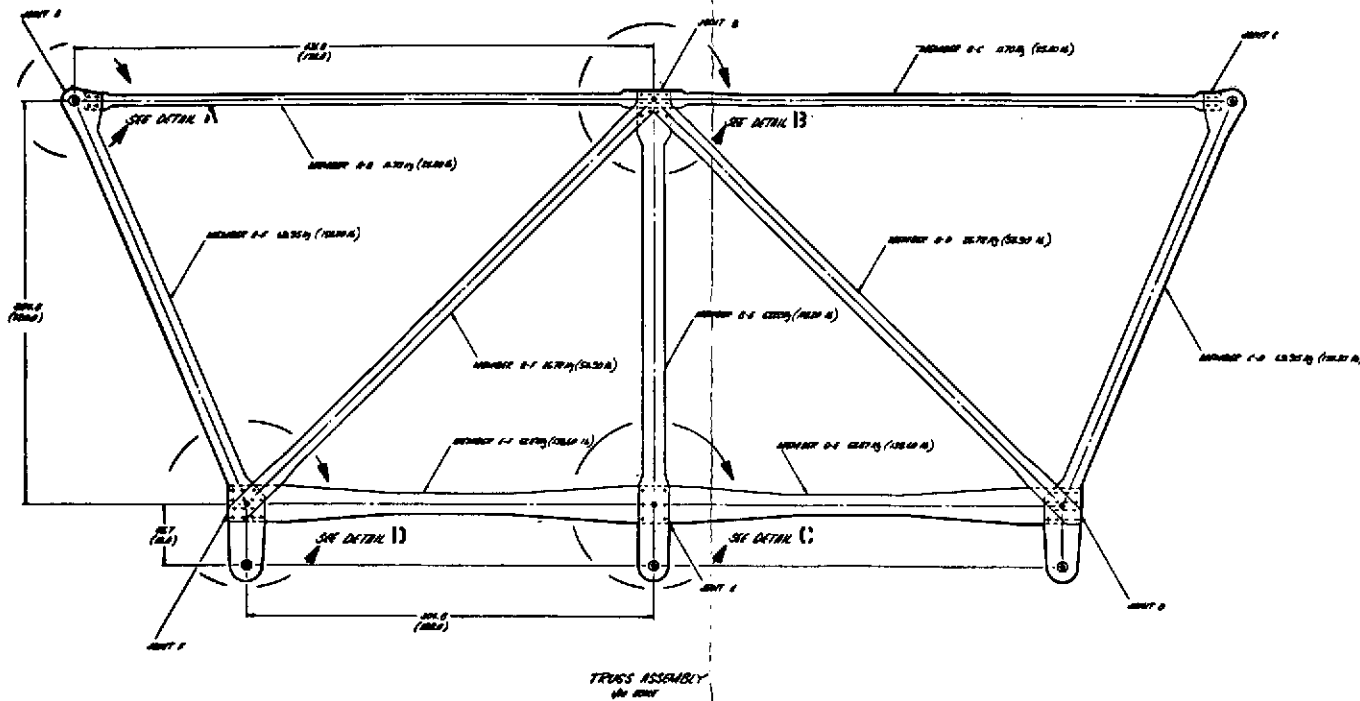
Figure 2-96
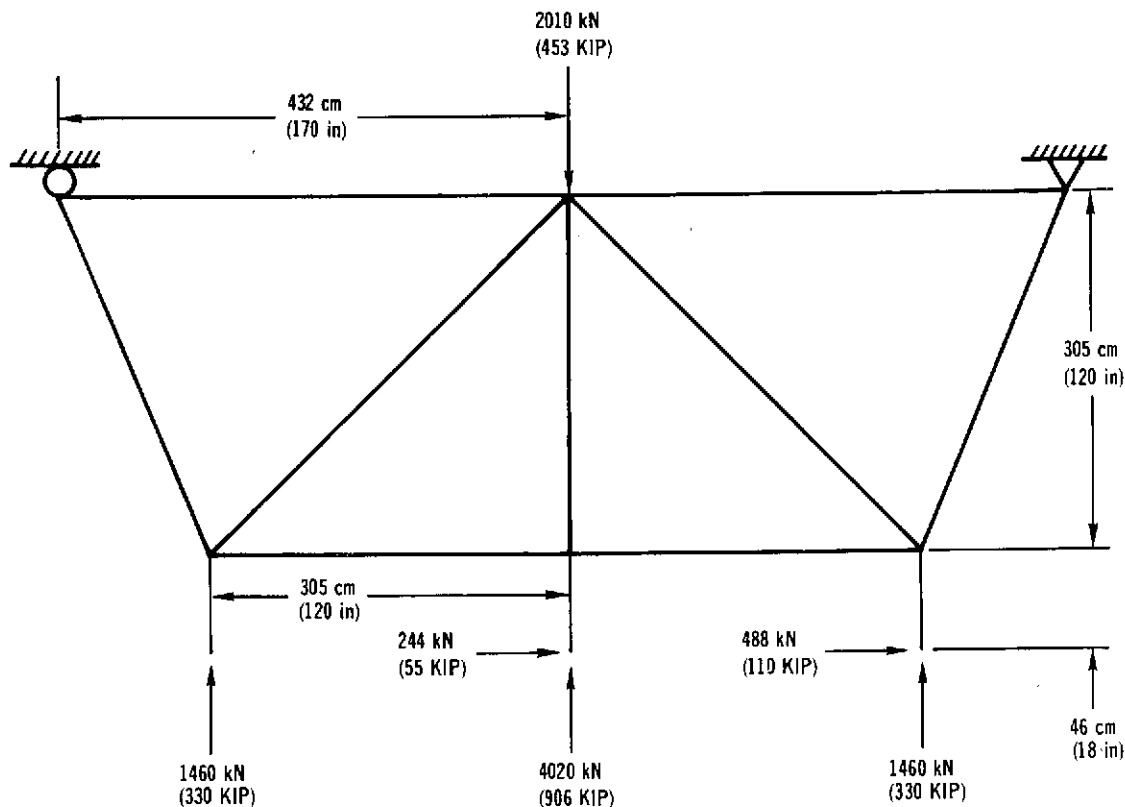
TRUSS BEAM GEOMETRY AND APPLIED LOADS

Figure 2–97
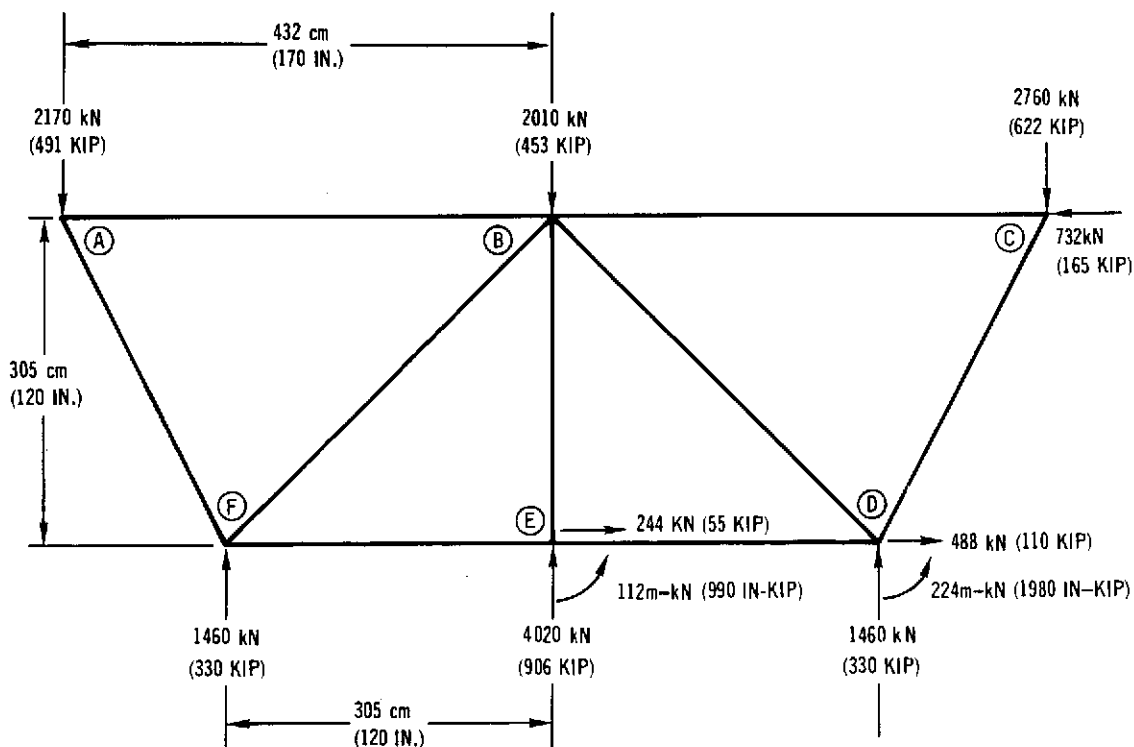
TRUSS BEAM FINITE ELEMENT MODEL WITH APPLIED LOADS

Figure 2–98
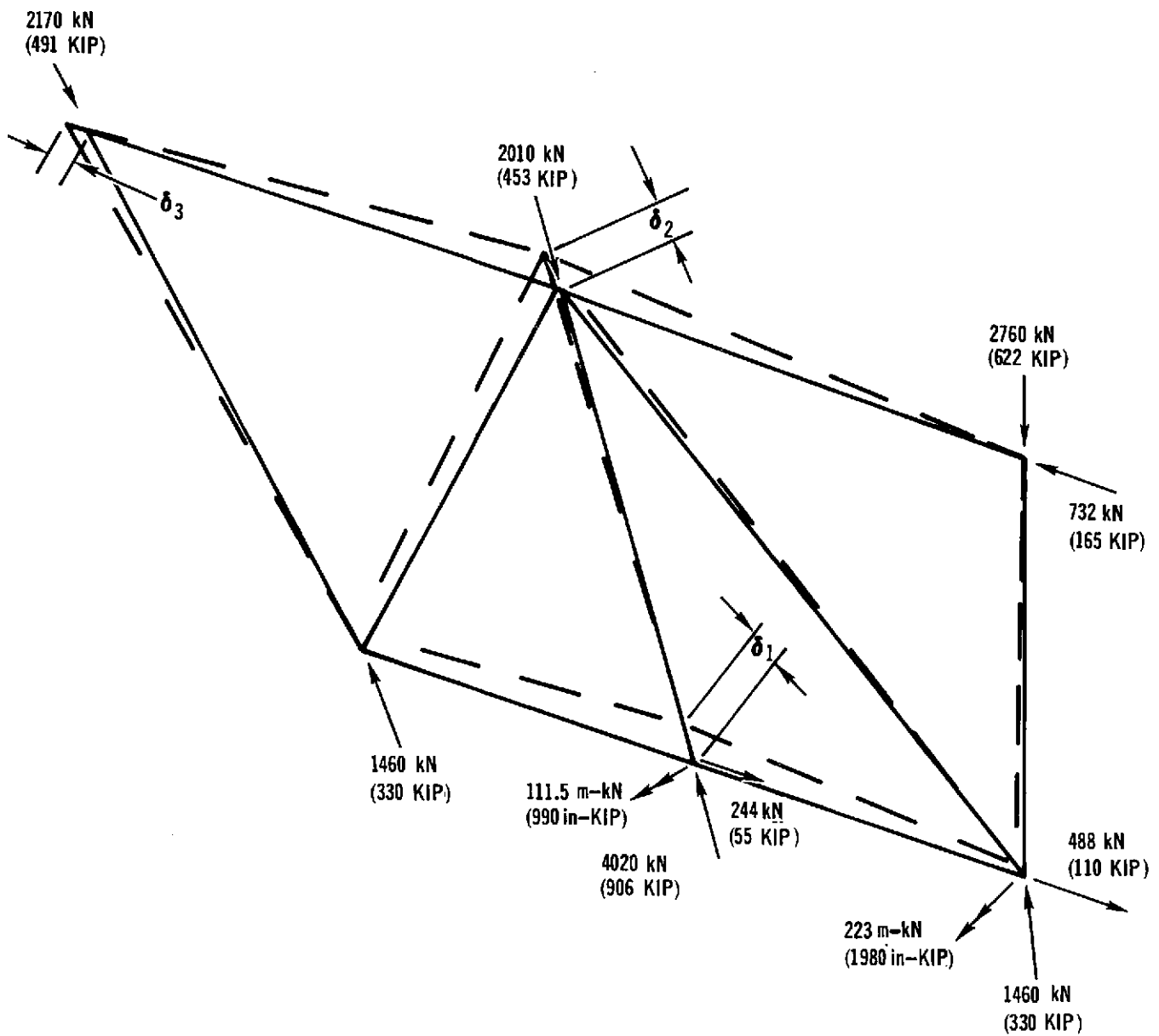
DEFLECTED SHAPE OF TRUSS BEAM

(FINITE ELEMENT ANALYSIS)

Figure 2-99
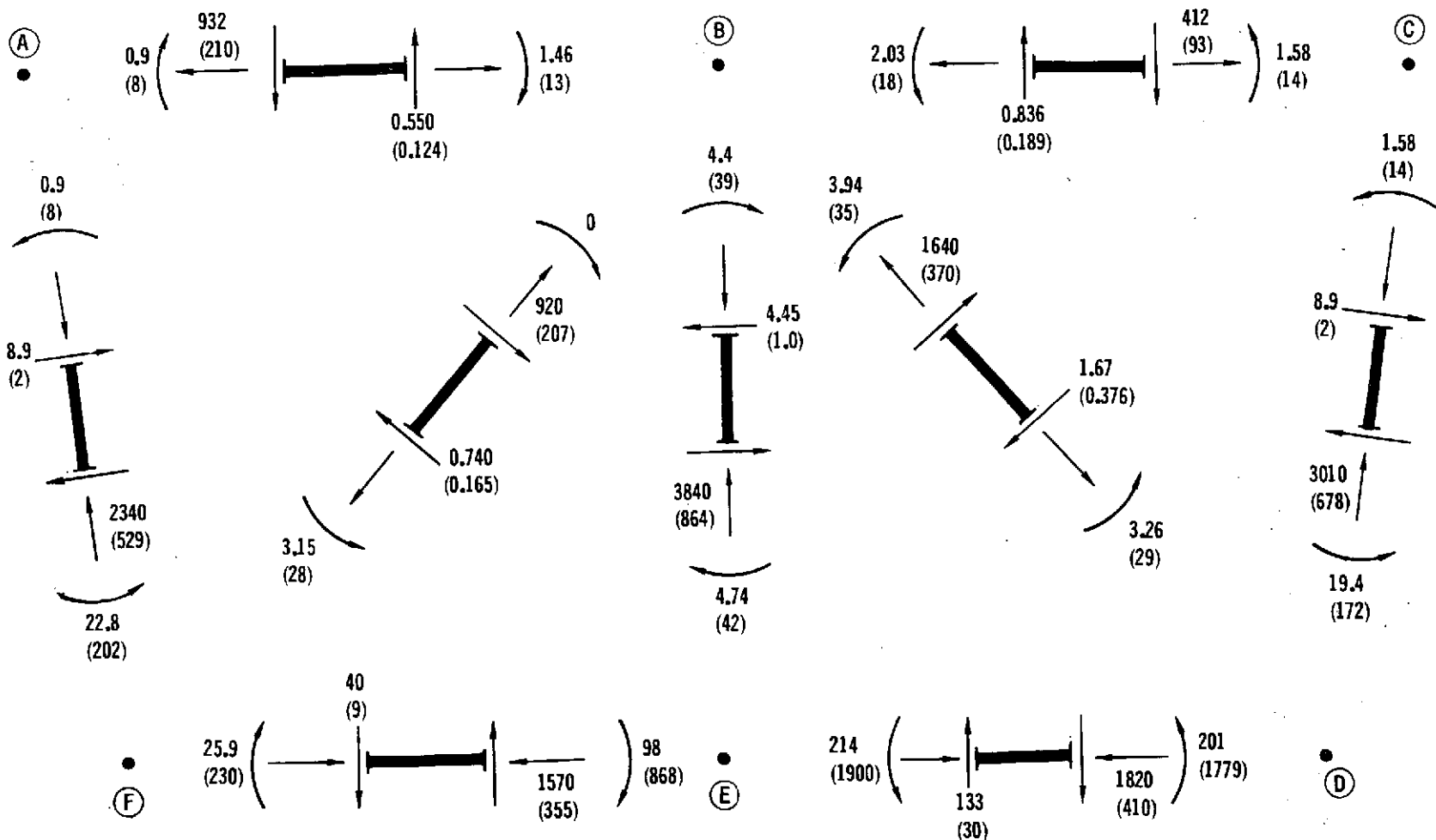
NOTE: LOADS ARE GIVEN IN kN OR (KIPS)
MOMENTS ARE GIVEN IN m–kN OR (IN-KIPS)

TRUSS BEAM INTERNAL MEMBER LOADS
(Finite Element Analysis)

2.2.2.2 <u>Detailed Strength Analysis</u> – Analysis of the truss structure required

no unusual analytical methods as all members were subjected to a simple combination

of compressive or tensile stress, shear stress and bending stress.

Tensile members contain sufficient area to carry tensile loads based on room

temperature ultimate tensile strength (1110.0 MN/m^2) of the material. Because

the compressive load for these members is small compared to the tensile load, the

required moments-of-inertia are small. As a result, when loaded in compression

they respond as slender columns and the allowable column load is given by the

Euler Column Formula:

$$P_{col} = \frac{\pi^2 E_L I_{min}}{L^2}$$

where, $\quad E_L$ = Elastic modulus in the longitudinal direction

$\quad\quad L$ = effective column length

$\quad I_{min}$ = minimum moment of inertia

Optimization of compression members for minimum weight involved the use of

Johnson's column formula to include interaction of primary flexural mode of failure

and local crippling mode.

$$P_{col} = P_{cc} \left[1 - \frac{P_{cc} L^2}{4\pi^2 E_L I_{min}} \right]$$

where $\quad P_{cc} = \sum_{i=1}^{n} F_{cc_i} b_i t_i$

and $\quad F_{cc_i}$ = crippling strength of the ith element

$\quad b_i$ = width of the ith element

$\quad t_i$ = thickness of ith element

$\quad L$ = effective column length

$\quad I_{min}$ = minimum moment of inertia

Crippling strength (F_{cc}) is based on test data for unidirectional boron-aluminum,

discussed in Section 2.1.2. For compression members which also carry high bending

moments, additional strength over that determined by the optimization procedure

was required. For these members, cap areas were increased as necessary to limit the combined compressive and bending stress to the crippling strength of the cap.

The final cross section geometry of each member was determined by an iterative process based on requirements for strength, stability and dimensional compatibility with other members. Centerline member B-E was used as the base member with other members sized for proper fit.

Analysis of compression member E-D is shown to illustrate checks made of each member in the truss. Member E-D has both high compressive and bending loads, as indicated by the shear, moment and axial load diagram shown in Figure 2-101. The cross section A-A shown in Figure 2-102 is that of the center one-third of the member. Since this member must fit inside the caps of member B-E, its depth is established at 8.38 cm (3.30 in.). As a result, this section has more than adequate stability to resist column buckling about the y-axis. However, the section must also have sufficient strength to carry axial load and bending about the x-axis. Section A-A has the following properties related to the x-axis,

$$A = 52.8 \text{ cm}^2 \ (8.2 \text{ in.}^2)$$
$$I_x = 1165 \text{ cm}^4 \ (28.0 \text{ in.}^4)$$
$$\bar{y} = 6.35 \text{ cm} \ (2.5 \text{ in.})$$

From Figure 2-101, the maximum ultimate axial and bending loads acting on Section A-A are,

$$P = 1820 \text{ kN} \ (410 \text{ KIP})$$
$$M = 78 \text{ m-kN} \ (700 \text{ in. - KIP})$$

Substitution of these values in the following equation for determining maximum axial stress yields,

$$F = \frac{P}{X} + \frac{M\bar{y}}{I_x}$$
$$= 345 + 430 = 775 \text{ MN/m}^2 \ (112.5 \text{ KIP/in.}^2)$$

The allowable crippling strength of cap elements at Section A-A is

$$F_{cc} = 1040 \text{ MN/m}^2 \ (150 \text{ KIP/in.}^2)$$

Therefore, the margin of safety for Section A-A is,

$$M.S. = \frac{F_{cc}}{F} - 1$$
$$= 1.33 - 1 = .33$$

A similar analysis performed at the end of member E-D where the moment is 214 m-kN results in a margin of safety of .08.

2-95
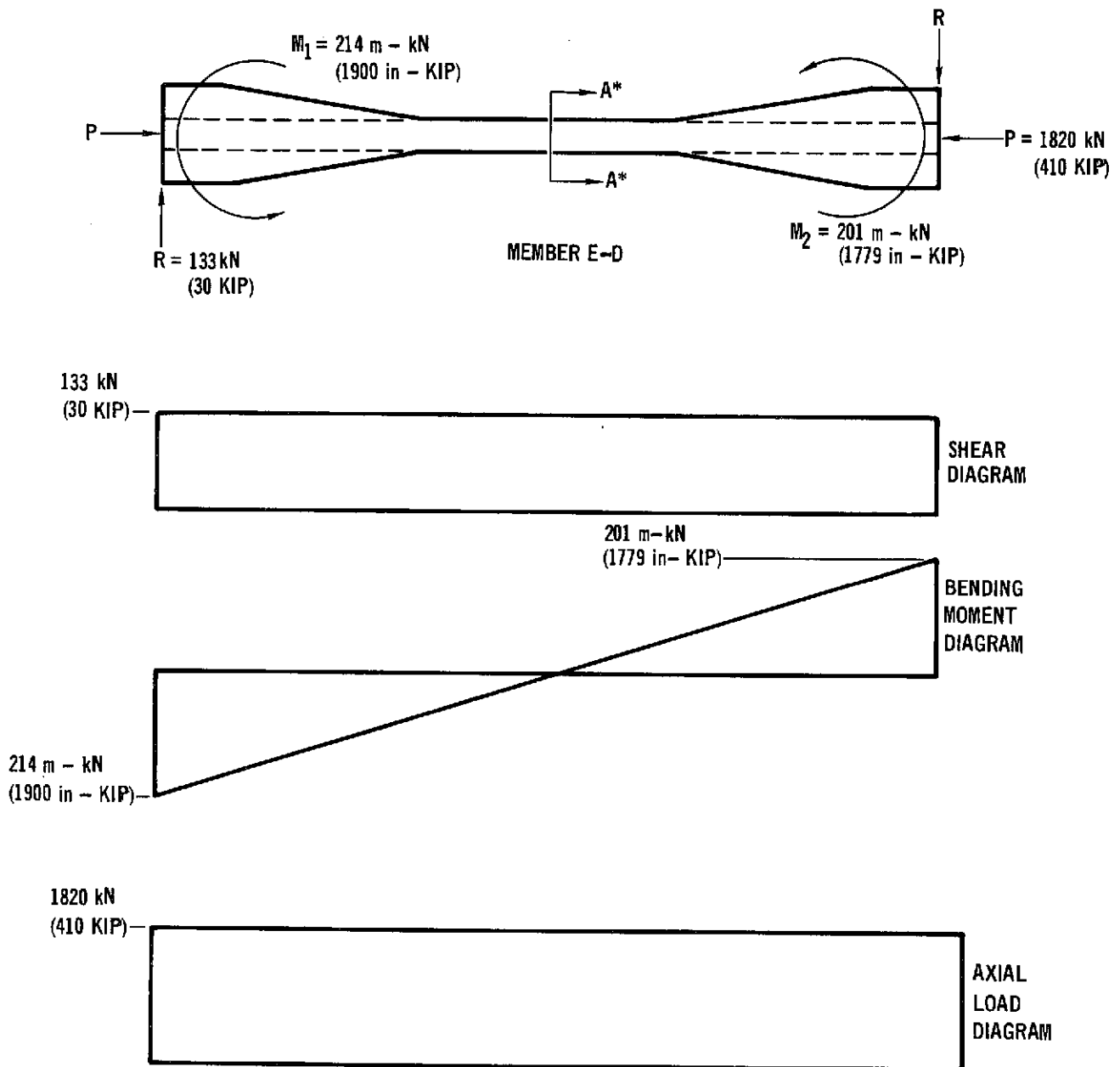
MEMBER E-D INTERNAL LOADS

*SEE FIGURE 2-102
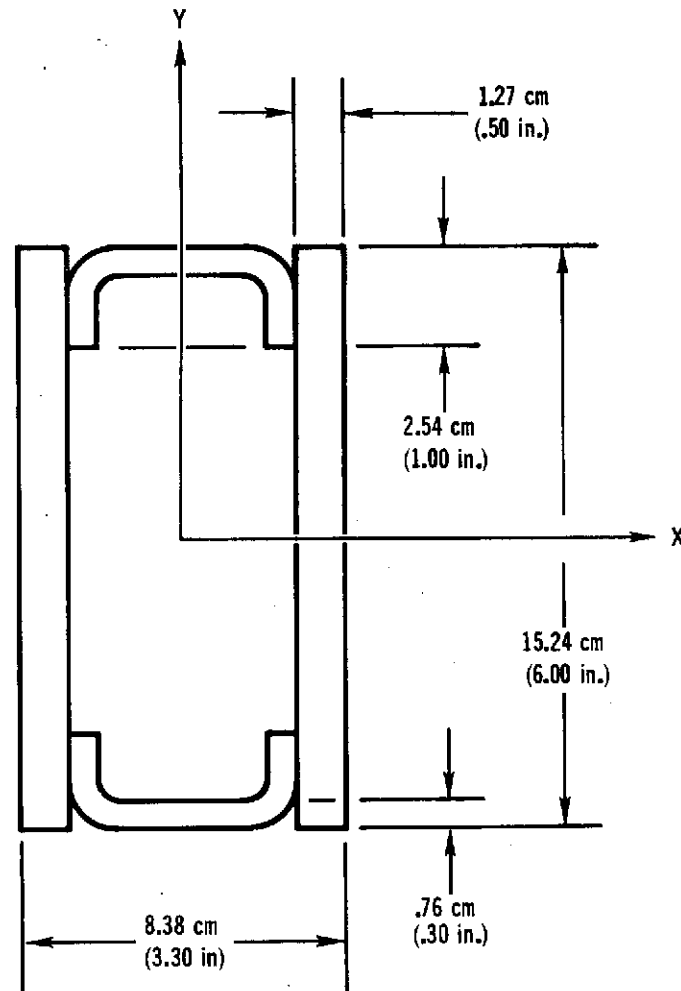
Figure 2-101

**TRUSS MEMBER E-D CROSS SECTION GEOMETRY
SECTION A-A (FIGURE 2-101)**

Figure 2-102

2.2.2.3 <u>Truss Beam Weight Summary</u> - The following distribution of estimated
weight for the truss structure includes the use of titanium interleaves, titanium
fittings, and steel fasteners. It does not include weight for contingencies or
nonoptimum factors.

Individual Members:			
	B-A	11.70 kg	(25.80 lb)
	B-C	11.70 kg	(25.80 lb)
	A-F	69.95 kg	(154.20 lb)
	C-D	69.95 kg	(154.20 lb)
	B-F	26.79 kg	(58.90 lb)
	B-D	26.79 kg	(58.90 lb)
	E-F	62.87 kg	(138.60 lb)
	E-D	62.87 kg	(138.60 lb)
	B-E	67.22 kg	(148.20 lb)
Fasteners:		28.95 kg	(64.00 lb)
Web Fittings and Shear Clips:		20.30 kg	(45.00 lb)
Total Weight:		459.1 kg	(1012.2 lb)

2.2.3 <u>Shear Web Beam Design and Analysis</u>

Selection of the shear web beam design shown in Figures 2-103 and 2-104 was
based on an investigation of the following shear panel configurations:

(1) an unstiffened $\pm$ π/4 rad ($\pm$45°) laminated skin

(2) a stiffined $\pm$ π/4 ($\pm$45°) laminated skin

(3) an unstiffened, braze bonded honeycomb sandwich with $\pm$ π/4 rad ($\pm$45°)
     face sheets and titanium core

(4) a stiffened, braze bonded honeycomb sandwich

The unstiffened braze bonded honeycomb sandwich configuration was selected
because it was lighter and easiest to fabricate. Use of titanium honeycomb core
rather than aluminum honeycomb core allows the face sheet plies to be eutectically
bonded at the same time the face sheets are braze bonded to the core. Each face
sheet on the two outboard shear panels is a six ply [+45°, ti, -45°]$_s$ laminate
while each face sheet on the inboard panels is a three ply [+45°, ti, -45°]
laminate. Titanium interleaves are used in the face sheets to increase in-plane
shear strength. The titanium honeycomb core for all panels is 2.54 cm (1 in.)
thick and has a density of 78.5 kg/m^3 (4.9 lb/ft^3).

Vertical stiffening members of the beam are formed by joining two unidirectional
boron aluminum hat sections to edge members on the shear panels as shown in Figure
2-104. Since three of the vertical members are also subjected to in-plane bending
moments, these members have a cap added to the crown of the hat section. The

Figure 2-103

caps are extended to form lugs at the load introduction end of the structure. Vertical members are tapered in height, width, and thickness, commensurate with axial load distribution, to achieve minimum weight.

Both the compression and tension caps are constant width channel sections tapering in thickness as permitted by axial load distribution.

2.2.3.1 <u>Shear Web Beam Internal Loads Distribution</u> - Basic geometry and external loads applied to shear web beam are shown in Figure 2-105. Loads applied to the three inboard vertical members are reacted by the two outboard vertical members and the lower cap member. For these reactions, the structure is externally statically determinate.
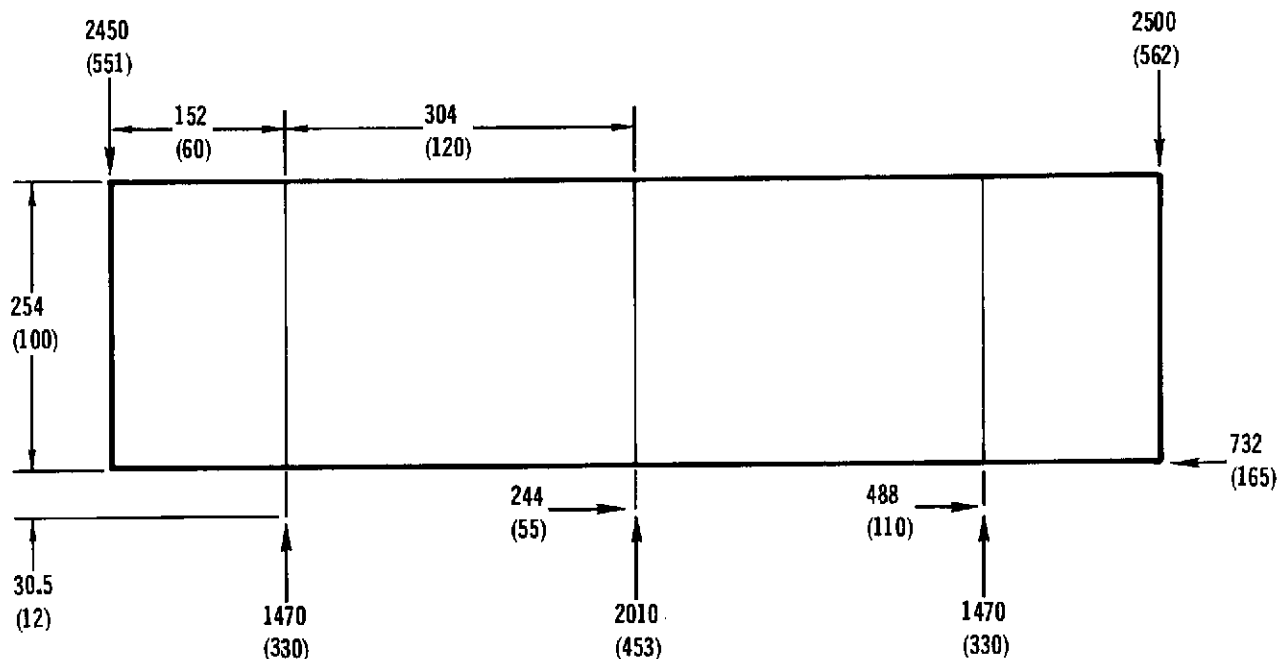
NOTE: LOADS ARE GIVEN IN kN OR (KIPS)
      LENGTHS ARE GIVEN IN cm OR (IN.)

SHEAR WEB BEAM GEOMETRY AND EXTERNAL LOADS

Figure 2-105

The internal loads distribution used in sizing the shear web members is shown in Figure 2-106. This distribution is based on the assumption that bending moments caused by eccentrically applied external side loads are carried entirely by the three inboard vertical members.

2.2.3.2 <u>Detailed Strength Analysis</u> - Face sheets of honeycomb sandwich structures loaded in shear are designed primarily on the basis of strength. The honeycomb core density and cell size are selected to preclude local instability
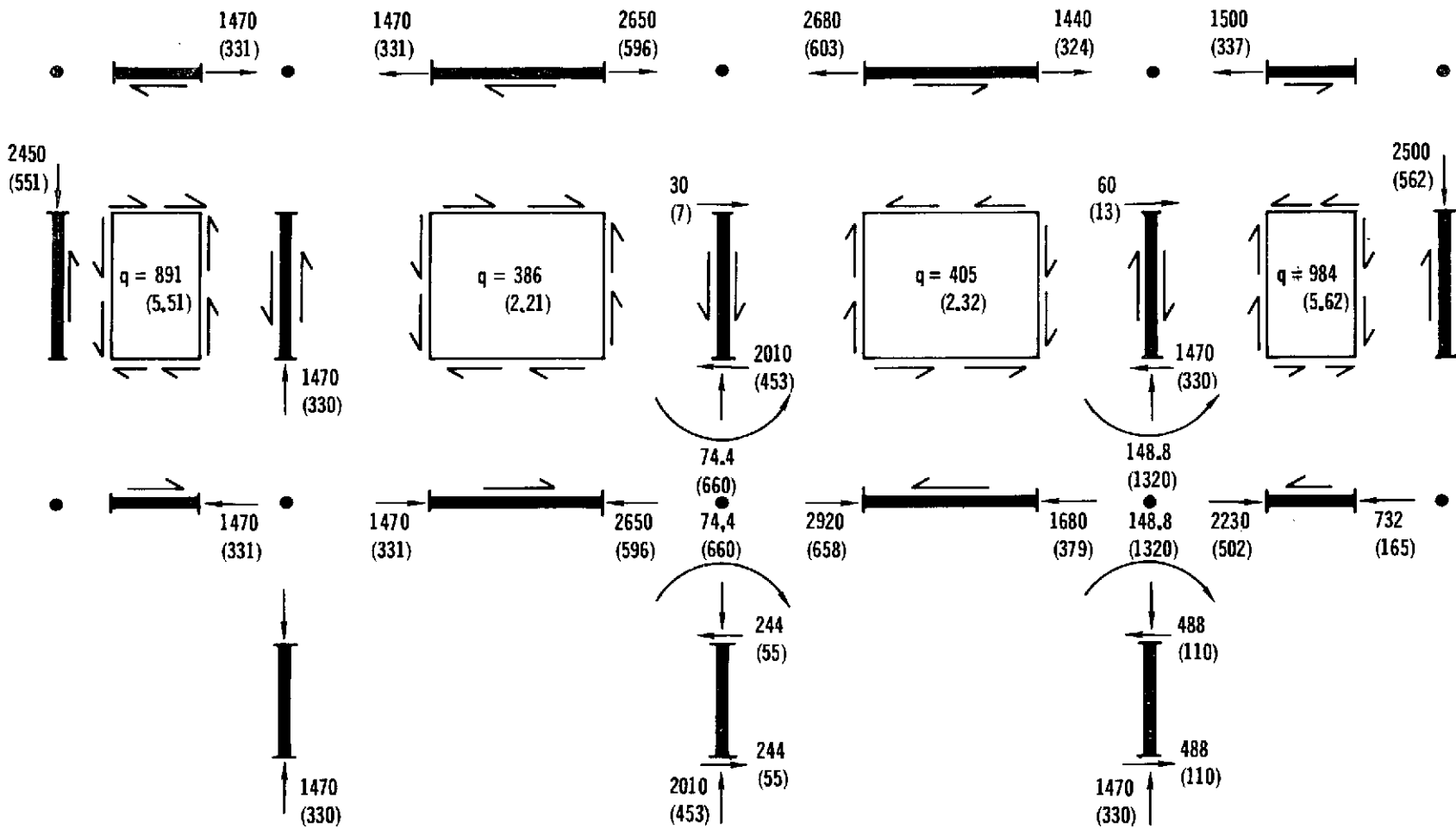
NOTE: AXIAL LOADS ARE GIVEN IN kN OR (KIPS)
MOMENTS ARE GIVEN IN m–KN OR (IN-KIPS)
SHEAR FLOWS ARE GIVEN IN kN/m OR (KIPS/IN.)

SHEAR WEB BEAM INTERNAL MEMBER LOADS

failures of face sheets such as wrinkling and intracell buckling. Core thickness
is selected to prevent overall shear buckling of the panel.

Based on an ultimate strain failure criteria, it can be shown analytically
that the shear strength of a $\pm$ $\pi/4$ rad ($\pm 45°$) laminate is directly proportional to
the transverse tensile strain capability of the plies. Tests have verified that
titanium interleaves will improve the transverse tensile strength of unidirectional
boron-aluminum and the effect of adding one titanium ply to four boron aluminum
plies is shown in Figure 2-107. A comparison of the stress-strain response curves
shows that the transverse strength is improved by a factor of three and, of more
significance, the ultimate strain increases from about 3300 μ m/m to more than
12000 μ m/m.

Improvement in transverse ultimate strain using titanium interleaves is
expected to have a marked effect on shear strength of $\pm$ $\pi/4$ rad ($\pm 45°$) laminates.
Since shear strengths of 297 MN/m^2 (43 KSI) were consistently obtained in rail
shear tests of $\pm$ $\pi/4$ rad ($\pm 45°$) laminates without titanium reinforcement (Reference
Section 2.1.2), a significantly higher shear strength may be anticipated when
titanium interleaves are used. Therefore, a shear strength of 448 MN/m^2 (65 KSI)
was used to determine face sheet thicknesses of the shear panels.

The overall thickness of the shear panels is determined by stability require-
ments. Core thickness is selected such that the applied shear flow q is equal to
or less than the shear flow causing buckling, q_{cr}.

$$q_{cr} = (\tfrac{2}{b})^2 \; (D_{11}D_{22}^3)^{1/4} \; (8.125 + \tfrac{5.05}{\theta}); \text{ if } \theta > 1$$

Or: $\quad q_{cr} = (\tfrac{2}{b})^2 \; \sqrt{D_{22}(D_{12} + 2D_{66})} \; x \; (11.7 + .532\,\theta + .938\theta^2); \text{ if } \theta < 1$

where, $\qquad \theta \;=\; \sqrt{D_{11}D_{22}}\big/(D_{12} + 2D_{66})$

$\qquad\qquad$ b $\;=$ shear panel width

$\qquad\qquad$ D_{ij} $=$ honeycomb sandwich stiffness coefficients (includes
$\qquad\qquad\qquad$ core and face sheets)

Caps and vertical members loaded in compression or tension were analyzed using
the same procedures discussed in Section 2.2.2.2. Although members loaded in
compression and bending are stabilized in-plane by the shear panels, they were
sized to prevent out-of-plane instability failure as well. Applied compressive
and bending loads reduce linearly in these members as load is introduced into the
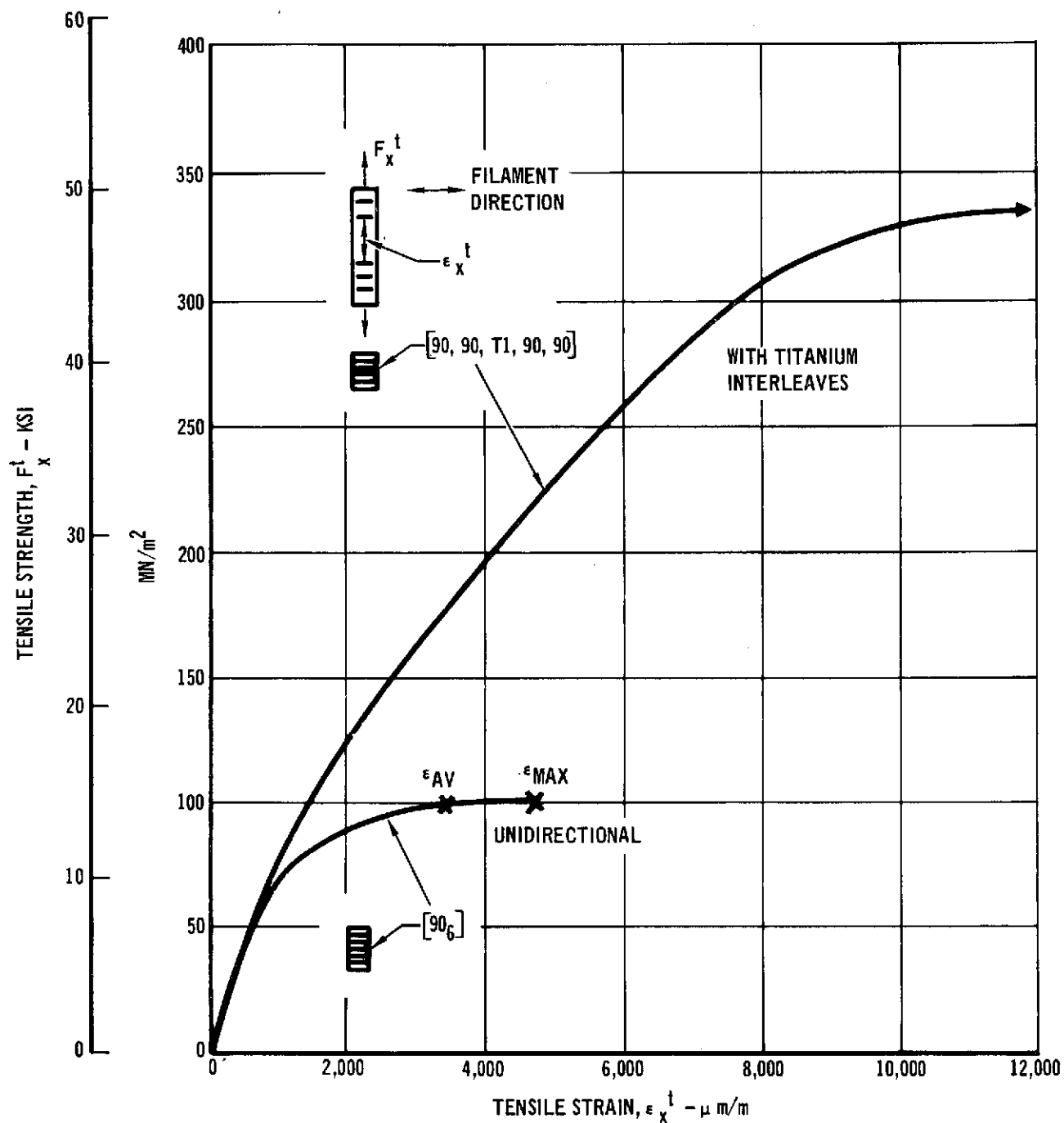
TITANIUM INTERLEAVES IMPROVE TRANSVERSE TENSION FAILURE STRAINS

Figure 2-107

MCDONNELL DOUGLAS ASTRONAUTICS COMPANY - EAST

shear panels. Consequently, both the moment of inertia and cross sectional area have been reduced accordingly by tapering the section.

The outboard shear panel experiencing the highest shear load is selected for analysis to illustrate primary checks made of all shear panels. Each six ply face sheet has a thickness (t_f) of .114 cm (.045 in.) and an ultimate shear strength, F_{xy}^{su}, of 448 MN/m^2 (65 KSI). Therefore, the allowable shear flow, q_{all}, is,

$$q_{all} = F_{xy}^{su} (2t_f)$$

$$= 1.02 \text{ MN/m (5.85 KIP/in.)}$$

From Figure 2-106, the applied shear flow, q, in this panel is

$$q = .984 \text{ MN/m (5.62 KIP/in.)}$$

Therefore, the margin of safety for face sheet strength is,

$$\text{M.S.} = \frac{q_{all}}{q} - 1 = \underline{.04}$$

To determine shear buckling strength of the panel, the equation given above for the case where $\theta < 1$ is used,

$$q_{cr} = (\frac{2}{b})^2 \sqrt{D_{22}(D_{12} + 2D_{66})} [11.7 + .532\theta + .938\theta^2]$$

The outboard shear panel has the following properties;

$$b = 1.52 \text{ m (60 in.)}$$

$$D_{11} = D_{22} = 47.4 \text{ m} - \text{kN (420 in.-KIP)}$$

$$D_{12} = 14.2 \text{ m} - \text{kN (126 in.-KIP)}$$

$$D_{66} = 25.4 \text{ m} - \text{kN (225 in.-KIP)}$$

$$\theta = .730$$

Substitution of these values into the buckling equation, yields the following,

$$q_{cr} = 1.20 \text{ MN/m (6.90 KIP/in.)}$$

The margin of safety for shear buckling is,

$$\text{M.S.} = \frac{q_{cr}}{q} - 1 = \underline{.22}$$

2.2.3.3 <u>Shear Web Beam Weight Summary</u> - The following distribution of estimated weights for the shear web structure includes the use of titanium inter-leaves, shear panel edge members, and fasteners. Weight for contingencies and nonoptimum factors is not included.

Outer Shear Panels:	60.5 kg	(133.4 lb)
Inner Shear Panels:	80.5 kg	(177.9 lb)
Inner Vertical Members:	110.0 kg	(243 lb)
Outer Vertical Members:	27.5 kg	(60.8 lb)
Compression Cap:	64.8 kg	(142.7 lb)
Tension Cap:	20.8 kg	(46.1 lb)
Fittings and Shear Clips:	48.4 kg	(106.5 lb)
Fasteners:	8.6 kg	(19 lb)
Total Weight:	421.1 kg	(929.4 lb)

2.3 Phase III - Process Technology Development

The objective of this phase of the program was to improve the procedures and techniques used to fabricate boron-aluminum structural components. Within this phase the development work was divided into four major tasks. These were:

° Improvement of the eutectic bonding process

° Improved manufacturing methods

° Metallurgical joining development

° Preparation of process specifications

Results of studies conducted in each of these areas are summarized in this section.

2.3.1 Eutectic Bonding Process Development - Eutectic bonding is a diffusion brazing process developed by MDAC-E for fabricating B/Al structural components from monolayer foil. This process relies on the diffusion of a thin surface film of copper into the aluminum matrix to form a liquid phase when heated above the copper-aluminum eutectic temperature of 821°K (1018°F). The basic bonding parameters had been defined and the process feasibility demonstrated prior to the onset of this program. Therefore, development studies undertaken in this program were directed toward the optimization of the process to ensure successful fabrication of the compression panel and test components. The process optimization was concerned with chemical cleaning and copper coating of monolayer foils and the selection of bonding conditions to minimize fiber degradation. In addition, the ability to include titanium interleaves in eutectic bonded laminates was demonstrated.

2.3.1.1 Optimization of Chemical Cleaning - Chemical cleaning is important in eutectic bonding for several reasons. Clean surfaces are required to ensure adherence of copper during the subsequent vapor deposition process and to permit free atomic movement during the diffusion process which results in the formation of a liquid phase and metallurgical joining of adjacent monolayers. Also, surface films due to lack of cleaning, present at the time of copper coating, could be trapped in the joint area and, if present in sufficient quantities, could lower joint properties.

The approach to improving the cleaning process consisted of rating several standard cleaning solutions according to their ability to remove surface films and the rate at which they dissolved aluminum. An "optimum" method was selected on the basis of these ratings. Then, the rate of film build-up was related to

environment to establish storage conditions and time limits for monolayer foils after cleaning and before coating.

Selection of a Test Method - Several standard cleaning procedures were used during the initial development of eutectic bonding to prepare boron-aluminum mono-layer foils for coating. Also, efforts were made to compare them and select an optimum process. However, initially, the principal test method employed was peel-testing of bonded samples. This approach was considered to be of limited value because the cleaning methods could not be rated quantitatively. Also, the bonding process itself may have introduced other variables, unrelated to cleaning, and influenced peel strength. A better method of comparing the effectiveness of various cleaning methods was needed to optimize the processing of boron-aluminum foils. The method selected for this program was to measure the residual film thickness, assumed to be an oxide, immediately after cleaning. Ellipsometry was selected as the technique for measuring these thin films, and 1100-0 aluminum foil was used for test specimens.

An ellipsometer is an optical instrument which has sufficient sensitivity to detect a single layer of adsorbed oxygen or oxide molecules on a metallic surface. This high degree of sensitivity made it an ideal instrument for comparing cleaning solutions by measuring residual film thickness. Ellipsometry measures changes in the polarization of monochromatic light upon reflection at an optical boundary. The magnitude of the change can be used to calculate the thickness of surface films provided the composition and optical properties of the film and substrate are known. A photograph of the ellipsometer is shown in Figure 2-108.

Comparison of Cleaning Processes - A standard method of cleaning aluminum alloys for removal of surface oxides consists of solvent or vapor degreasing followed by alkaline cleaning to remove soil and finally acid pickling or deoxidiz-ing to remove smut and oxide films. Several commercial cleaners and deoxidizers are approved for use at MDAC-E and are listed as options in various process specifications for cleaning aluminum. These materials were compared to determine if any particular combination of alkaline cleaner, deoxidizer and immersion time was superior from the standpoint of residual film thickness. Three alkaline cleaners plus four deoxidizers were evaluated, and the immersion times were varied to provide 108 combinations of cleaning procedures. Triplicate specimens of 1100-0 aluminum, .15 mm (.006-in.), were tested under each condition. The cleaning solutions and test conditions are listed in Table 2-1 and are summarized as follows:

Alkaline Cleaner		Deoxidizer	
Solution	Time (min.)	Solution	Time (min.)
Turco 4215S	5, 17, 30	Amchem 7	3, 6, 10
Turco 4090	5, 17, 30	4 Acid Type	3, 6, 10
Pennsalt 85	5, 17, 30	Smut Go #1	3, 6, 10
		Acid Pickle	1, 8, 15
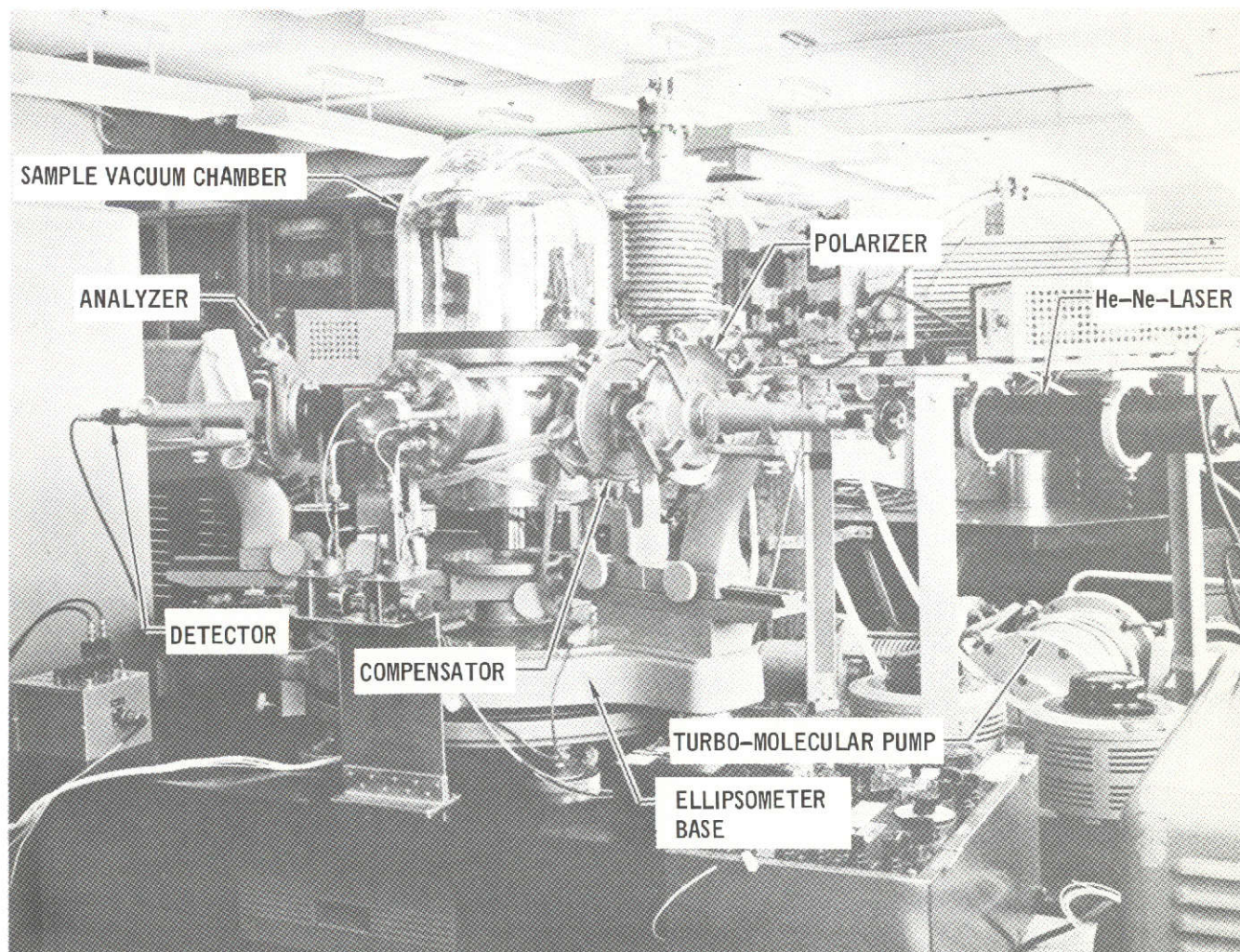
ELLIPSOMETER AND ASSOCIATED EQUIPMENT

457-3519

Figure 2-108

Alkaline Cleaners

	CHEMICAL	CONCENTRATION	TEMPERATURE	IMMERSION
1.	TURCO 4215S – CHROMATED NON-SILICATED CLEANER TURCO 4215 ADDITIVE	5.5–7.0 OZ/GAL 1 FL OZ/ OF CLEANER	$150 \pm 5^{o}F$	5, 17, 30 MIN
2.	PENNSALT 85 – NON-SILICATED CLEANER	3–6 OZ/GAL	170–180°F	5, 17, 30 MIN
3.	TURCO 4090 – SILICATED CLEANER	4–6 OZ/GAL	$180 \pm 10^{o}F$	5, 17, 30 MIN

Deoxidizers

TYPE	CHEMICAL	CONCENTRATION	TEMPERATURE	IMMERSION
AMCHEM	AMCHEM DEOXIDIZER NO. 7 NITRIC ACID 42° Be' WATER, TAP	3 OZ/GAL 12% BY VOLUME REMAINDER	70–100°F	3, 6, 10 MIN
4 ACID	CHROMIC ACID – FLAKES (FED SPEC O–C–303) SULFURIC ACID, 66° Be' (SPEC O–S–809, TYPE 1, CLASS 1) PHOSPHORIC ACID (75%) (TECH GRADE, O–O–670, CLASS 1) HYDROFLUORIC ACID, 70% (SPEC O–H–795) WATER, TAP	6 OZ/GAL 18% BY VOLUME 30% BY VOLUME 0.15% BY VOLUME REMAINDER	70–100°F	3, 6, 10 MIN
SMUT-GO	SMUT-GO NO. 1 WATER, TAP	8–16 OZ/GAL TO MAKE 1 GALLON	70–100°F	3, 6, 10 MIN
ACID PICKLE	NITRIC ACID, 42° Be' (SPEC O–N–350) CHROMIC ACID FLAKES (SPEC O–C–303, TYPE 2) HYDROFLUORIC ACID, 70% (SPEC O–H–795) WATER, TAP	9.3 TO 10.5 GALLONS 38–42 LB 0.85 TO 1.0 GALLON TO MAKE 100 GALLONS	70–100°F	1, 8, 15 MIN

CLEANING SOLUTIONS AND IMMERSION TIMES EVALUATED FOR APPLICATION TO BORON-ALUMINUM MONOLAYER PRIOR TO COPPER COATING

Table 2-1

Test samples were rinsed thoroughly after both alkaline cleaning and deoxidizing treatments and, after a final rinse in hot, deionized water, they were dried with gaseous nitrogen. Ellipsometer readings were made at several stages during the processing. Selected samples were checked for film thickness in the as-received condition, after vapor degreasing and after alkaline cleaning. All 324 specimens were measured after the final deoxidizing treatment. These measurements are based on the assumption that the film consisted entirely of aluminum oxide. However, atmospheric exposure probably resulted in the formation of a film of moisture (<1 nm) over the oxide so that the measurements did not represent the absolute thickness of the oxide film. This factor was not considered a drawback in measuring the efficiency of cleaning techniques. The error introduced by ignoring the moisture was slight, and since all the test specimens were subjected to atmospheric exposure, they all contained some adsorbed moisture and a similar degree of error.

The ellipsometry data showed no general trend for increased cleaning efficiency with increased immersion times. However, there were differences in residual film thickness attributable to variations in alkaline cleaning and deoxidizing solutions. Generally, the most efficient alkaline cleaner, regardless of the deoxidizer used was the Pennsalt 85 solution. Also, the most efficient deoxidizer was the HNO_3-HF-CrO_3 acid pickle. These general trends are shown in Figure 2-109 which compares the optimum results obtained with each cleaner/deoxidizer combination. On an overall basis, the systems can be grouped according to residual film thickness as follows:

1. <u>Residual Film Thickness: <3nm</u>

   Pennsalt 85 + HNO_3-HF-CrO_3 Acid Pickle

2. <u>Residual Film Thickness: <4nm</u>

   Pennsalt 85 + Amchem 7

   Pennsalt 85 + Smut Go No. 1

3. <u>Residual Film Thickness: <5nm</u>

   Turco 4090 + HNO_3-HF-CrO_3 Acid Pickle

   Turco 4090 + Amchem 7

   Turco 42155 + HNO_3-HF-CrO_3 Acid Pickle

ALKALINE CLEANERS

PENNSALT 85   TURCO 4090   TURCO 4215S

IMMERSION	ALKALINE	5	5	17		5	5	30		5	17	30		30	5	30	
TIME, MIN	DEOXIDIZER	3	6	3		6	10	3		6	3	10		8	15	1	
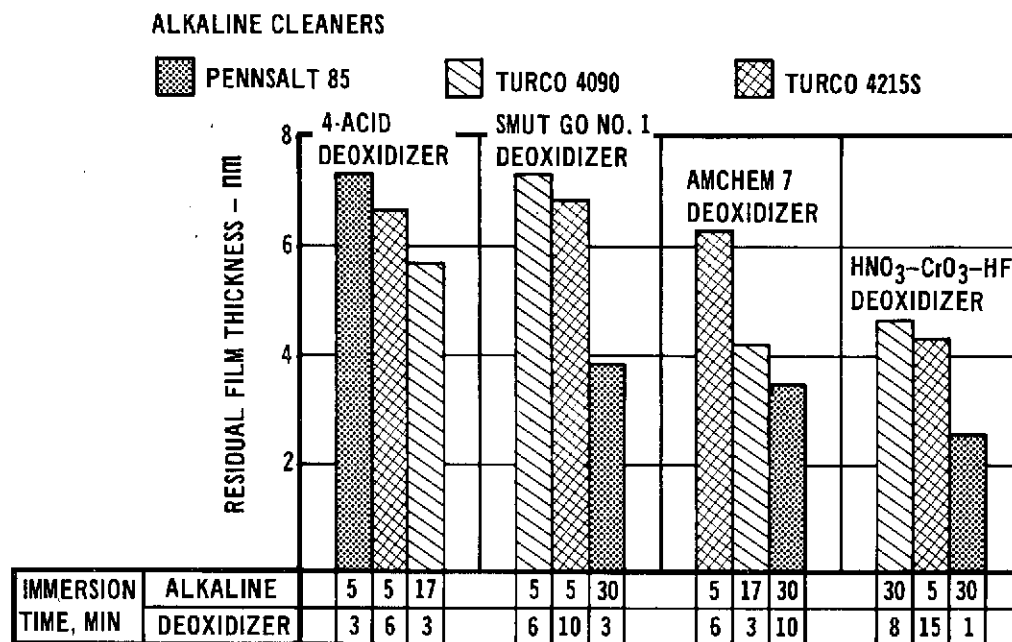
NOTE: CONDITIONS SHOWN REPRESENT "OPTIMUM" RESULTS FROM 108
COMBINATIONS OF CLEANER, DEOXIDIZER AND TIME (324 SPECIMENS)

EFFECT OF CHEMICAL TREATMENT ON 1100 ALUMINUM RESIDUAL FILM THICKNESS

Figure 2-109

Rate of Metal Removal During Cleaning - Although the ellipsometer showed which
of the cleaning methods was most efficient from the standpoint of oxide removal,
the amount of metal removal also had to be considered. Metal removal during chemical
cleaning is considered important for boron-aluminum because the layer of matrix
material covering the filaments in boron-aluminum monolayer foil is very thin.
The thickness of composite foil fabricated with .14 mm (.0056-in.) diameter boron
is about .20 mm (.008-in.) so that the filaments are covered by less than 30μm per
side of aluminum; hence, even a small loss of surface metal could amount to an
appreciable percentage of this layer. This potential problem assumes greater
proportions if recleaning should be required for some reason, because significant
reduction of this thin layer could reduce transverse tension properties appreciably.

The comparison of cleaning procedures indicated significant differences
existed in the aggressiveness of various alkaline cleaner - deoxidizer combinations.
Therefore, a check was made of three of these combinations to determine the
relative amounts of material removed and the influence of immersion times.
Selection of the three systems was made to represent three degrees of severity.
The conditions studied in increasing order of severity of the cleaner-deoxidizer
combination were:

1. Turco 4215S/10 min. + Amchem 7M for 3, 7 and 10 min.

2. Turco 4215S/10 min. + HNO_3-HF-CrO_3 Acid Pickle for 3, 7 and 10 min.

3. Pennsalt 85/30 min. + HNO_3-HF-CrO_3 Acid Pickle for 3, 7 and 10 min.

The latter system had produced the thinnest residual film thickness (less than 3 nm) in the ellipsometric evaluation of cleaning processes.

Samples of 1100-0 aluminum alloy, approximately 25.4 mm x 76.2 mm x .152 mm (1-in. x 3-in. x 0.006-in.) were weighed and then subjected to the candidate cleaning methods and reweighed. The weight difference was used to calculate the metal thickness removed per side. The results of the tests are shown graphically in Figure 2-110. In general, the mildest cleaning method (Turco 4215S + Amchem 7M) removed about .15 to .30 µm (6 to 12 µ-in.) as the deoxidizing time was increased from 3 to 10 minutes. A removal of .3 µm (12 µ-in) would result in a loss of about 1% of the matrix material covering the boron filaments. Therefore, monolayer foils could be recleaned many times (perhaps up to 10 times) in this cleaner-deoxidizer combination without removing more than 10% of the matrix thickness over the center of the filament. Removal of this small % of material is not considered detrimental.
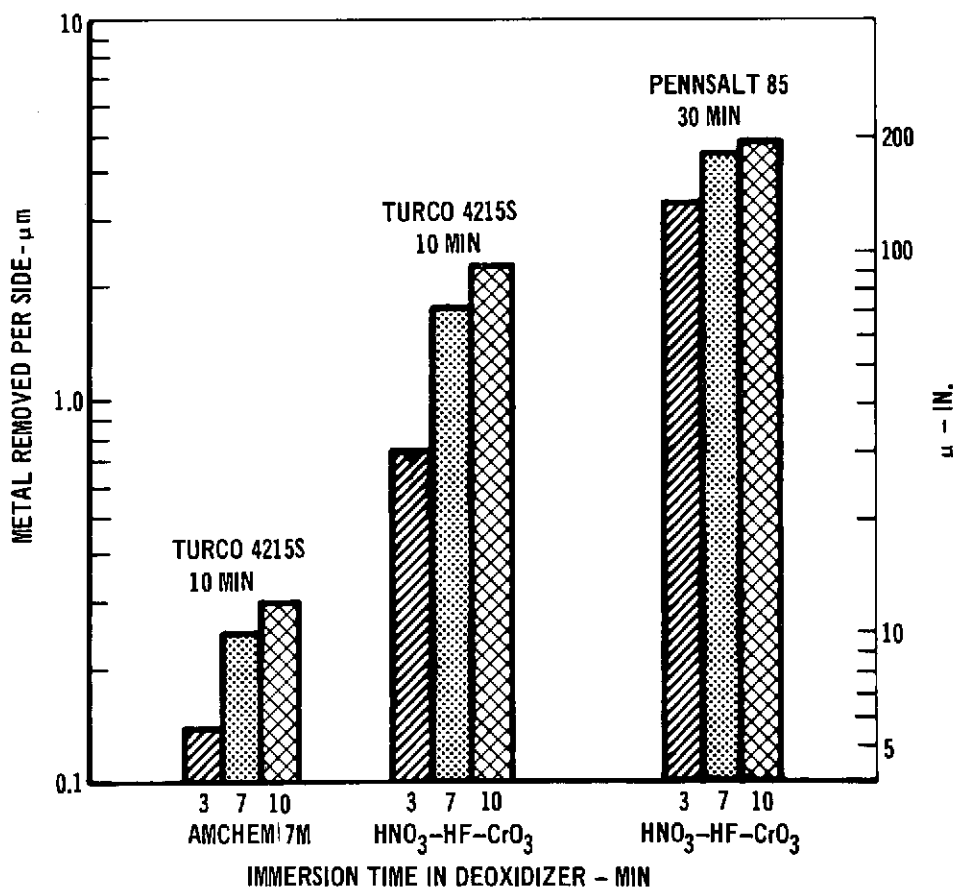
EFFECT OF CLEANING CONDITIONS ON DISSOLUTION OF 1100-0 ALUMINUM FOIL

Figure 2-110

On the other hand, a single cleaning in the most efficient combination, Pennsalt 85/30 min. + HNO_3-HF-CrO_3 Acid Pickle, for as short a time as 3 min. in the deoxidizer would result in the loss of 3.56 μ-m (140 μ-in.) or about 12% of the matrix material covering the filaments. This loss would be acceptable, but cleaning in this combination would have to be limited to a single cycle to avoid a severe loss, and this limitation was considered too restrictive.

The intermediate combination of Turco 4215S + Acid Pickle resulted in metal removal ranging from .76 to 2.3 μm (30 to 90 μ-in.) as the deoxidizing time was increased from 3 to 10 minutes. In this case, a 3 min. immersion would result in the loss of about 2.5% of the aluminum covering the filaments.

This series of tests indicated that although the Pennsalt 85 + HNO_3-HF-CrO_3 Acid Pickle produced the cleanest surface, it would dissolve more than 10% of the aluminum matrix in a single cleaning operation. Therefore, using this combination for chemical cleaning of monolayer foils would prohibit recleaning if needed for any of a variety of reasons. At the other extreme, the mildest combination – Turco 4215S plus Amchem 7M–is relatively inefficient for oxide removal. Samples measured by ellipsometry during this series of tests showed residual film thickness of about 6 nm with this mild combination.

The intermediate combination of Turco 4215S + HNO_3 + HF + CrO_3 Acid Pickle for 3 min. offered a good compromise. The metal removal rate ($\sim$ 2.5%) was sufficiently low to permit recleaning. Also, this combination is considerably more efficient than the milder Turco 4215S plus Amchem 7M. Ellipsometer readings made during this series showed residual films after cleaning in the intermediate system to be about 3.7 nm, or 40% less than measured on specimens subjected to milder environment. Therefore, the Turco 4215S plus HNO_3 + HF + CrO_3 Acid Pickle was selected as the method of cleaning boron-aluminum monolayer foils prior to copper coating.

Finally, a limited test series was made to determine if the boron filaments would be attacked in the cleaning solutions. This was accomplished by immersing duplicate samples of boron filament in Amchem 7 deoxidizer for periods up to 20 minutes and in the HNO_3 – HF – CrO_3 deoxidizer for intervals up to 30 minutes. There was no change in weight of the boron filaments as a result of these exposure conditions.

Effect of Storage Conditions – One of the tasks in the cleaning optimization study was determining the rate at which an oxide film forms on a freshly cleaned aluminum surface. This investigation was undertaken to determine if a time limit should be imposed on the interval between cleaning and coating and if storage in an

inert environment would retard the rate of film build-up. In this evaluation, strips of 1100-0 aluminum foil were chemically cleaned in Pennsalt 85 and HNO_3 - HF - CrO_3 deoxidizer and then stored in small controlled atmosphere chambers and exposed to a continual uniform flow of air, nitrogen or argon. Ellipsometer readings of oxide thickness were taken on each sample immediately after cleaning and at intervals during the test period.

Ellipsometer readings taken immediately after cleaning showed the oxide film on the test samples to be about 2.2 nm thick. At the end of 1 hour exposure to the test environments, the film thickness had increased significantly. The oxide continued to increase throughout the test period of 960 hours but at a slower rate. After 960 hours, the oxide film thickness had increased about 80% overall; however, during the first hour alone, the increase amounted to 40%. Also, the rate of increase was not influenced appreciably by environment. These relationships are shown in Figure 2-111.
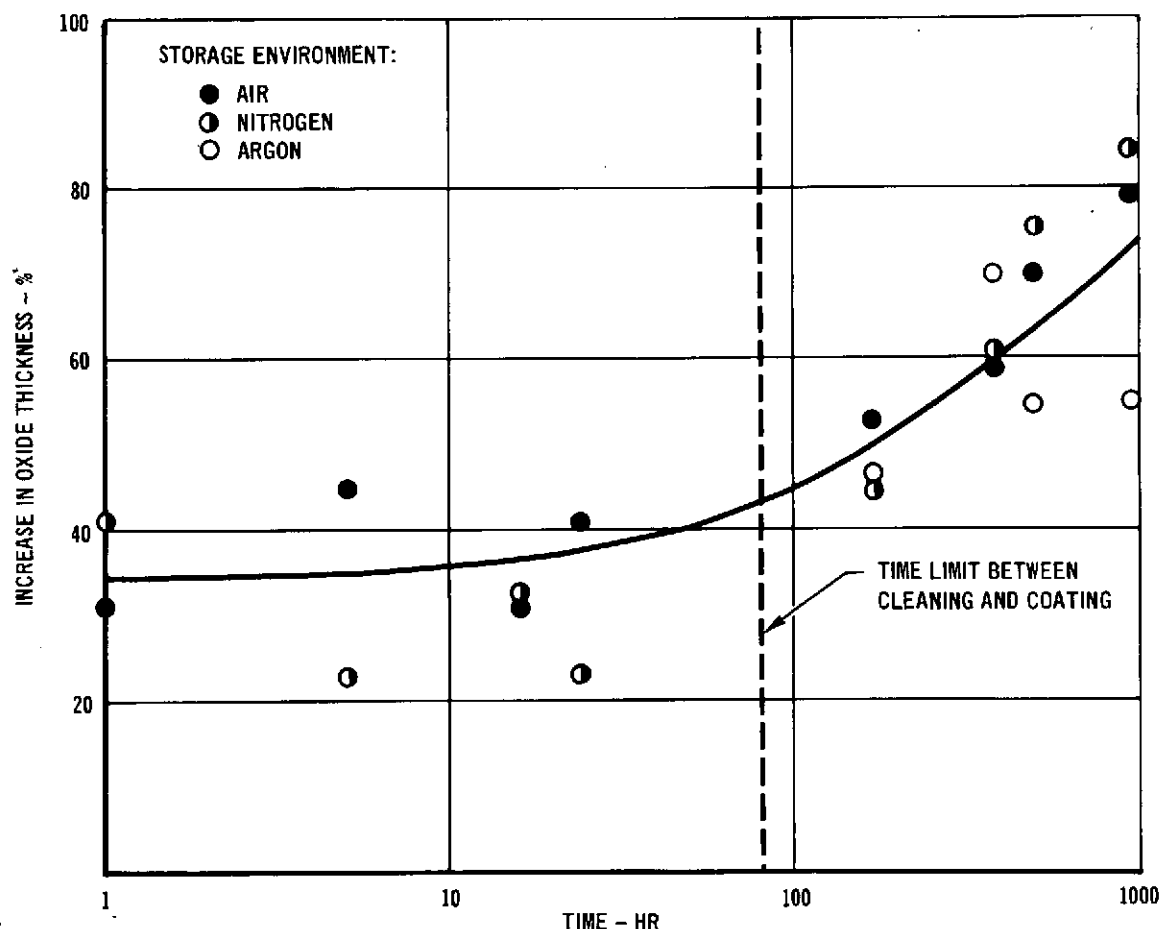
EFFECT OF STORAGE ENVIRONMENT ON BUILD-UP OF OXIDE FILM
ON CHEMICALLY CLEANED ALUMINUM

Figure 2-111

2-115

These test results showed that unless coating was begun almost immediately after the cleaning operation, an increase in oxide film thickness on monolayer foils could not be avoided even if stored in an inert gas environment. This was not considered practical for a production operation. Therefore, it was necessary to set a limit on the storage time between cleaning and coating based on the test data and practical considerations. A limit of 80 hours was established to be consistent with a normal production flow cycle. Also, this extended interval would result in very little increase in oxide thickness over a one-hour exposure, as shown in Figure 2-111.

2.3.1.2 <u>Vapor Deposition Studies</u> - During this program, a study was under-taken to improve the techniques for vapor depositing copper on the boron-aluminum foils for eutectic bonding. This evaluation was concerned with the parameters of the glow discharge process (ion bombardment) which cleans the monolayer foil just prior to vapor deposition. The purpose of the evaluation was to determine the effect of current density and time on oxide removal. This was accomplished in the ellipsometer which was modified to accommodate an atmosphere chamber in which a sample could be glow-discharge cleaned and the surface film measured without exposure to air. Test samples were .15 mm (.006 in.) thick 1100 aluminum alloy discs, 28.4 mm (1.12 in.) dia.

The test procedure consisted of evacuating the sample chamber and imposing a high voltage between the chamber wall and the sample, with the sample as the cathode. A glow discharge was then initiated by backfilling the chamber with argon until the desired argon ion current was achieved. Ellipsometer measurements were made prior to and during the discharge to determine the thickness of the oxide film. The dis-charge was continued until the measurements indicated that a minimum or threshold film thickness had been achieved. All the tests were made at 3700 volts but the current density was varied for each run.

Test results showed that the oxide was removed at a rapid rate during the early stage of glow discharge but the rate decreased with time and eventually a threshold value of oxide thickness was reached and the removal rate approached zero. Increas-ing the current density reduced the time required to reach the threshold film thickness, but did not change the minimum value appreciably. The removal rate, defined as the ratio of total film removed to the time required to reach the threshold value, was essentially a linear function of ion current as shown in Figure 2-112.

ALL TESTS RUN AT 3700 VOLTS
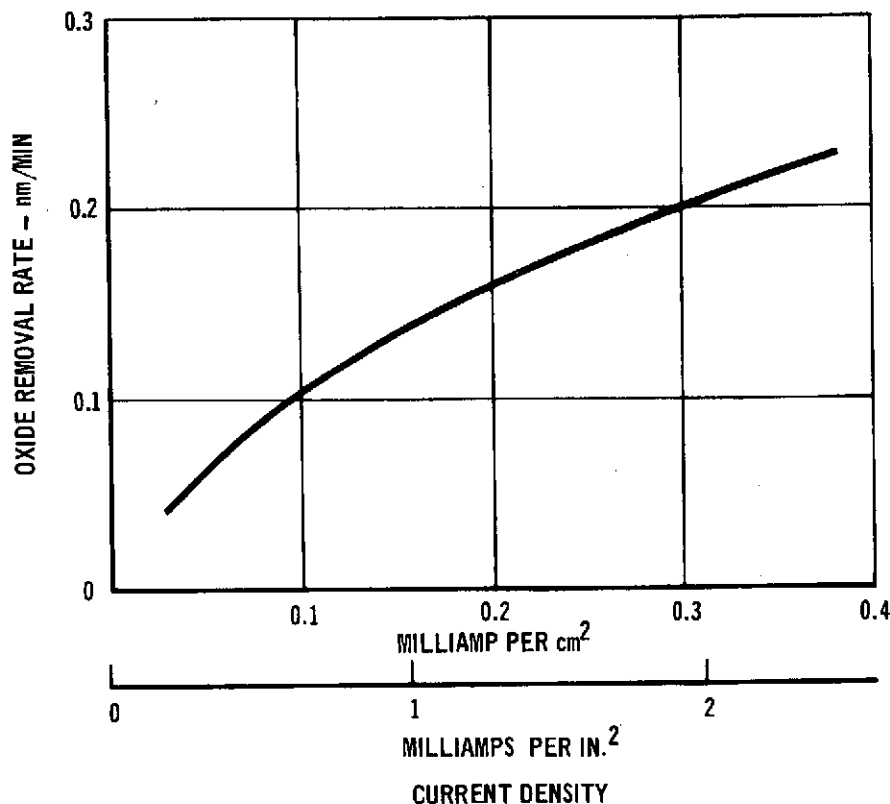
**EFFECT OF CURRENT DENSITY ON RATE OF OXIDE REMOVAL
DURING GLOW DISCHARGE CLEANING**

Figure 2-112

Since oxide-free surfaces can be achieved by glow discharge just prior to coating, it is theoretically possible to eliminate all the chemical cleaning operations with the exception of vapor degreasing. However, the rate of oxide removal from aluminum is slow even at the highest current densities evaluated (Figure 2-112). Since the oxide film on the starting material would exceed 10 nm, which was demonstrated in the cleaning optimization study, glow discharge times would exceed one hour even under high current densities to ensure an oxide free surface. Therefore, chemical cleaning was selected as the primary means to minimize the surface oxide on monolayers prior to copper coating. Glow discharge was relied upon primarily to remove only surface layers of adsorbed gases and water vapor and thereby ensure adherence of the vapor deposited layer.

The final experiment in the glow discharge study was designed to determine if an oxide-free surface could be maintained under ideal conditions. This was carried out in an Auger electron spectrometer which is used to determine the chemical compositon of surface deposits. The test procedure consisted of sputtering the

oxide off a sample of aluminum, holding it under a partial pressure of argon
$(9 \times 10^{-5}$ torr), and analyzing the surface periodically. The initial scan, taken
30 seconds after ion bombardment was completed, showed a single 67 eV peak char-
acteristic of pure aluminum. As the holding time was increased, the amplitude of
this peak decreased and this was accompanied by the appearance of a second peak at
57 eV. This second peak is associated with the formation of aluminum oxide and
eventually becomes more prominent than the pure aluminum peak. The build-up was
charted by the change in the aluminum peak which diminished as oxide was formed.

Results of the test, shown in Figure 2-113, indicate that oxide begins to
form on a clean aluminum surface almost immediately upon exposure to even a high
purity (vacuum) environment. These measurements indicate that even under ideal
glow discharge conditions, an oxide film would form on the metal surface during the
ten minute period required for evacuation of the chamber to the coating pressure.
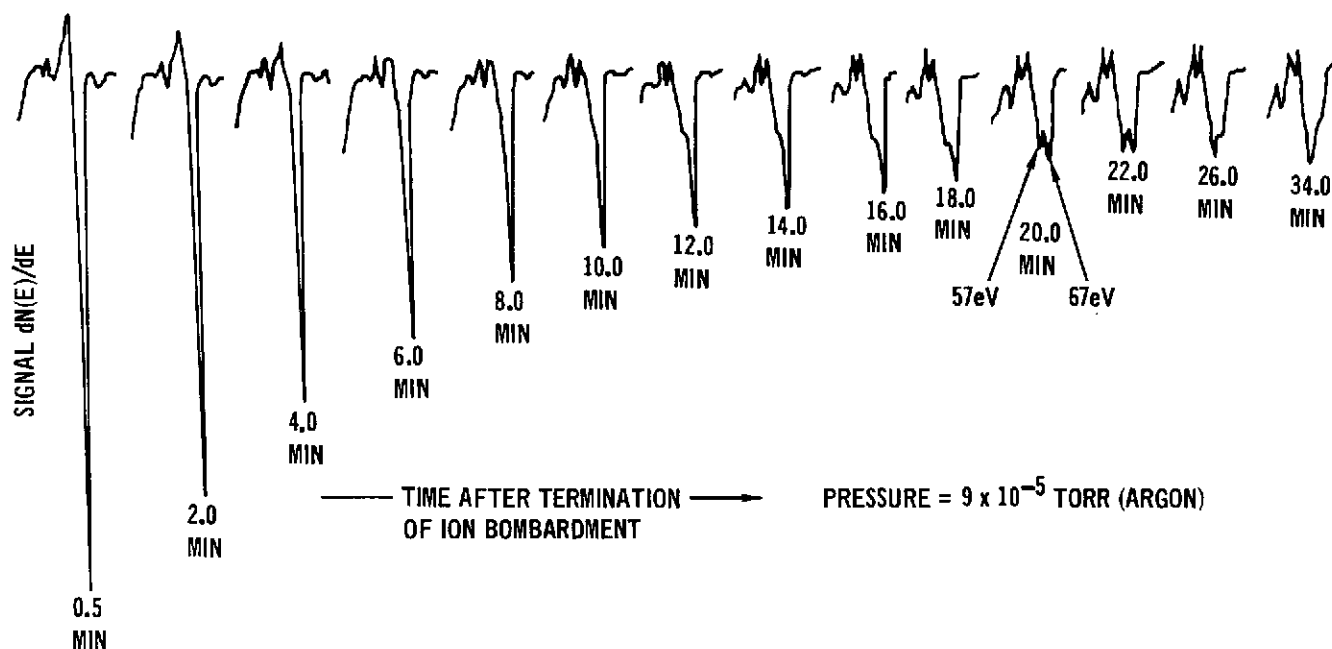
OXIDATION OF ALUMINUM, AS STUDIED BY CHEMICAL SHIFTS
IN 67 eV AUGER PEAK FOR ALUMINUM

Figure 2-113

Effect of Storage Environment on Copper Surfaces - The possibility that freshly
deposited copper would oxidize during the interval between coating and bonding was
investigated. This was also done using ellipsometry. Freshly coated samples of
1100-0 aluminum foil were subjected to several different environments and the film
thickness measured periodically. Initially, specimens were exposed for 168 hours

and no appreciable difference was noted in the rate of oxidation as a function of
environment. In a second test series, samples were exposed for a total of 960
hours in argon. Oxidation occurred throughout the test period, but the rate
appeared to decrease with time. At the end of the 960 hour exposure, the film
thickness was less than 4 nm. This thickness or amount was not considered
excessive. To ensure that oxidation would be kept within acceptable limits, the
time between coating and bonding was limited to 700 hours and nitrogen was specified
for the storage environment.

2.3.1.3 Effect of Bonding Cycle on Fiber Strength - Eutectic bonding involves
heating above 821°K (1018°F), the aluminum-copper eutectic temperature. When
exposed to elevated temperatures for extended periods of time, boron and aluminum
will interact which degrades the strength of the boron filaments. Therefore, a
study was undertaken to determine the extent of filament strength degradation for
the times and temperatures associated with eutectic bonding. This study was con-
ducted in two phases. The first was preliminary in nature and made with composite
samples containing 0.10 mm (.004-in.) dia. boron fibers. These tests showed that
some degradation could be expected as a result of the thermal cycle associated with
eutectic bonding.

The second phase of the investigation was more extensive and its objective was
to better define the effects of exposure at temperatures ranging from 549° to 593°K
(1020° to 1100°F). For this purpose, a single sheet of 1100 aluminum-matrix com-
posite foil containing 0.14 mm (0.0056 in.) diameter boron fibers was cut into
seven groups of specimens. All the specimens to be exposed to a given time-
temperature cycle were from the same group. This procedure was followed to reduce
the normally high data scatter associate with composite materials by providing
samples that shared common filaments. The method of selecting test specimens and
the exposure conditions are shown in Figure 2-114.

Thermally exposed samples were heated in a vacuum furnace (1×10^{-5} torr) to
the desired temperature at a rate of 11°K (20°F) per minute, and held for the
required time. Then the specimens were fast cooled to 755°K (900°F) by back-
filling the furnace with argon and furnace cooled to 394°K (250°F).

Tensile test results, listed in Table 2-2 show that some boron fiber
degradation occurred throughout the time/temperature range evaluated. The amount
of degradation varied with both time and temperature and increased with the
severity of exposure. For example, at 844°K (1060°F), a holding period of 7 min

SEVEN GROUPS OF SPECIMENS – NINE SPECIMENS PER GROUP –
CUT FROM ONE MONOLAYER SHEET:

2.87 cm (1.13 IN.)

1.78cm (7 IN.)

FILAMENT
DIRECTION

0.97 CM(0.38 IN.)
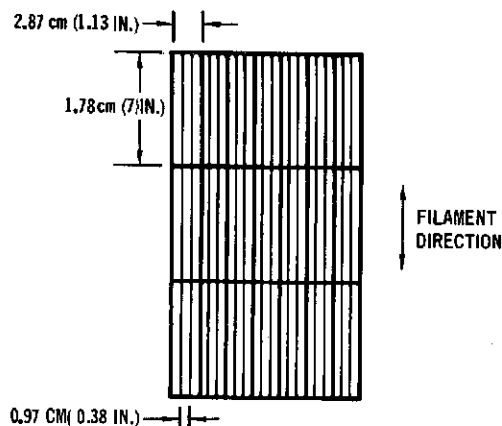
THREE SPECIMENS FROM EACH GROUP TESTED IN AS–RECEIVED CONDITION
TO SERVE AS CONTROLS

REMIANING SAMPLES HEATED IN VACUUM TO SIMULATE TYPICAL BONDING
CYCLES PRIOR TO TESTING:

549°K (1020°F) – 30 MIN
554°K (1030°F) – 7 MIN OR 15 MIN
571°K (1060°F) – 7 MIN, 15 MIN OR 30 MIN
593°K (1100°F) – 7 MIN

FIBER DEGRADATION STUDY CONDITIONS

Figure 2–114

EXPOSURE CONDITION	AVERAGE MONOLAYER ULTIMATE STRENGTH MN/m^2 (KSI)	AVERAGE FILAMENT BUNDLE STRENGTH MN/m^2 (KSI)	PERCENT DEGRADATION (1)
UNEXPOSED CONTROL	1272 (185)	3062 (441)	–
818°K (1020°F) – 30 MIN.	1034 (150)	2509 (364)	17.6
827°K (1030°F) – 7 MIN	1152 (167)	2681 (389)	11.9
827°K (1030°F) –15 MIN	1096 (159)	2468 (358)	19.0
844°K (1060°F) –7 MIN	1082 (157)	2578 (374)	15.5
844°K (1060°F) – 15 MIN	917 (133)	2186 (317)	28.3
844°K (1060°F) –34.5 MIN	848 (123)	1993 (289)	34.6
866°F (1100°F) –7 MIN	931 (135)	2179 (316)	28.6

$$(1) \% \text{ DEGRADATION} = \frac{\text{CONTROL STRENGTH} - \text{EXPOSED STRENGTH}}{\text{CONTROL STRENGTH}} \times 100\%$$

LONGITUDINAL TENSILE
STRENGTH OF EXPOSED AND UNEXPOSED BORON-ALUMINUM MONOLAYER FOIL

Table 2–2

resulted in a strength loss of about 15%; extending the time to 30 min increased the loss to 35%. A similar effect occurred when the temperature was increased. Holding at 827°K (1030°F) for 7 min resulted in a 12% strength loss while exposure to 866°K (1100°F) for the same amount of time produced a 29% loss. The combined effect of both time and temperature is shown in Figure 2-115 where the exposure conditions are expressed in terms of a Larson-Miller parameter.

$$P = T_{^\circ R} (36 + 3 \ \log_{10} t_{min}) \times 10^{-3}$$
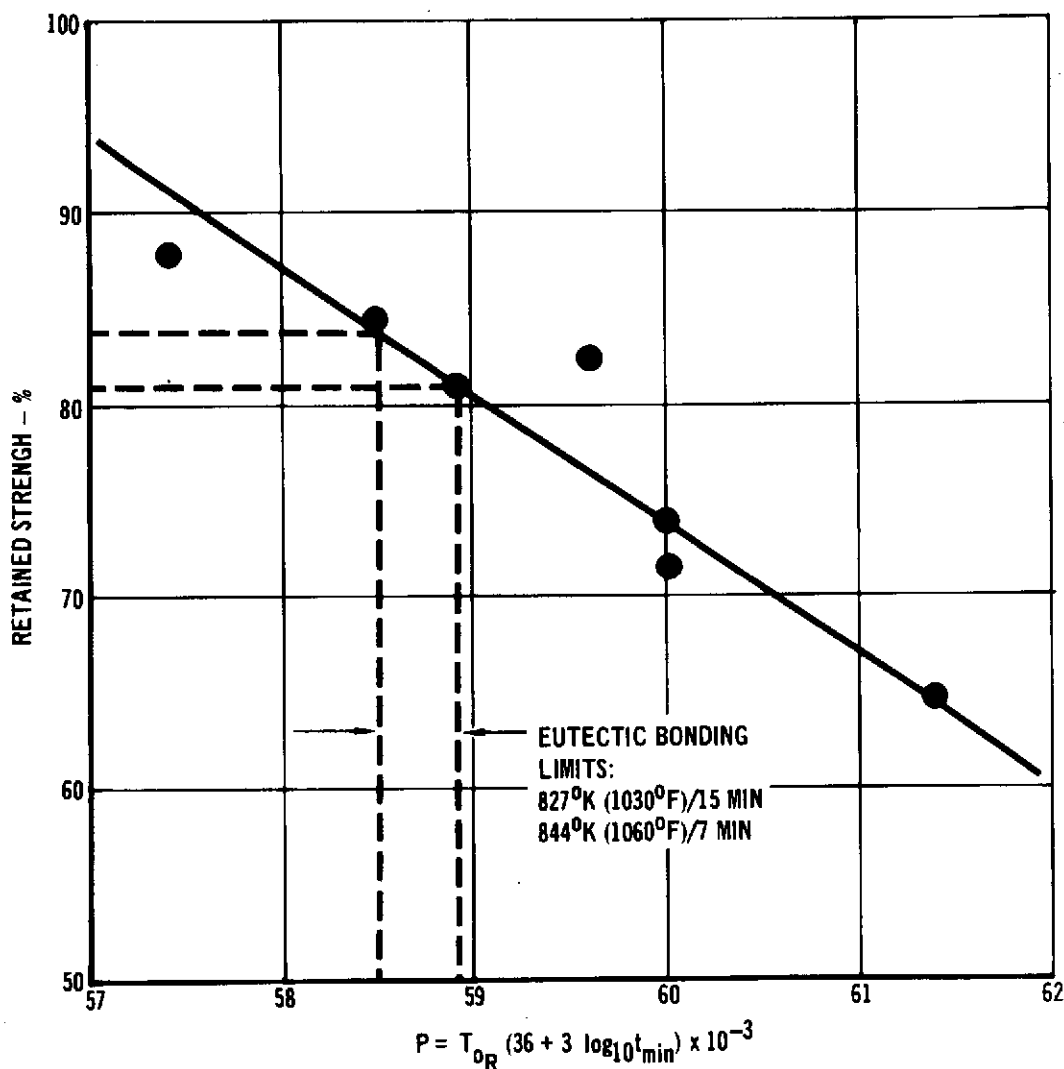
EFFECT OF ELEVATED TEMPERATURE EXPOSURE
ON STRENGTH OF BORON-ALUMINUM MONOLAYER FOIL

Figure 2-115

On the basis of these tests, limits were established for eutectic bonding mechanical property test specimens and structural components. The lower limit for bonding was selected to be 827°K (1030°F) for no more than 15 minutes. An upper limit of 844°K (1060°F) for a maximum of 7 minutes was specified. Under these

conditions, the amount of degradation could not exceed 20% as shown in Figure 2-115 This amount was not considered excessive for the compression panel. Further strength evaluations using multiple specimens inserted in production packs for quality assurance purposes showed that the range of realized strength reduction was usually less than this value (see Section 2.3.2.3).

2.3.1.4 - Co-Eutectic Bonding Boron-Aluminum to Titanium - When structural analysis of various assemblies in this program indicated the need for local reinforcement, tests were initiated to determine if titanium interleaves could be incorporated into boron-aluminum laminates during eutectic bonding to provide such reinforcement. Initial tests were made on a multi-ply laminate consisting of copper coated boron-aluminum and bare Ti-6Al-2Sn-4Zr-2Mo alloy. The lay-up contained three plies of boron-aluminum interleaved with two plies of 0.30 mm (0.012 in.) thick Ti alloy. Metallographic examination was used to evaluate the joint and showed the bond to be continuous and of high quality with an interaction zone less than 1 μm (40 μ-in.) thick (Figure 2-116). Microprobe analyses were made to determine if the eutectic former had diffused into the titanium. This analysis indicated that no significant amount of diffusion had occurred.
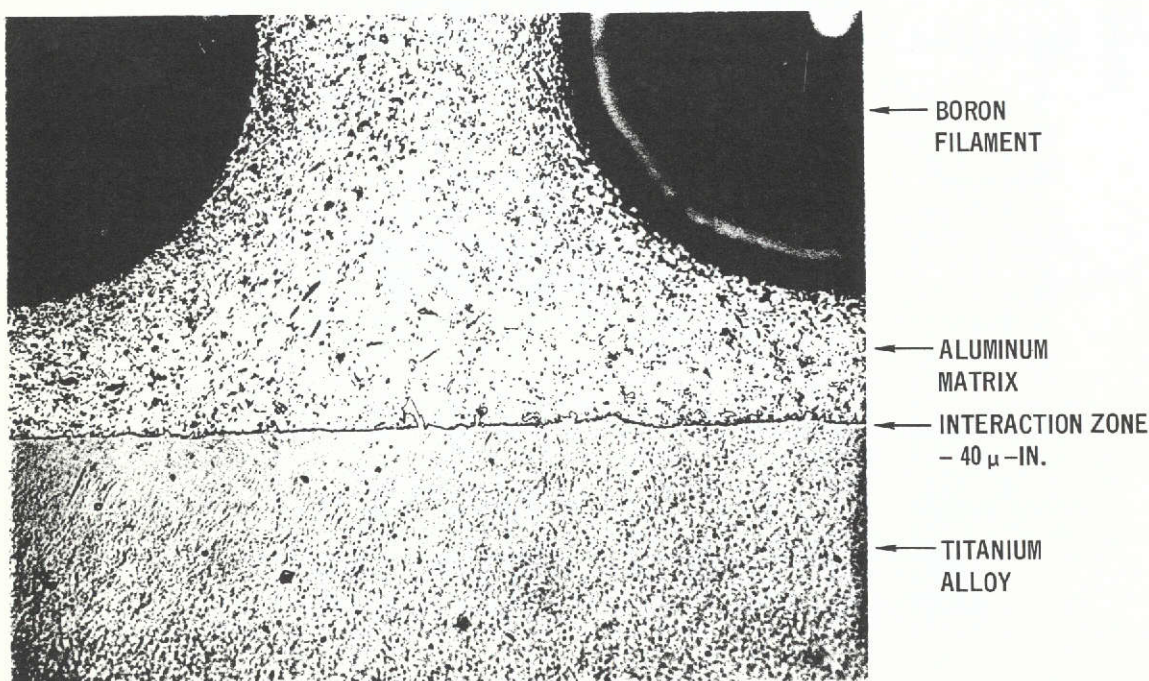
AS POLISHED   500X

**TITANIUM ALLOY JOINED TO BORON-ALUMINUM BY AL-CU LIQUID
FORMED DURING EUTECTIC BONDING CYCLE**

Figure 2-116

Because the initial results were encouraging, the evaluation was extended to determine the interlaminar shear strength between the Ti alloy and boron-aluminum. For these tests, specimens measuring 8.6 mm x 20.32 mm (.3 in. x .8 in.) were cut from a multi-ply laminate and tested in three point bending (15.24 mm span) with the principal bending stress parallel to the fiber direction. The basic laminate contained nineteen plies, of which three were Ti-6Al-2Sn-Zr-2Mo alloy. These Ti plies were located in the center of the laminate (maximum shear) and were separated from each other by a single boron-aluminum ply.

Five interlaminar shear specimens were tested at room temperature. Failure loads ranged from 5293 to 5382 N (1190 to 1210 lbs) with the average equivalent to a nominal shear strength in excess of 110 MN/m^2 (16,000 psi) at the titanium alloy - boron-aluminum interfaces. This shear strength exceeds the levels developed by previous all-boron-aluminum specimens. All the specimens failed in tension and the failures originated in the outer boron-aluminum plies at stress levels in excess of 1103 MN/m^2 (160,000 psi); hence, the maximum shear strength was not reached. On the basis of these tests, it was concluded that titanium interleaves could be included in a boron-aluminum laminate during a normal eutectic bonding cycle.

2.3.2 Improved Manufacturing Methods - One of the objectives of the process technology development phase of the program was to reduce costs and increase quality through improved manufacturing methods. The three processing steps singled out for such improvement were: (1) copper coating of monolayer foils, (2) lay-up of structural shapes and (3) control of eutectic bonding thermal cycle. Significant improvements were made in each of these processing steps and they will be discussed individually.

2.3.2.1 Copper Coating - During the initial development of the eutectic bonding process, the minimum copper thickness required for bonding had been defined and a production physical vapor deposition coating facility constructed. The major process improvement undertaken in this program was concerned with the quality of the copper coating from the standpoint of increased ability to control thickness and uniformity.

Such a study was considered necessary because of the importance of coating thickness to eutectic bond quality. A certain minimum amount, about 0.3 μm (12 μ-in.) is needed to ensure that some of the coating at the surface of the monolayer will remain after the diffusion during heating to the bonding temperature to be available to form an adequate amount of liquid phase for bonding. On the other hand, an

excessive amount could result in a brittle bond. A coating thickness of 0.5 μm
(20 μ-in.) had been previously established as a satisfactory level that would pro-
duce sufficient liquid phase without the danger of joint embrittlement. The
objective of the study was to refine the coating technique to ensure that the desired
coating thickness could be obtained consistently within narrow tolerance limits,
and that the coating would be uniform over the entire surface of each monolayer foil.

Vapor deposition of copper on boron-aluminum monolayer foils is accomplished
in a modified electron-beam welding chamber. A drum, 61 cm (24 in.) in diameter by
2.28 cm (90 in.) long, is used to hold the monolayer foils. The outer surface of
the drum is electrically insulated so that the entire outer surface on which the
monolayer foils are wrapped can be glow-discharge cleaned. A single molybdenum boat
source, positioned 30.5 cm (12-in.) below the outer surface of the drum, is kept
continuously filled with molten copper by filler wire additions. The boat is
surrounded by a metal shield and a cut-out area in this shield limits the deposi-
tion area. An ion rate monitor is used in the system to measure evaporation rate
which is controlled by the rate at which wire is fed into the boat. This equipment
is shown in Figure 2-117.
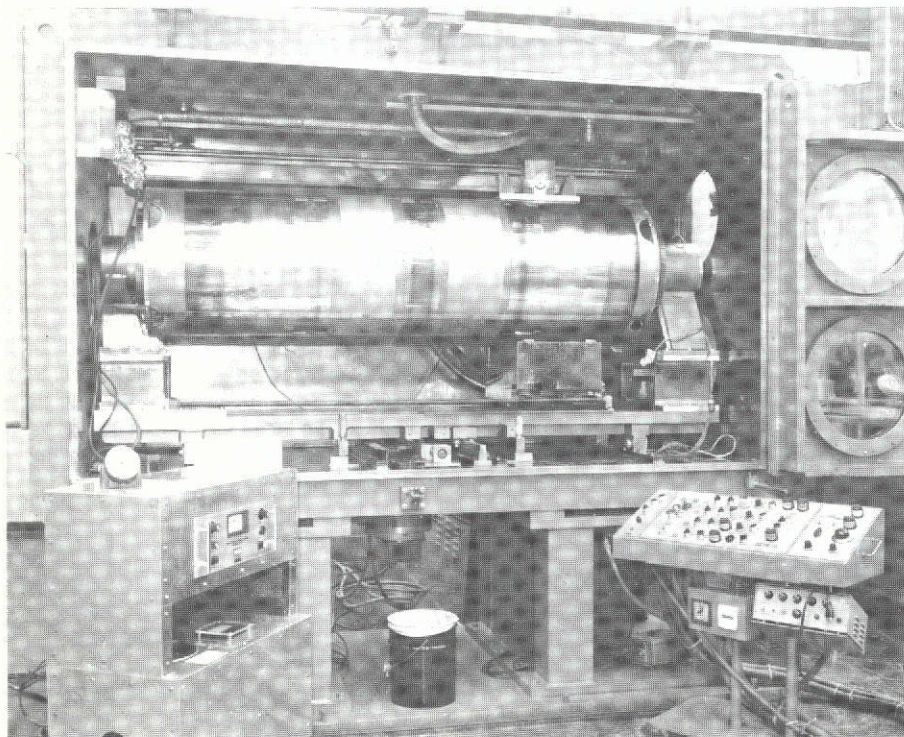
VACUUM DEPOSITION FACILITY

Figure 2-117

Initially, the coater was operated with the boat held stationary and the drum
rotated past the shield cut-out while maintaining a constant evaporation rate. Two
passes of the drum were required to attain a coating about .35 μm (14 μ-in.) thick.
Under this system of operation, the monolayers were located in zones along the drum.
When coating of the material within a given zone was completed, the boat was then
moved to the next zone without opening the chamber and the process repeated. This
method provided acceptable coating thicknesses, but over a relatively narrow width.

In order to improve the coating uniformity, the mode of operation was changed
from the stationary boat-zone method to a traveling boat procedure. The initial
objective was to determine if this change would provide control of the coating over
a narrow thickness range. The target value selected was 0.35 to 0.50 μm (14 to 20
μ-in.).

The traveling mode of operation consists of moving the boat containing the
copper from one end of the drum to the other as the drum rotates. Approximately
25 test runs were made to develop operating parameters of boat travel speed, drum
rotational speed, power input to the boat and deposition rate. For these tests,
3 rows of 6 specimens each, located 120° apart were coated under various conditions
and the resulting coating thickness measured by weight change. The samples covered
46 cm (18 in.) of drum length. These tests indicated that on any given run, coating
uniformity within the 18 sample grouping did not vary more than about .076 μm
(3 μ-in.) with an average uniformity variation of .053 μm (2.1 μ-in.).

These initial test results were better than could be attained by the zone
method. In addition, the traveling mode offered the potential of plating wider
sheets of monolayer foil than could be accommodated in the zone method. While the
uniformity in the initial tests was consistent within a given run, the thickness
itself varied from run to run but could be contained in the target range of .35 to
.51 x μm (14 to 20 μ-in.). This inconsistency was traced to variations in the
travel speed of the boat caused by operating the motor at the very low end of its
speed range where accuracy was not reproducible. This was overcome to some extent
by increasing the speed of the motor, changing gear ratios and depositing the
copper in multiple passes.

On the basis of the good results obtained during the development tests, the
decision was made to use the traveling boat mode for coating material to be used
in this program. The next step was to certify the new procedure for production.
For this purpose a coating run was made with 240 weight samples to cover a larger

area on the drum. These 7.62 cm (3 in.) long samples were placed end-to-end
longitudinally to cover the central 152.4 cm (60 in.) of the 228.6 cm (90 in.) long
drum. Twelve such rows of twenty specimens each were spaced at 30° intervals
around the circumference. Within the central 127.0 cm (50 in.) of the drum, coat-
ing thicknesses ranged from .36 to .40 μm (14.0 to 16.8 μ-in.) for a two-pass
coating run. A similar run, made with more passes, showed good uniformity but with
the resulting coating thickness on the high side of the target range. In other
respects, the run was satisfactory.

The certification tests demonstrated that the vapor deposition equipment was
capable of depositing a uniform copper coating of closely controlled thickness.
Therefore, the travelling boat mode of operation was selected to be used for the
remainder of the program. In order to check coating thickness on each run, seven
weight samples are included with each drum load. These samples are commercial
aluminum kitchen wrap cut into samples 51 cm x 76 cm (2 in. x 3 in.) and randomly
distributed on the coating drum. The material coated for the compression panel
was specified to meet the following conditions:

a. The average coating thickness based on all seven weight samples must
fall between .44 and .57 μm (17.5 and 22.5 μ-in.).

b. The coating thickness on any one sample could not exceed .67 μm
(26.5 μ-in.).

c. The coating thickness of any one sample could not be less than .34 μm
(13.5 μ-in.).

The coating thickness requirements were met during the production phase with
little difficulty. This is shown in Figure 2-118 which represents an analysis of
coating thickness control during the first 63 coating runs on monolayer foil used
in the full size panel. The average of all weight specimens (441 total) was .497
μm (19.57 μ-in.) which is very close to the middle of the specified range. Sixty
of the individual runs (∿95%) met the requirements for average thickness and
the remainder exceeded the upper or lower bound by less than 6%. Of all the first
sixty-three runs, the upper or lower limits specified for single specimens were
exceeded only twice and in both cases by .025 μm (1 μ-in.) or less.

This analysis demonstrates that coating thickness can be closely controlled
although some average run-to-run variation within a narrow range can be expected.
No requirements were specified to ensure a minimum variation among the seven
specimens from the same coating run. However, coating parameters were selected to
reduce the variation within the individual groups, with the objective of holding
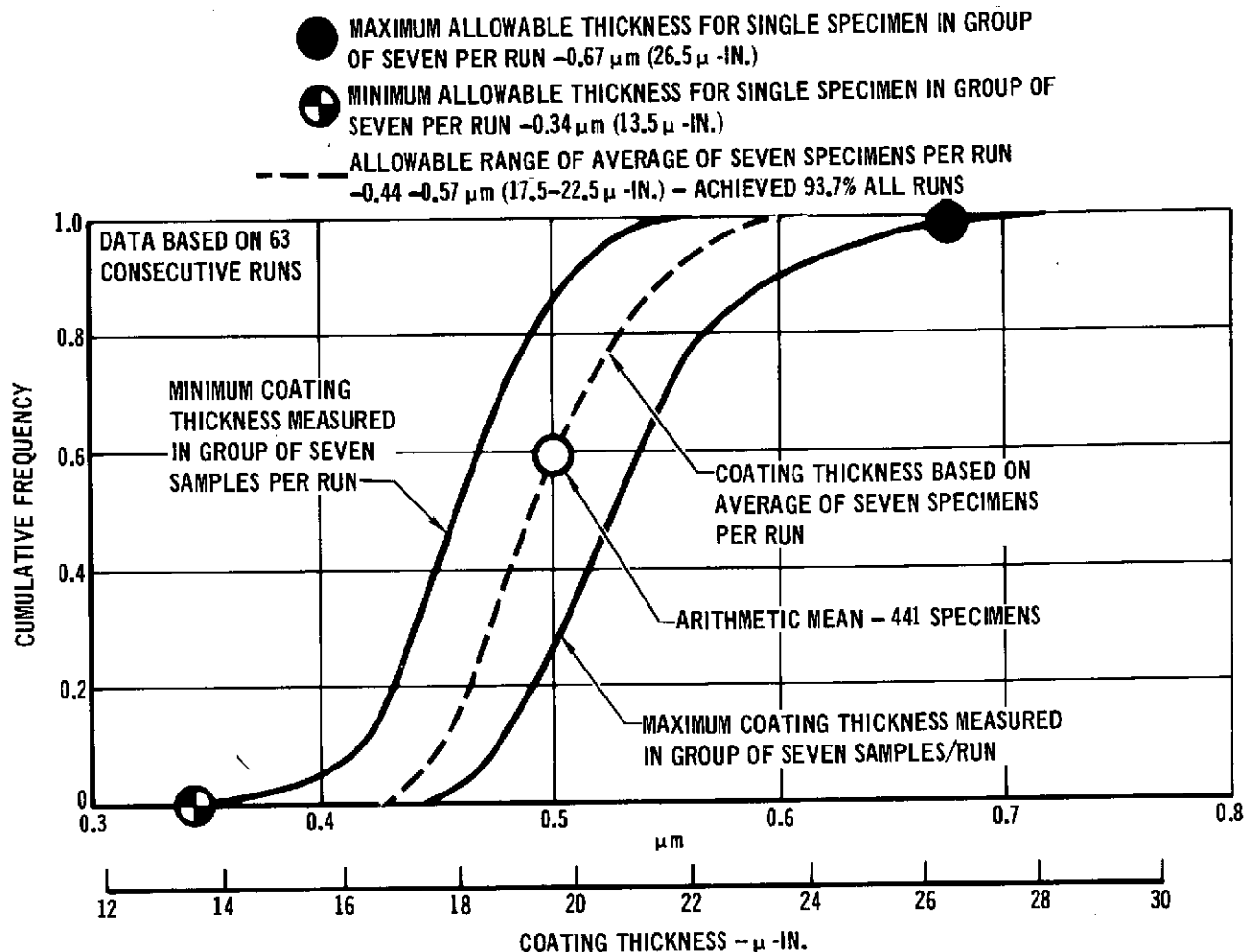
**RESULTS OF WEIGHT CHANGE QUALITY CONTROL SAMPLES SHOWING
RUN-TO-RUN VARIATION IN COPPER COATING THICKNESS ON B/AL MONOLAYER**

Figure 2-118

this variation to .10 μm (4 μ-in.) or less. The frequency distribution of this difference for all sixty-three runs is shown in Figure 2-119 . These data show that the average of all runs was .07 μm (2.9 μ-in.); 86% showed a variation of less than .1 μm (4 μ-in.).

The sixty-three runs described above are typical of the thickness and uniformity observed throughout the program. The change in technique which resulted in this improvement also reduced costs by virtually eliminating the need for rework and reducing the overall time required for coating.

2.3.2.2 Layup Techniques - A principal advantage of fabricating structural shapes from individual monolayer foils is the versatility this approach offers for producing complex shapes of varying thickness. At the onset of this program, layups of this type were made by hand-forming each ply over a shaped tool. This pro-

2-127
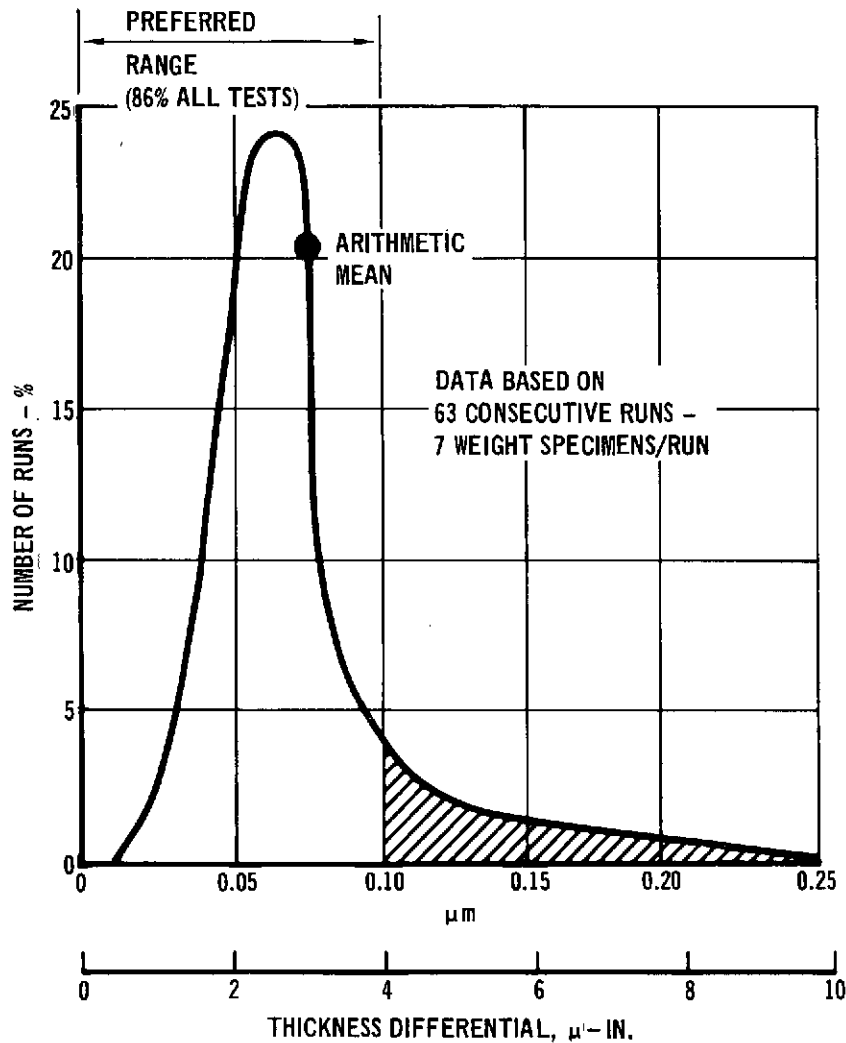
MAXIMUM VARIATION IN COPPER THICKNESS
PER RUN BASED ON QUALITY CONTROL SAMPLES

Figure 2-119

cedure was costly and the quality of the finished parts was questionable because good contact between adjacent layers was not always attained. Therefore, a study was undertaken to develop layup procedures that would reduce costs and improve quality. At the same time it became necessary to further increase the versatility of the monolayer approach to permit the inclusion of local reinforcement in the form of titanium interleaves. The use of individual monolayers was ideally suited to interleaving, but hand layup techniques were not because of the springback characteristics of titanium.

The need for an improved process led to the development of a mechanical forming procedure. This concept, shown schematically in Figure 2-120 utilizes a flat layup consisting of a cover sheet and slip and spacer sheets as well as the

2-128

boron-aluminum interleaved with titanium. This entire pack is formed as a single unit and the forming pressure maintained until the cover sheet is welded to the bonding tool and the pack evcuated.

a) Before Forming

b) After Forming
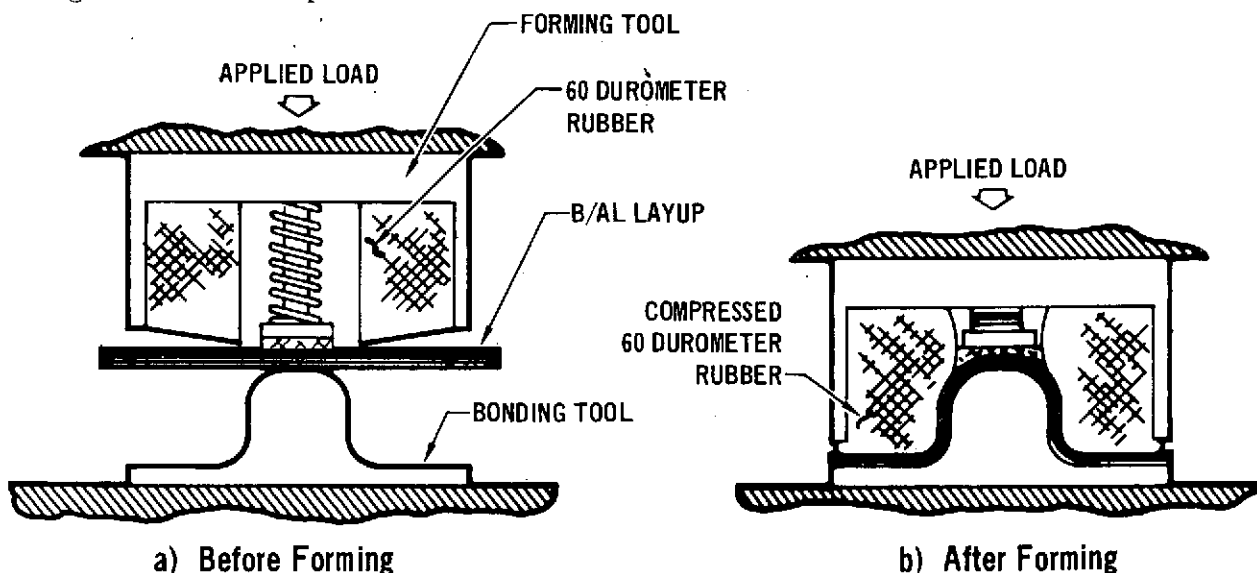
A FLAT PACK LAY-UP IS MADE CONSISTING OF COPPER-COATED BORON/ALUMINUM MONOLAYER FOILS, TITANIUM FOIL INTERLEAVES,STOP-OFF COATED SLIP SHEETS AND AN OUTER ENVELOPE SHEET. THIS LAY-UP IS THEN PLACED IN A BRAKE PRESS ON THE BONDING TOOL AS SHOWN IN (a). PRESSURE THEN IS APPLIED AS IN (b) TO FORM THE ENTIRE LAY-UP. FORMING PRESSURE IS MAINTAINED WHILE THE OUTER ENVELOPE SHEET IS WELDED ALL AROUND THE PERIPHERY OF THE BONDING TOOL. THE INTERIOR OF THE WELDED PACK IS EVACUATED AND THE FORMING PRESSURE THEN RELEASED. ATMOSPHERIC PRESSURE HOLDS THE LAY-UP TO THE TOOL AND PREVENTS SPRINGBACK OF THE B/AL AND TITANIUM FOILS.

MECHANICAL FORMING OFFERS THE FOLLOWING ADVANTAGES:

1. SUBSTANTIAL REDUCTION OF LAY-UP COSTS
2. HIGHER QUALITY OF FINAL PRODUCT BY VIRTUE OF BETTER CONTROL OF RADIUS CONTOUR AND CONTACT BETWEEN PLIES
3. PERMITS INCLUSION OF TITANIUM ALLOY INTERLEAVES – SPRINGBACK OF TITANIUM CANNOT BE PREVENTED IN HAND LAY-UP OPERATIONS.

PROCEDURES FOR MECHANICALLY FORMING B/AL STRUCTURAL SHAPES PRIOR TO EUTECTIC BONDING

Figure 2–120

Several small hat-section test assemblies were fabricated with prototype tooling to develop tooling shapes, materials, etc. These parts were complex in that thickness was varied by terminating plies externally and titanium alloy inter-leaves were included. Some of the titanium plies were continuous while others were terminated internally at an abutting boron-aluminum ply. These conditions duplicated designs that were being considered for the compression panel. Metallo-

graphic examination of these test assemblies, which were bonded in the conventional manner after forming, showed them to be of high quality with good contact between adjacent plies. On the basis of the good results obtained on the subsize assemblies, mechanical forming was selected for use in fabricating the stringers for the test components and full-size compression panel. A typical stringer cross-section is shown in Figure 2-121. The development of mechanical forming represents a significant advance in boron-aluminum fabrication. Mechanical forming, followed by eutectic bonding or some other low-pressure, liquid-phase bonding system, permits the fabrication of thick, complex structural shapes which vary in thickness and incorporate titanium interleaves. Such assemblies cannot be fabricated by other manufacturing methods.

2.3.2.3 Bonding Cycle Control - The fiber degradation studies conducted to support the optimization of the eutectic bonding process showed that some degradation could be expected as a result of bonding but that the degree could be minimized by controlling the thermal cycle. On the basis of these studies, parameters were established for the bonding cycle to limit the degradation to an acceptable amount. The lower temperature limit was established at 827°K (1030°F) with the time at this temperature not to exceed 15 min. An upper limit of 844°K (1060°F) was selected with the time at this temperature not to exceed 7 min.

In order to achieve the degree of control needed to meet the selected bonding cycle parameters, an on-line, closed-loop, proportional control system was added to the bonding furnace. This furnace has six independently controlled zones, each of which is programmed to provide the same cycle of heating rate, maximum temperature, and time at temperature.

After this improved control system was added to the furnace, a series of calibration runs were made. These tests showed the system capable of producing actual time-temperature cycles that fell within the specified limits. As a result, this system was used for the bonding of most of the element test specimens, the component test assemblies and the full size panel.

Generally, the amount of degradation which occurred during the over-all program was less than predicted on the basis of the fiber degradation studies. This was demonstrated by quality control specimen test results. Each bonding run contained tensile-test samples which were eutectically bonded along with the components in the pack. These tensile specimens had filaments in common with material tested in the as-received condition. A direct comparison of tensile strengths before and after bonding was made for each run. The results of the test specimens

48 PLIES B/AL
4 PLIES Ti–6AI–4V

5X

100X

100X
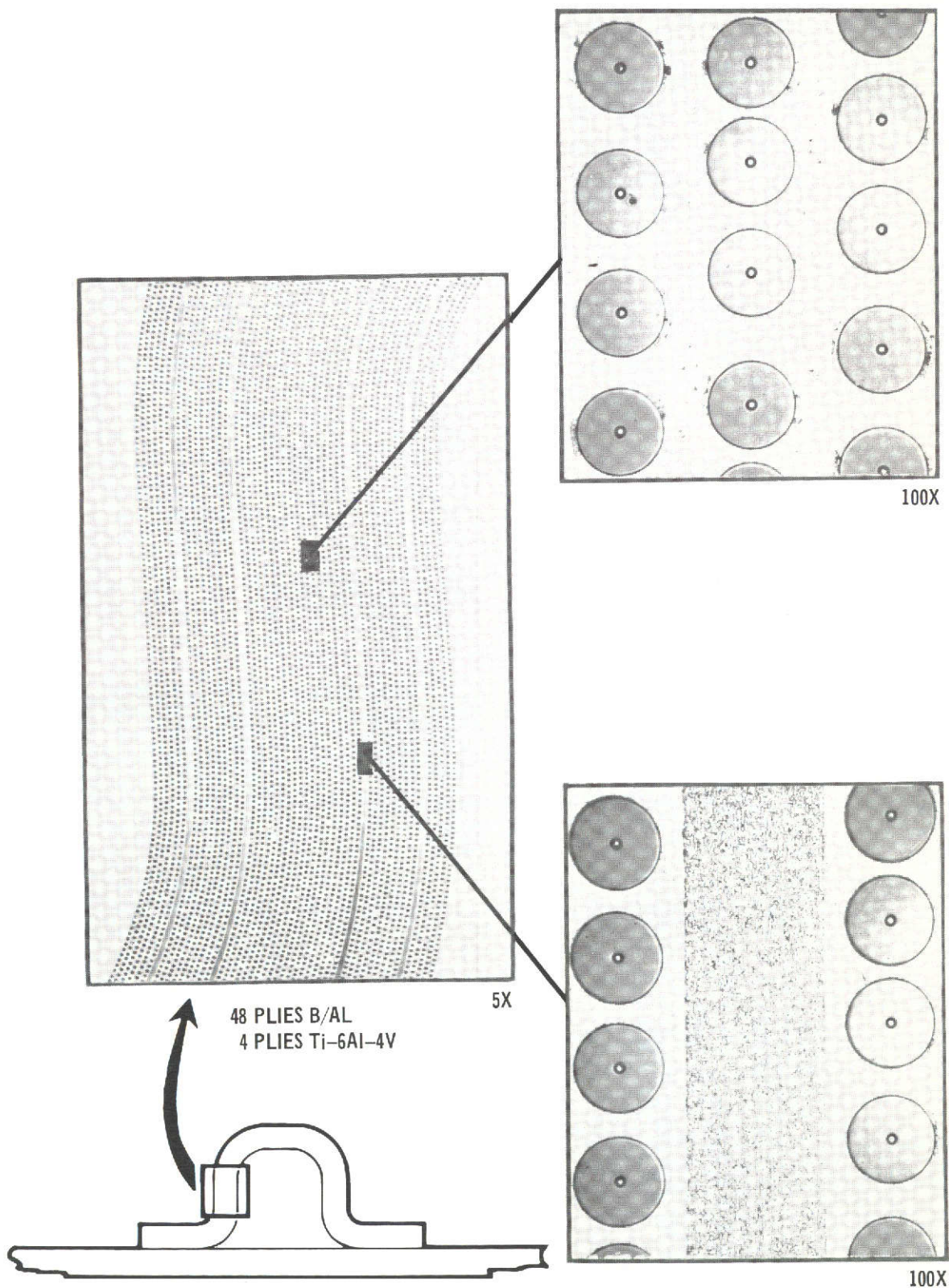
CROSS-SECTION THROUGH EUTECTIC BONDED CENTER-LINE
STRINGER OF COMPONENT PANEL

Figure 2–121

2–131

from the first 35 runs made after the installation of the improved controls are
shown in Figure 2-122. These data show that the average bundle strength of all the
runs was well above the predicted value based on the filament degradation studies
(Figure 2-115). Also, less than the minimum expected amount of degradation was
observed in more than 60% of the runs. These results demonstrate that the improved
control system, with few exceptions, does maintain the eutectic bonding cycle with-
in the desired limits.

AVERAGE FILAMENT BUNDLE STRENGTH AFTER BONDING
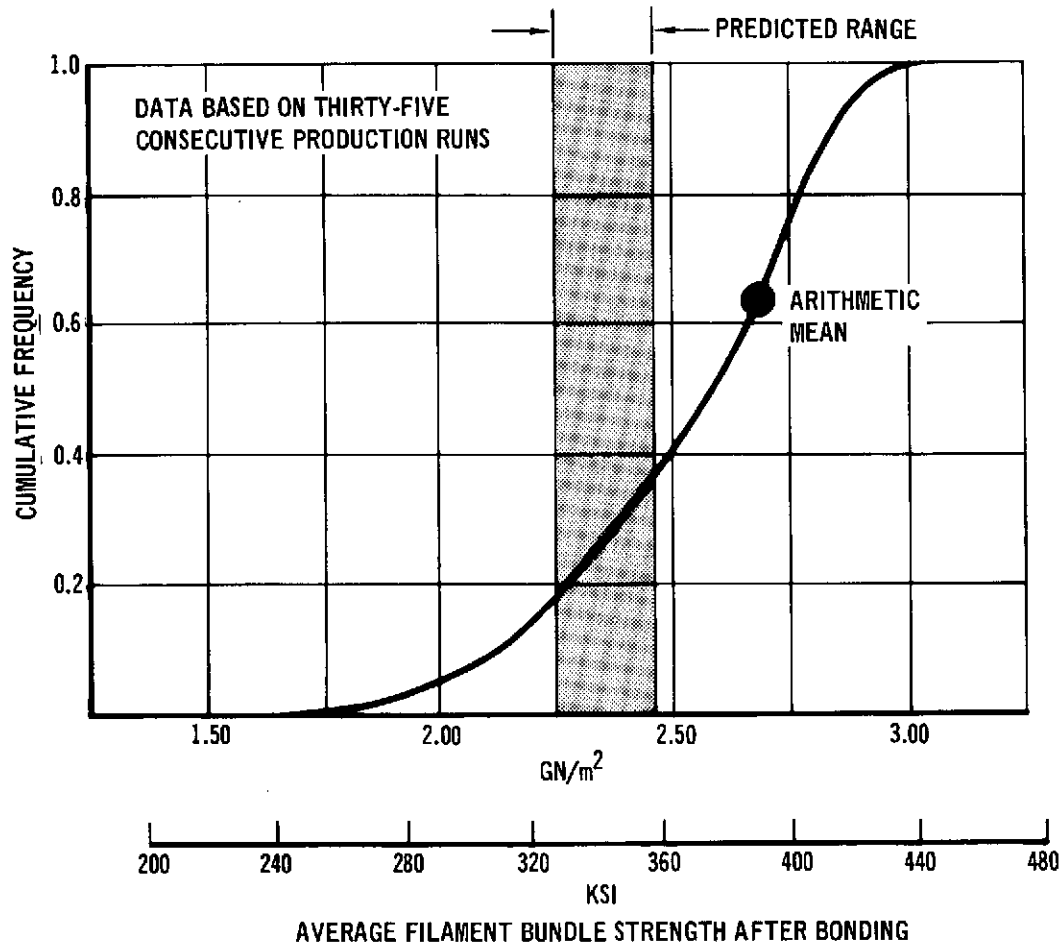
STRENGTH OF BORON FILAMENTS AFTER EUTECTIC BONDING BASED ON TENSILE SPECIMENS BONDED WITH PRODUCTION PARTS

Figure 2-122

2.3.3 Metallurgical Joining Development - One of the tasks in the process develop-
ment phase was to evaluate metallurgical joining methods that might be applied to
the compression panel, truss beam or shear web to be designed in Phase II of this
program. Two processes expected to have wide application in fabricating boron-
aluminum structures are brazing and resistance spotwelding. Therefore, these
processes were selected for a preliminary evaluation.

2-132

2.3.3.1 <u>Resistance Spotwelding</u> - Resistance welding and weldbonding investigations were conducted on boron-aluminum composite for possible application to the compression panel skin-to-stringer joints. Weldbonding is a combination of resistance welding and adhesive bonding developed to improve fatigue properties. Most weldbonding studies have utilized epoxy type adhesive because the design temperatures were less than 422°K (300°F). These adhesives would not withstand the 589°K (600°F) compression panel test temperature so a commercial polyimide adhesive, BR-34, was selected to provide high temperature properties needed for this program.

Preliminary resistance welds were made in 2.29 mm (0.090 in.) thick 1100 aluminum to establish a weld schedule. Weldbonds then were made in 1100 sheet. Just prior to welding, the adhesive was applied to the faying surfaces of joints and the welds were made with the schedule developed for conventional resistance welding. Control specimens which had been adhesive bonded only also were prepared. The cure cycle consisted of heating at 450°K (350°F) for 1 1/2 hour in vacuum under a positive pressure of 275.7 MN/m^2 (40 psi). After cooling to room temperature, the specimens were reheated to 574°K (575°F) for 2 hours. The failure loads of all of the joints - resistance welded, weldbonded and adhesive bonded - were comparable and the shear strengths of the adhesive bonded and weldbonded joints were comparable. The weld strengths were well above the minimum average specified in MIL-W-6858.

Preliminary resistance welds then were made in 4 ply 0.86 mm (0.031 in.) and 8 ply mm (0.060 in) thick boron-aluminum composite eutectic bonded laminates. Excellent resistance welds were obtained with no apparent difficulties provided the basic composite monolayer was satisfactorily diffusion bonded. Weld strengths obtained in establishing weld schedules are shown in Table 2-3. These strengths were also above the minimum averages specified for 1100 aluminum in MIL-W-6858. Attempts to weld material with marginal diffusion bonds resulted in melting of the spot area near the electrode and delamination of the composite along the diffusion bondline.

Preliminary weldbonds and adhesive bonds also were made in 4 ply 0.86 mm (0.031 in.) thick boron-aluminum composite. Weldbonded specimens were made using the resistance weld schedules developed for the boron-aluminum composite. All the other procedures and cure cycles were the same as those used for the 1100 aluminum. Shear strength tests made on the specimens resulted in fractures of the composite

NO. OF PLIES	ORIENTATION	THICKNESS		TEST FAILURES		SPEC. MIN. FOR EQUIV. ALUMINUM,	
		mm	(IN.)	N/SPOT	(LB/SPOT)	N/SPOT	(LB/SPOT)
4	$[+45]_S$	0.76	(0.303)	1334–1557	(300 – 350)	934	(210)
8	$[+45_2]_S$	1.52	(0.060)	3114–3558	(700–800)	2202	(495)
5	$[90_2, T]_S$	0.97	(0.038)	2224–2758	(500–620)	–	–
10	$[Ti, 45, -45_2, 45]_S$	1.93	(0.076)	6005–6450	(1350–1450)	–	–

STRENGTH OF RESISTANCE WELDS IN EUTECTIC BONDED BORON-ALUMINUM COMPOSITE

Table 2-3

material away from the joint or by delamination along diffusion bondlines in the joint area. These latter failures were attributed to unsatisfactory diffusion bonds in the initial monolayers. However, these preliminary tests indicate that the composite material can be resistance welded either with or without the use of the high temperature polyimide adhesive.

The possibility of spotwelding boron-aluminum laminates which contained .20 mm (.008 in.) thick titanium alloy interleaves was investigated also. These studies included tests on material with the titanium sandwiched between the boron-aluminum and also with titanium on the outer surface of the laminates. Good results were obtained under both conditions (Table 2-3).

Although preliminary tests showed that boron-aluminum, both with and without titanium interleaves, can be readily joined by resistance welding methods, this procedure was not applied to the fabrication of the compression panel. The config- uration of the panel precluded its consideration for two reasons. First, at the point of load introduction, the skin and stringer are about 12.7 mm (.5 in.) and 10.2 mm (.4 in.) thick respectively; this combination could not be readily joined with welding equipment available at MDC-St. Louis. In addition, both the skin and stringer thickness vary along their length, requiring the development of a very large number of welding schedules and new welding techniques. Such a study was beyond the scope of the program. For these reasons, resistance welding was not selected for the compression panel design.

2.3.3.2 Brazing Feasibility Study - The high modulus of elasticity of boron- aluminum makes it an attractive candidate for honeycomb sandwich structures. Therefore a study was undertaken to determine if such structures could be fabricated

by brazing B/Al face sheets to Ti-alloy honeycomb core. An additional objective
was to demonstrate that the multi-ply facing sheets could be joined by eutectic
bonding during the brazing cycle. To accomplish this, a brazing alloy was needed
that would melt and flow within the eutectic bonding temperature limits. There-
fore, both commercial and experimental Al-base brazing alloys were evaluated for
potential application to boron-aluminum/titanium honeycomb structures.

The brazing alloy study included Al-Si-Cu, Al-Cu-Mg and Al-Si-Zn-Cu alloys
which were compared on the basis of their flow temperature and ability to wet 1100
aluminum. Several compositions were found that had the desired characteristics.
Of these, the commercial alloy designated 719 by Alcoa was selected for further
evaluation. The nominal composition of this alloy is Al-10Si-10Zn-4Cu and it
melts within the temperature range from 788° to 839°K (960° to 1040°F).

In the final stage of the brazing study, small honeycomb samples were prepared
by eutectic bonding the boron-aluminum facing sheets while brazing the face sheets
to the titanium alloy core. Figure 2-123 shows a section of one of these samples
which consists of 4 ply ($\pm$45°) face sheets, Ti-3Al-2.5V alloy core, 19 mm (.75 in.)
thick, and a titanium edge member. Five day salt spray tests were conducted per
Fed. Std. 151, Method 811.1 on a similar section. There was no visual evidence of
braze joint deterioration. These tests demonstrated that boron-aluminum can be
used to fabricate honeycomb sandwich and applied to structures such as the shear
web (Phase II). The braze approach utilizing titanium alloy core could provide
elevated temperature capability for these structures.

2.3.4 <u>Preparation of Process Specifications</u> – During the initial stages of this
investigation a major portion of the effort was directed toward process develop-
ment. The major objectives of this phase were accomplished well before fabrication
of test components or the compression panel was begun; hence, the improved processing
was used for the successful fabrication of these major structures. The incorporation
of the improved processing was accomplished through the preparation and application
of several process specifications.

Three basic specifications were prepared. The first was MDC-St. Louis
Specification PS 12071, "Cleaning Boron Filament-Aluminum Matrix Composite Foil".
This specification was based on the cleaning optimization studies and the solu-
tions and immersion times found to be the most suited from the standpoint of
oxide removal and dissolution rate are included together with requirements to
prevent contamination during handling and storage.
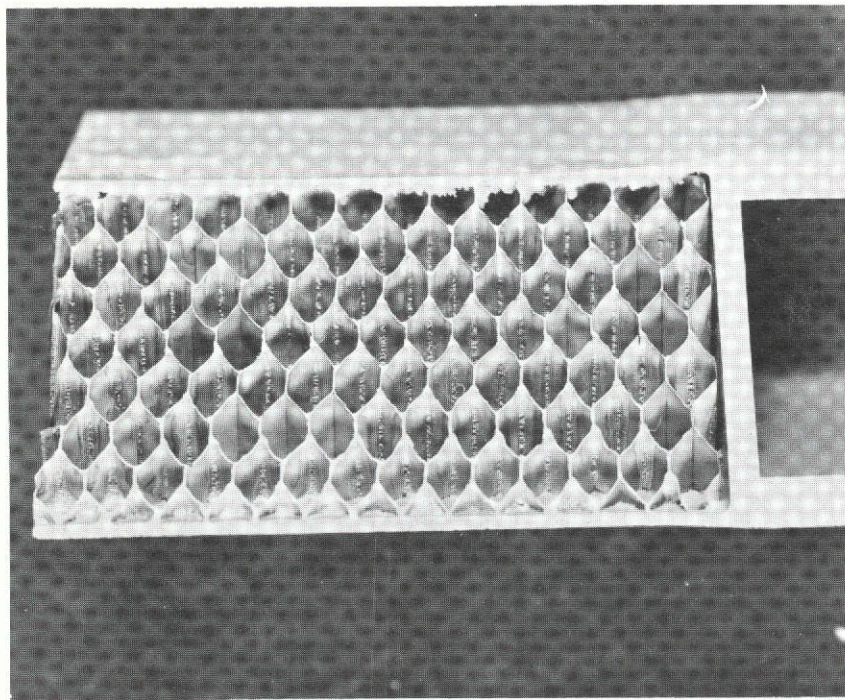
EUTECTIC BONDED FOUR PLY BORON/ALUMINUM FACE
SHEETS BRAZED TO TITANIUM CORE. ALL BONDING
COMPLETED IN ONE THERMAL CYCLE

Figure 2-123

The second specification, PS 13130, "Vacuum Deposition of Copper on Boron Filament-Aluminum Matrix Composite Foil" outlines certification procedures for both the coating process, which includes glow discharge cleaning, and operators. Quality control procedures to ensure proper coating thickness and adherence are included. Storage requirements based on the ellipsometry evaluations of oxide built-up on cleaned and on coated surfaces.

Eutectic bonding time and temperature parameters, selected on the basis of fiber degradation studies are covered in PS 22617 (Preliminary) - "Eutectic Bonding of Boron Filament - Aluminum Matrix Composite Foil Assemblies".

2.4 Fabrication and Assembly

2.4.1 General – Fabrication and assembly in Phase IV consisted of the manufacture
of selected items designed in Phase II for test. These items were: (1) Component
Test Panel Test Assembly, (2) Stringer Test Assembly with typical splice joint,
and (3) the Compression Panel.

The 1.22 m x 1.83 m (4 ft x 6 ft) compression panel design required fabrica-
tion of skins and hat section boron-aluminum stringers with interleaves of titanium,
tapered in thickness and using the eutectic bonding process. Thicknesses of the
stringers ranged from 5 plies to 52 plies and the skin thickness varied from 10
plies to 62 plies. Assembly of the panel component parts was accomplished by using
Hy-Lok fasteners and other standard aerospace bolt-nut combinations. All the
above test assemblies were successfully fabricated and delivered to the responsible
test agencies (MDC or NASA).

Boron-aluminum composite foil material used in this phase was of good quality,
readily fabricable; however, bilayer material used in the panel skins was found to
have a pronounced tendency to separate at the diffusion bonds during machining
operations. The diffusion bond deficiencies of the bilayer material could not be
determined in standard quality control material tests; consequently, bilayer usage
was restricted to noncritical applications for the remainder of the program.

Manufacturing and quality assurance procedures followed on this program
are illustrated on the flow chart presented in Figure 2-124. As evidenced by the
chart, frequent inspection steps during fabrication assured quality workmanship
for the complex assemblies for this program.

2.4.2 Tooling – Major tooling required for this phase consisted of tools for
eutectic bonding the panel skin and hat section stringers and a mechanical forming
tool for forming the stringers.

An existing MDC tool was used for eutectic bonding the panel skins. This
tool is essentially a large flat, stainless steel plate with stiffened egg crate
type support structure as shown in Figure 2-125.

For the hat section stringers, a double sided hat stainless steel tool shown
in Figure 1-126 was constructed. The tool is of balanced construction to minimize
thermal distortion during the bonding cycle. A tool for mechanical forming
resulting from studies reported in Section 2.3.3.3 was also constructed (Figure
2-127) which enabled forming the stringer ply layups directly onto the bonding

```
┌──────────┐   ┌──────────────┐   ┌─────────┐   ┌────────┐   ┌─────────────┐
│ B/AL PER │───│ INSPECT PER  │───│ TRIM TO │───│ CLEAN  │───│ COPPER COAT │───┐
│ MMS 584  │   │ FIGURE 2-1   │   │ SIZE    │   │        │   │             │   │
└──────────┘   └──────────────┘   └─────────┘   └────────┘   └─────────────┘   │
                                                                               │
┌──────────┐   ┌──────────────┐   ┌─────────┐   ┌────────┐                     │
│ Ti-6Al-4V│───│ REVIEW       │───│ TRIM TO │───│ CLEAN  │─────────────────────┤
│ FOIL PER │   │ CERTIFICATION│   │ SIZE    │   │        │                     │
│ AMS 4911 │   └──────────────┘   └─────────┘   └────────┘                     │
└──────────┘                                                                   │
```

```
        ┌───────────────────┐          ┌───────────────────┐
        │ STRINGERS         │          │ SKINS-LAYUP       │
        │ LAY-UP FLAT       │          │ SUBASSEMBLIES     │
        │ PACKS-INSPECT     │          │ INSPECT           │
        └───────────────────┘          └───────────────────┘
                 │                               │
        ┌───────────────────┐          ┌───────────────────┐
        │ MECHANICAL        │          │ LAYUP SUBASSEMBLIES│
        │ FORM              │          │ TO COMPLETE SKIN   │
        │                   │          │ LAYUP             │
        └───────────────────┘          └───────────────────┘
                 │                               │
           ┌──────────┐                   ┌──────────┐
           │ INSPECT  │                   │ INSPECT  │
           └──────────┘                   └──────────┘
                 │                               │
                 └───────────────┬───────────────┘
                          ┌───────────────────┐
                          │ COMPLETE BONDING  │
                          │ PACK-WELD         │
                          │ PULL VACUUM       │
                          └───────────────────┘
                                  │
                          ┌───────────────────┐
                          │ EUTECTIC BOND     │
                          └───────────────────┘
                                  │
                          ┌───────────────────┐
                          │ INSPECT           │
                          └───────────────────┘
                                  │
                          ┌───────────────────┐
                          │ MACHINE TO        │
                          │ FINAL SIZE        │
                          └───────────────────┘
                                  │
                          ┌───────────────────┐
                          │ LOCATE ON         │
                          │ ASSEMBLY -        │
                          │ DRILL             │
                          └───────────────────┘
                                  │
                          ┌───────────────────┐
                          │ ASSEMBLE          │
                          └───────────────────┘
                                  │
                          ┌───────────────────┐
                          │ INSPECT           │
                          └───────────────────┘
                                  │
                          ┌───────────────────┐
                          │ SHIP TO           │
                          │ TEST AGENCY       │
                          └───────────────────┘
```

MANUFACTURING AND QUALITY ASSURANCE FLOW CHART

Figure 2-124
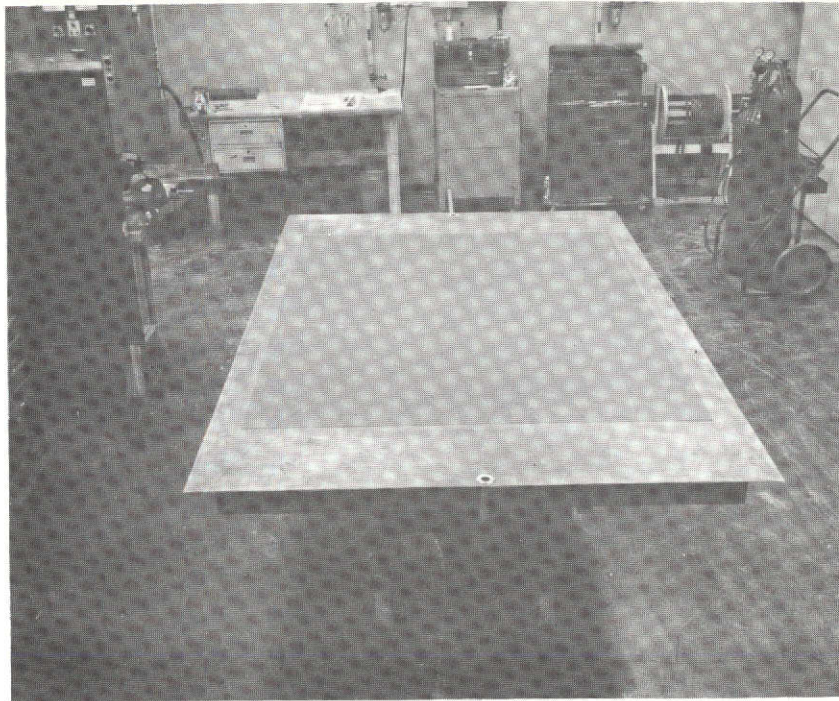
TOOL FOR COMPRESSION PANEL SKIN

Figure 2—125
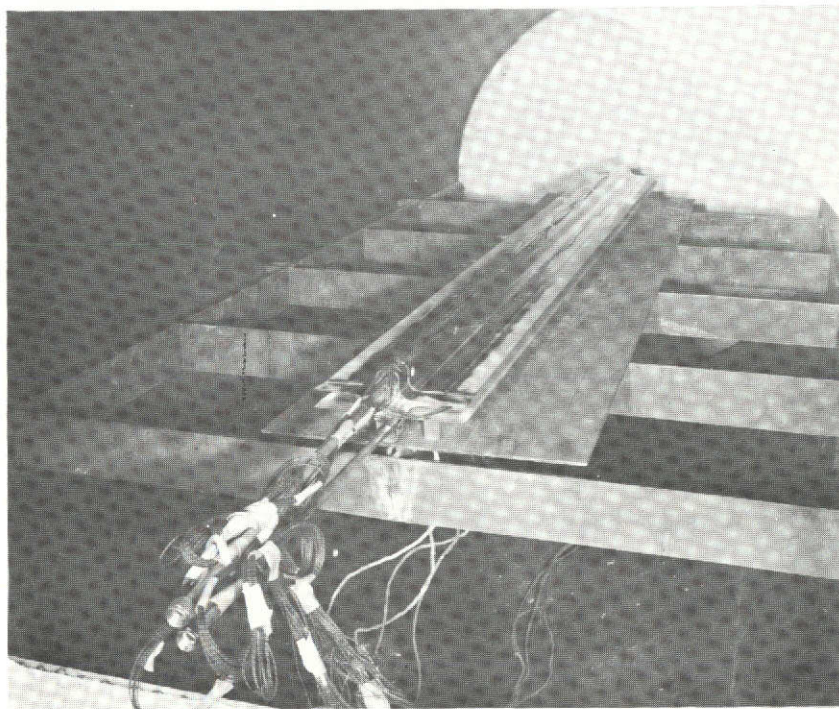
TOOL FOR COMPRESSION PANEL STRINGER

Figure 2—126

tool prior to the bonding cycle. Heat surveys conducted on the bonding tools
proved temperature response and thermal gradient acceptability and determined the
control settings for semiautomatic control of the cycle.
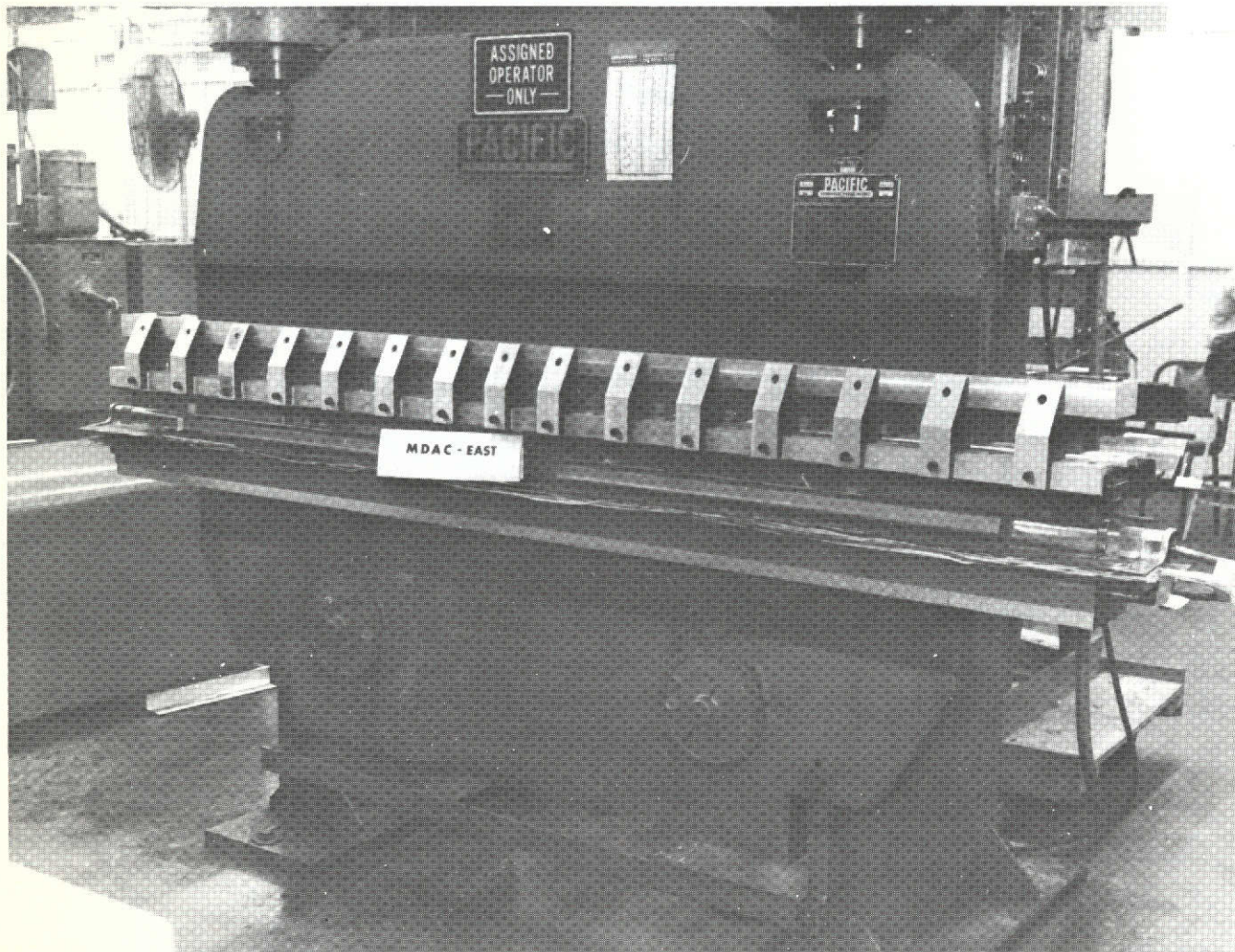
STRINGER FORMING TOOL

Figure 2-127

2.4.3 Lay-Up Technique - The varying thickness and the large number of plies (up
to 62 plies) of the panel skin required lay-up procedures that would insure proper
orientation and fitting of plies. To accomplish this, the skin assembly was
divided into subassemblies of four plies each. The detail plies were fitted and
poke welded together in the conventional manner to form the subassemblies; these
subassemblies were then fitted and poke welded together to complete the skin lay-up.
Mylar templates such as shown in Figure 2-128 were used to aid in the location,
ply orientation and inspection to assure proper lay-ups.

STRINGER ASSY SKIN LAYUP

Figure 2–128

Lay-up techniques for the hat sections were greatly simplified by the mechanical forming process as the lay-up portion only involved stacking of a flat pack which would subsequently be mechanically formed. A typical flat pack lay-up for a stringer prior to forming is illustrated in Figure 2–129.
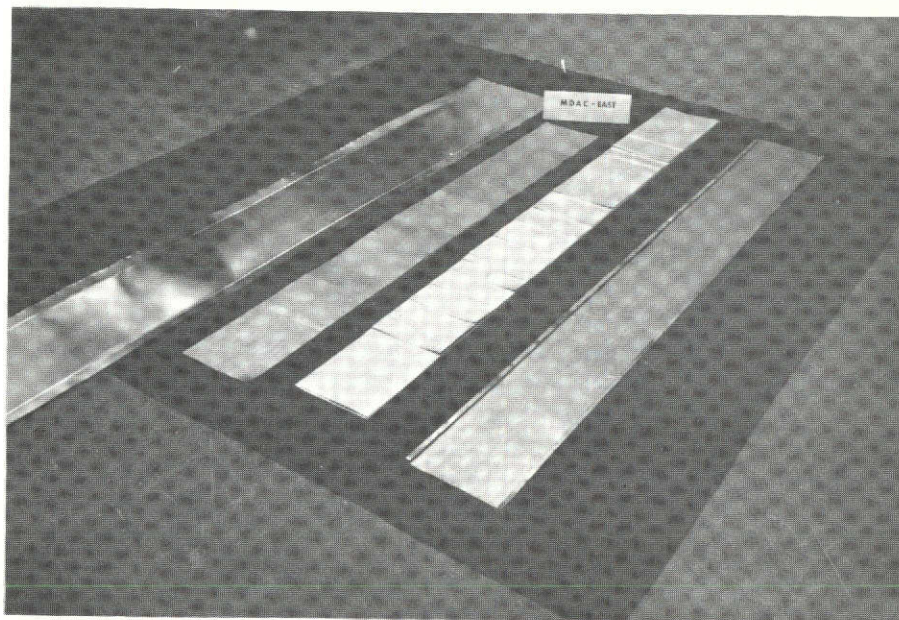
STRINGER FLAT PACK LAYUP DETAILS

Figure 2–129

2–141

2.4.4 Mechanical Forming – Assurance of intimate contact between the plies for bonding in shaped parts and the varying thickness of the hat section stringers (up to 52 plies including "hard-to-form" titanium interleaves) led to the development of a mechanical forming technique as described in Section 2.3.2.2 to replace the marginal hand forming and fitting process previously employed. All hat section stringers fabricated during this phase used this forming technique and resulted in well-bonded, controlled shapes.

2.4.5 Bonding Cycle – All bonding was performed in an autoclave under a nominal 2.1 MN/m^2 (300 psi) pressure using a large tube furnace for heating. The bonding cycle was automatically controlled as developed to conform to process standards set by project engineering. The tube furnace and autoclave are shown in Figure 2-130. The first stringer fabricated for the program was found to be deficient in accomplishment of the eutectic bond. Resultant investigation revealed that defective thermocouple readouts had indicated higher temperatures than were actually experienced; hence, sufficient temperatures were not achieved during the cycle for a well-bonded part. This discrepancy was corrected and with the institution of an automated bonding cycle; all cycles thereafter were controlled to within specification requirements and resulted in generally well-bonded parts.
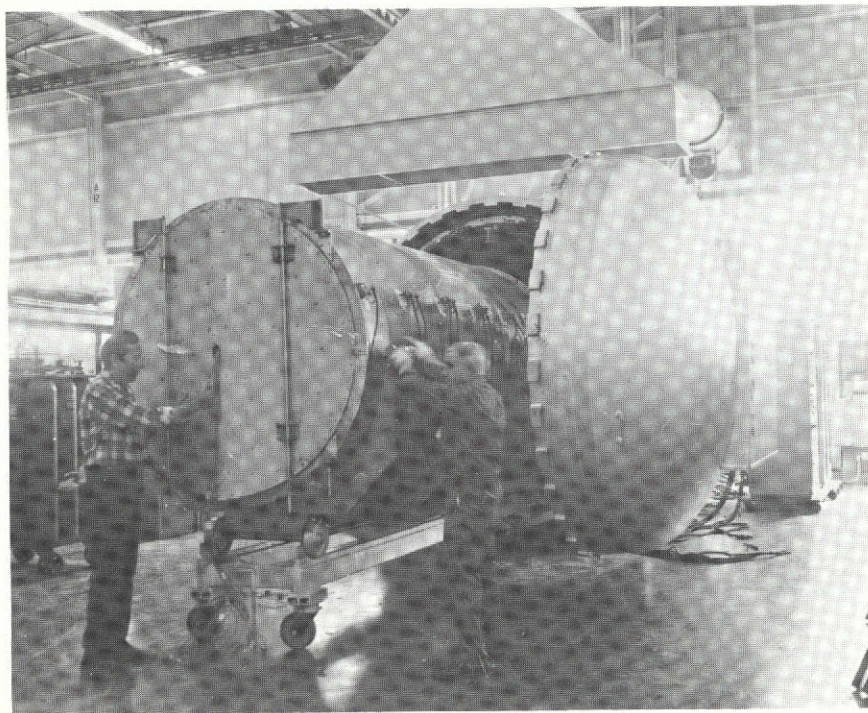
BONDING FURNACE AND AUTOCLAVE

Figure 2-130

2.4.6 <u>Machining and Drilling</u> - Emphasis in this program was placed on improvement and applicability of machining techniques to the more complex composite containing titanium interleaves. The addition of titanium to the composite was found to have little effect on the machining characteristics of the candidate techniques selected for this program.

The primary machining method selected for this program was ECG (Electro Chemical Grinding), supplemented where necessary by grinding with a diamond impregnated disc. A Marwin router converted for use with the ECG process resulted in significant improvement of the machining operations as compared to the modified Bridgeport mill previously used. The router was modified to include a large work table and a variable 0 to 51 cm/minute (0 to 20 inches per minute) feed system. Machining operations on the compression panel skin using the ECG process on the Marwin router are shown in Figure 2-131 with a hat stringer machining shown in Figure 2-132. With these modifications, improvements in the machining quality, setup time and feed rate were realized. The parameters used were:

    Electrolyte - Sodium Nitrate (NaNO$_3$) .9 kg per 3.78 1 (2 lbs per gal) of H$_2$0
    Wheel - .36 m (14 in.) Metal Bonded Diamond
    Voltage - 6 Volts
    Current - 200 to 250 amps (maintained by adjusting the feed rate)
    Feed Rate - 2.5 to 25 cm (1 to 9 in.) per minute dependent on material
            configuration.

The relatively thick sections of boron-aluminum composite with titanium inter-leaves in the test articles necessitated re-evaluating of candidate drilling techniques. Drilling investigations conducted on manufacturing test plans resulted in the selection of the Branson ultrasonic unit using diamond core drills as the most promising technique. This unit required very rigid mounting, necessitating a stationary location, consequently requiring the work piece to be moved into position for the drilling operation. Although the drilling time and drill life with this method was superior to other methods and provided the means for drilling the thick composite sections, this technique was discarded during the fabrication of the Component Panel Test Assembly as attempts to make the unit portable were not successful and setup time using the rigidly mounted drill unit was prohibitive. A DeSoutter rack feed drill unit (Figure 2-133) providing a semiportable drilling operation was evaluated using high speed steel drills and, although an approximate usage of one drill per hole was experienced, the total of the drilling and setup time was substantially reduced. With this method, an acceptable hole could be
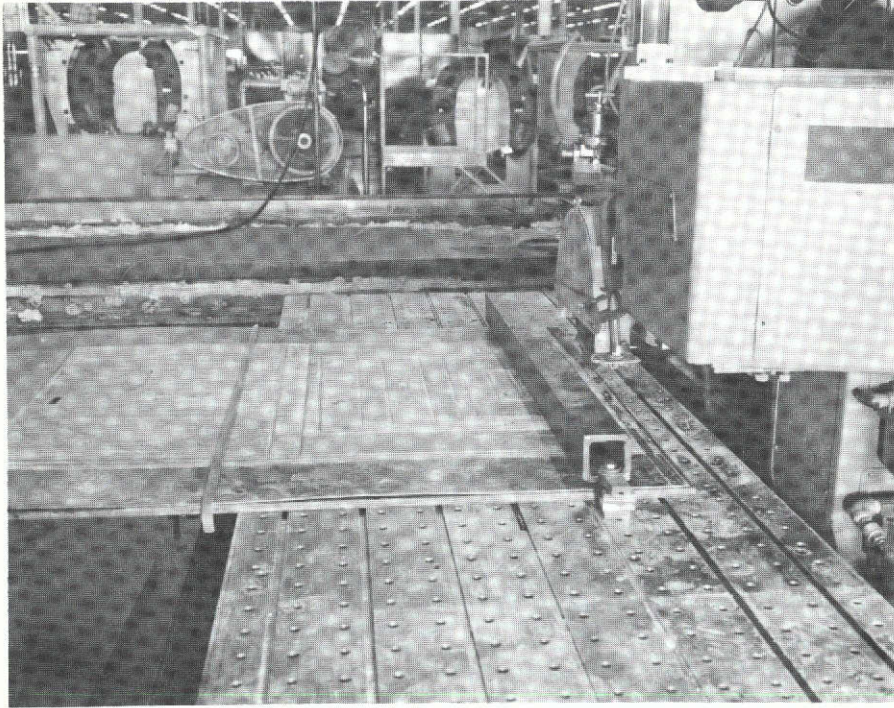
ECG MACHINING OF PANEL SKIN

Figure 2-131
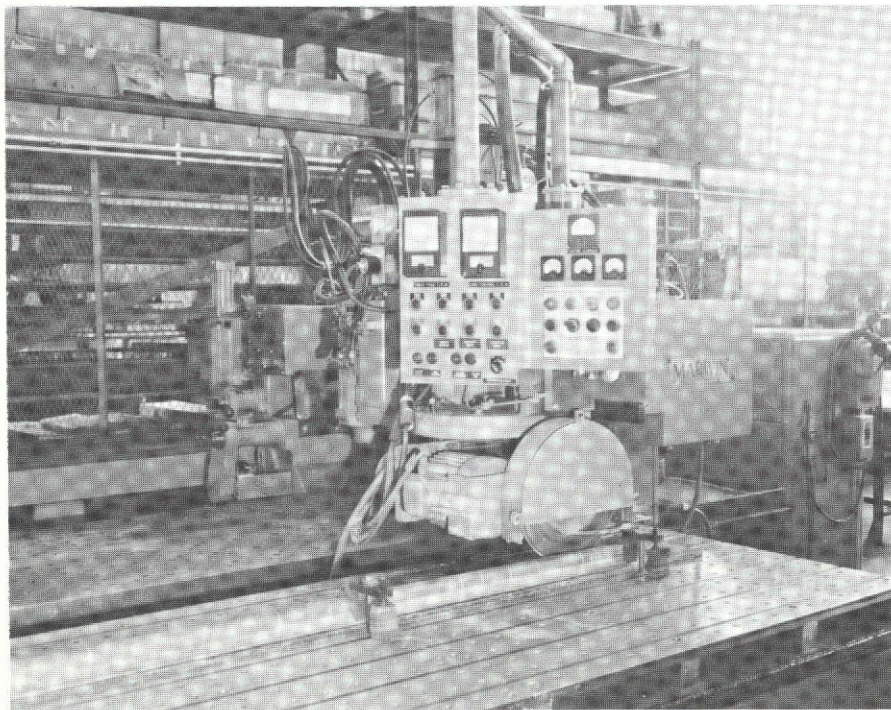
ECG MACHINING OF HAT STRINGER

Figure 2-132

generated in the assembly within two minutes. This technique was adopted and proved reliable and efficient in the remaining assembly work.

RACK FEED DRILL SETUP

Figure 2-133

2.4.7 <u>Stringer Test Assembly</u> - This was the first article fabricated for this phase consisting of a boron-aluminum stringer similar to the outboard stringer of the compression panel with an eight ply $\pm \frac{\pi}{4}$ rad ($\pm 45°$) boron-aluminum skin and a load introduction stringer of sheet metal design. A typical splice joint fitting similar to the compression panel joint design at the load reaction end of the stringer was included to prove the joint design of the compression panel. This assembly as fabricated is shown in Figure 2-134.

2.4.8 <u>Component Panel Test Assembly</u> - The Component Panel Test Assembly, identical to the first bay of the Compression Panel, was fabricated next. This panel represented the more difficult fabrication and assembly tasks associated with the Compression Panel as it involved complex lay-ups of stepped (tapered) construction and large numbers of plies in both skin and stringers. The hat stringer and skin detail parts are pictured in Figures 2-135 and 2-136 with assembled panel views shown in Figures 2-137 and 2-138. A close-up of the load introduction is as shown in Figure 2-139 with the thrust post as assembled as well as the stepped detail of the skin detailed in Figure 2-140. Fabrication of this assembly proved lay-up and assembly techniques and provided experience for production personnel for the full compression panel fabrication task.
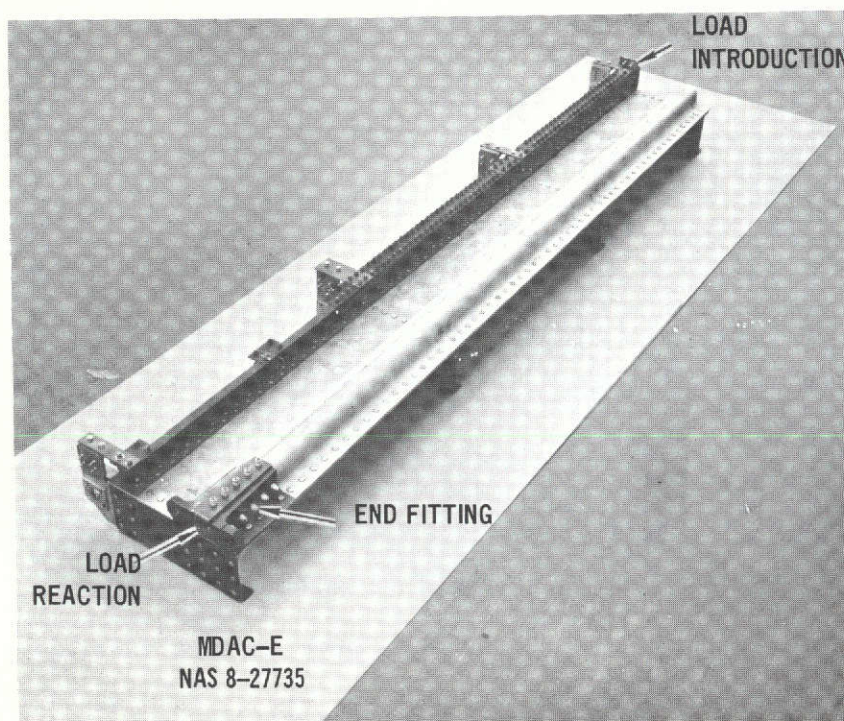
Figure 2–134
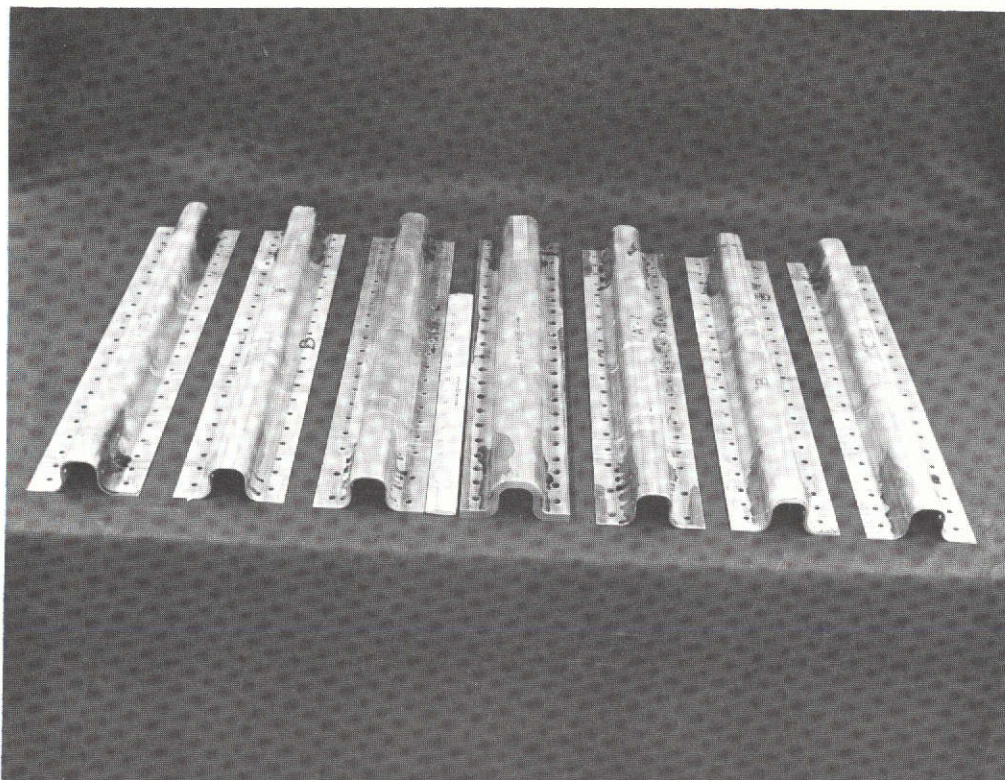
STRINGERS FOR COMPONENT TEST PANEL

Figure 2-135
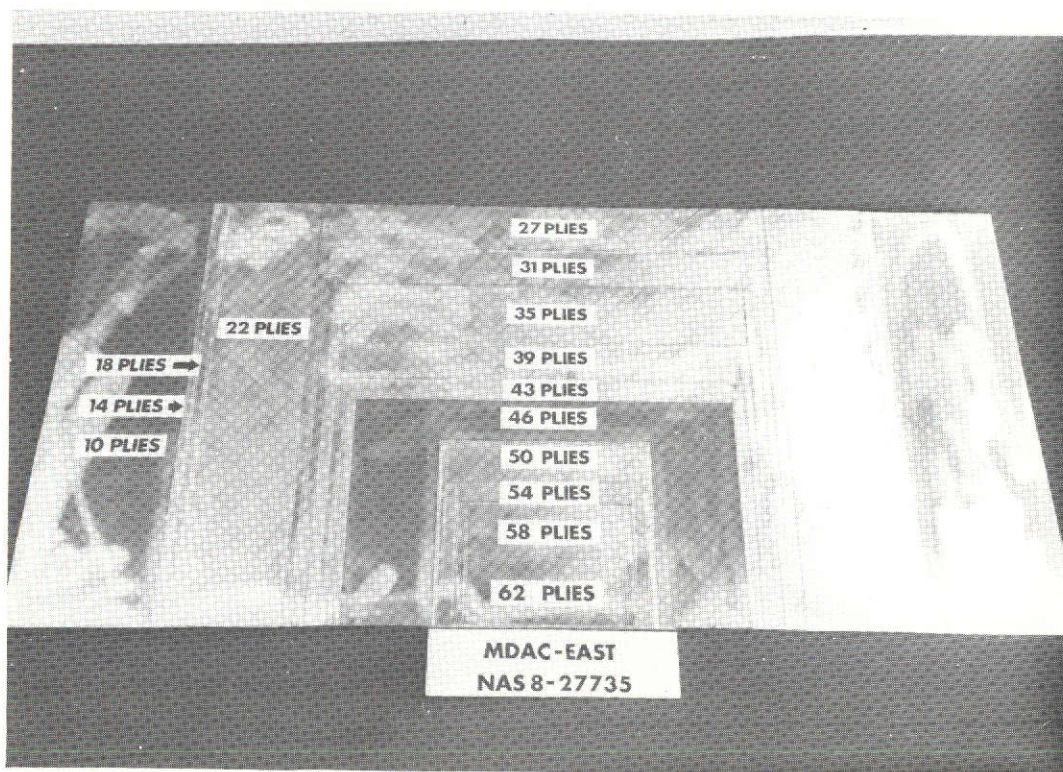
SKIN-COMPONENT TEST PANEL

Figure 2-136

Stringer Side
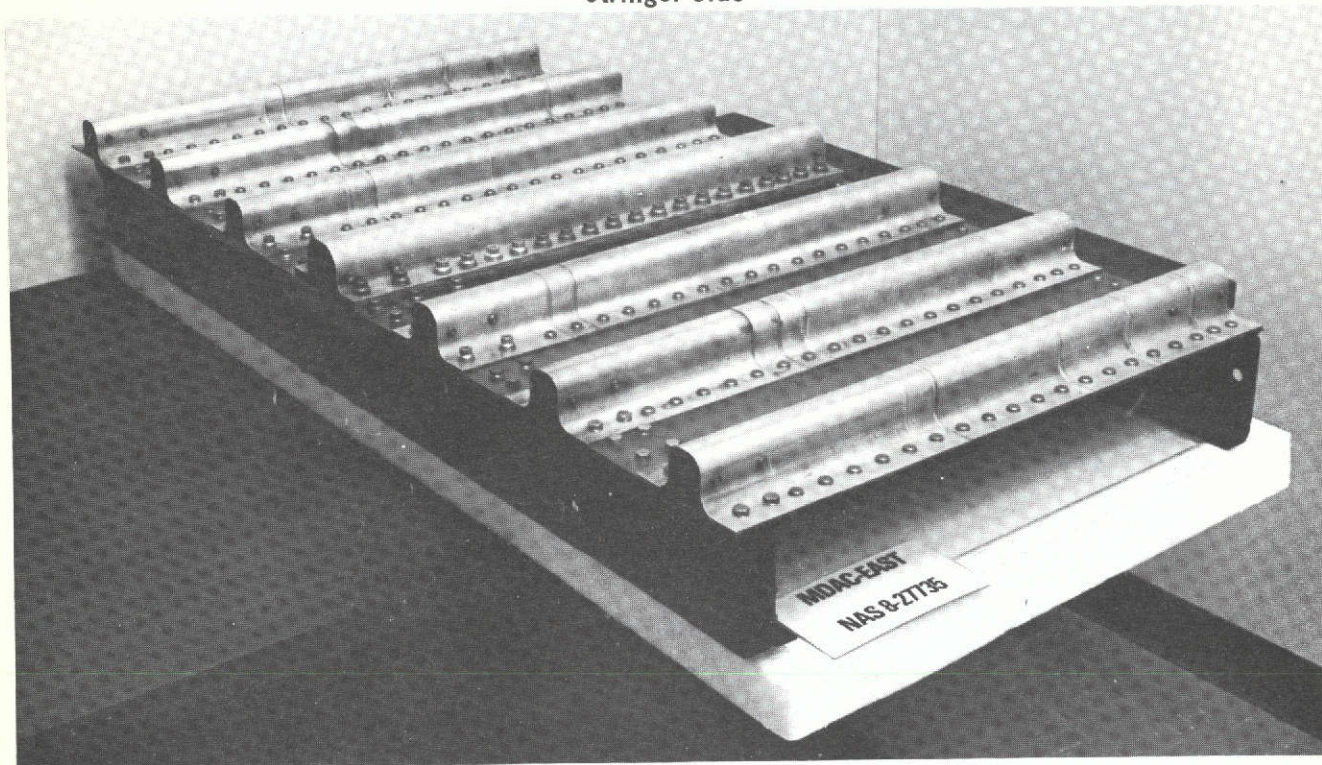
Skin Side
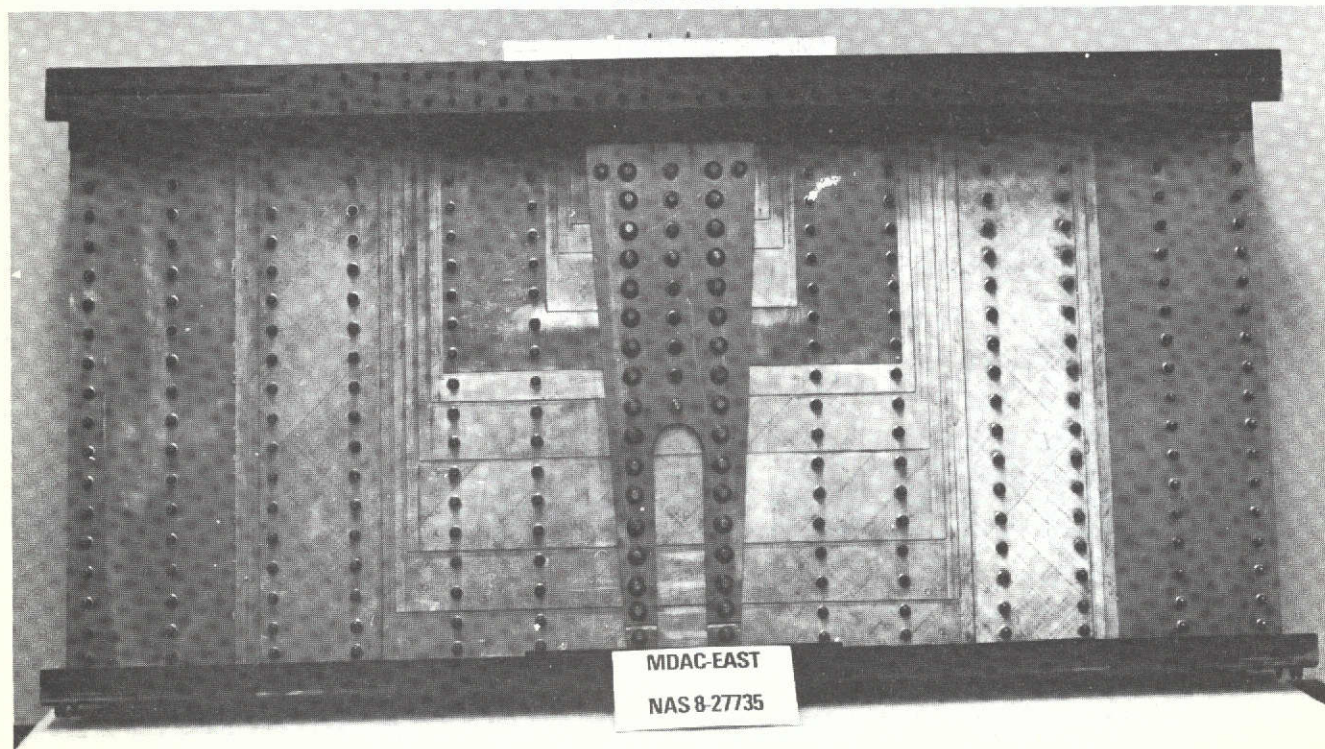
COMPLETED COMPONENT PANEL ASSEMBLY

Figure 2–138

2–148
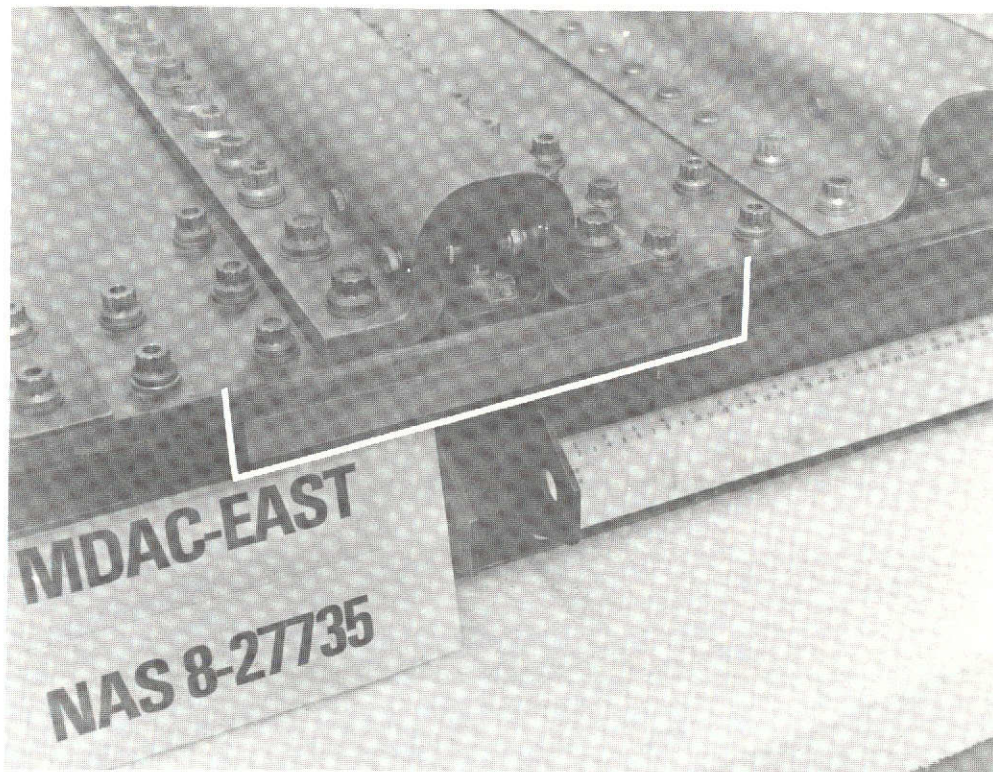
LOAD INTRODUCTION AREA – COMPONENT TEST ASSEMBLY

Figure 2–139
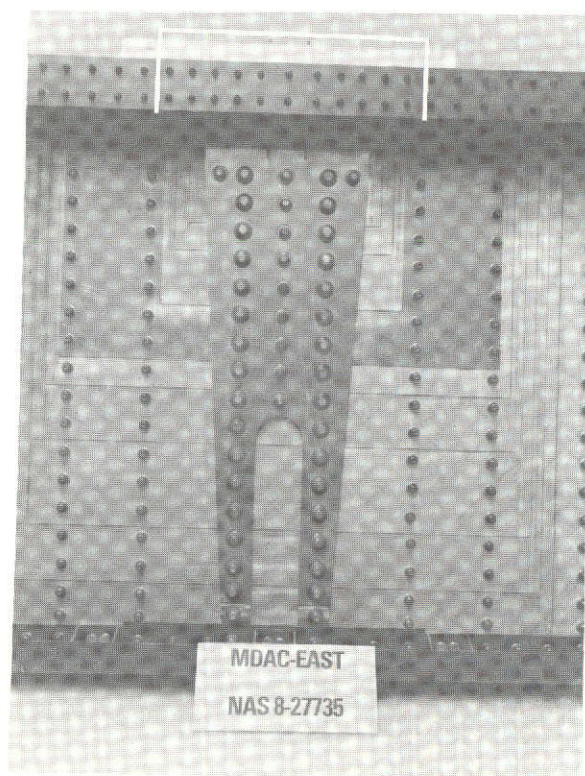
THRUST POST AREA – COMPONENT TEST ASSEMBLY

Figure 2–140
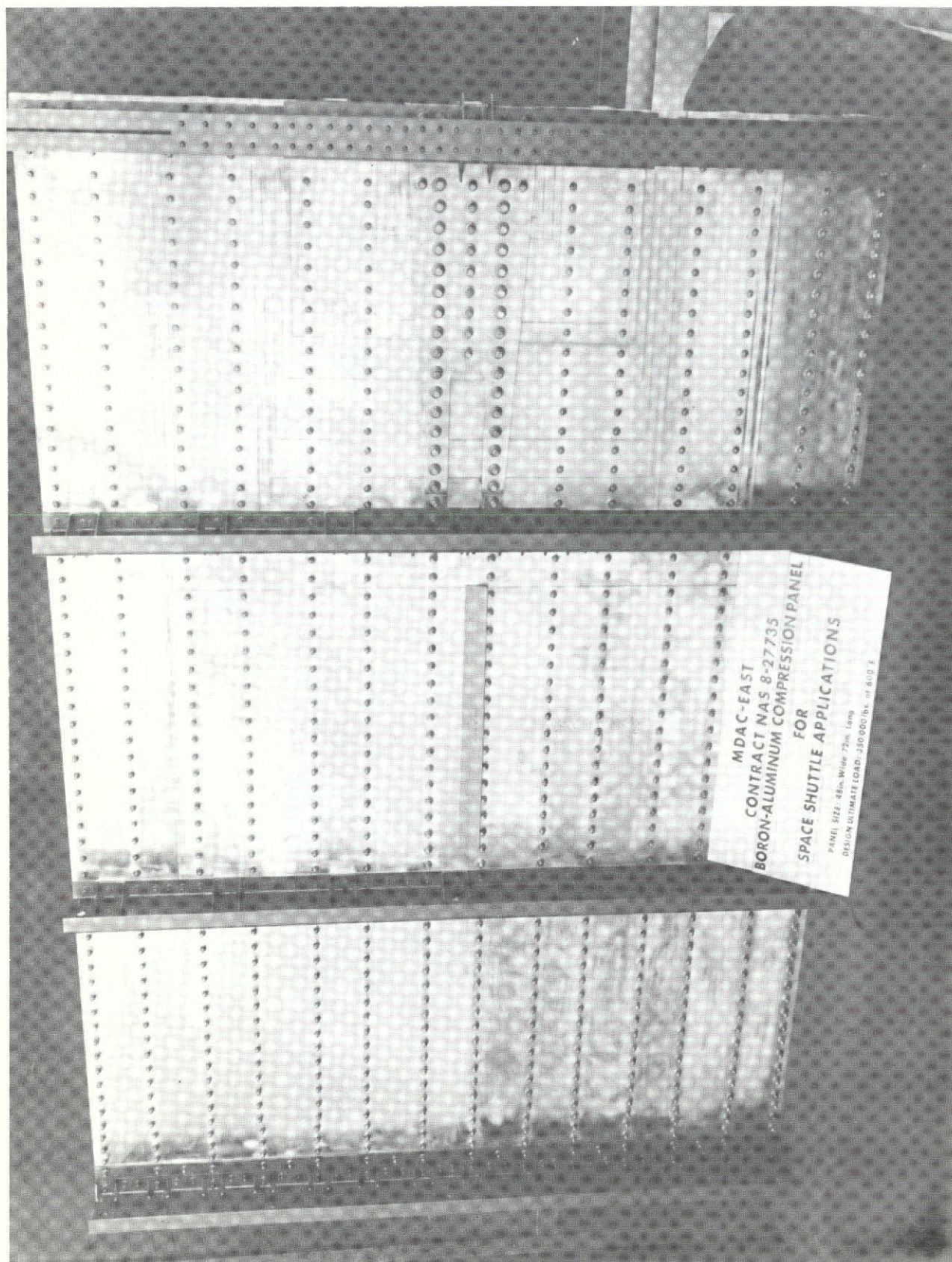
SKIN SIDE –COMPRESSION PANEL
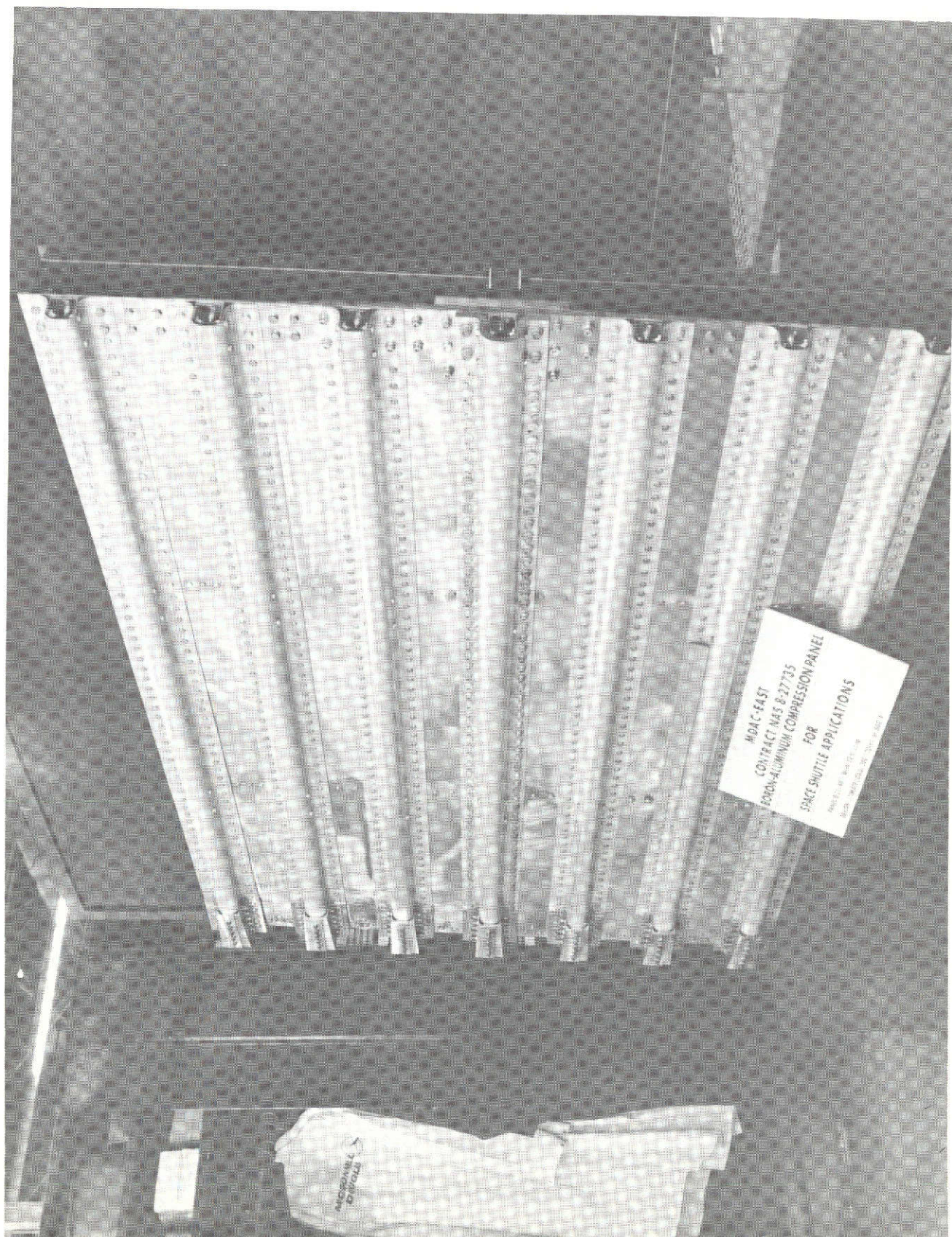
STRINGER SIDE – COMPRESSION PANEL

2.4.9 Compression Panel – After test results of the Stringer Test Assembly and
Component Panel Test Assembly units confirmed the panel design, fabrication of
the 1.22 x 1.83 m (4 x 6 ft) compression panel was initiated. Manufacturing
techniques and assembly procedures for the thick and tapered composite details of
the two test component proved reliable for the large panel enabling the fabrication
and assembly to proceed routinely to completion. The completed panel as viewed from
the skin side in FIgure 2-141 illustrates the precision stepped details of the
large skin as assembled with the thrust post and conventional support frames.
The tapered and variable thickness hat section stringers are evident in Figure
2-142 viewing the panel from the stringer side. The load introduction and load
reaction ends of the panel are shown in Figures 2-143 and 2-144, respectively,
where the thicknesses and built-up assembly of the details are emphasized including
the production splice closeout fittings.

The fabricated structure is sound and well-bonded with the exception of edge
delaminations located in the diffusion bonds of the skin bilayer material. These
delaminations were discovered during machining of the skin after bonding.
Ultrasonic C scans indicated these delaminations to be in localized areas at
the skin edges. Analysis indicated that since the skin in this area is well
supported by the hats and mechanical fasteners, the discrepancies were acceptable.
Further, the ultimate strength of the panel would not be degraded.

It is believed that these defective diffusion bonds in the bilayer material
existed in incoming material as supplied by Amercom, Inc., but were not discoverable
using available material inspection techniques. It is the nature of multilayer
diffusion bonded material to form a mechanical lock between the foil and filaments,
making detection of lack of diffusion bond (especially when the joint is tight)
very difficult. The decision was made to limit the use of the bilayer material to
noncritical applications for the remainder of this program.

LOAD INTRODUCTION END – COMPRESSION PANEL

Figure 2–143
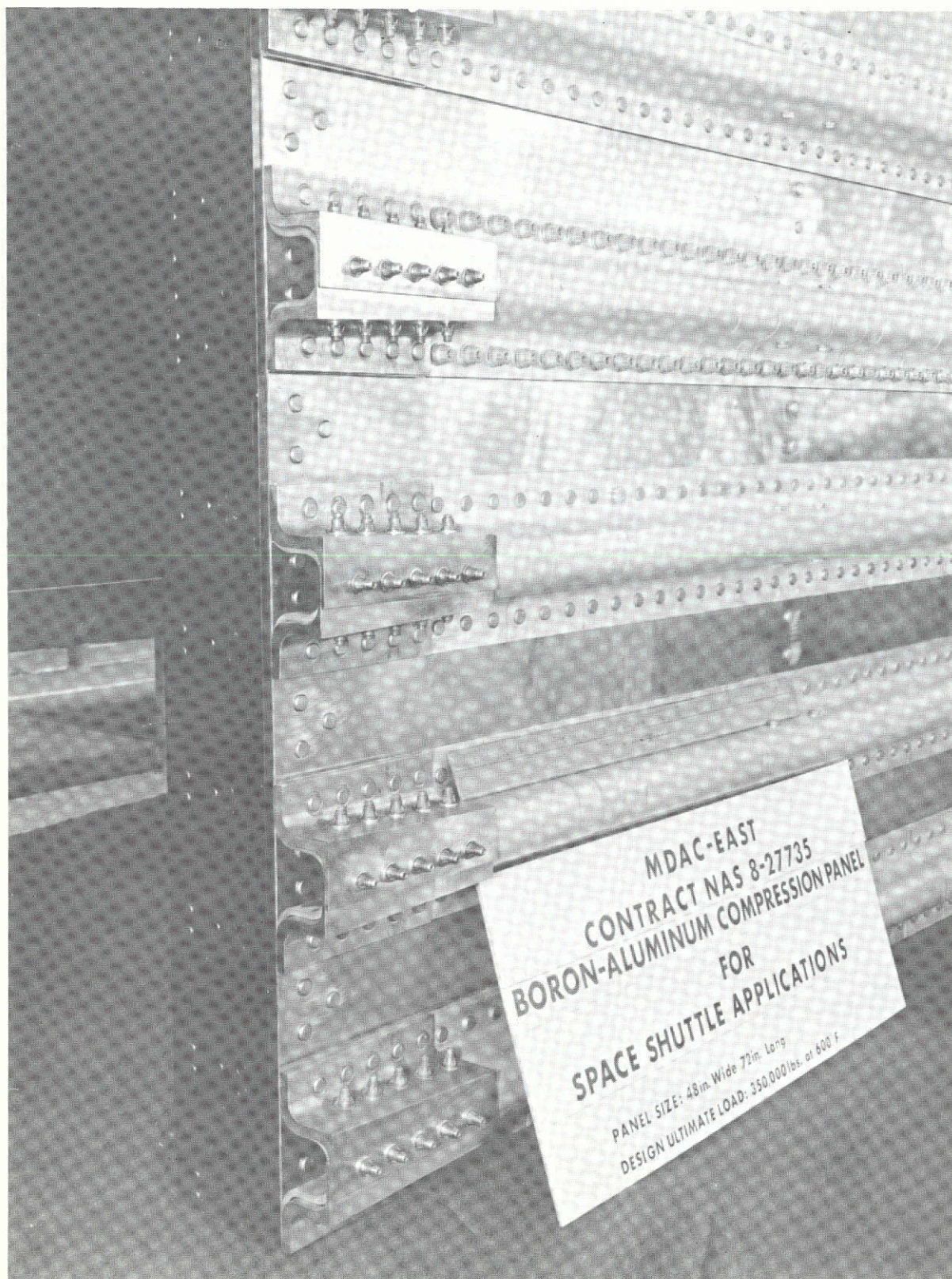
LOAD REACTION END — COMPRESSION PANEL

Figure 2-144

2-154

MCDONNELL DOUGLAS ASTRONAUTICS COMPANY - EAST

2.5 Phase V – Test and Evaluation

The 1.22 m (48 in.) by 1.83 m (72 in.) boron-aluminum Compression Panel
contains many unique design features including titanium interleaves, internal
and external boron aluminum ply terminations, and tapered thickness stringers
and skin. In addition, the concentrated load applied at one end reacted by a
uniformly distributed load at the opposite end causes complex internal loads.
No composite structure has been designed and tested for shear lag loading in the
past, particularly at an elevated temperature of 589°K (600°F). For these reasons,
it was advisable to fabricate and test structural components which verified primary
structural features of the Compression Panel. Two components were chosen. One
was a stringer assembly to demonstrate the overall axial compressive strength
of a long element of the panel. The Stringer Test Assembly is described in
Section 2.5.1. The other structural test article was a Component Panel Test
Assembly which is an exact duplicate of one-third of the Compression Panel at the
concentrated load end. Test of the Component Panel Test Assembly verified internal
loads distribution. Component Panel test results are described in Section 2.5.2.
English units have been used in illustrations for Sections 2.5.1 and 2.5.2 for
clarity.

2.5.1 Boron Aluminum Stringer Test Assembly – The three span 1.83 m (72-in.) long
tapered boron aluminum stringer column specimen shown in Figure 2-145 was selected
to verify the design and analysis of stringers on the Compression Panel. The
stringer for the Stringer Test Assembly is identical to the outboard stringer of
the Compression Panel. This specimen was successfully tested at room temperature
to 355 kN (80K) and 445 kN (100K) during two different loading sequences without
failure. Axial load was applied to the unidirectional boron aluminum stringer of
this test assembly by panel shear using a 12 ply $\pm\pi/4$ rad (±45°) boron aluminum
skin. It will be shown that the 455 kN (100K) load level demonstrates ultimate
strength of the outboard stringer on the compression panel when loaded to the
ultimate design load at 222 kN at 589°K (600°F). In addition, this is the first
major boron aluminum test article to utilize titanium interleaves eutectically
bonded to the boron aluminum. Results of this test showed that the use of
titanium interleaves significantly increased shear strength and bearing strength
of unidirectional boron aluminum stringers.
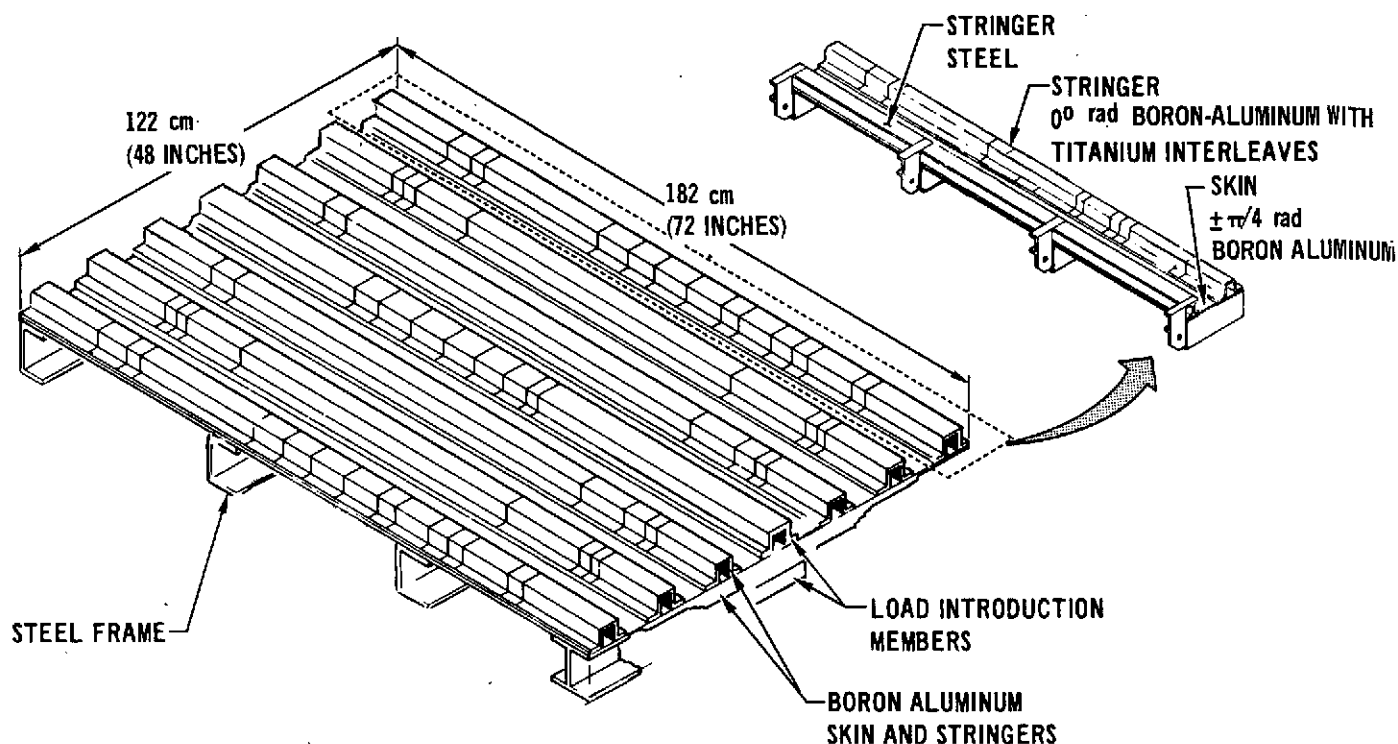
ACCOMPLISHED OBJECTIVES

- DEMONSTRATE COLUMN CAPABILITY OF STRINGER INCLUDING CRIPPLING
- VERIFY THAT TITANIUM INTERLEAVES INCREASE IN-PLANE SHEAR STRENGTH
- VERIFY THAT TITANIUM INTERLEAVES INCREASE BEARING STRENGTH

STRINGER ASSEMBLY AIDED EVALUATION OF COMPRESSION PANEL DESIGN

Figure 2-145

Design loads at 589°K (600°F) for the outboard stringer on the compression panel are shown in Figure 2-146. The maximum shear flow occurs approximately 50.8 cm (20 in.) from the unloaded end of the stringer, while the maximum axial compressive load occurs at the stringer closeout. The small predicted shear flows shown for the area near the distributed load end of panel indicate that the internal loads distribution required to achieve a nearly-uniform ultimate reaction load (222 kN, 50,000 lb per stringer) has been accomplished in less than the full panel length.

Analysis showed that a unidirectional boron aluminum stringer, if sized to carry only the axial compressive load, would possess insufficient in-plane shear strength to carry the shear loads. Therefore, one 8 mil titanium ply was added over the entire length and a 38.1 cm (15 in.) long ply was added near the thin end of stringer as shown in Figure 2-147. The allowable shear flow which can be

P_X

50,000 LB
PER STRINGER

350,000 LB

TEMP = 600°F

X = 0"   24"   48"   72"

SHEAR FLOW

q – 1000 LB/IN.

1.5

1.0

0.5

0   24   48   72
STRINGER LOCATION, X – IN.

AXIAL LOAD

P_X – 1000 LB

50

30

10

0   24   48   72
STRINGER LOCATION, X – IN.
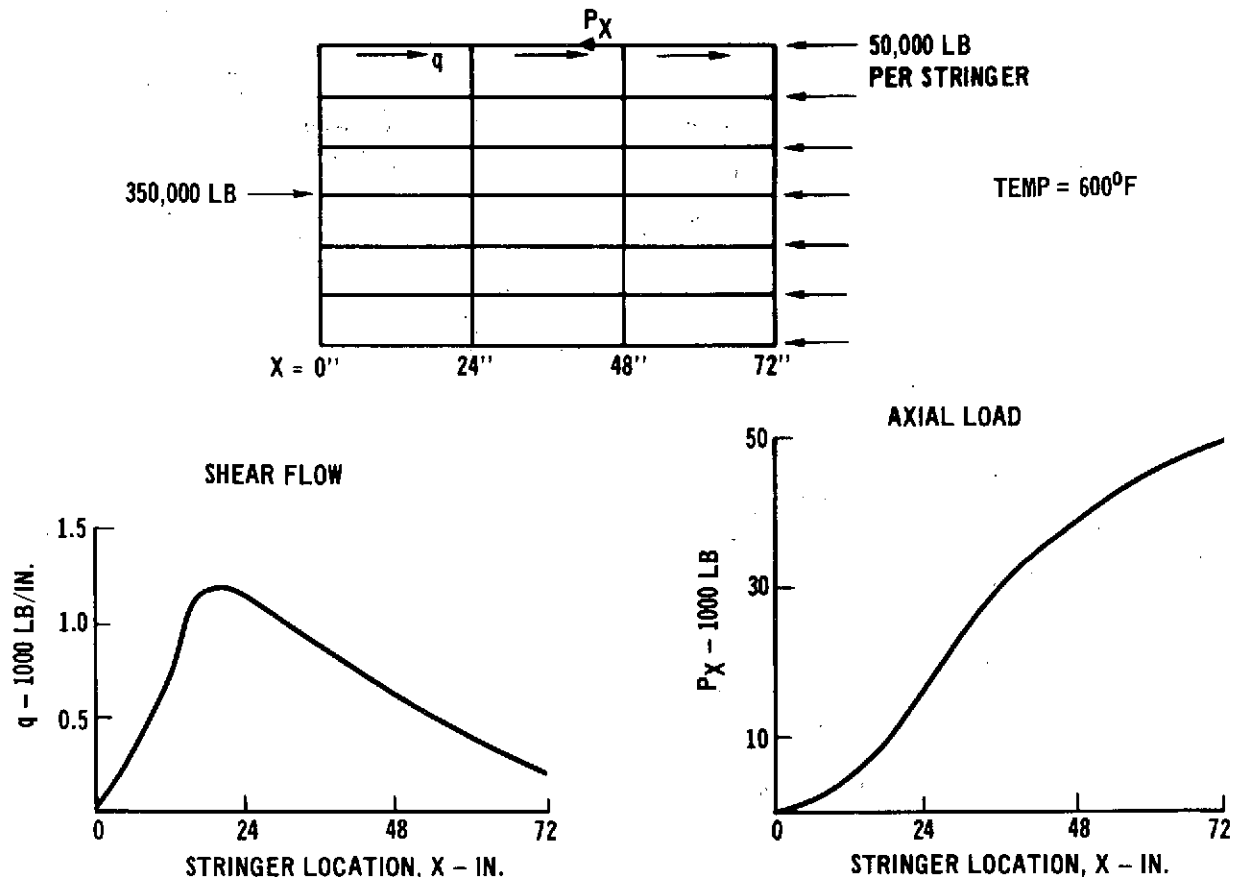
DESIGN LOADS FOR STRINGER ON COMPRESSION PANEL

Figure 2-146

applied to a stringer with boron aluminum plies only and to a boron aluminum stringer with titanium interleaves is shown in Figure 2-148. Additional titanium plies are used at the opposite end to provide sufficient bearing strength for the closeout fitting loads. Note that some of the boron aluminum and titanium plies are terminated internally. The terminations are staggered a minimum of 1.27 cm (.50 in.). The external ply terminations were selected to meet the axial load and stiffness requirements of stringer.

All attachments have been made using HI-LOK mechanical fasteners. The lateral frames are steel channel members and the closeout fitting is a machined steel part attached to the boron aluminum stringer with 25 fasteners. Figure 1-149 shows the boron aluminum stringer assembly located in test machine. Note the turn buckle arrangement used to provide lateral support without restricting axial motion of the stringer.

STRINGER

SKIN

12 PLY

±45° LAYUP

——— BORON ALUMINUM MONOLAYER
– – – 8 MIL TITANIUM INTERLEAF

23 PLY

72.0 IN.

5 PLY

—STRINGER
STEEL

—STRINGER
0° BORON ALUMINUM WITH
TITANIUM INTERLEAVES

SKIN ±45°
BORON ALUMINUM

RING
STEEL (TYP)

SECTION A-A STRINGER LAYUP
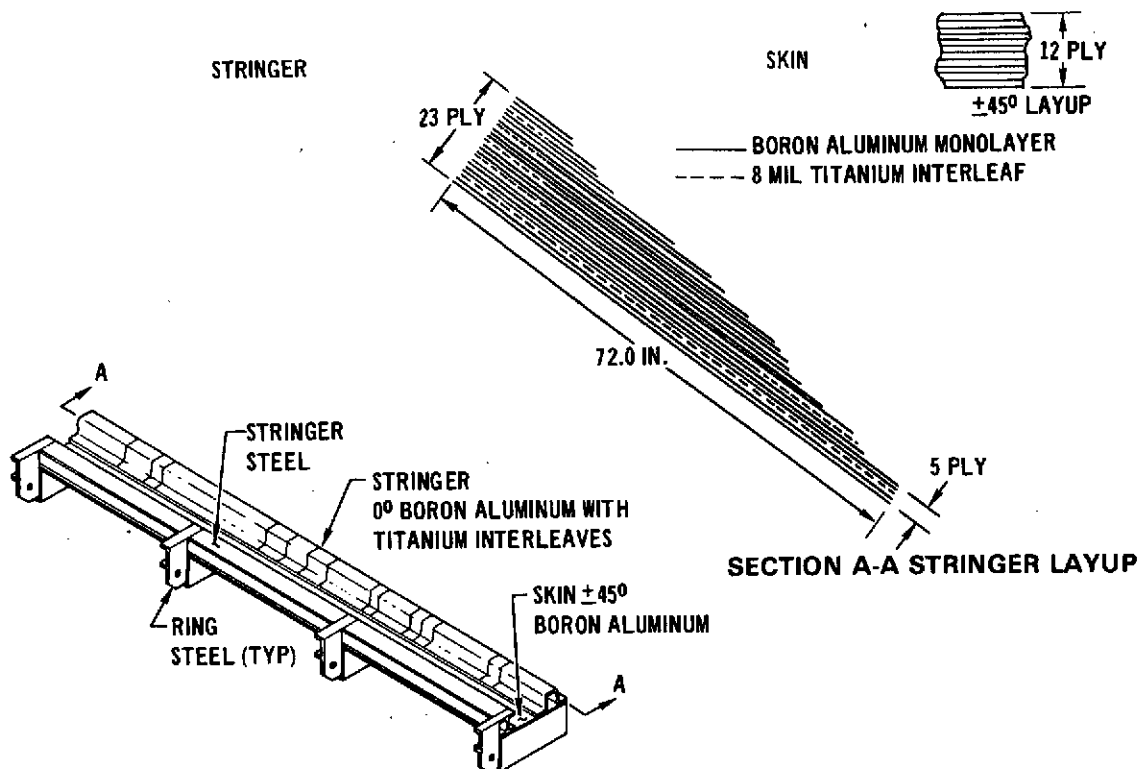
SIGNIFICANT FEATURES OF BORON-ALUMINUM STRINGER ASSEMBLY

Figure 2–147

TEMPERATURE = 600°F

0.4q

0.6q

P_x

ALLOWABLE
B–AL + TI

ALLOWABLE
B–AL

DESIGN
(0.6q)

SHEAR FLOW, q – 1000 LB/IN.

STRINGER LOCATION, X – IN.
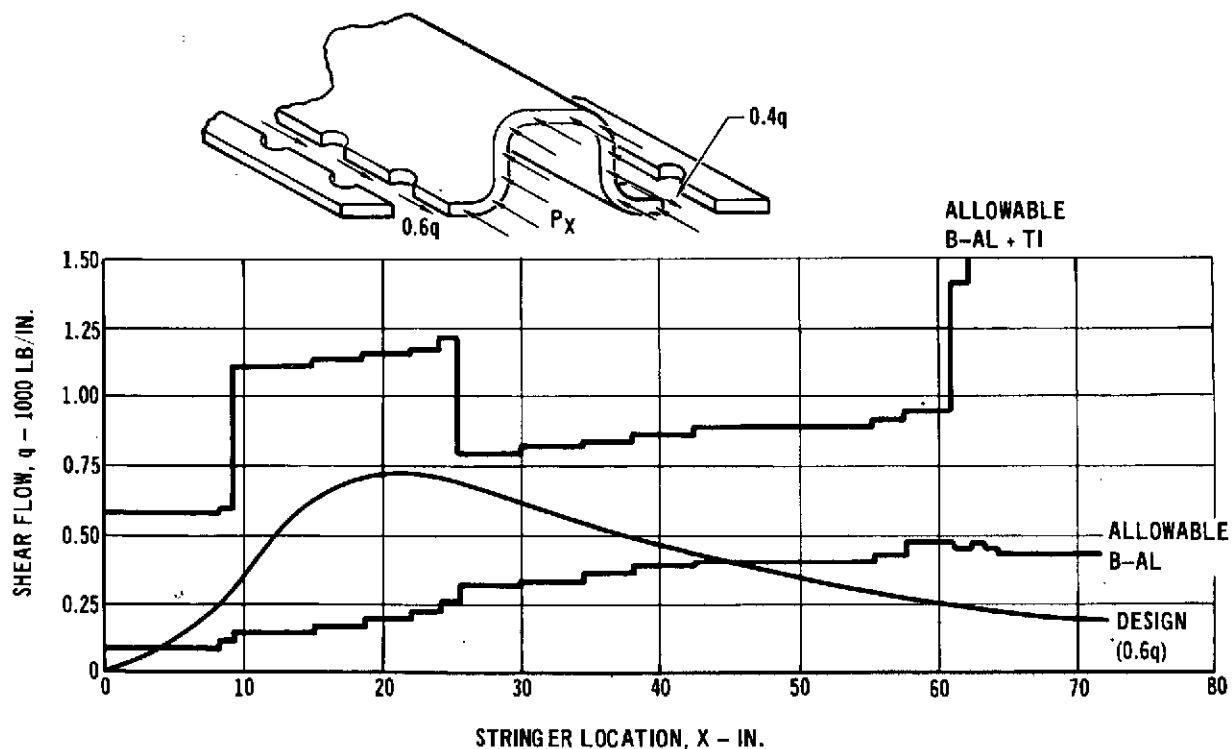
TITANIUM PLIES USED TO INCREASE IN–PLANE
SHEAR STRENGTH

Figure 2–148
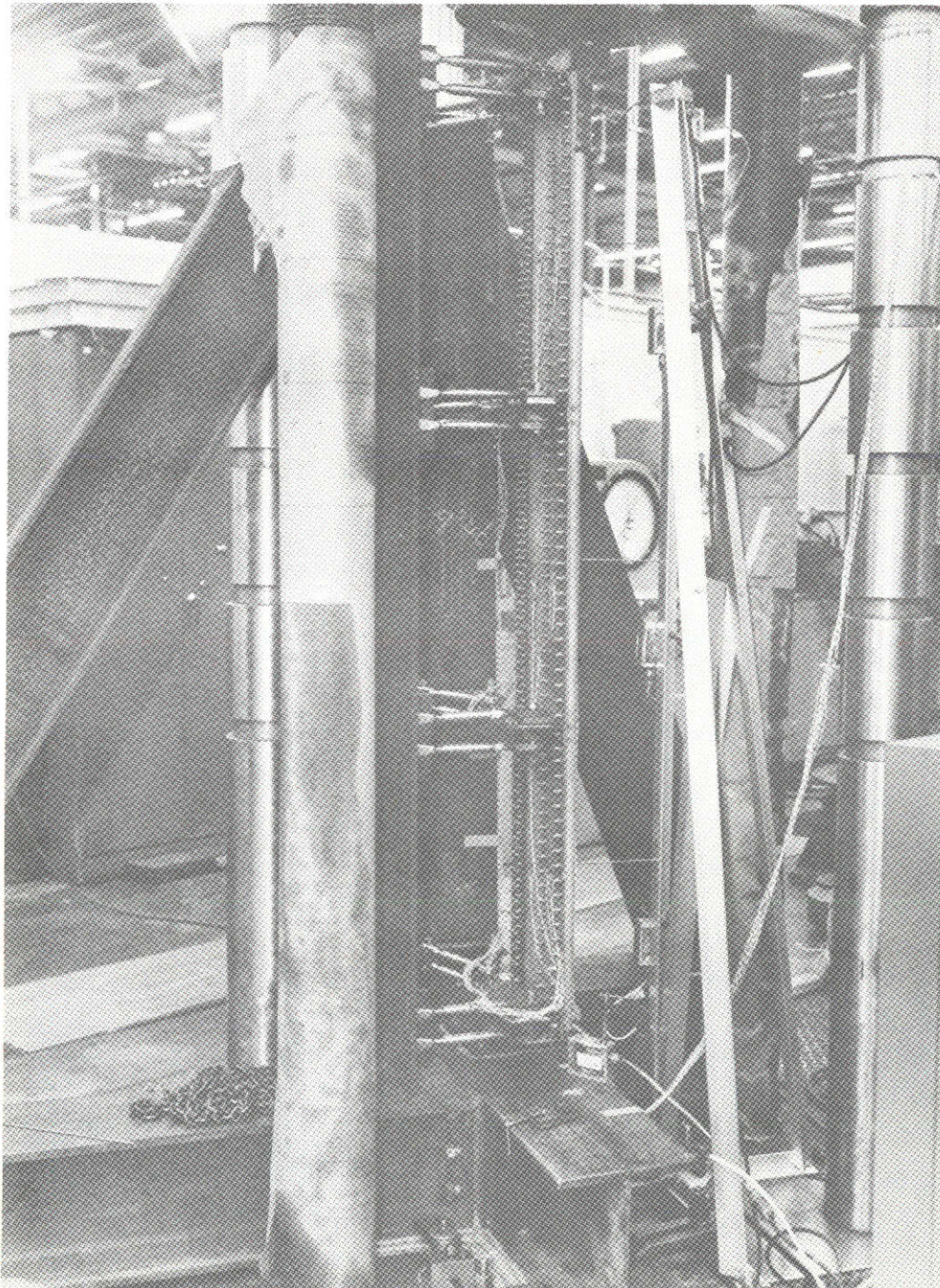
STRINGER ASSEMBLY IN TEST MACHINE

Figure 2–149

The assembly was loaded twice at room temperature without failure. During the first test, the maximum axial load applied to the stringer was 355 kN (80K). In the second test, the maximum load was 445 kN (100K). When the stringer successfully carried 445 kN (100K) at room temperature, ultimate strength was demonstrated of a similar stringer on the compression panel at 589°K (600°F).

Strain gages for the stringer assembly were located as shown in Figure 2-150. In addition, three deflection gages were located midway between each frame for recording deflection of the stringer normal to the skin. A fourth deflection gage was used to record overall shear deformation of the panel.
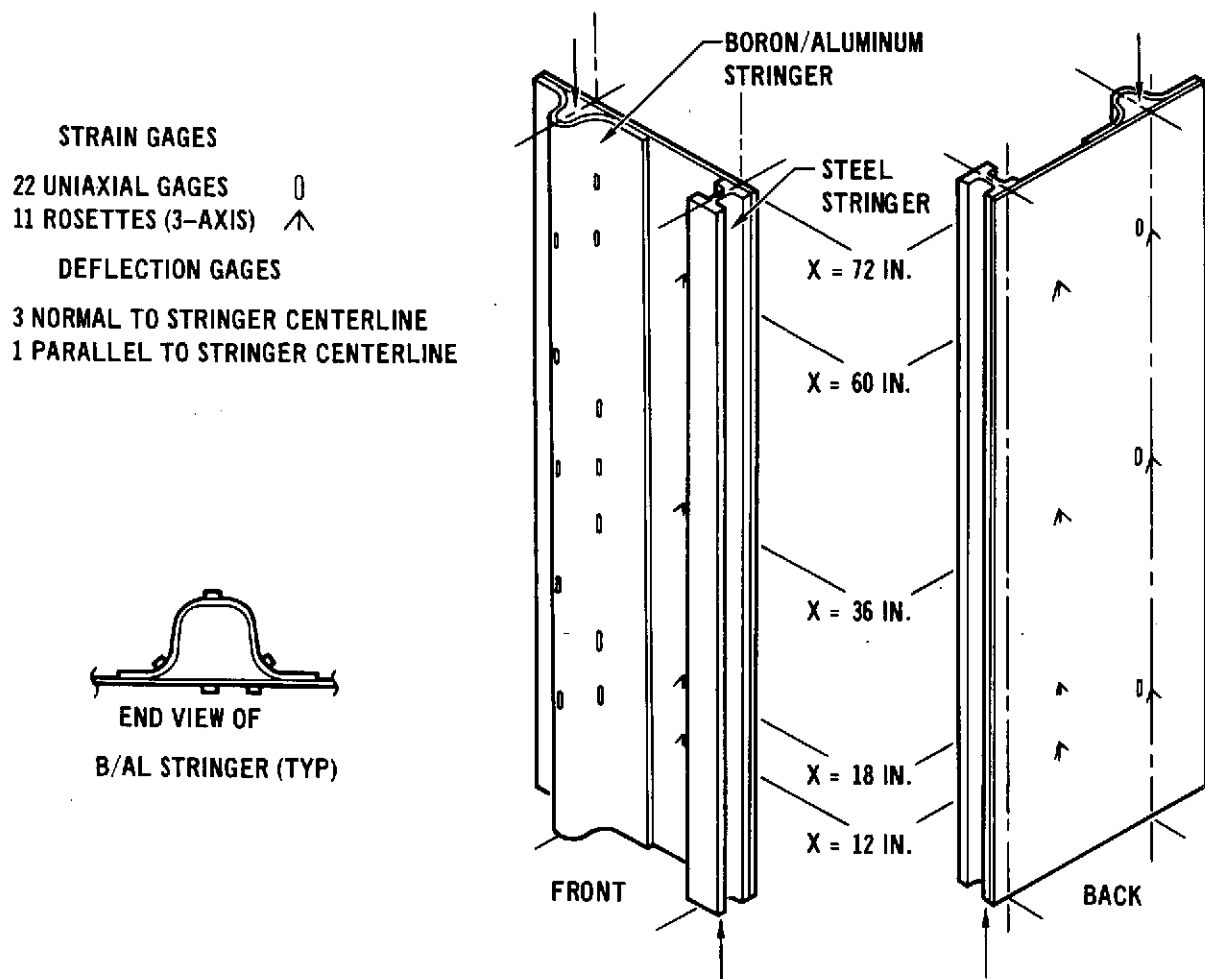
STRAIN AND DEFLECTION GAGES MONITOR RESPONSE DURING TEST

Figure 2-150

The uniaxial strain gages located on the stringer cross-section were used to
determine the presence of bending as well as axial load. Figure 2-151 shows strain
readings taken from three such gages located 30.5 cm (12 in.) from the highly
loaded end of the stringer. A predicted load-strain curve for the stringer under
pure axial load is shown also. There was considerable difference between the com-
pressive strain measured by the gage on the crown of the stringer and the gages
located near the attachment legs, indicating that the stringer cross section was
subjected to bending as well as axial load.
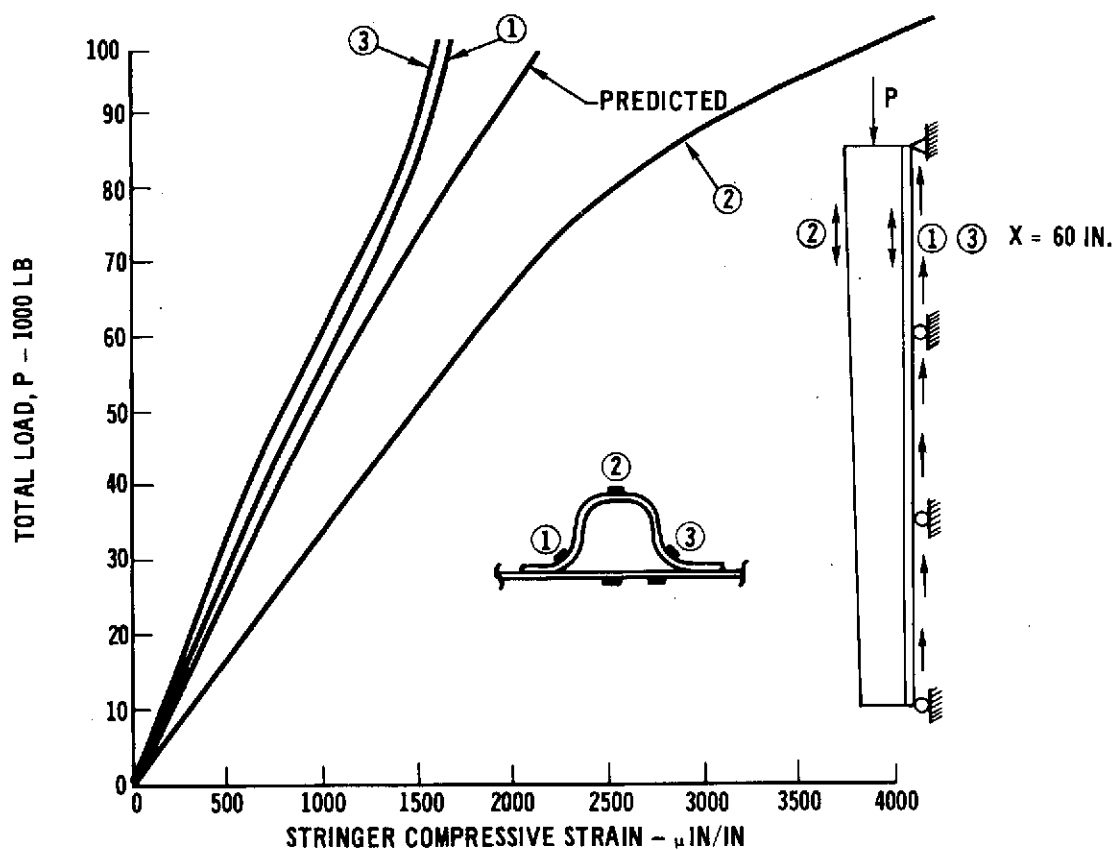
STRAIN GAGE DATA SHOW STRINGER BENDING STRESSES

Figure 2-151

Figure 2-152 illustrates the stringer deflected shape under 445 kN (100,000
lbs) load. The high bending strains in the thick end of the stringer were
attributed to an initial curvature in the stringer caused either during stringer
fabrication or induced into the specimen by the lateral support adjustment struts
in the test setup. It can be shown that an initial eccentricity of .10 cm
(.04 in.) is sufficient to produce the bending strains observed during this test.
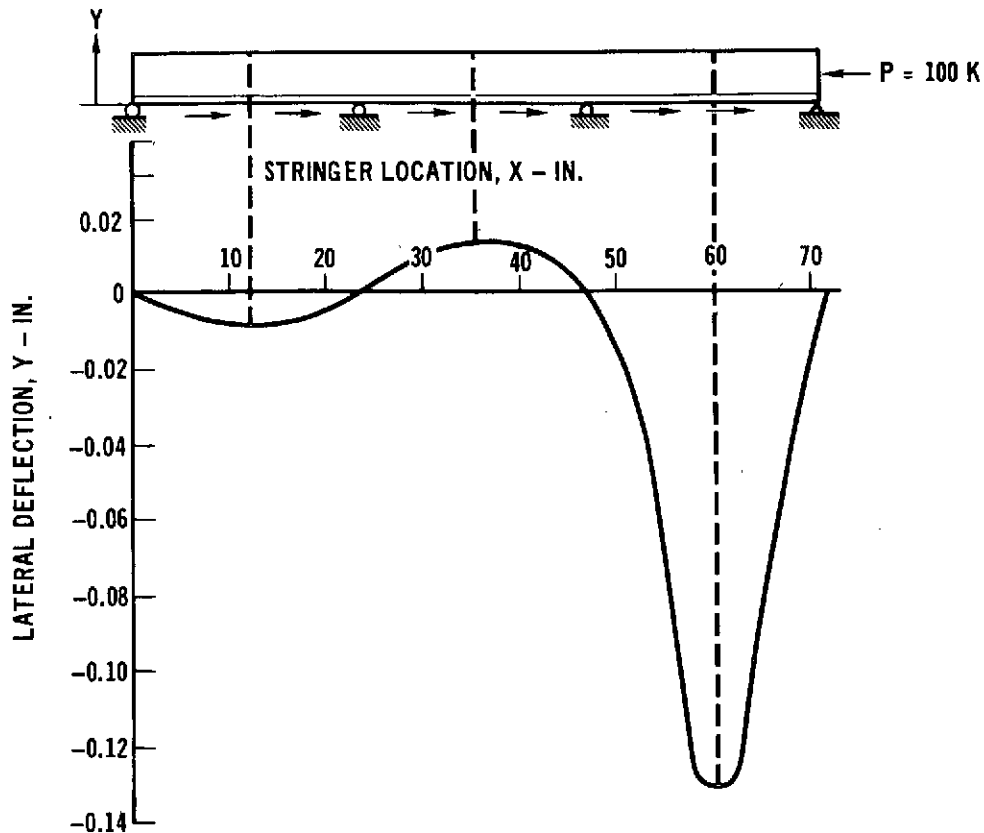
DEFLECTION GAGES VERIFY STRINGER BENDING

Figure 2-152

Figure 2-153 shows the 589°K (600°F) predicted axial load curve used to design the stringer on the compression panel. Also shown is the allowable load curve for the stringer based on recent crippling tests. The allowable load curve markedly exceeds the predicted curve at most locations due to improvements in actual crippling strength over predicted values used to design the stringer.

The lower portion of Figure 2-153 shows the room temperature axial loads carried by the stringer during the actual stringer assembly test along with the allowable load curve based on recent room temperature crippling tests. With 445 kN (100,000 lb) load on the assembly, the loads in the thin end of the stringer were almost the same as the allowable loads. The stringer did not fail at this load level. The critical region on the stringer during test is about the same as expected for the stringer on the compression panel. It occurs approximately 50.8 cm (20 in.) from the thin end of the stringer.

Figure 2-154 illustrates the use of titanium interleaves to increase the allowable fastener load in the leg of the stringer. The load introduced at the
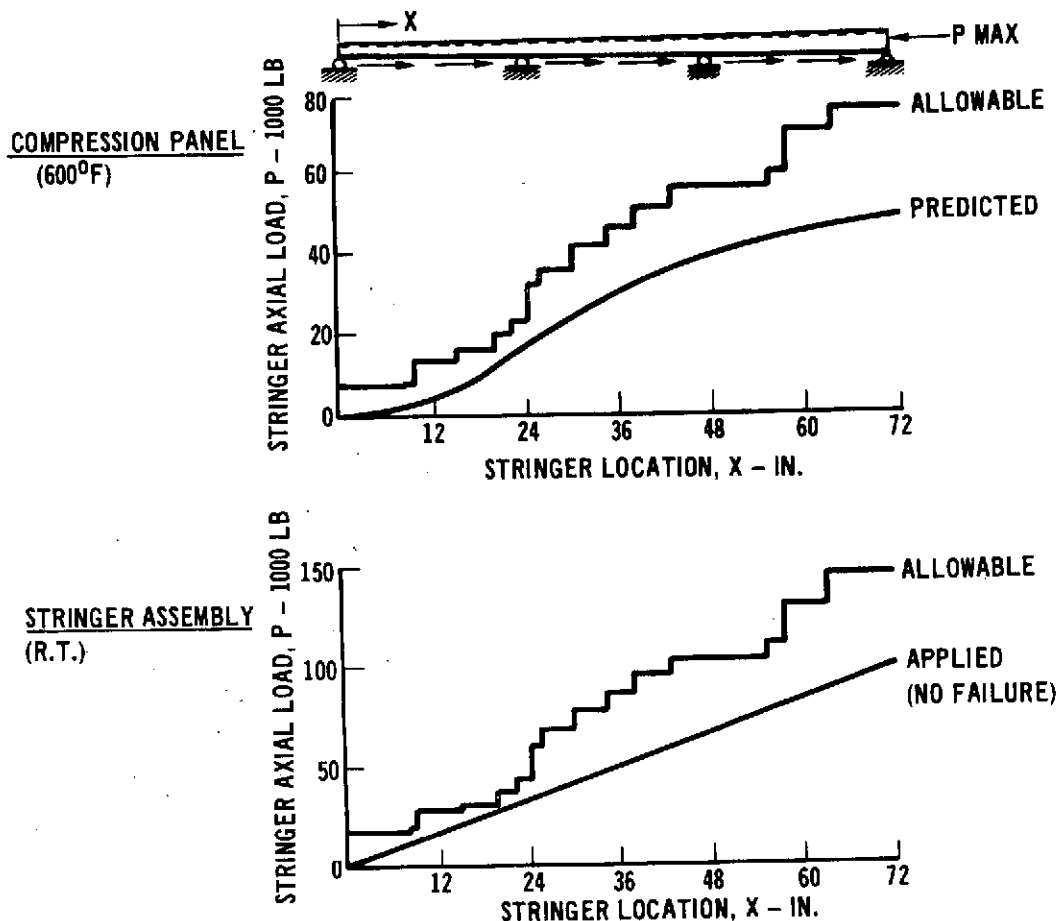
ULTIMATE COLUMN STRENGTH OF BORON ALUMINUM STRINGER VERIFIED BY TEST

Figure 2-153

fastener is reacted by both the boron aluminum and titanium and must be sheared into the main portion of the stringer. Since the titanium shear allowable is considerably above that of the unidirectional boron aluminum, the shear-out strength of the joint is greatly increased.

The stringer closeout fitting, Figure 2-155 simulates a typical load introduction splice joint. All loads in the stringer are transferred to the end fitting through 25 fasteners. In this case, loads are applied to the fastener on both sides resulting in a double shear condition for the boron aluminum stringer. The end fitting extends beyond the panel skin and stringer to ensure that the entire load in the assembly is reacted at the steel end fitting.

Predicted fastener allowables for unidirectional 0 rad (0°) boron aluminum are shown in Figure 2-155. Also, curves are for boron-aluminum only and for boron-aluminum combined with five, .0203 cm (.008 in.) thick annealed 6Al-4V titanium

2-163
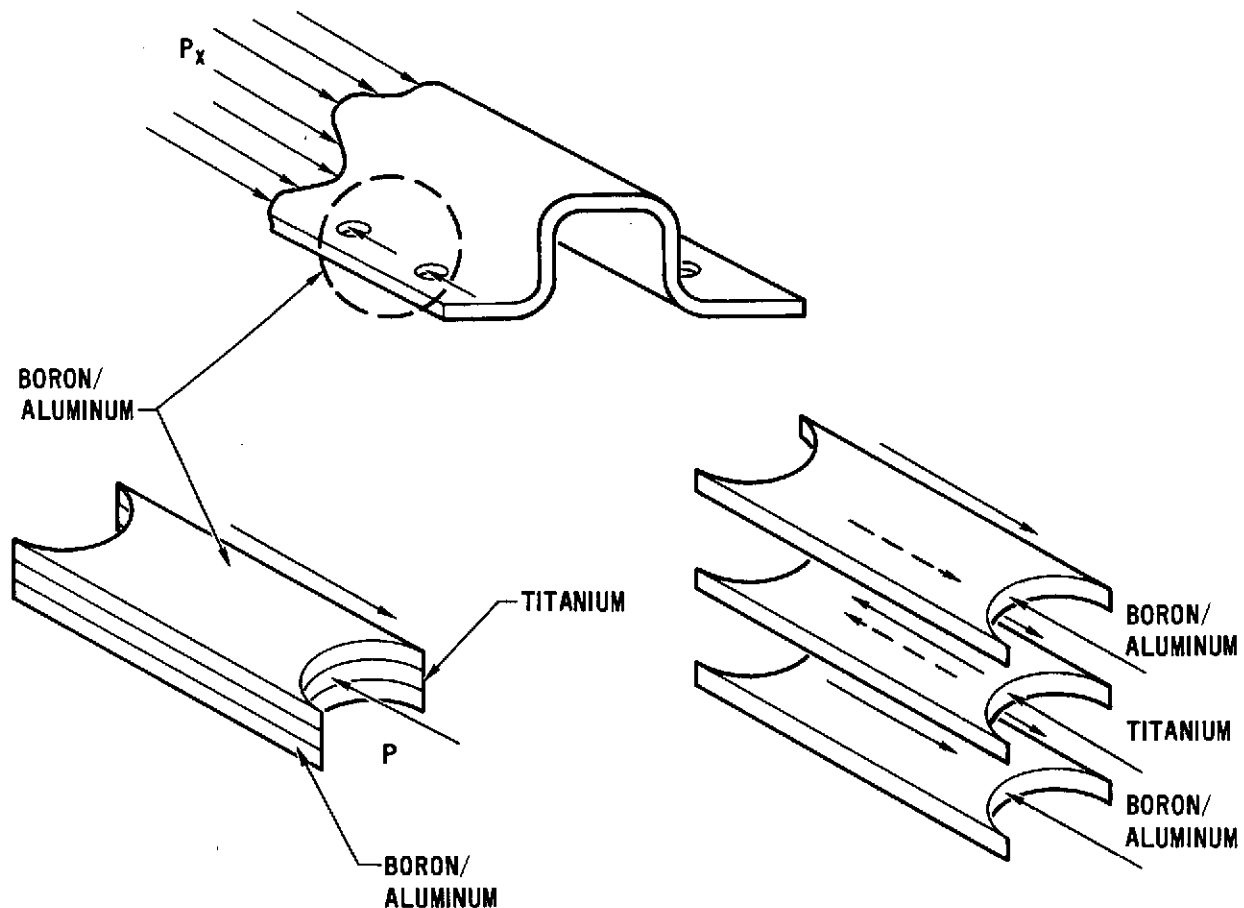
TITANIUM AND BORON ALUMINUM SHARE FASTENER BEARING LOADS
(Single Shear)

Figure 2-154

plies. The latter curve applies to stringer closeout fitting region where 5
titanium plies are used.

The point designated closeout fitting represents the load experienced by
each of the 25 fasteners in the closeout region of the stringer when the total
load was 445 kN (100,000 lb). This assumes each fastener is carrying an equal
portion of the total load. Since no failures occurred in the stringer, predicted
ultimate strength of the joint was not completely proven.

The other point shown represents the average of three unidirectional boron
aluminum, titanium interleaf lug tests at room temperature. The actual lug
specimens were made up of 28 plies of 0 rad (0°) boron aluminum and eight,
.0304 cm (.012 in.) thick titanium plies. Their average failing load was 62.3 kN
(14,000 lb). To plot these results on this curve, the failing load and number of
boron aluminum plies was scaled down so that the thickness of titanium was
equivalent to five, .0203 cm (.008 in.) thick titanium plies.
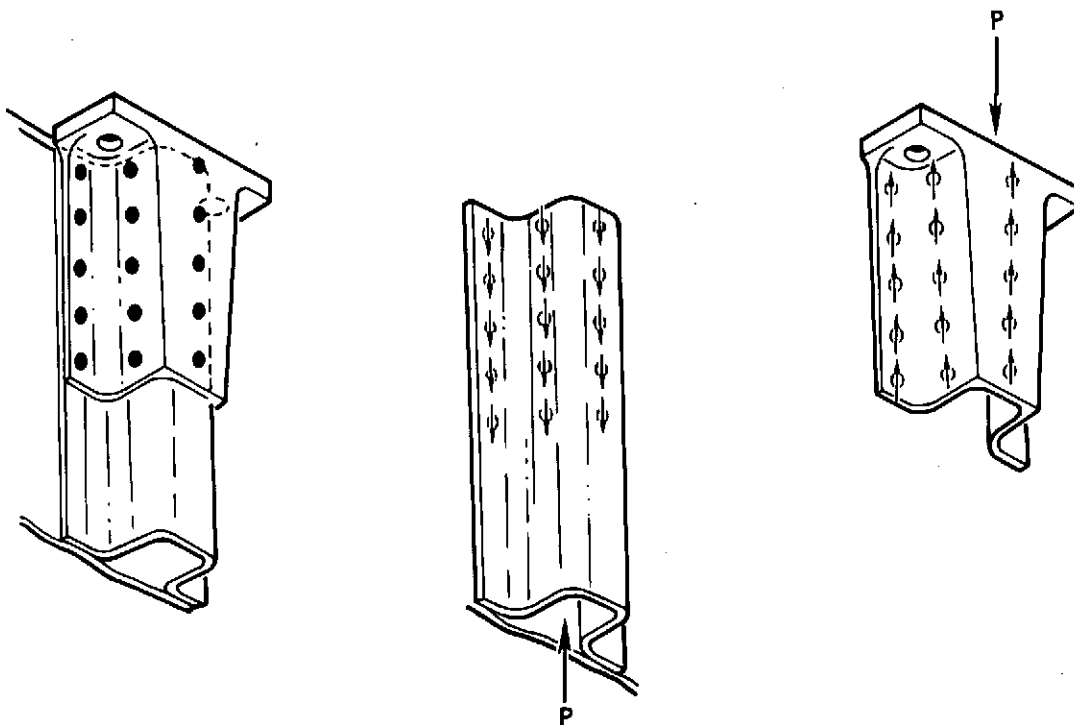
STRINGER CLOSEOUT FITTING
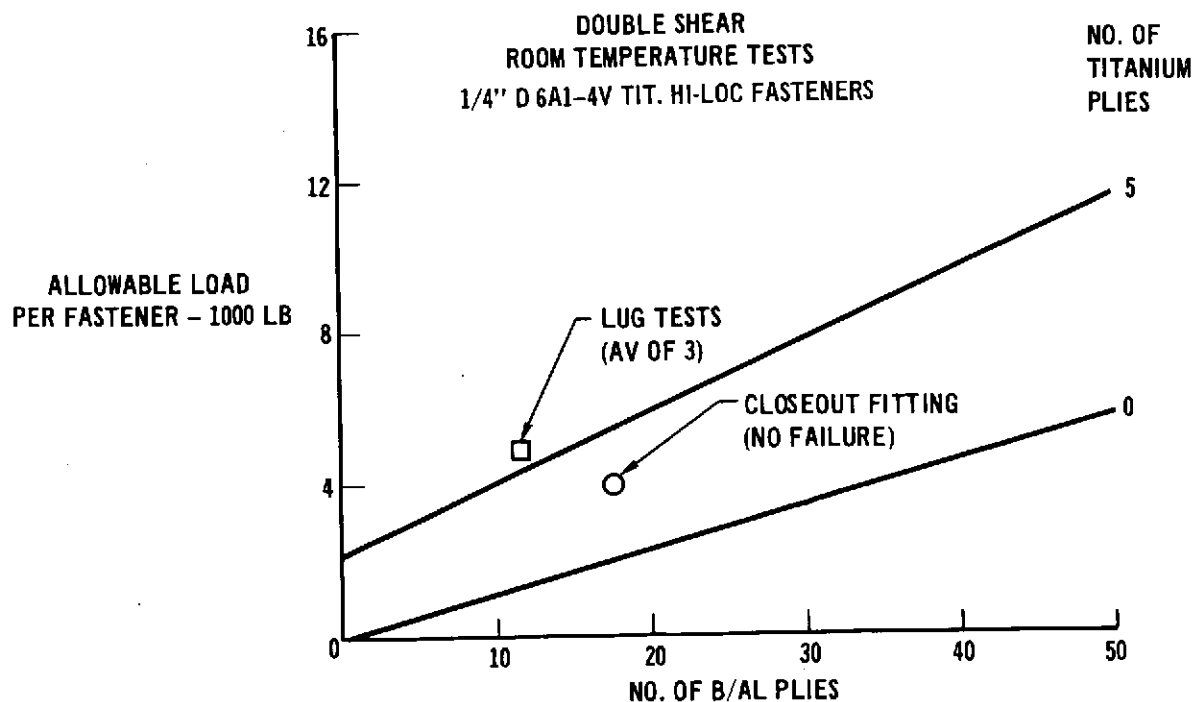
ANALYTICAL PROCEDURES FOR PREDICTING BEARING STRENGTH
PARTIALLY VERIFIED BY TEST

Figure 2–155

In summary, a considerable amount of significant data was obtained from the stringer assembly during fabrication and test. Fabrication procedures necessary to construct a long stringer with tapered thickness and containing titanium interleaves were developed. In addition, several structural features incorporated in the stringer were demonstrated including the following:

o Unidirectional boron aluminum can be used as stringers

o Titanium interleaves increase in-plane shear strength

o Titanium interleaves increase fastener bearing strength.

2.5.2 <u>Boron Aluminum Component Panel Test Assembly</u> - The Compression Panel will experience very high internal shear and compressive loads when subjected to the concentrated ultimate load of 1.55 MN (350K) at 589°K (600°F). Since no composite structures have experienced this type of loading and the unique design features incorporated in the panel had not been proven, the component panel shown in Figure 2-156 was fabricated and tested. This component panel, .61 m (2 ft) long and 1.22 m (4 ft) wide, is an exact duplication of the highly loaded Compression Panel first bay. Seven unidirectional boron-aluminum stringers carry the axial compressive load and a $\pm \frac{\pi}{4}$ rad (+45°) cross-plied skin carries the shear load. With the exception of the centerline stringer which is constant thickness in this bay, both the stringers and skin are tapered in thickness to achieve an efficient design.

Very high shear loads exist in this bay of the Compression Panel. Unidirectional boron-aluminum stringers sized to carry axial compressive loads possess insufficient in-plane shear strength to carry the applied shear loads. Therefore, 8 mil titanium interleaves were added to the stringers to provide the required shear and bearing strengths as shown in Figure 2-157. The titanium interleaves and boron-aluminum plies are eutectically bonded simultaneously in one operation.

The component panel skin is shown in Figure 2-158. It is made up of both $\pm \frac{\pi}{4}$ rad (+45°) boron-aluminum plies and some titanium interleaves. Skin thickness is designed to carry the shear flow occurring at various locations on the panel. All tapering of the skin occurs on one side. Skin thickness varies from a maximum of 58, $\pm \frac{\pi}{4}$ rad (+45°) boron-aluminum plies with four additional titanium interleaves at the load introduction end to a thickness of $8 \pm \frac{\pi}{4}$ rad (+45°) boron aluminum plies with two additional titanium interleaves at the distributed load end of panel in the outboard bays.

Stringer Side
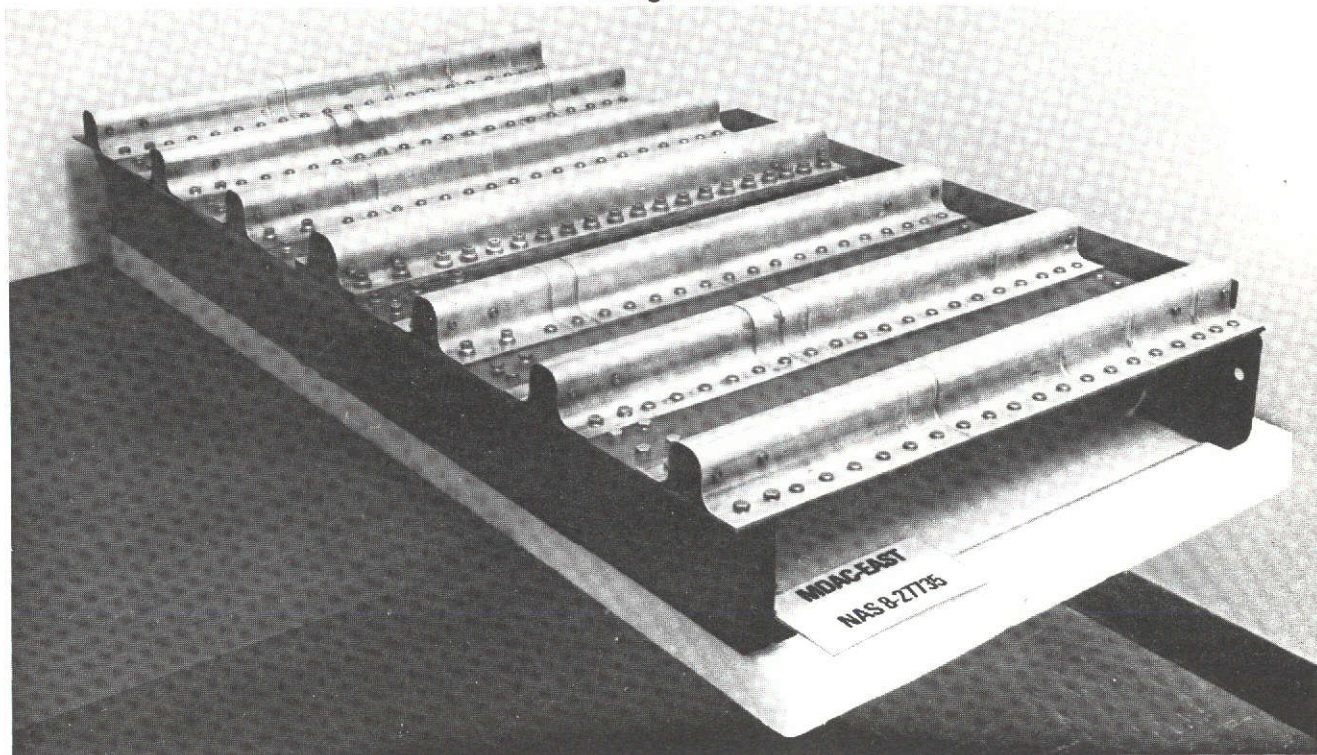
Skin Side
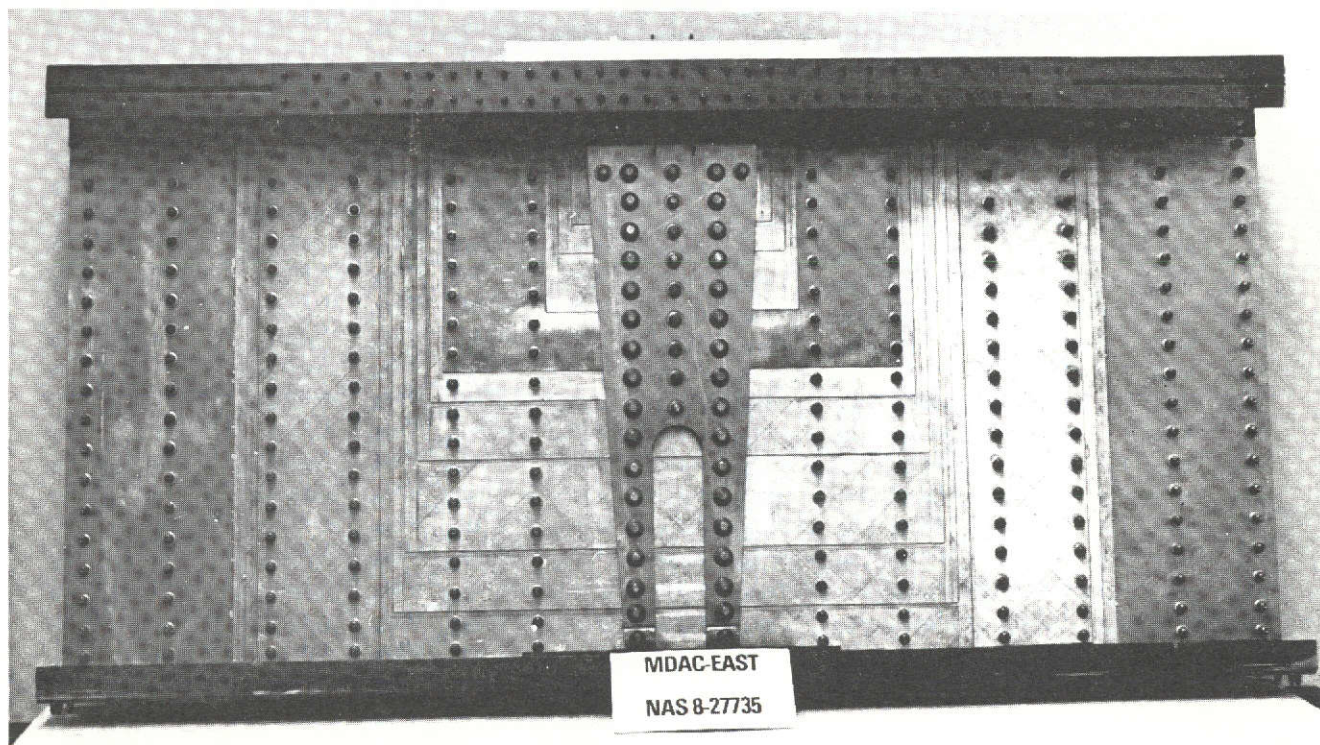
COMPLETED COMPONENT PANEL ASSEMBLY

Figure 2-156
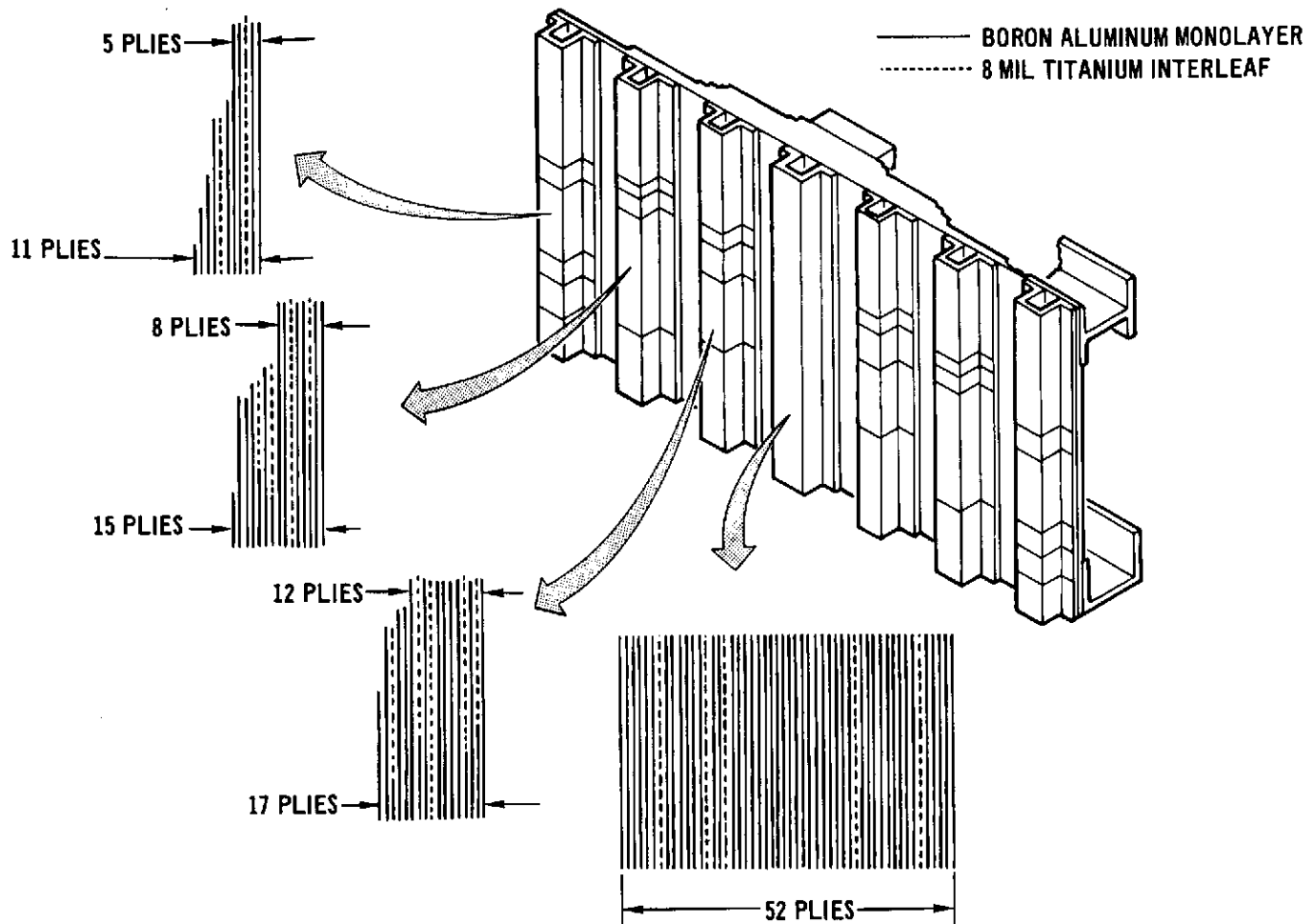
MCDONNELL DOUGLAS ASTRONAUTICS COMPANY - EAST

5 PLIES

11 PLIES

8 PLIES

15 PLIES

12 PLIES

17 PLIES

52 PLIES

——— BORON ALUMINUM MONOLAYER
---------- 8 MIL TITANIUM INTERLEAF

TITANIUM INTERLEAVES ARE ADDED TO STRINGERS TO PROVIDE NECESSARY SHEAR AND BEARING STRENGTH
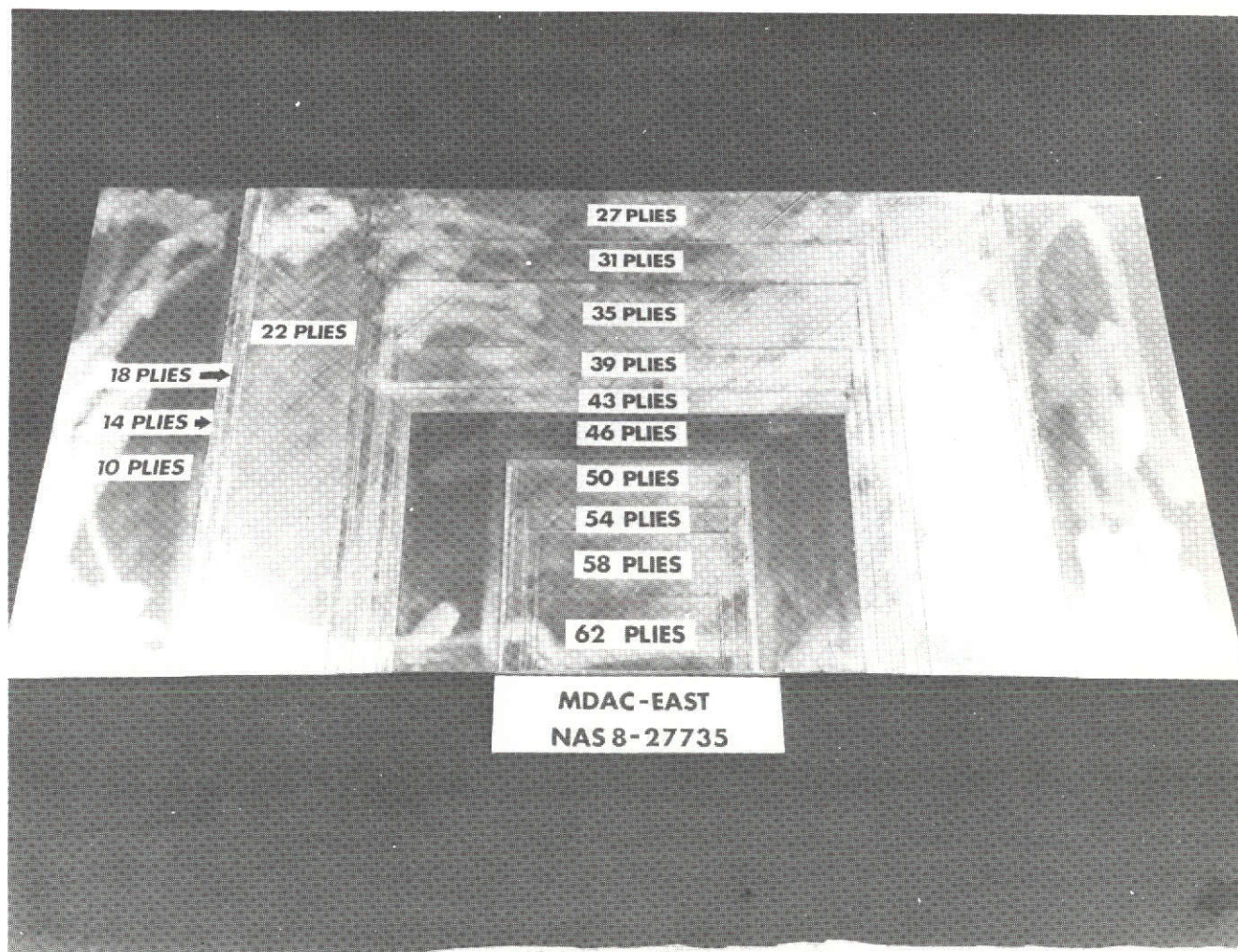
Figure 2—157

COMPONENT PANEL SKIN BEFORE ASSEMBLY

Figure 2-158

MCDONNELL DOUGLAS ASTRONAUTICS COMPANY - EAST

Two separate tests were conducted on the panel. During the first test conducted at room temperature, the maximum applied load was 1.33 MN (300K) to check out overall test setup and load distribution. In the second test conducted at a temperature of 589°K (600°F), the panel actually was tested to 1.78 MN (400K) or 115% of design ultimate load. Examination of the panel after test showed indications of the beginnings of crippling failures on the outboard stringers. These can be observed in Figure 2-159 which shows the panel in the test machine after test.

Figure 2-160 shows in detail one of the outboard stringers on the component panel after the 589°K (600°F) test. The opposite outboard stringer contains a similar blister. It is estimated that some additional load above the 1.78 MN (400K) level could have been carried by the panel before a complete crippling failure of outboard stringers would have occurred.

In Figure 2-161, the predicted and measured loads distribution for the component panel when subjected to 1.55 MN (350K) at 589°K (600°F) are shown. For comparison, the loads distribution predicted at this location for the complete compression panel are shown also. The good agreement between predicted and measured loads for the component panel increased confidence in procedures used for design and analysis.

In summary, many unique design features incorporated in the Compression Panel were verified by the component panel test program. Also, the ability of a boron aluminum structure to sustain a complex shear lag load distribution was demonstrated. In addition, it was proven that analytical tools, such as finite element programs, for conventional materials and structures can be successfully applied to analysis of composite structures. Other specific accomplishments include:

o Capability to design B/Al load redistribution structures for 589°K (600°F) environment

o Additional strength at minimum weight provided by titanium interleaves

    o In-plane shear strength

    o Fastener bearing strength

    o Overall improvement in apparent ductility

o Design and fabrication of tapered B/Al stringers with titanium interleaves

o Design and fabrication of contoured B/Al skins with titanium interleaves

o B/Al stringer closeout fitting design

o Panel thrust post area design using mix of both composite and conventional materials

o General improvement in overall B/Al manufacturing and design technology
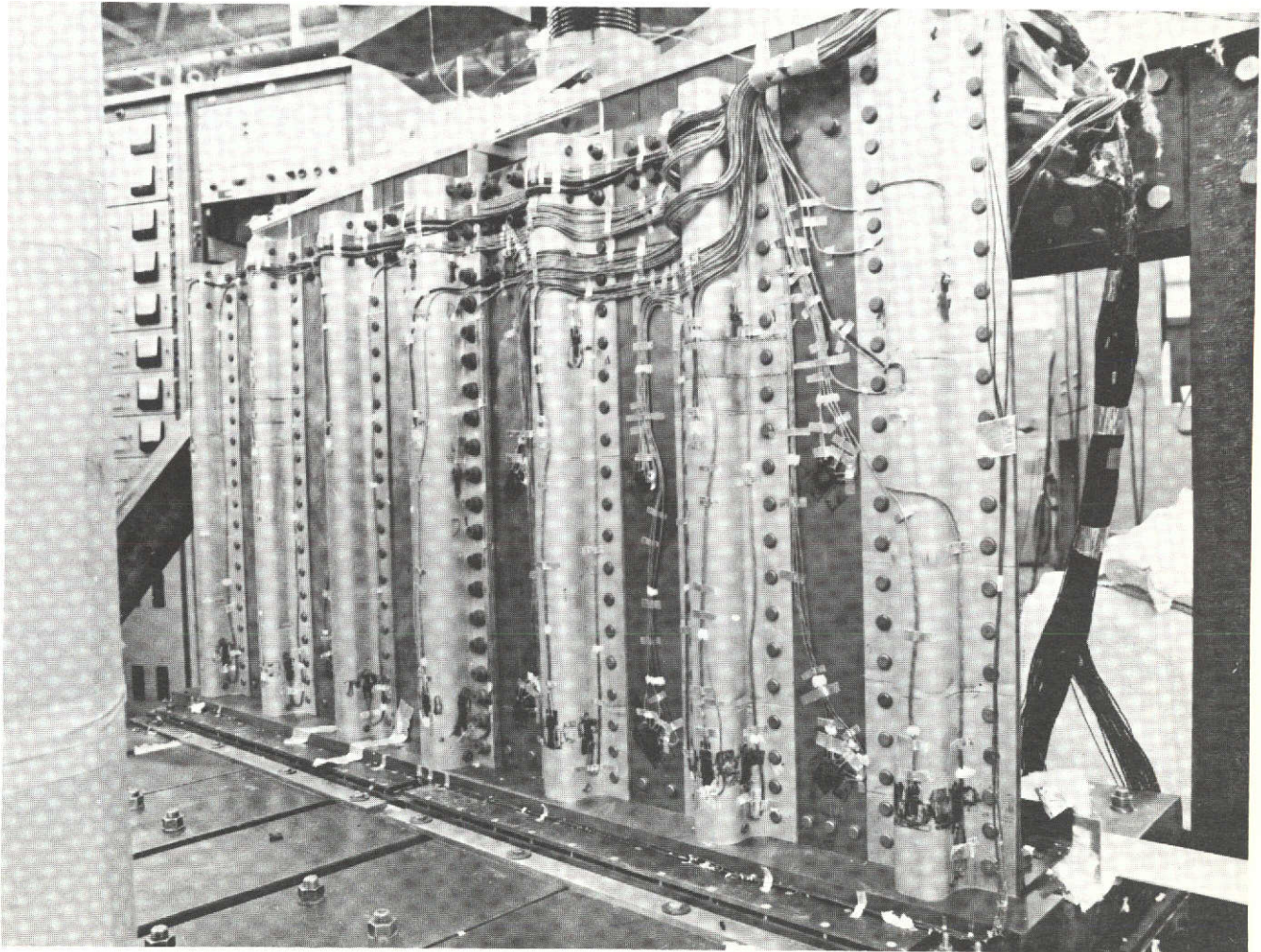
COMPONENT PANEL IN TESTING MACHINE

Figure 2—159
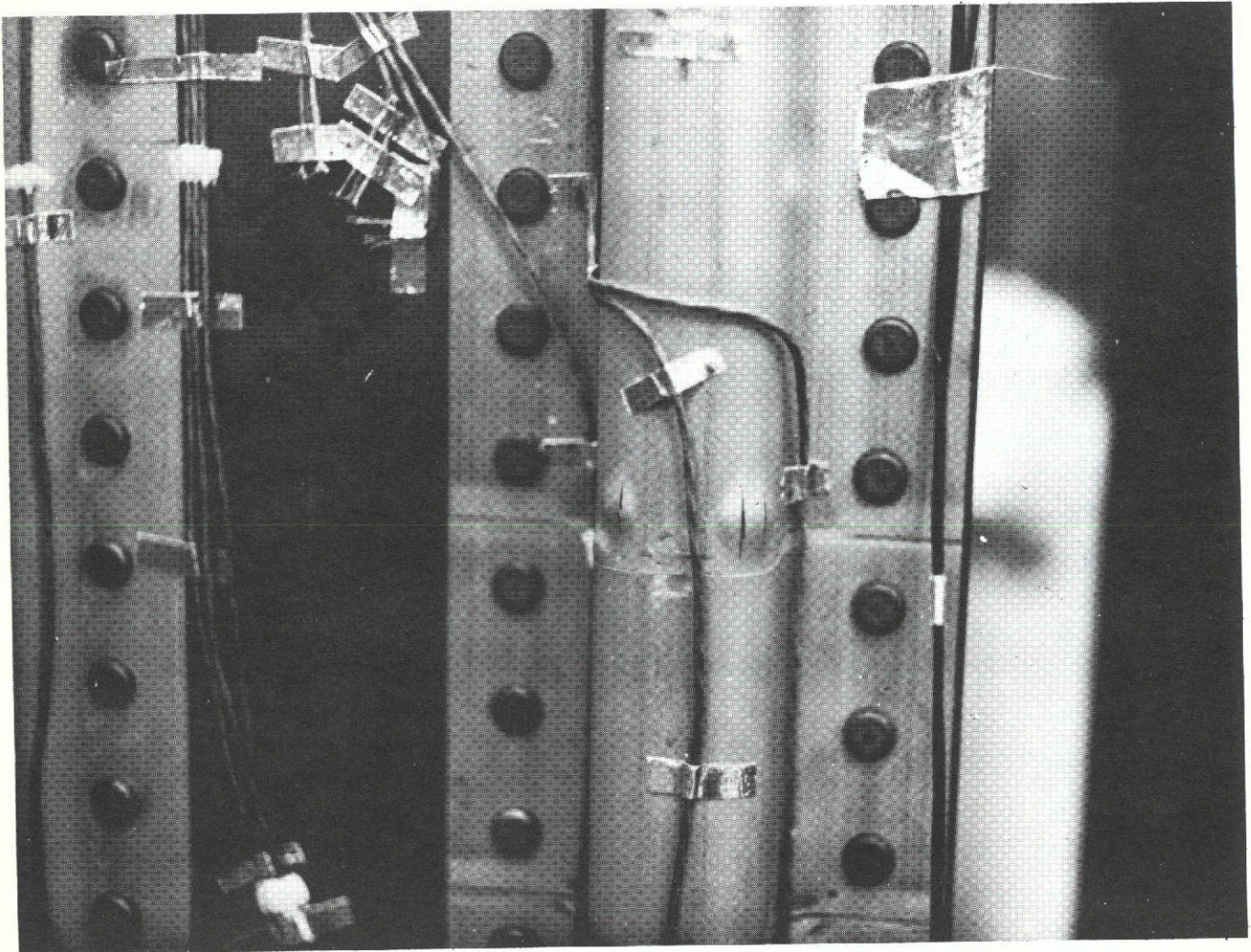
CRIPPLING FAILURE OF STRINGER ELEMENT

Figure 2—160

LOADS DISTRIBUTION
(600°F)

P = 350 (KIPS)

PREDICTED – COMPRESSION PANEL	17.8	34.7	49.7	145.5	49.7	34.7	17.8
– COMPONENT PANEL	23.0	37.2	48.0	133.5	48.0	37.2	23.0
MEASURED – COMPONENT PANEL	23.6	–	–	135.0	45.0	40.0	21.2
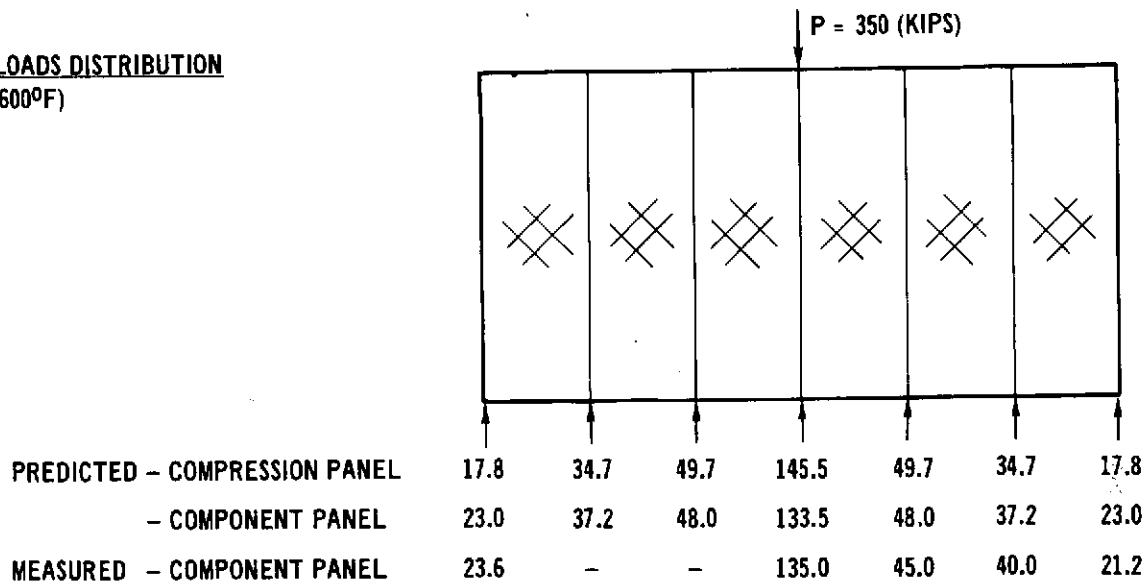
STRUCTURAL INTEGRITY
  MAXIMUM TEST CONDITION: P = 400K (115% DUL)
                           TEMPERATURE = 600°F
                           CRIPPLING FAILURES BEGINNING ON OUTBOARD STRINGER

PREDICTED LOADS DISTRIBUTION AND STRUCTURAL INTEGRITY
OF COMPONENT PANEL VERIFIED BY TEST AT 600°F

Figure 2–161

MCDONNELL DOUGLAS ASTRONAUTICS COMPANY - EAST

3.0 REFERENCES

1. First Quarterly Report, "Design, Process Development, Manufacture, Test and Evaluation of Boron-Aluminum for Space Shuttle Components", McDonnell Douglas Corporation Report E0491, dated 10 November 1971.

2. Second Quarterly Report, "Design, Process Development, Manufacture, Test and Evaluation of Boron-Aluminum for Space Shuttle Components", McDonnell Douglas Corporation Report E0555, dated 10 March 1972.

3. Third Quarterly Report, "Design, Process Development, Manufacture, Test and Evaluation of Boron-Aluminum for Space Shuttle Components", McDonnell Douglas Corporation Report E0650, dated 10 August 1972.

4. Sandwich Construction for Aircraft, Part II, Material Properties and Design Criteria", MIL-HDBK-23 (ANC-23), Second Edition, 1955.

5. "Structural Design Guide for Advanced Composite Applications", Air Force Materials Lab, Second Edition, January 1971.

6. "Development of the Shim Joint Concept for Composite Structural Members", F33(615)-67C1263, Bendix Corp., August 1967.

7. Lehman, G. M. and A. V. Hawley, "Investigation of Joints in Advanced Fibrous Composites for Aircraft Structures", AFFDL-TR69-43, Vol. 1, April 1969.

8. "Military Standardization Handbook: Metallic Materials and Elements For Aerospace Vehicle Structures", MIL-HDBK-5B, Volume 2, September 1971.

APPENDIX A - STRUCTURAL CONCEPTS EVALUATED FOR COMPRESSION PANEL

Three structural concepts for the compression panel were evaluated in sufficient depth for weight and structural arrangement comparison purposes. These concepts are: skin-stringer, honeycomb sandwich and contoured plate. The skin-stringer concepts was selected for the design of the compression panel.

The three compression panel concepts considered were 48 inches (1.22 m) wide and 72 inches (1.83 m) long and were designed for a concentrated ultimate compressive load of 350,000 lbs (1555 kN) applied at one end and reacted by a distributed load at the opposite end. Peaking of the distributed load must not exceed a uniformly distributed load by more than 30% as illustrated in Figure A-1. Shown in Figure A-2 is a weight comparison of the three concepts considered. Including support frame weight, the skin-stringer and honeycomb sandwich concepts are nearly equal in weight while the contoured plate concept is considerably heavier because of the numerous frames required. Methods of analysis and assumptions used in evaluating the three concepts are summarized in the following paragraphs.

(a) Skin-Stringer Concept Analysis - A finite element idealization of the skin-stringer concept was used to obtain preliminary sizes for the shear panels and stringers. The use of a MDAC-E computer program (CASD) allowed a rapid determination of preliminary estimates for a minimum weight structure capable of distributing a concentrated applied load at one end into a uniformly distributed load at the opposite end. A deflection criteria of uniform deflection at the distributed load end was also imposed for later element sizing.

The structural arrangement of the skin-stringer panel is shown in Figure A-3 and the finite element idealization is shown in Figure A-4. Due to symmetry of structure and loads, only one half of the panel was idealized. A typical stringer-skin cross-section is shown in Figure A-5. The unidirectional boron-aluminum stringers and steel frames are assumed to carry longitudinal and transverse loads only and are simulated by 49 bar elements. The $\pm 45°$ ($\pm \pi/4$ rad.) mid-plane symmetric laminate skins are assumed to carry shear only and are idealized by 20 shear panels. Skin buckling is assumed to be negligible.

Mechanical properties used for the frames, stringers and skin in this study are given, in Table A-6. Past boron-aluminum properties at 500°F (534°K) are assumed equivalent to 600°F (588°K) properties for improved material. Four

A-1
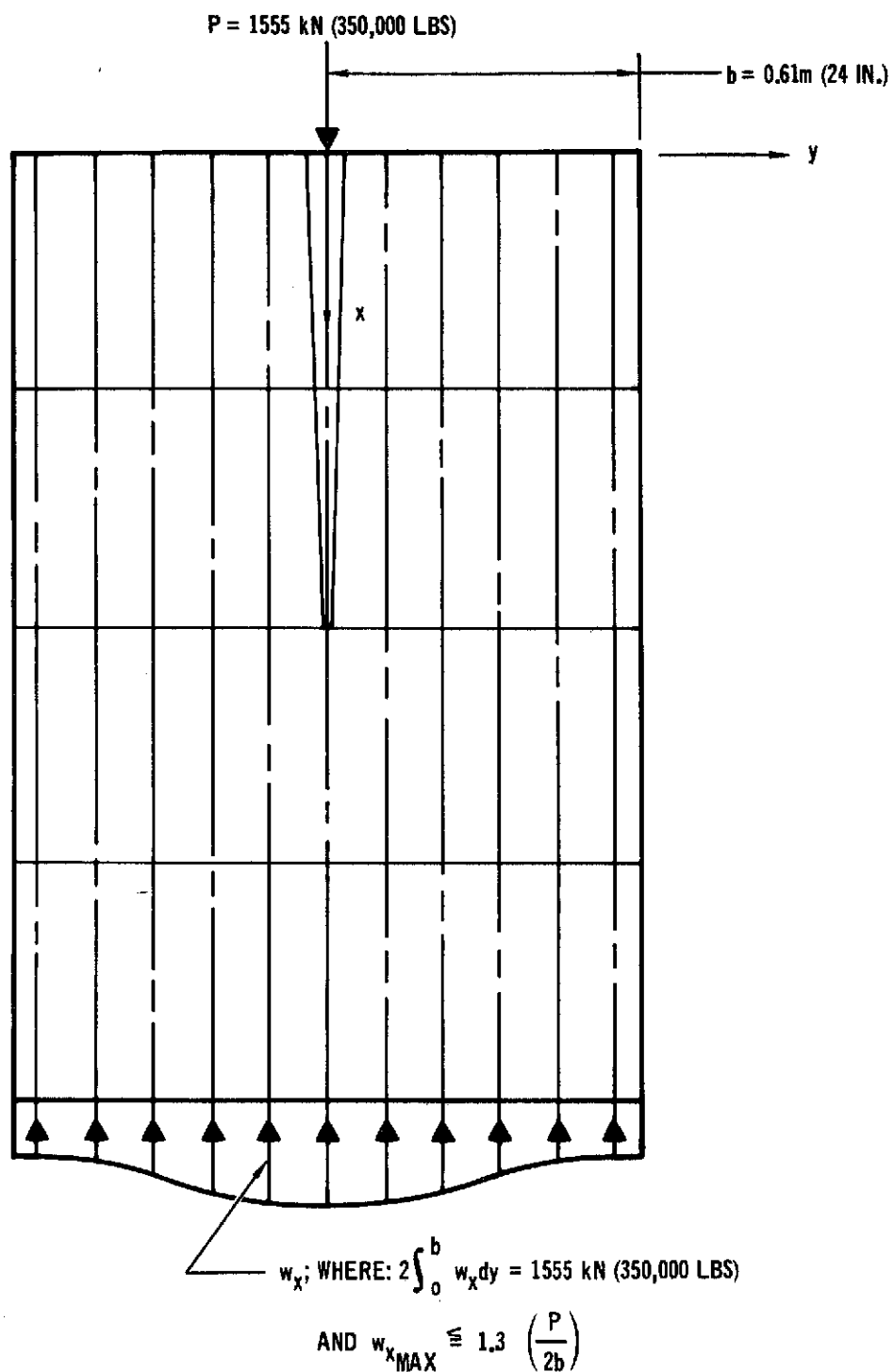
COMPRESSION PANEL EXTERNAL LOADS

Figure A–1

CONCEPT		WEIGHT		REMARKS
		LB	kg	
SKIN-STRINGER ±45° SKIN 48 IN. (1.22 m) 18" TYP 0° STRINGERS B-AL SKIN-STRINGER STEEL FRAMES	B-AL SKIN B-AL STRINGER ST FRAMES TOTAL	24.0 38.5 27.0 89.5	10.9 17.5 12.2 40.6	1. LOADS DISTRIBUTION OBTAINED FROM ASD ANALYSIS 2. STRINGER AREAS OBTAINED USING PRELIMINARY CRIPPLING & COLUMN ESTIMATES 3. SHEAR PANELS SIZED BY STRENGTH 4. DESIGNED FOR CONCENTRATED LOAD OF 350,000 LB (1.56 MN) AT 600°F (589°K)
SANDWICH PANELS 90° FACE SHEETS 0°, 90°, ±45° 0° TITANIUM CORE h h = 2.8 IN. (0.071 m)	B-AL FACE SHEETS BRAZE ST FRAMES Ti CORE TOTAL	51.8 2.9 11.0 28.4 94.1	23.5 1.3 5.0 12.9 42.7	1. LOADS DISTRIBUTION ASSUMED SAME AS SKIN-STRINGER CONCEPT 2. TITANIUM CORE DENSITY ASSUMED 5.0 LB/FT^3 (0.080 gm/cm^3) 3. BRAZE WEIGHT BASED ON 0.06 LB/FT^2 (0.0292 gm/cm^2)
SOLID TAPERED LAMINATE 0°, 90°, ±45° P 72 IN. (1.83 m) P	B-AL SKIN ST FRAMES	51.8 HIGH	23.5 HIGH	1. LOAD DISTRIBUTION ASSUMED SAME AS SKIN-STRINGER CONCEPT FRAME SPACING REQUIREMENT BECOMES IMPRACTICAL AT DISTRIBUTED LOAD END

WEIGHT COMPARISON OF THREE COMPRESSION PANEL CONCEPTS

72 IN.
(1.83 m)

48 IN.
(1.22 m)

RING
(TI OR
STEEL)

STRINGER
(BORON-
ALUMINUM)

SKIN
(BORON-
ALUMINUM)

LOAD INTRODUCTION
MEMBER (BORON-
ALUMINUM)
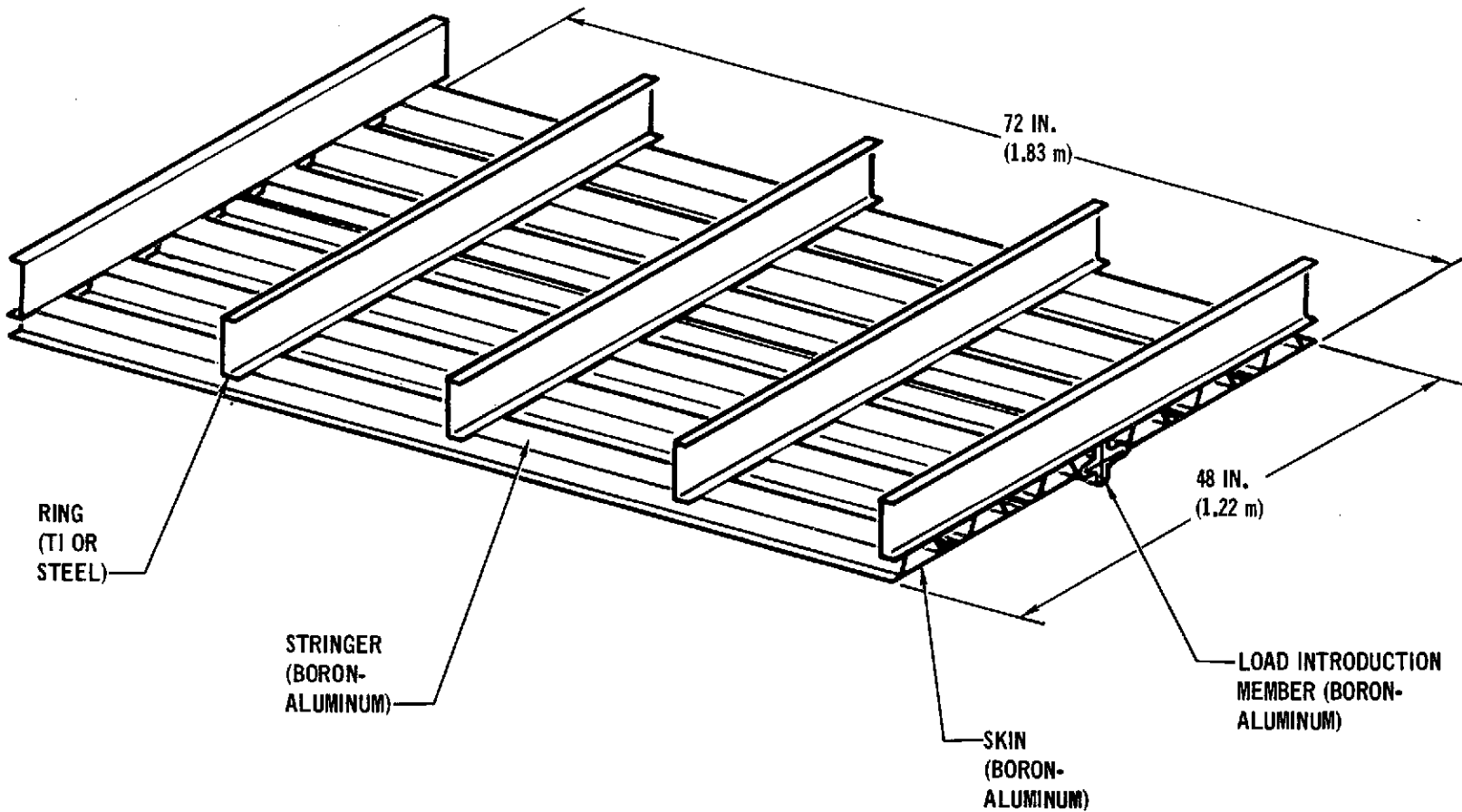
SKIN-STRINGER COMPRESSION PANEL DESIGN
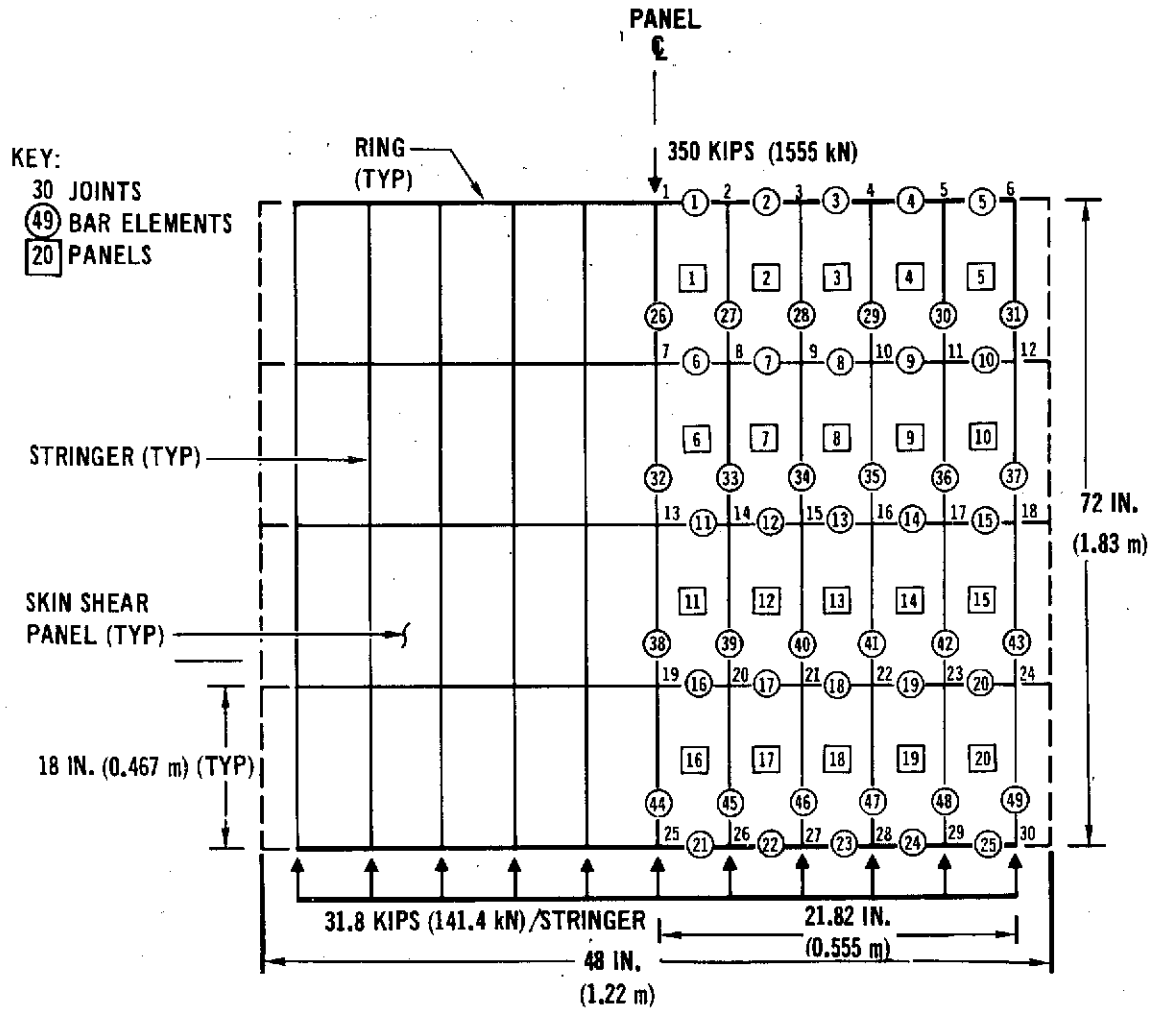
FINITE ELEMENT IDEALIZATION OF SKIN STRINGER CONCEPT

Figure A–4
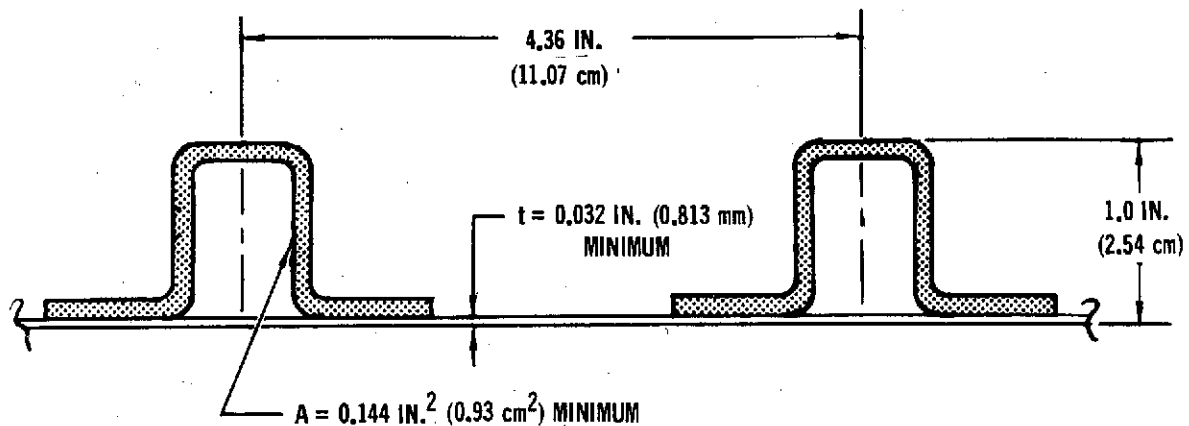
SKIN STRINGER CONCEPT USED FOR PRELIMINARY STRENGTH ANALYSIS

Figure A–5

RINGS –	4130 STEEL AT 600°F (589°K) $E = 29.0 \times 10^6$ PSI (200 GN/m²) $G = 10.0 \times 10^6$ PSI (69 GN/m²) $\rho = 0.283$ LB/IN.³ (7.83 gm/cm³)
STRINGERS –	U.D. BORON-ALUMINUM AT 600°F (589 °K) $E^C_L = 24.0 \times 10^6$ PSI (165 GN/m²) $G_{LT} = 6.02 \times 10^6$ PSI (41.5 GN/m²) $Ftu_L = 143.0$ KSI (0.985 GN/m²) $\rho = 0.095$ LB/IN.³ (2.63 gm/cm³)
SKIN –	± 45° BORON-ALUMINUM AT 600°F (589°K) $G_{xy} = 6.65 \times 10^6$ PSI (45.8 GN/m²) $F^{su}_{xy} = 20$ KSI (0.138 GN/m²) $\rho = 0.095$ LB/IN.³ (2.63 gm/cm³)

MATERIAL PROPERTIES

Figure A-6

analysis steps as outlined in Figure A-7 were used to obtain stringer areas and
skin gages for a minimum weight structure satisfying both the uniform loading and
deflection constraints required at the distributed load end. In the first step,
the panel was sized to meet the uniform load constraint only, without satisfying
the deflection criteria. The structure so determined was the minimum weight
structure meeting the uniform loading constraint. However, a support of variable
stiffness is required at the uniform load end and the allowable strength of all
stringers was assumed to be 100 ksi (.69 GN/m²).

In step two, the panel was resized to determine the minimum weight structure
meeting both uniform loading and deflection criteria with allowable stringer
strengths of 100 ksi (.69 GN/m²). The deflection criteria used in step 2 is
that all deflections shall be equal to or less than the center deflection obtained
during step one (Figure A-7).

Based on the internal loads distribution found in step two, revised allow-
ables were determined for each stringer element and employed in step three.
These preliminary revised stringer allowables were based on stringer crippling
strength and long column considerations. The uniform load and deflection con-
straints were again employed in step three.

Based on the stringer areas determined in step three, the stringer allow-
ables were again revised for the fourth resizing step. An additional requirement

A-6

that all $\pm 45°$ ($\pm \pi/4$ rad.) skin laminate thicknesses should reflect multiples of four plies to maintain mid-plane symmetry was employed in the fourth resizing step.

LOADING (ALL CASES):
31.8 KIPS (141.4 KN)
PER STRINGER

DEFLECTED
SHAPE

I. • STRUCTURE SIZED FOR STRENGTH
   • ALLOWABLE STRENGTH OF STRINGERS = 100 KSI
                                        (0.69 GN/m²)

III. • STRUCTURE RESIZED FOR STRENGTH AND STIFFNESS
     • ALLOWABLE STRENGTH OF STRINGERS BASED ON
       LOADS FROM STEP II

II. • STRUCTURE RESIZED FOR STRENGTH
      AND STIFFNESS
    • DEFLECTION $\delta \leq \delta_1$
    • ALLOWABLE STRENGTH OF STRINGERS = 100 KSI
                                         (0.69 GN/m²)

IV. • STRUCTURE RESIZED FOR STRENGTH AND STIFFNESS
    • ALLOWABLE STRENGTH OF STRINGERS BASED ON
      AREAS DETERMINED IN STEP III
    • MINIMUM GAGES FOR SKIN REVISED TO MULTIPLES OF
      FOUR PLIES $\geq$ GAGES DETERMINED IN STEPS III

STEPS LEADING TO PRELIMINARY SKIN AND STRINGER SIZES

Figure A-7

Preliminary stringer and skin loads and sizes obtained from step four are shown in Figures A-8 through A-11 and represent minimum weight structure satisfying both loading and deflection constraints. A summary of weights for the compression panel based on step four analysis is given in Figure A-12. The resulting structure has a load distribution at the distributed load end which is within the design requirement of less than a 30% load peaking as outlined in Figure A-1.

The skin-stringer concept was selected for the compression panel and additional analyses to support detail design were identified in the following areas:

1. Verify loads distribution for equal deflection as distributed load end.

2. Refine idealization of panel

   (a) Increase number of elements

A-7

    (b) Idealize skin with plate elements

        ° orthotropic

        ° nonlinear

    (c) Utilize multiple elements for stringer cross section

    (d) Update allowables based on test results

    (e) Revise skin allowables to reflect combined compression
          and shear loads

3. Increase number of iterations for improved convergence of stringer
    and skin gages.

4. Determine thermal stress distributions.
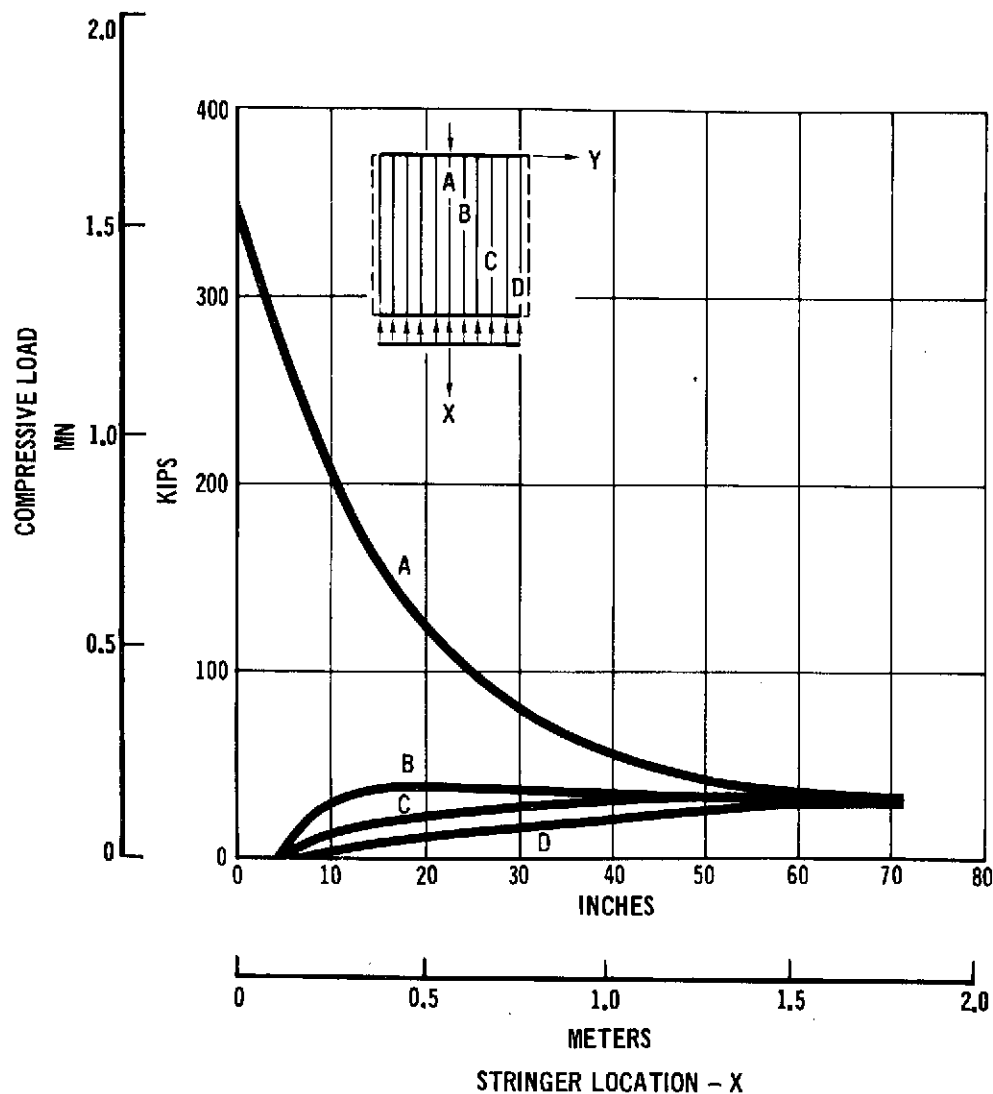
STRINGER AXIAL LOADS DETERMINED IN STEP IV

Figure A-8

A-8
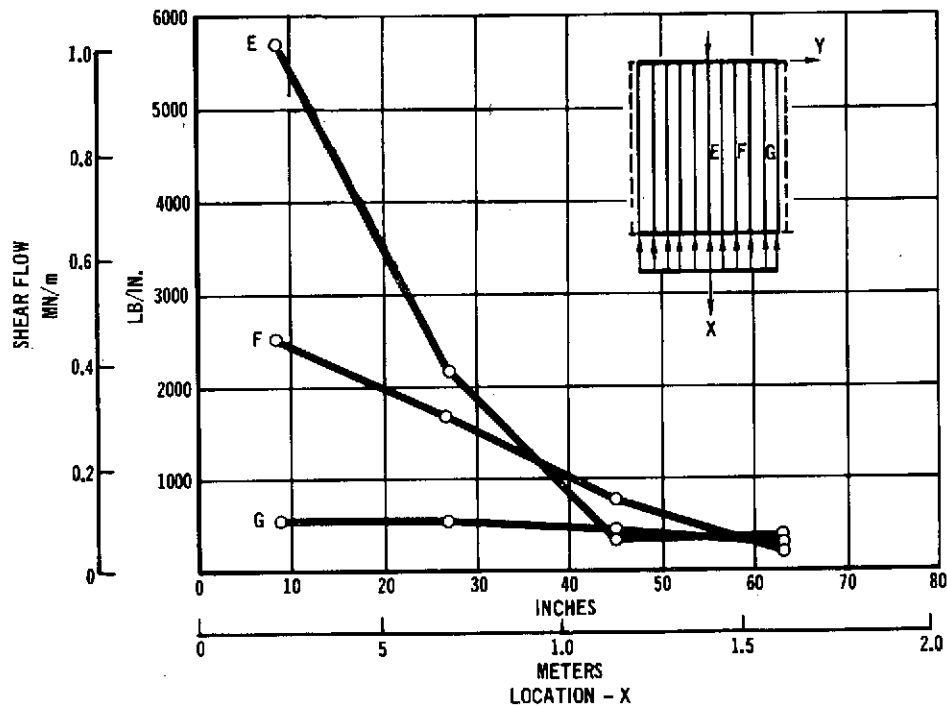
PANEL SHEAR FLOWS ARE LARGE ADJACENT TO CENTER STRINGER

Step IV

Figure A-9
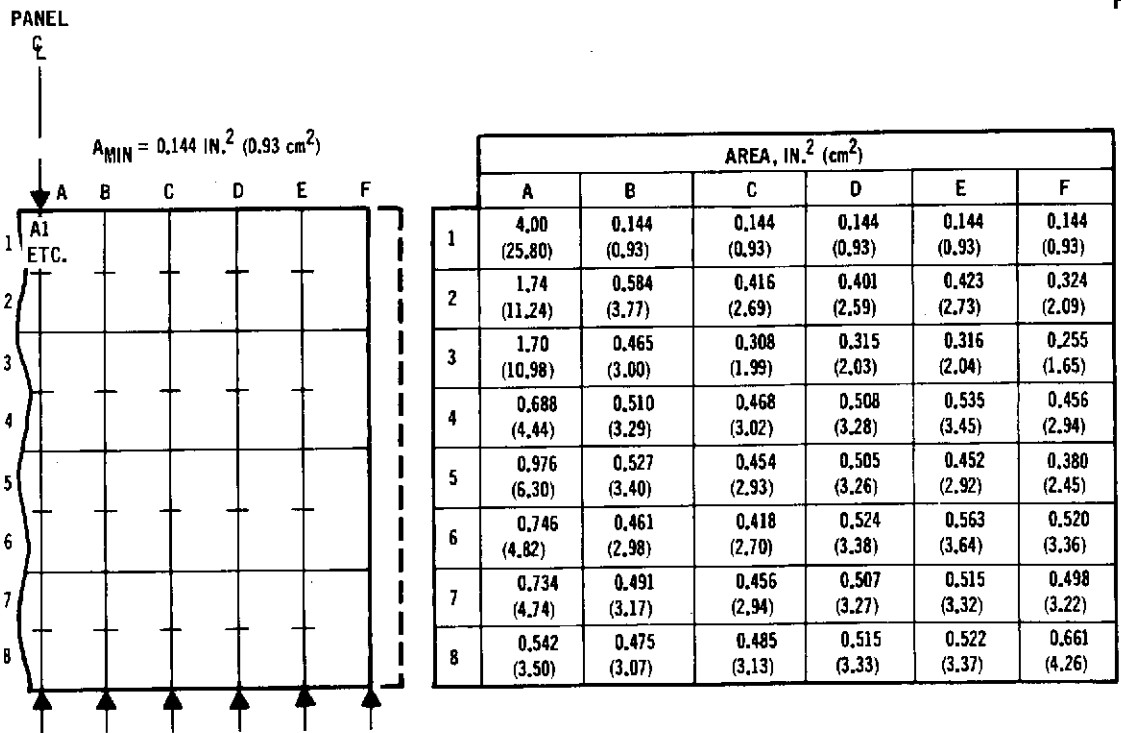
LARGE VARIATION IN STRINGER AREAS REQUIRED

Step IV

Figure A-10

A-9

$t_{MIN} = 0.032$ IN. (0.08 cm)

TYPICAL THICKNESS CALLOUT, IN. (cm)

					0.288 (0.73)	0.192 (0.49)	0.128 (0.33)	0.064 (0.16)	0.032 (0.08)	0.032 (0.08)
					0.128 (0.33)	0.128 (0.33)	0.096 (0.24)	0.064 (0.16)	0.032 (0.08)	0.032 (0.08)
					0.032 (0.08)	0.032 (0.08)	0.064 (0.16)	0.064 (0.16)	0.032 (0.08)	0.032 (0.08)
					0.032 (0.08)	0.032 (0.08)	0.032 (0.08)	0.032 (0.08)	0.032 (0.08)	0.032 (0.08)
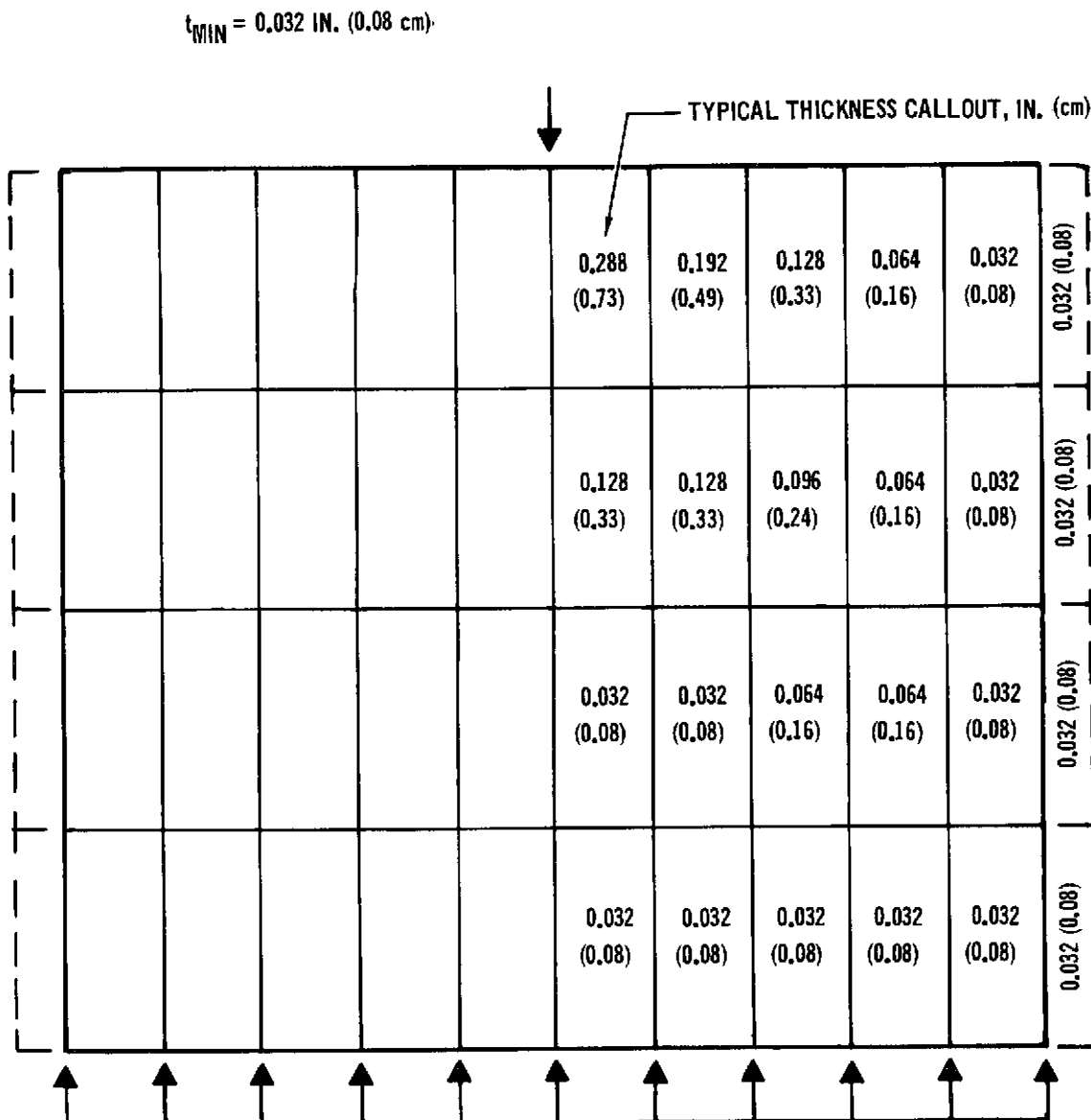
LARGE VARIATION IN SKIN THICKNESS REQUIRED
Step IV

Figure A–11

WEIGHT:

STRINGERS	38.5 LB (17.50 kg)	62.5 LB (28.4 kg)
SKIN	24.0 LB (10.90 kg)	
RINGS	27.0 LB (12.25 kg)	
TOTAL	89.5 LB (40.65 kg)	

DEFLECTIONS:

350 KIPS (1555 kN)

DEFLECTED SHAPE

0.241 IN. (0.612 cm)

0.220 IN. (0.559 cm)

LOADING: 31.8 KIPS (141.4 kN) PER STRINGER

% VARIATION IN DEFLECTION = 9.5
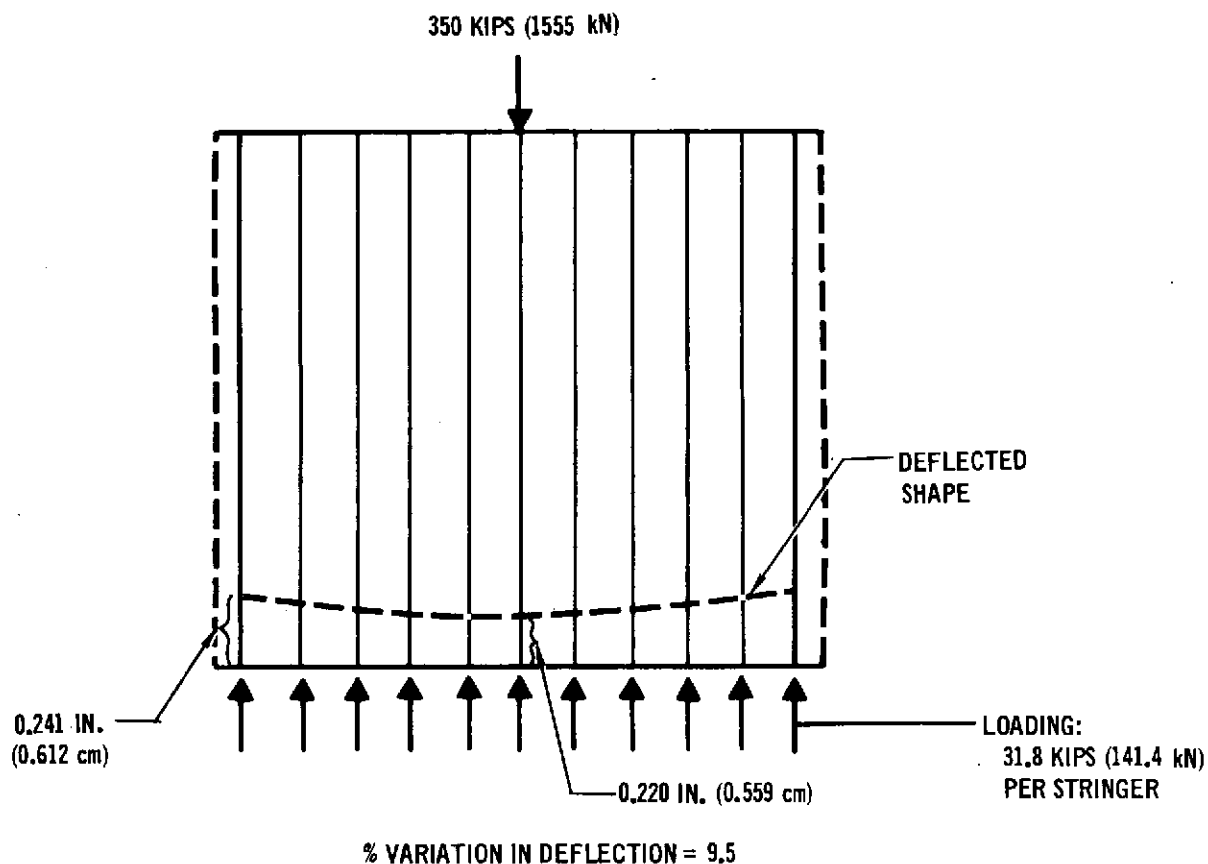
SUMMARY OF COMPRESSION PANEL SKIN-STRINGER CONCEPT

Figure A—12

(b) Honeycomb Sandwich and Contoured Plate Concept Analyses – The sandwich
panel and contoured plate design requirements are identical to those of the skin-
stringer as defined earlier. The basic design of the honeycomb sandwich panel is
that the boron-aluminum laminate skins contain lamina oriented to efficiently re-
sist the external loads. Sandwich core height was determined from stability re-
quirements considering the panel as simply supported at the concentrated load and
distributed load ends.

The contoured plate design is identical to the sandwich panel skins since
both are designed for strength. Therefore, the contoured plate thickness is
equal to the sum of the two faceplate thickness of the sandwich panel. Frame
spacing for the contoured plate design is based on stability requirements.

Design Points and Loads Criteria – Twenty-one points on one-half of the
panel were selected for the skin thickness calculations. Loads obtained in the
analysis of the skin-stringer concept were used to obtain loads per inch in the
plane of the panel. Shear flow distributions across the panel, q, at various
distances from the concentrated load are shown in Figure A-13. Distributions of
the longitudinal loads, W_X, are shown in Figure A-14. All design points selected
correspond to mid-points between stringers of the skin-stringer concept. There-
fore, the W_X load at each point was derived form the average of the two adjacent
stringer loads at the corresponding X-distance, using an effective width of 4.36
inches (.111 m) (the stringer spacing in the skin-stringer concept). Transverse
loads, W_Y, for points located between transverse frames were obtained in a
similar manner, using appropriate effective widths.

Determination of Laminate Allowables – In both concepts, internal loads
carried by the boron-aluminum vary greatly over the entire surface. Therefore
it was necessary to determine the proper ply orientations to withstand these
loads. For these studies laminate ply orientations were limited to combinations
of 0°, $\pm$45°, 90° (0, $\pm$ π/4, $\pm$ π/2 rad.) plies. Initially a minimum weight ulti-
mate shear and compression strength envelope shown in Figure A-15 was developed
for laminates containing combinations of 0° and $\pm$45° (0 and $\pm$ π/4 rad.) plies
only. This envelope was developed based on lamination theory and the maximum
strain failure criteria.

The ultimate strength analysis computer program was used to develop the
ultimate strength envelope. Within this program, the basic lamina and laminate
constitutive relations as well as the lamina stress-strain properties are used to
determine the stress-strain response of the laminate under biaxial in-plane load-

A-12

ing. By this procedure, the nonlinear stress-strain properties of the boron-
aluminum can be accurately included.

Using this shear and compressive strength envelope, minimum weight combina-
tions of 0° and ±45° (0 and ± π/4 rad.) plies to carry the loads at various points
on the panel were determined.
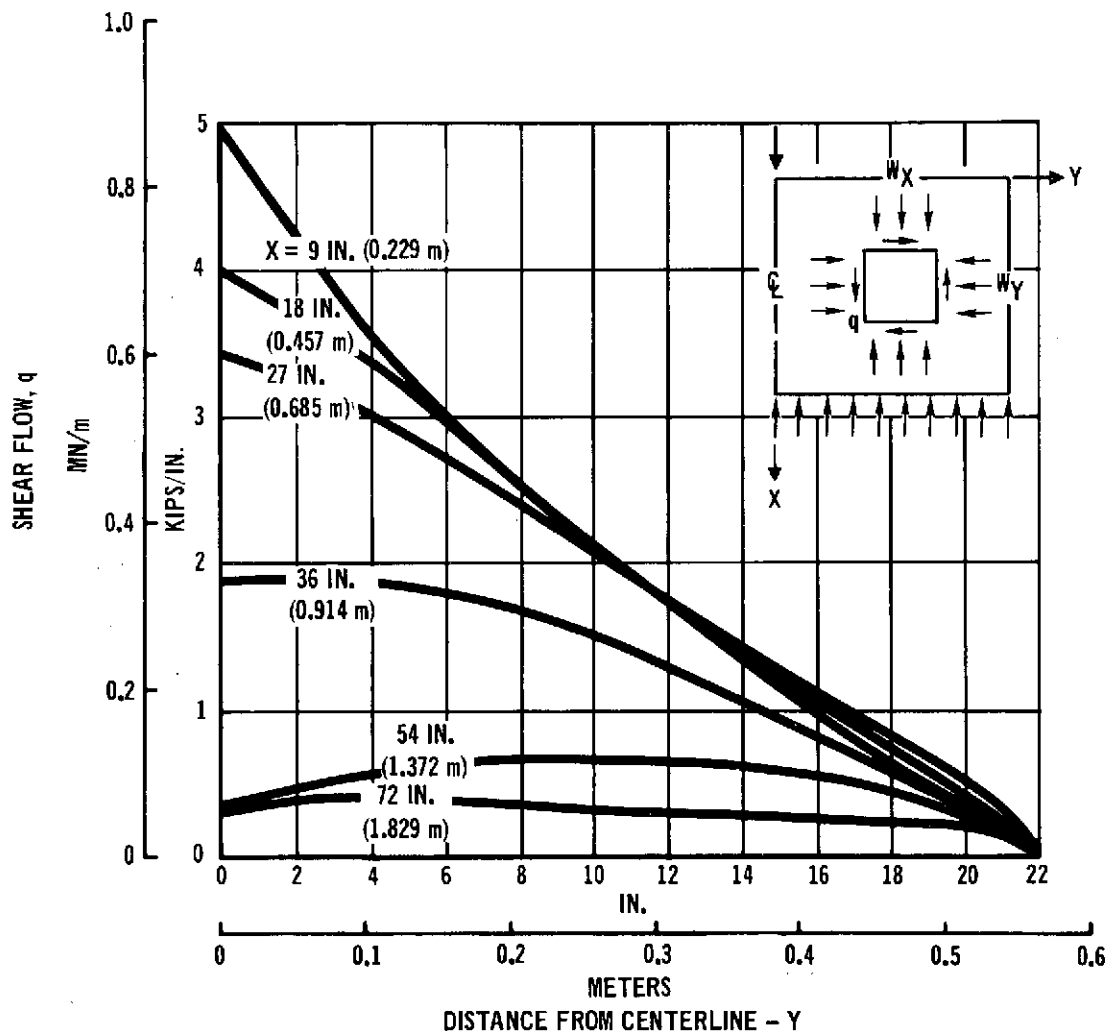
SHEAR LOADS OBTAINED FROM ANALYSIS OF SKIN-STRINGER CONCEPT

Figure A-13
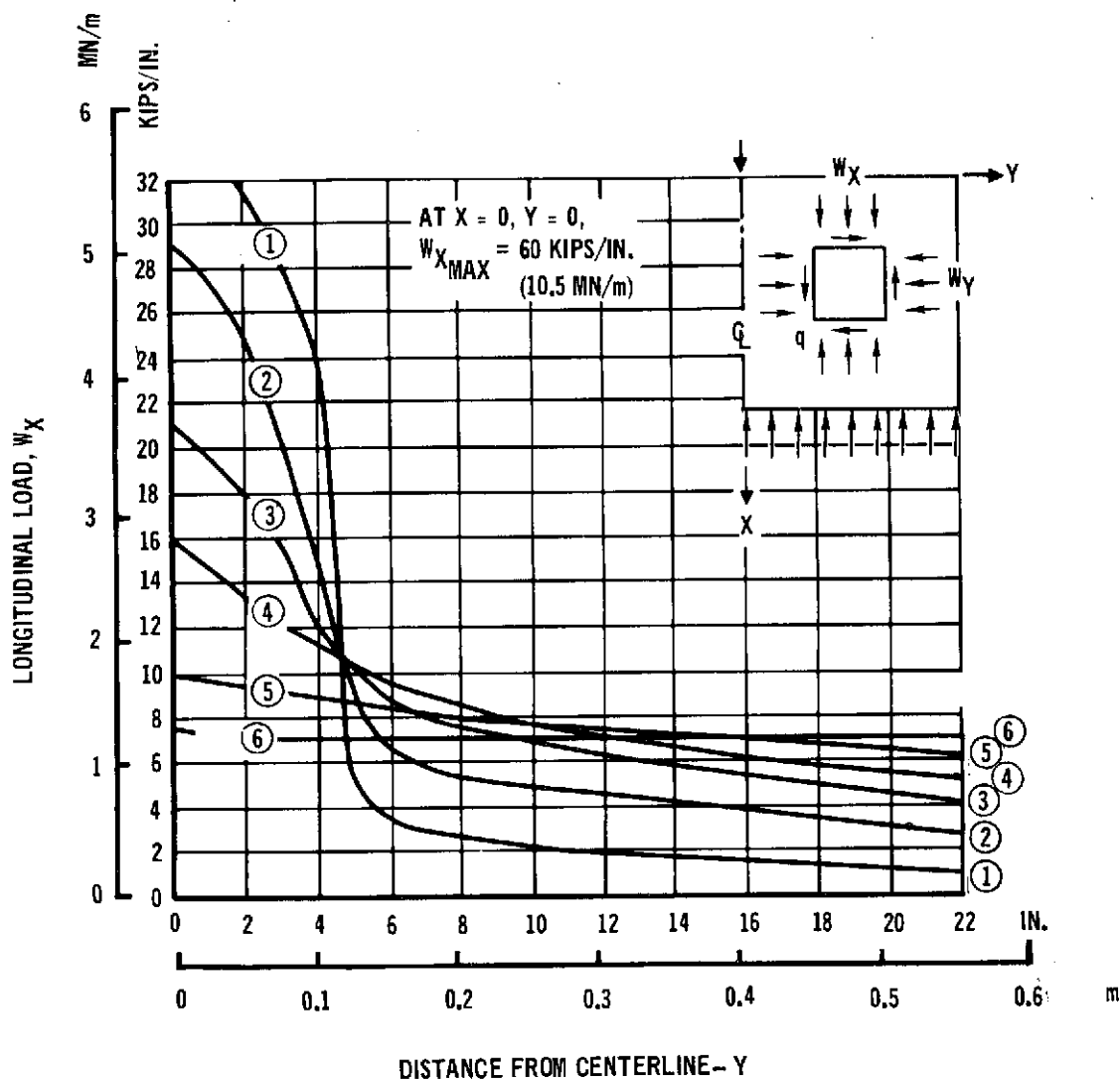
CURVE NO.		①	②	③	④	⑤	⑥
X	IN.	9	18	27	36	54	72
	m	0.229	0.457	0.685	0.914	1.372	1.829

LONGITUDINAL LOADS OBTAINED FROM ANALYSIS OF SKIN-STRINGER CONCEPT

Figure A—14

$$F_X = W_X / t$$

$$F_{XY} = q/t$$

COMBINED ULTIMATE SHEAR AND COMPRESSIVE
STRENGTH ENVELOPE
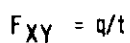
Figure A-15

Skin Thickness Design Curve - Using the allowable compressive strength, F_X, and the corresponding 0 rad ply percentages at five selected points (A to E as shown in Figure A-15) the ply thickness design curve shown in Figure A-16 was obtained. It should be noted that since the allowable strengths, F_X and F_{XY}, are based on the total laminate thickness, the ratio W/q, the design curve ordinate, is also equal to the ratio F_X/F_{XY}.

Skin Thickness Example Calculations - From Figure A-14 at X = 9 in. and Y = 2.16 inches:

$$W_X = 31.2 \text{ kips/in. } (5.46 \text{ MN/m})$$

$$q = 4.15 \text{ kips/in. } (.73 \text{ MN/m})$$

$$\text{and, } \frac{W}{q} = 7.5$$

From the design curve, Figure A-16: $X_o = 0.70$
Using Figure A-16, a line with a slope of 7.5 intersects the allowable strength envelope at F_X = 66 ksi (.455 GN/m^2). The total laminate thickness, t, is

$$F = \frac{W_X}{F_X} = \frac{31.2}{66}$$

$$t = 0.473 \text{ in. } (1.20 \text{ cm})$$

The 0° ply thickness, t_o, is

$$t_o = t \ (X_o)$$

$$t_o = 0.331 \text{ in. } (.84 \text{ cm})$$

The cross-ply ($\pm 45°$, $\pm \Pi/4$ rad.) thickness, t_s, is

$$t_s = t - t_o = 0.473 - 0.331$$

$$t_s = 0.142 \text{ in. } (.36 \text{ cm})$$

Skin Thickness Contours - The theoretical cross-ply and 0° ply laminate thicknesses were calculated for the 21 selected points and tabulated on plan view sketches representing one-half of the panel. Using linear interpolation between adjacent values, contour lines for several thicknesses were obtained as shown in Figures A-17 and A-18. The values were selected so that regions of laminate thicknesses corresponding to multiples of the assumed lamina thickness, .008 inch (.203 mm), were obtained. For the cross-plies, thickness increments of 4 laminae, i.e. .032 in. (.812 mm), were used since the sandwich panel design must utilize one +45° (+ $\Pi/4$ rad.) and one -45 (- $\Pi/4$ rad.) lamina per facesheet.

Thickness increments of .016 in. (.406 mm), or multiples thereof, were used for the 0° laminae.

Using the transverse loads, W_y, a preliminary analysis was made to determine the requirements for 90° ($\pi/2$ rad.) plies. As a result of this investigation, the laminate configuration shown in Figure A-19 was selected.

Final Laminate Configuration - After obtaining the contour sketches described above, actual lay-up of the corresponding laminates was investigated, using the following three constraints: (1) no joggling of cross-plies, (2) no joggling of 90° or 0° plies in the filament direction, and (3) no curved laminate boundaries. This study led to the configuration consisting or rectangular-shaped laminates shown in Figure A-20.

Sandwich Panel Core Height - These calculations were based on the assumption that the panel buckles as a simply supported, pin-ended column having a 72 inch (1.83 m) length. It was also assumed that core height could vary linerally from top to bottom and that the panel stiffnesses at each end are equal. Using the design ultimate load of 350,000 lbs (1555 KN) and an additional 1.5 factor on the effective area to account for uncertainties such as neglecting the reduction in stiffness due to shear deformation, etc., the required core heights were 2.0 inches (5.08 cm) and 3.7 inches (9.36 cm) at the concentrated-load and uniform-load end, respectively.

The resulting sandwich panel weights are given in Figure A-2 and include weights of the boron-aluminum facesheets, braze for joining facesheets to core, titanium core and steel frames.

Contoured Plate Concept - The third structural concept considered is the contoured plate concept with closely spaced frames. This concept utilizes the same total skin thickness as required by the honeycomb sandwich concept since both concepts are assumed to have the same internal loads distribution. It was determined from buckling analyses that numerous frame supports are required to stabilize the contoured plate concept. As a result, this concept is not competitive with the skin-stringer or honeycomb sandwich concept designs. However, this concept may be competitive for a curved panel design where a major portion of stability is provided by curvature.
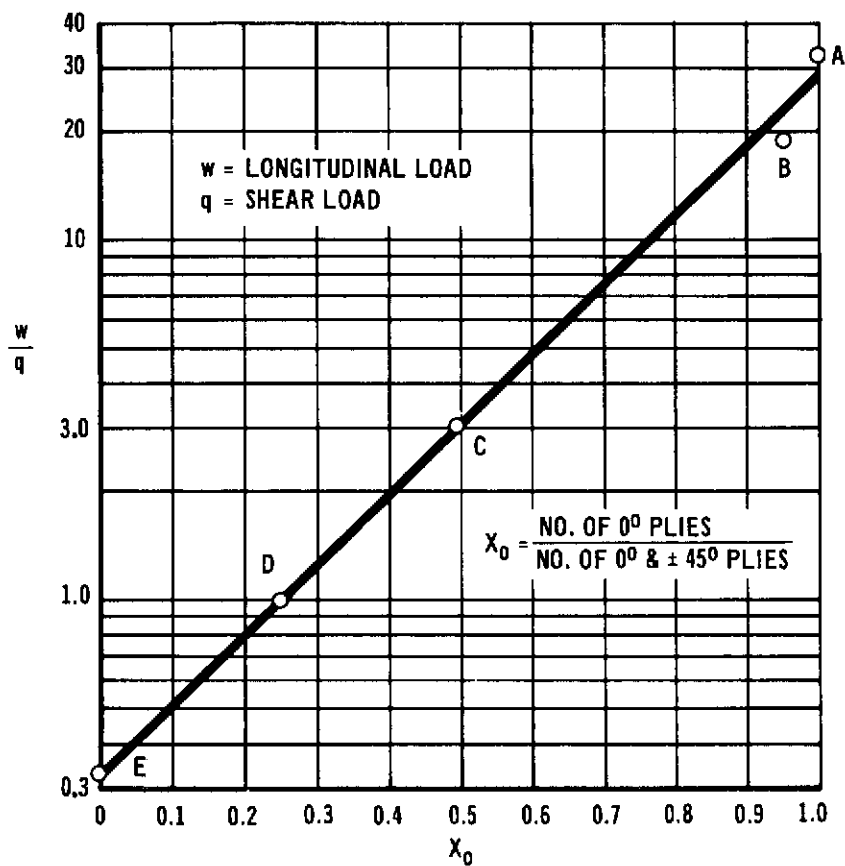
PLY ORIENTATION REQUIREMENTS DEFINED BY LOADING RATIO, W/q

Figure A—16

NO.	THICKNESS	
	IN.	cm
1	0.656	1.67
2	0.512	1.30
3	0.368	0.93
4	0.272	0.69
5	0.240	0.61
6	0.208	0.53
7	0.176	0.45
8	0.144	0.37
9	0.112	0.28
10	0.080	0.20
11	0.064	0.16
12	0.048	0.12
13	0.032	0.08
14	0.016	0.04

PLY THICKNESS — 0.008 IN. (0.0203 cm)
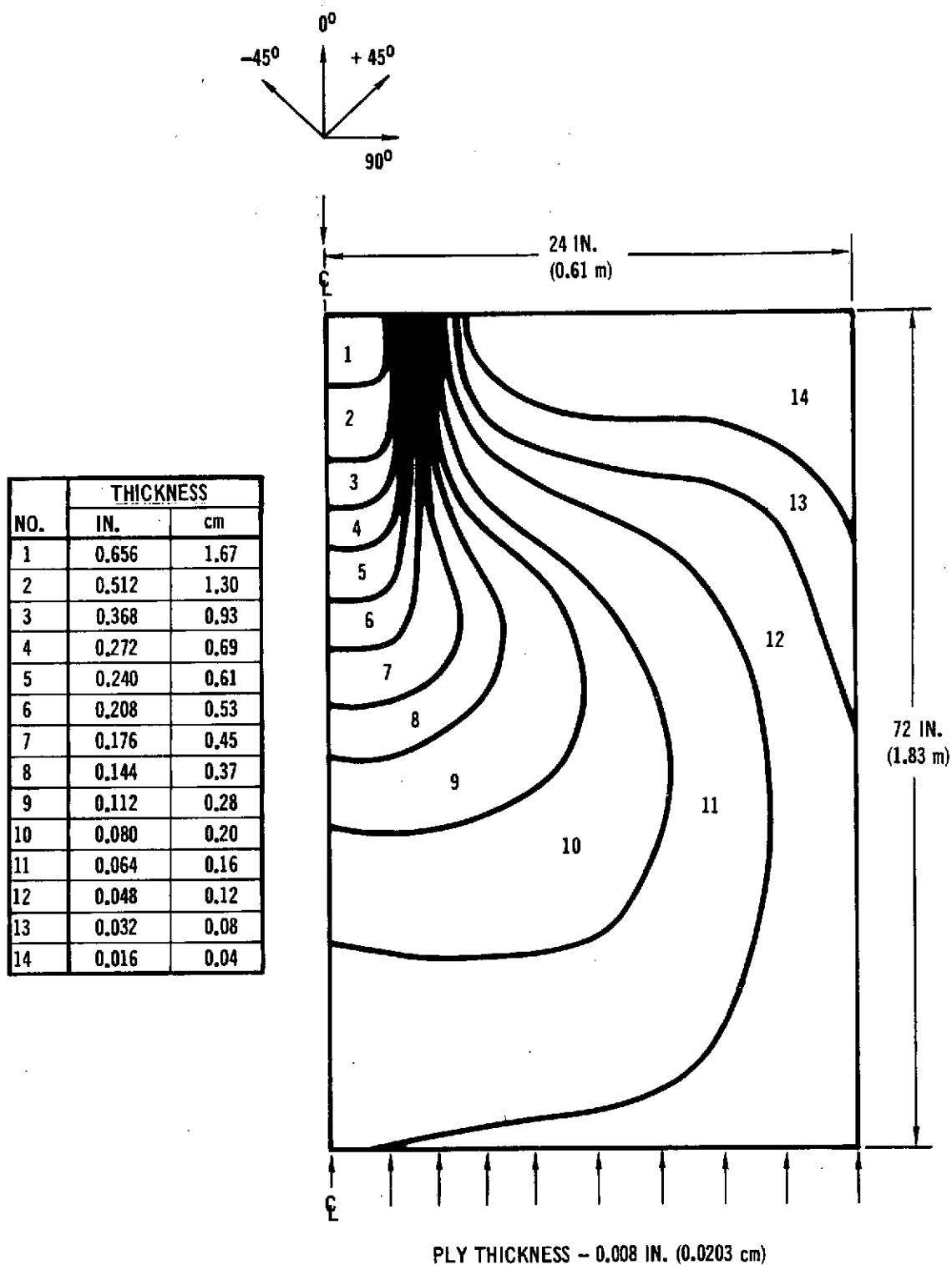
THEORETICAL THICKNESS OF 0° PLIES FOR HONEYCOMB SANDWICH
AND CONTOURED PLATE CONCEPTS

Figure A-17

A-19
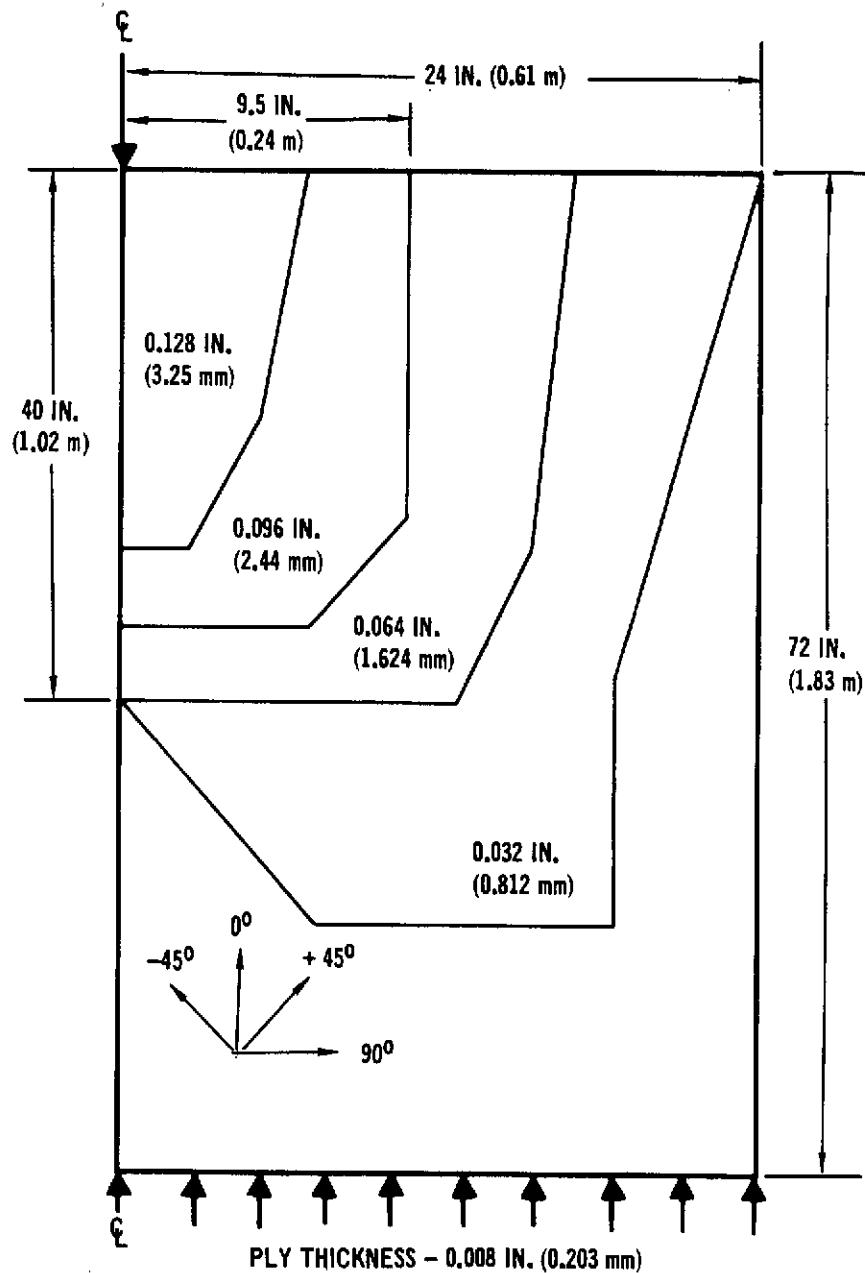
**THEORETICAL THICKNESS OF ± 45° PLIES FOR HONEYCOMB SANDWICH
AND CONTOURED PLATE CONCEPTS**

Figure A-18
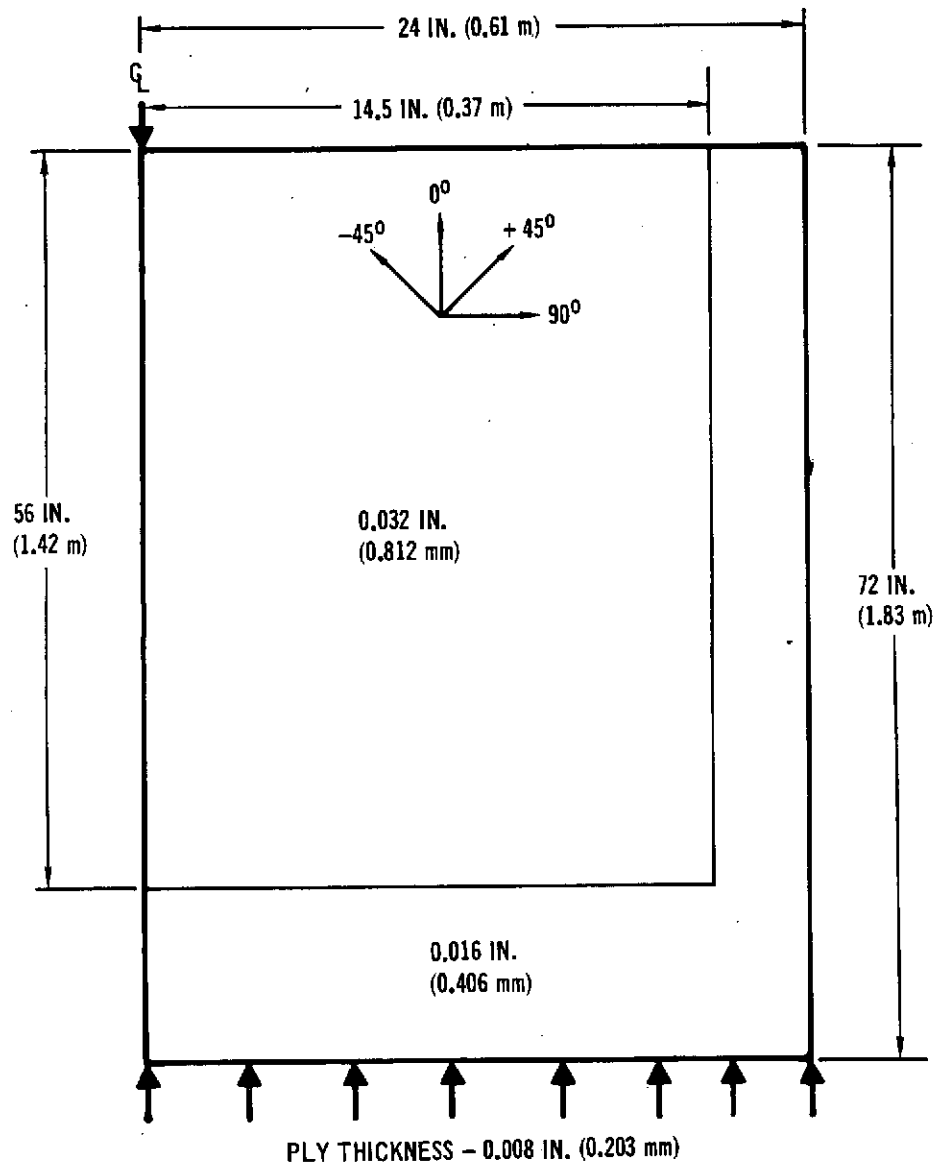
**THEORETICAL THICKNESS OF 90° PLIES FOR HONEYCOMB SANDWICH
AND CONTOURED PLATE CONCEPTS**

Figure A-19

BORON ALUMINUM FOR
SPACE SHUTTLE COMPONENTS

FINAL REPORT

REPORT MDC E0825
30 JULY 1973

MCDONNELL DOUGLAS ASTRONAUTICS COMPANY - EAST

A-22

HORIZONTAL DIMENSION	CODE	A	B	C	D	E	F	G	H
	(IN.)	2.5	3.5	5.5	7.5	9.5	14.5	18.0	24.0
	(m)	0.064	0.089	0.140	0.190	0.241	0.368	0.457	0.610
VERTICAL DIMENSION	CODE	J	K	L	M	N	P	R	S
	(IN.)	6	12	16	25	34	45	56	72
	(m)	0.152	0.305	0.407	0.635	0.863	1.143	1.422	1.829
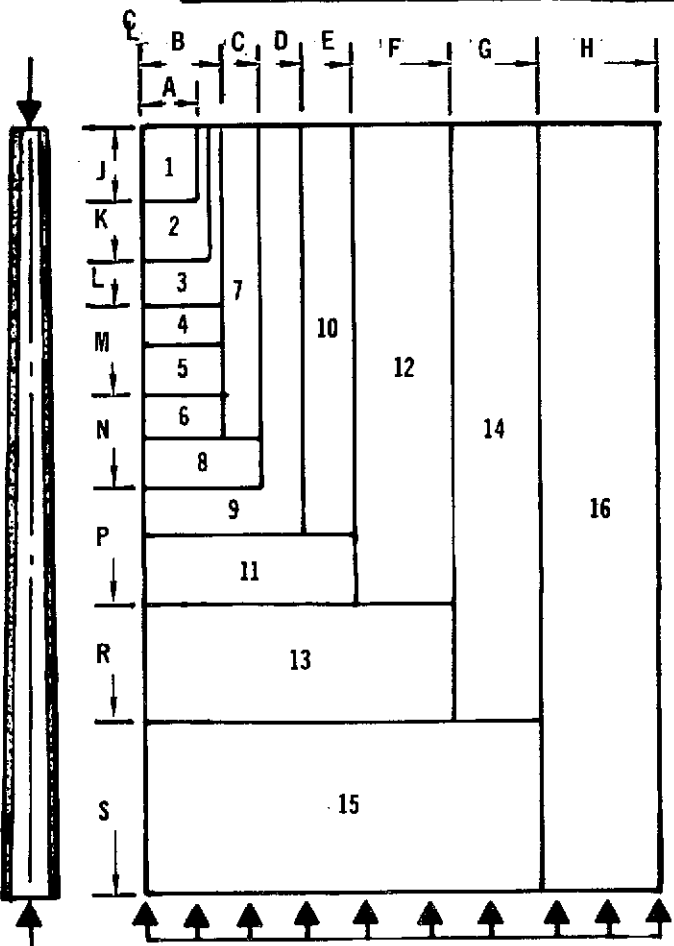
REGION	THICKNESS		NO. OF PLIES		
	IN.	cm	$0°$	$\pm 45°$	$90°$
1	0.816	2.07	82	16	4
2	0.672	1.71	64		
3	0.528	1.34	46		
4	0.432	1.10	34		
5	0.400	1.02	30		
6	0.368	0.93	26		
7	0.336	0.85	22	16	
8	0.304	0.77	22	12	
9	0.272	0.69	18	12	
10	0.240	0.61	14	12	
11	0.208	0.53	14	8	
12	0.176	0.45	10	8	
13	0.144	0.37	10	4	4
14	0.112	0.28	8	4	2
15	0.080	0.20	8	0	2
16	0.064	0.16	6	0	2

TOTAL SKIN THICKNESS OF HONEYCOMB SANDWICH AND CONTOURED
PLATE CONCEPTS USED IN WEIGHT ANALYSIS

APPENDIX B - TEST PLAN - BORON-ALUMINUM COMPRESSION PANEL

1.0. INTRODUCTION - The purpose of this test plan is to define the procedures required for performing a structural test at 589°K of the boron-aluminum compression panel. Instrumentation requirements are defined and recommendations for achieving uniform elevated temperatures on the compression panel are given. In addition, requirements for supporting the panel during test are specified and a suggested test sequence is included. The test plan is compatible with the following design criteria established for the compression panel:

a)   Design limit load (D.L.L.) = 1.11 MN (250,000 lbs)

b)   Factor of safety = 1.40

c)   Design ultimate load = 1.40 (D.L.L.) = 1.56 MN (350,000 lbs)

d)   Design temperature at (D.L.L.) or (D.U.L.) = 589°K (600°F)

e)   Prolonged temperature soak, large thermal gradients during heating, cyclic loading or temperature cycling are not design conditions.

2.0 COMPRESSION PANEL STRUCTURAL DESCRIPTION - The compression panel is composed of a 1.83 m (6 ft.) x 1.22 m (4 ft.) boron-aluminum tapered skin; seven boron-aluminum hat section stringers of tapered thickness; and four steel, channel section frames of constant cross section as shown in Figure B-1. The four frames are spaced on two foot centers dividing the compression panel into three equal bays. Three stringers are symmetrically located either side of the centerline stringer on approximately seven inch centers. The centerline stringer is part of the load introduction member. A steel plate attached to the panel on the side opposite the stringers completes the load introduction member. The stringers and frames are joined to the skin with mechanical fasteners.

3.0 INSTRUMENTATION - Approximately 190 gages are required to monitor deflections, strains, and temperature distribution throughout the compression panel. Figures B-2, B-3 and B-4 indicate only the approximate locations suggested for these gages. The specific placement of instrumentation will be based on location of existing fasteners and unique structural details. MDAC-E recommendations for exact location of gages will be supplied at the request of NASA-MSFC.

Deflection gages will record out-of-plane deflections of the centerline stringer and one outboard stringer. These gages will be located at the midpoint of each bay as shown in Figure B-3.

Twenty-eight rosette gages are required to monitor shear and biaxial strains in the skin. Suggested locations of the rosette gages are shown in Figure B-2. Twelve rosettes will monitor the strain distribution of the upper bay, six for the second bay and ten for the third. Rosette gages will be mounted back-to-back near the center of the shear panels indicated in Figure B-2 to determine any evidence of panel buckling or bending.

Fifty-two uniaxial strain gages will record longitudinal strain distribution in the seven hat-section stringers. Gages are placed in groups of two or three as indicated in Figure B-3. Each group consists of two gages symmetrically positioned on opposite sides of the stringer. Near the maximum load end of each stringer, a third gage mounted on the crown is added to the group. In the load introduction region two additional gages are attached to the steel thrust plate. This arrangement will indicate any evidence of twisting or bending during the heating and loading cycles.

Nine uniaxial strain gages monitor the response of the upper and lower frames. When grouped in pairs, the gages are attached to both legs of the frame. When only a single gages is used, it is placed on the inner leg of the frame. Gages are located at four inches and ten inches from the panel center line in the regions of high load.

The number of data recording channels selected for continuous review of the structure under load is twenty-three. These channels are reserved for monitoring those structural areas shown by analysis to be critical. Following is a description of the critical areas and the number of channels required for each.

a)   The two inboard shear panels of the upper bay on either side of the centerline stringer. Three channels are required for each rosette gage mounted in the center of the panel. Total channels required is six.

b)   The two outboard shear panels of the upper bay on either side of the centerline stringer. Six channels are required for the two "back-to-back" rosette gages mounted in the center of each panel. Total channels required is twelve.

c)   The centerline stringer. Two channels are required, one for each deflectometer located on the stringer.

d)   The outboard stringer. Three channels are required, one for each deflectometer located on the stringer.

Ninety-five thermocouples are required to control and monitor the temperature distribution of the compression panel. Forty-one thermocouples are located in the

critical areas of the structure, and provide input signals to a "Data Trak" Programmer
(See Section 4.0). Forty-one monitor thermocouples located adjacent to the control
thermocouples provide temperature read out, and may be used to maintain correct
panel temperature by manual control of the heat lamp bank in the event of a control
thermocouple malfunction. Thirteen additional thermocouples are suggested to
monitor temperature of the steel frames, thrust plate area, and panel base.

Thirty-six thermocouples placed on the frame side of the panel at locations
shown in Figure B-4, monitor and control the skin temperatures of the panel. Forty-
two thermocouples record and control temperature along the length of the seven
stringers, and are mounted in pairs on the stringers on 24 in. centers starting
11 inches from the top of the panel. Eight thermocouples, (2 control and 6 monitor)
are positioned along the panel base. Seven monitor thermocouples are located on
the steel frames nearest the heat lamp banks. The two remaining thermocouples
monitor the temperature in the thrust plate region.

3.1 STRAIN GAGE RECOMMENDATION AND INSTALLATION - Because of the temperature
environment, 589°K (600°F), rosette and uniaxial gages designated as WK-06-250W-350,
WK-03-250BG-350 and WK-09-259BG-350 are recommended for measuring strains in the
shear panels, stringers, and frames of the compression panel respectively. These
gages are of nickel-chromium wire, fully encapsulated in glass fiber reinforced
epoxy resin and are capable of withstanding a temperature of 603°K (625°F) or
greater. These gages are also selected on the basis of matching as near as possible
the coefficient of thermal expansion of the gage to that of the structural component.
The gages and the high temperature bonding cement (M-bond) required for installation
are manufactured by Micro-Measurement Company.

To assure a good bond at test temperature, the cement requires curing at 450°K
(350°F) for two hours followed by a post cure of 603°K (625°F) for one hour. Because
of the thermal stresses and the amount of time required in locally bonding small
groups of strain gages to the compression panel, the use of a furnace is recommended
for the first curing cycle.

Prior to starting the temperature cure, measure and record the "out-of-plane"
deflections at several points along each stringer and frame. The minumum number of
measurements along any member should be four. After curing at 450°K (350°F) and with
the compression panel at ambient temperature, repeat all of the "out-of-plane"
measurements. If the difference in deflections of the same member is .051 cm
(.020 inch) or greater after completion of the primary bonding cycle, contact MDAC-E
Composites Group before proceeding with the structural test.

The M-bond 610 is a non-tacky liquid at room temperature, therefore, the compression panel should be placed in a furnace in a horizontal, unrestrained position with all the gages on the upper surface in their proper position. Each gage requires a contact pressure of approximately 207 kN/m^2 (30 psi) which may be attained either by clamping or by weights. To assure a uniform pressure distribution on the bonding surface it is recommended that silicon rubber pads be placed between the clamps or weights and the gages. Care must be exercised to keep the temperature differential between adjacent structural components at a minimum, (approximately no greater than 13.9°K (25°F). Since the compression panel is of varying cross sectional area and consists of different materials, allowance must be made for temperature lag effects between furnace air temperature, compression panel temperature and compression panel support structure temperatures. The temperature of the structure should not be allowed to reach the maximum allowable differential before corrective measures are taken to return the temperature within limits.

When the gages are bonded to one surface of the compression panel, the panel may be turned over and the operation repeated for the remaining gages. The number of heating cycles to bond all strain gages and thermocouples shall not exceed four.

After curing at 450°K (350°F), the room temperature compression test as described in Section 6.1 may be performed. To minimize the number of thermal cycles, post curing at 603°K (625°F) should be done just prior to the elevated temperature test using the test heat source facilities. After one hour of post curing, the temperature may be reduced to the test temperature of 589°K (600°F) and the elevated temperature test conducted as described in Section 6.2.

3.2 STRAIN GAGE AND DEFLECTOMETER OUTPUT CORRECTIONS – Strain gage readings should be transmitted to the data acquisition system using the three-wire system to minimize temperature effects on lead wire resistance. Any zero offset in strain gage output voltage at room temperature due to unbalanced bridge completion networks, or at 589°K (600°F) due to differentials in thermal expansion coefficients of the gage and compression panel should be balanced before testing. This may be accomplished by either using a signal conditioner balancing network or the data acquisition system should subtract this offset from the voltage output when the compression panel is subjected to load.

Errors due to changes in Gage Factor from room temperature to 589°K (600°F) should be eliminated by programming the correct Gage Factor values, per manufacturer's specification into the data acquisition system both at room temperature and at 589°K (600°F).

B-4

3.3 <u>THERMOCOUPLE RECOMMENDATIONS AND INSTALLATION</u>. - The thermocouples recommended for monitoring and controlling the temperature of the compression panel are standard Chromel-Alumel thermocouples. These gages will require bonding to the structure with M-bond 610 at the locations shown in Figure B-4. Installation of these gages should be done simultaneously with the strain gage installation to keep the number of heating cycles to a minimum.

4.0 <u>HEAT SOURCE AND METHOD OF TEMPERATURE CONTROL</u> - The heat lamp system described in this section for the heat source is presented as an example only. This technique is not required and other techniques such as heated ovens, etc., are acceptable if the performance requirements stated herein are met.

One hundred and two standard T-3 quartz heat lamps manufactured by General Electric are recommended for heating the compression panel to a maximum temperature of 603°K (625°F) (Provision should be made to have about twenty percent spares). Each lamp is twenty-five inches long and has a power consumption of one hundred watts per inch. Sixty lamps will heat the frame side of the compression panel and forty-two lamps will heat the stringers. All heat lamps should be vertically oriented and located approximately 17 inches from either side of the compression panel skin as shown in Figure B-5.

The 60 lamps on the frame side of panel are grouped into 18 banks of lamps as shown in Figure B-5. The recommended spacing between each lamp is three inches. Vertical overlapping of the lamp holders of each bank of lamps is sufficient to assure an even temperature distribution to the compression panel skin. Each lamp bank should extend four and half inches beyond the vertical sides of the compression panel, one inch above the top edge and two inches below the base.

Heat lamps arranged in pairs at two inch spacing, located symmetrically on either side of each stringer are recommended. Six heat lamps are used for each stringer. Vertical overlapping of the lamps is the same as heat lamp banks for the skin. Aluminum foil facing the heat lamps and backed up with 0.25 inch "Refrasil" insulation should cover the shear panels in the areas between the stringers (See Figure B-5) to reduce the effects of secondary heating from the stringer heat lamps. To minimize heat radiation losses and assure a more even heat distribution, reflectors of Alsac-Aluminum are required for lamp banks on both sides of panel.

Control of the heat source to the compression panel may be accomplished by means of a temperature-time profile and a "Data Trak" programmer. ("Data Trak" is a trade name and is manufactured by Research Inc.). Each "Data Trak" programmer can control the temperature to six different areas of the compression in accordance with the

requirements of a given temperature-time profile. Three "Data Trak" programmers utilizing eighteen available channels are required for thermal control of the panel skin. Temperature control of the seven stringers, and base areas requires four additional programmers. It is suggested that the temperature time profile be programmed for a structural temperature rise of 2.22°K (4°F) per minute until the post curing temperature of 603°K (625°F) is reached. After one hour at temperature the temperature should be reduced to the test temperature of 589°K (600°F) at a temperature reduction rate of 2.22°K (4°F) per minute.

5.0   COMPRESSION PANEL SUPPORT STRUCTURE – The compression panel requires support structure to restrict "out-of-plane" deflections. Because of the elevated temperature environment, the support must allow "in-plane" growth in the vertical and horizontal planes to preclude thermal stresses. Support is required at the compression panel centerline and along the vertical edges at each of the four frames as shown schematically in Figure B-6. The clevis fitting and lug support concept shown in Figure B-6 is intended to show only the direction where support is required and where capability for panel motion is required.

Stiffness requirements of the lateral support structure for the compression panel test and the lateral loads to be reacted by the support structure are defined in Figures B-7 and B-8 respectively.

As shown in Figure B-7, the maximum lateral deflection permitted by the support structure at any frame support due to loads applied by the compression panel is 0.03 in. Also the total deflection at any support from all sources (including structural deflection, alignment, installation, etc.) cannot exceed 0.06 in. Furthermore, the lateral stiffness of support structure at any frame support point relative to an adjacent support point must exceed 200,000 lb/in.

Figure B-8 defines the ultimate lateral reactions expected when the 350,000 lb ultimate compression load is applied to the compression panel. It is recommended that the support structure at each frame support on a given frame be designed for the maximum load expected for that frame. These loads do not contain contingencies for additional loads which may occur due to tolerances in installation and alignment procedures.

The compression panel base support structure is assumed infinitely rigid. Because of the anticipated large mass of the base support structure, an insulation pad of sufficient thickness and compression strength or a heated platen placed between the compression panel and the base support is required to limit temperature differential during testing to 27.8°K (50°F). Temperature at the base of the compression panel may be monitored and controlled as described in Section 4.0.

The loading head or ram is assumed as infinitely rigid. Distribution of load from the ram to the compression panel will be by means of a loading plate located between the ram and the compression panel. Surfaces of the loading plate are to be flat, square and parallel to within 0.002 m/m. Steel heat treated to at least 1030 MN/m^2 (150 KSI) is recommended for the plate. Dimensions and clearances required are defined on Engineering Drawing TO-6192; the centroid of load application through the loading head is shown in Figure B-8 and is coincident with the panel centerline. Temperature control across the loading plate and ram may be attained in the same manner as that utilized for the base structure.

6.0   LOADING PLAN - The recommended loading plan is divided into two parts. In the first part, the design limit load (D.L.L.) of 1.11 MN (250,000 lbs) compression is applied to the compression panel at room temperature. This is followed by the elevated temperature test at 589°K (600°F) to the design ultimate load of 1.56 MN (350,000 lbs) (D.U.L. = 1.4 D.L.L.). Room temperature testing is recommended prior to post curing of the gage adhesive because the service life of strain gages at 589°K is limited. To minimize the effects of temperature, it is recommended that the post-cure of the adhesive and the elevated temperature test be combined into one operation as outlined in Section 3.1. Test procedures at room temperature are outlined in Section 6.1 and 6.2 respectively.

6.1   COMPRESSION PANEL ROOM TEMPERATURE STATIC TEST -

  a) Load the compression to 5% D.L.L. 55.5 kN (12,500 lbs compression).

  b) "Zero out" all structural gages per Section 3.2.

  c) Increase the compression load to 20% D.L.L. 222 kN (50,000 lbs) and record all gage readings.

  d) Increase the load in increments of 20% D.L.L. to 100% D.L.L.

  e) At each load level (40%, 60%, 80% and 100% D.L.L.) record load, deflections and strains.

  f) At 100% D.L.L., reduce load to 20% D.L.L. in 20% D.L.L. increments and record load, deflections and strains.

  g) It is recommended that a given load level be maintained just long enough to record all data and review data from critical areas identified in Section 3.0 only.

6.2   COMPRESSION PANEL ELEVATED TEMPERATURE STATIC TEST -

  a) With the heat lamps in place as described in Section 4.0, heat the compression panel to the post curing temperature of 603°K (625°F) at a temperature rise rate of 2.22°K (4°F) per minute.

b) Maintain the compression panel at the post-cure temperature for one hour.

c) After one hour at 603°K (625°F) reduce the temperature to the test temperatur of 589°K (600°F) at a temperature reduction rate of 2.22°K (4°F) per minute.

d) After panel temperature stabilization, apply 5% D.L.L. Allow panel temperatu to stabilize again if heat sinks influence temperature.

e) "Zero-out" all structural gages per Section 3.2

f) Increase the compression load to 20% D.L.L. and record all gage readings.

g) Increase the compression load in increments of 20% D.L.L. to 100% D.L.L. and in 10% increments beyond D.L.L. to design ultimate load (1.4 D.L.L. = D.U.L.).

h) If structure sustains D.U.L. without failure continue increasing load beyond D.U.L. in increments of 10% D.L.L. until failure occurs.

i) At each load level, record the applied load, deflections, strains and structural temperatures.

j) Remain at a given load level just long enough to record all data and review data as necessary from the critical areas identified in Section 3.0.
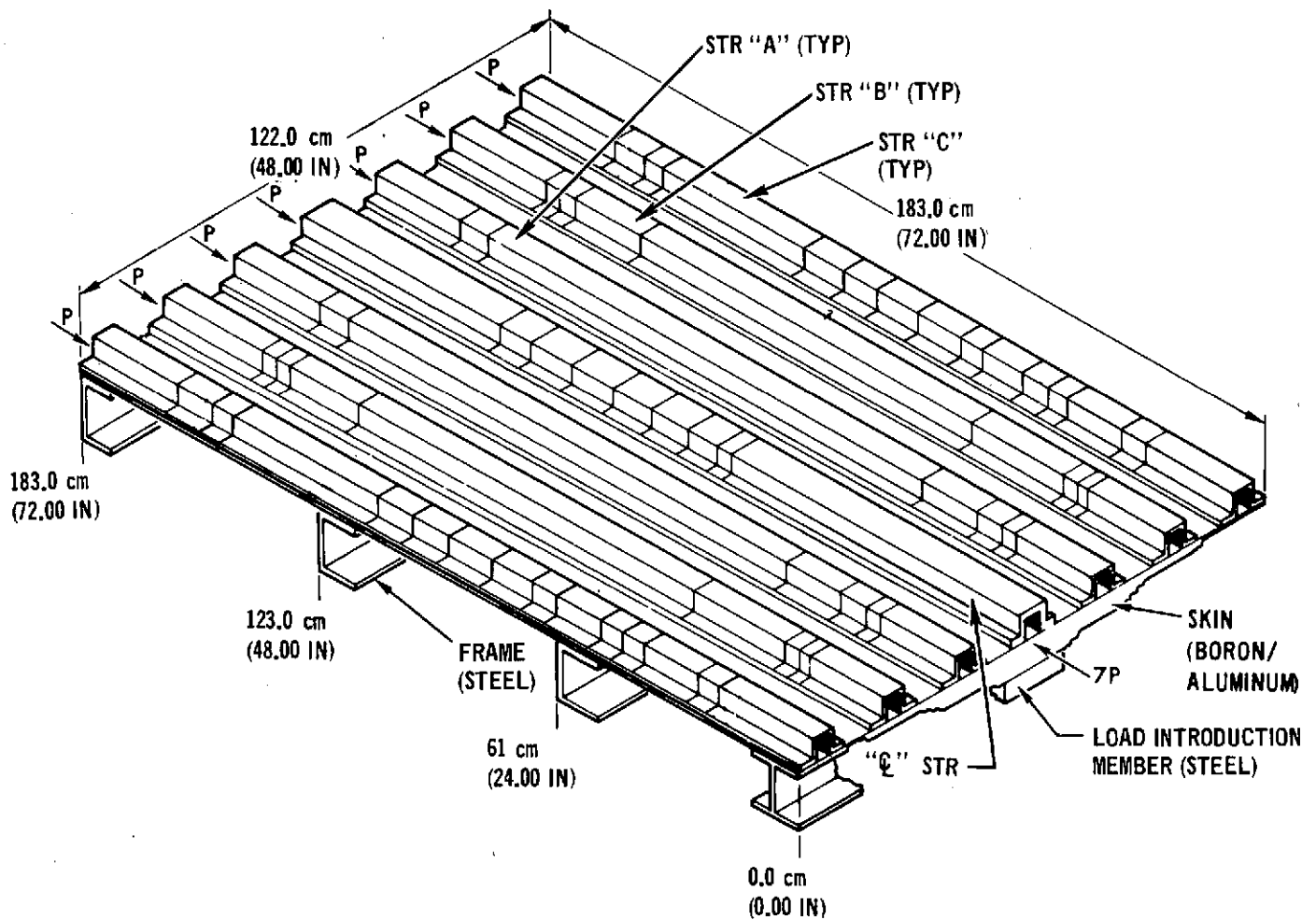
FIGURE B-1

COMPRESSION PANEL

FIGURE B-2

STRAIN GAGE ROSETTE LOCATIONS ON COMPRESSION

PANEL SKIN

- GAGES ARE SYMMETRICALLY LOCATED ABOUT THE PANEL ℄

- BACK TO BACK GAGES —◯
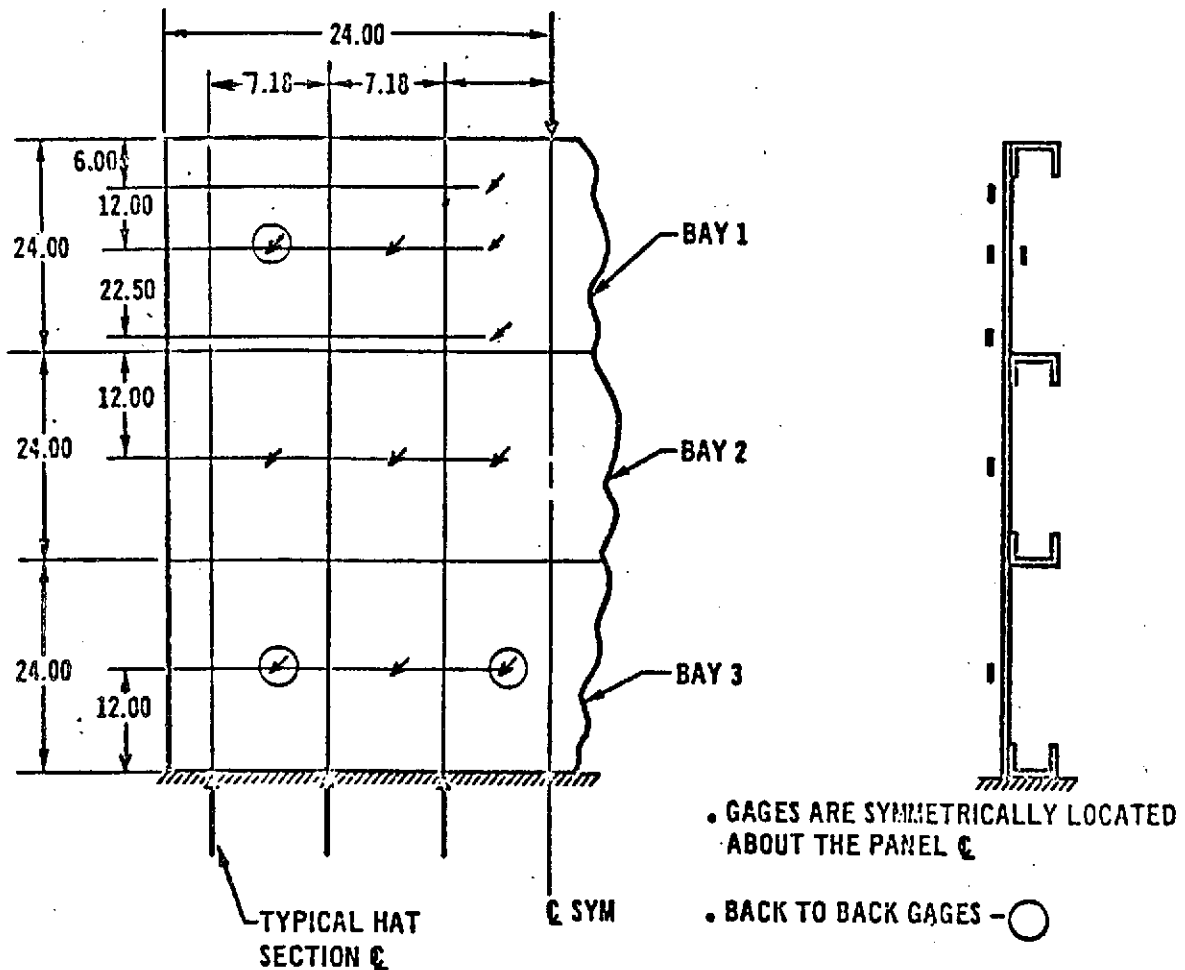
MCDONNELL DOUGLAS ASTRONAUTICS COMPANY - EAST

FIGURE B-2 NOTES:

1. Gages are symmetrically located about the panel center line; a total of 28 gages are used.

2. Gages are to be centered between stringers.

3. If necessary, the position of back-to-back gages should be shifted slightly to avoid skin tapering.

4. Details of channels and hat sections are omitted for clarity.

5. WK-06-250WR-350 rosette gages are recommended.

6. Mount gages to structure with high temperature adhesive M-bond 610. Cure bond at 450°K (350°F) for two hours followed by post curing at 603°K (625°F) for one hour. Post cure at the time of the elevated temperature test.

7. Maintain the entire panel at 589°K (600°F) for five minutes prior to loading at temperature.

FIGURE B-3

STRINGER AND FRAME STRAIN GAGE AND
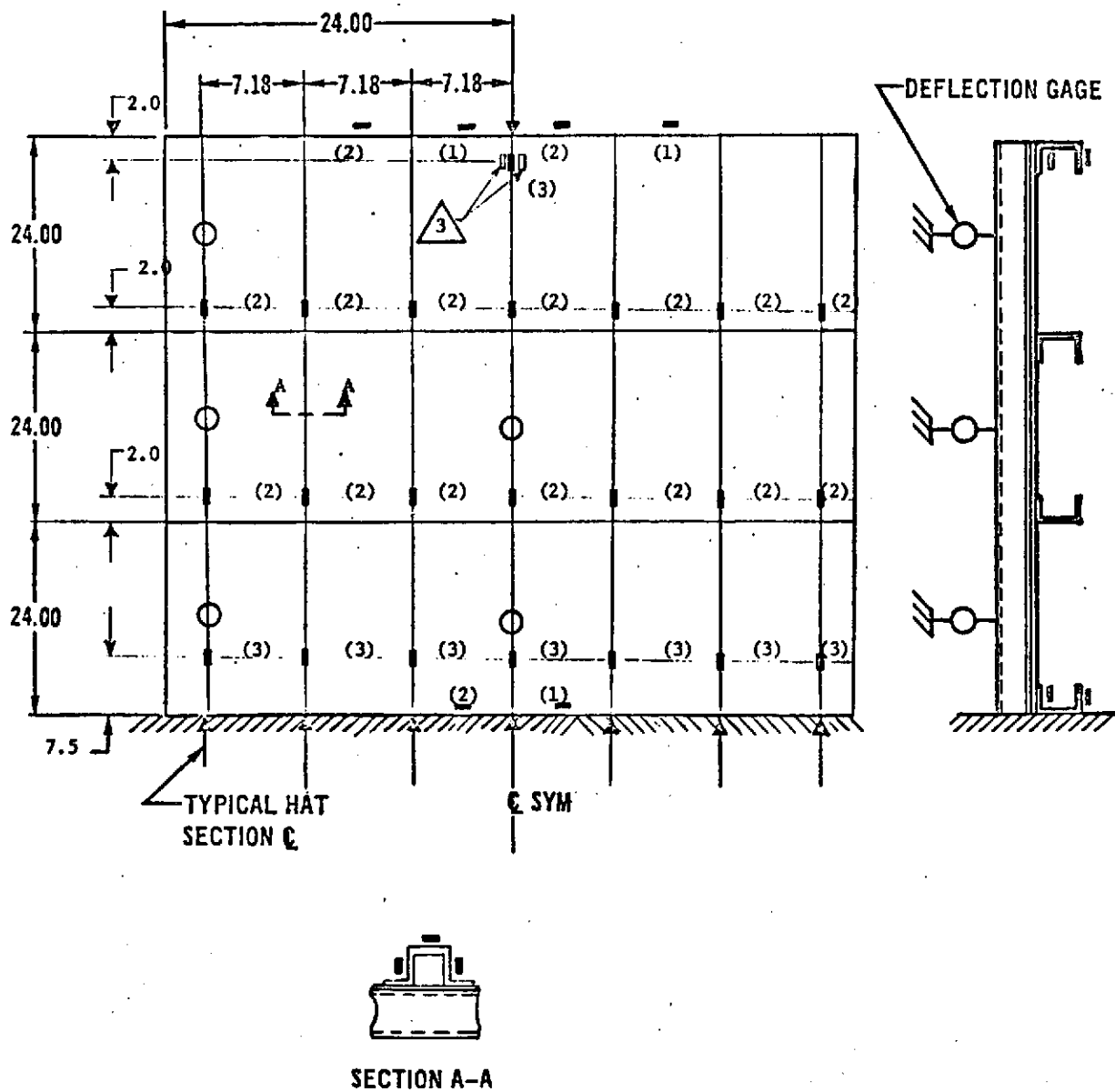
### DEFLECTOMETER LOCATIONS

SECTION A-A

FIGURE B-3 NOTES:

1. The total number of strain gages used is 63.

2. Number shown in parenthesis indicates a group of uniaxial gages used at that location.

3. Gages located on steel thrust plate.

4. Five deflectometers are used. Two are located on the center line and three on one outboard stringer.

5. WK-03-250BG-350 uniaxial strain gages required for stringers.

6. WK-09-250BG-350 uniaxial strain gages required for frames.

7. Mount gages to the panel structure with high temperature adhesive M-bond 610. Cure bond at 450°K (350°F) for two hours followed by post curing at 603°K (625°F) for one hour. Post cure at the time of elevated temperature test.

8. Maintain the entire panel at 589°K (600°F) for five minutes prior to loading at temperature.

FIGURE B-4

COMPRESSION PANEL THERMPCOUPLE LOCATIONS
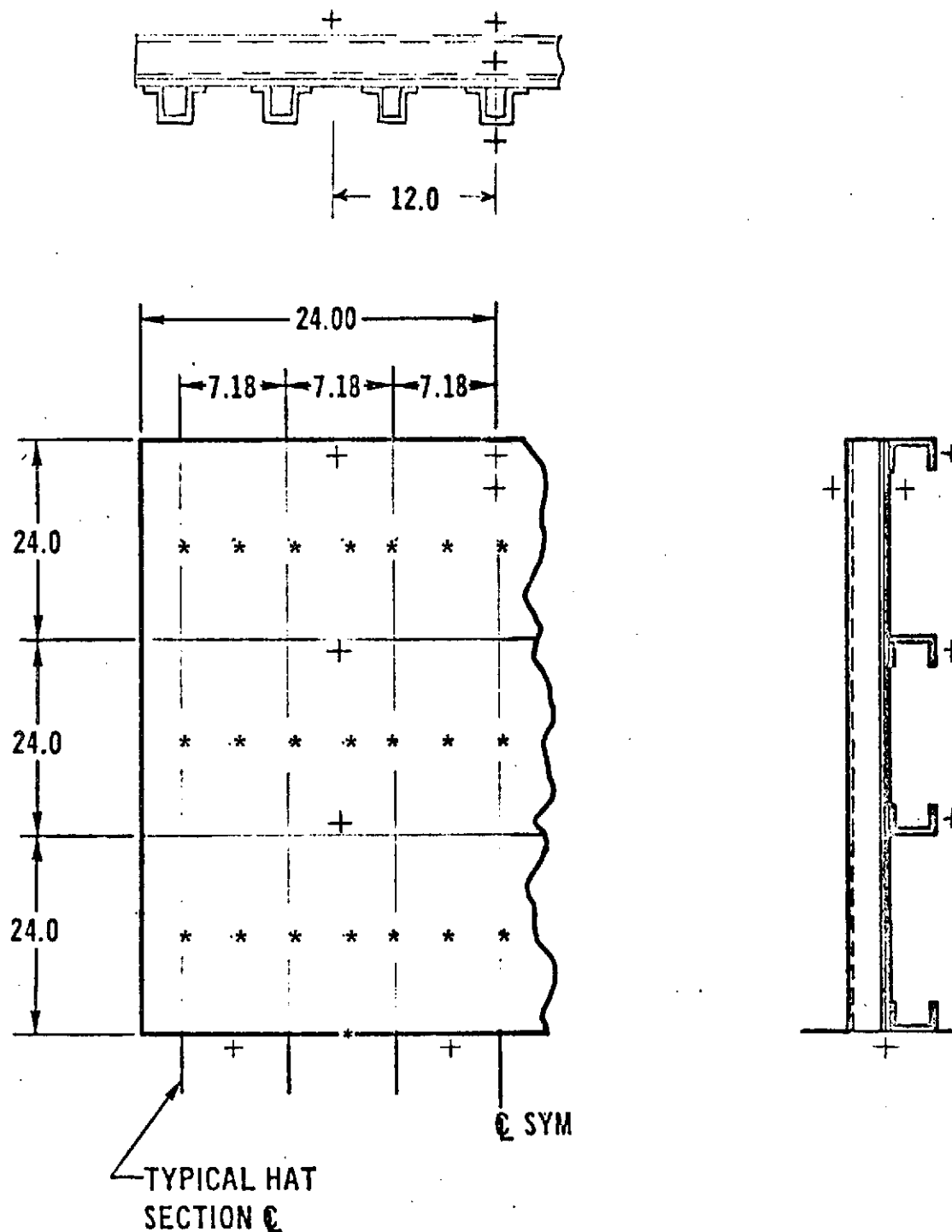
95 THERMOCOUPLES

* - INDICATES LOCATION OF TWO THERMOCOUPLES: ONE CONTROL, ONE MONI

\+ - INDICATES LOCATION OF A SINGLE MONITOR THERMOCOUPLE

FIGURE B-4 NOTES:

1. Ninety-five thermocouples are shown. Forty-one for control and fifty-four to monitor the panel temperature. They are located symmetrically about the panel center line.

2. Thermocouples mounted on the stringers are located on the crown near the midpoint of each bay.

3. Thermocouples mounted on the skin are located on the frame side near the midpoint of each shear panel.

4. Mount thermocouples to the compression panel with high temperature adhesive M-bond 610. Cure bond at 450°K (350°F) for two hours followed by post curing at 530°K (625°F) for one hour. Post cure at the time of elevated temperature test.
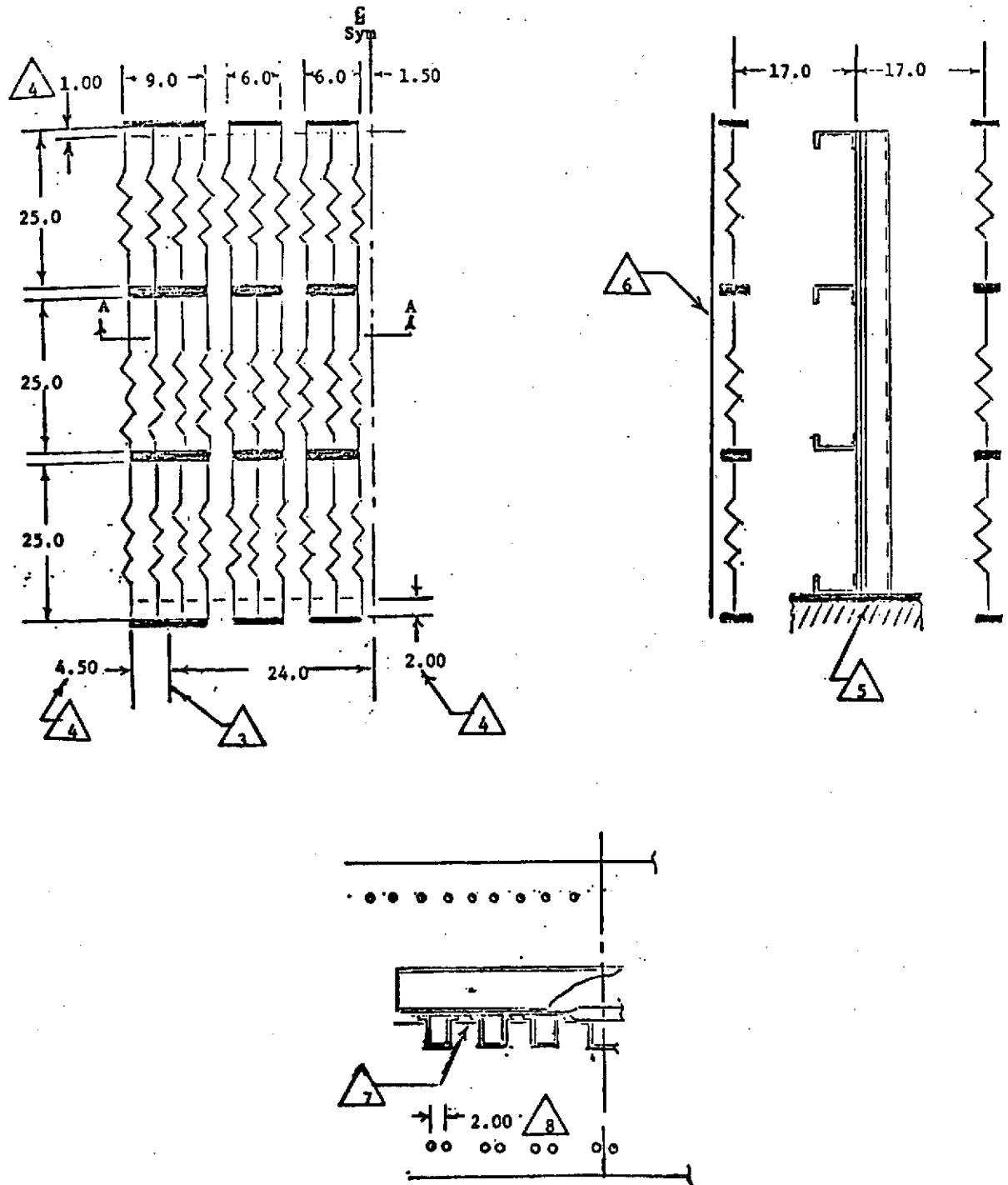
FIGURE B-5

HEAT LAMPS INSTALLATION

FIGURE B-5 NOTES:

1. Structure and reflectors not shown in plan view for clarity.

2. Three inch center to center distance between heating lamps on frame side

△3 Edge of structure.

△4 Extension of heat lamps beyond edge of structure.

△5 Insulation or heated platen.

△6 Heat lamp bank reflectors, typical for forward and aft side of compression panel.

△7 Typical heat insulator on stringer side of panel. One quarter inch thick "Refrasil" sandwiched between shear panels and aluminum foil reflectors.

△8 Distance between each pair of heat lamps symmetrically located about stringer centerline.

FIGURE B-6

COMPRESSION PANEL "OUT-OF-PLANE" SUPPORT FITTING CONCEPTS
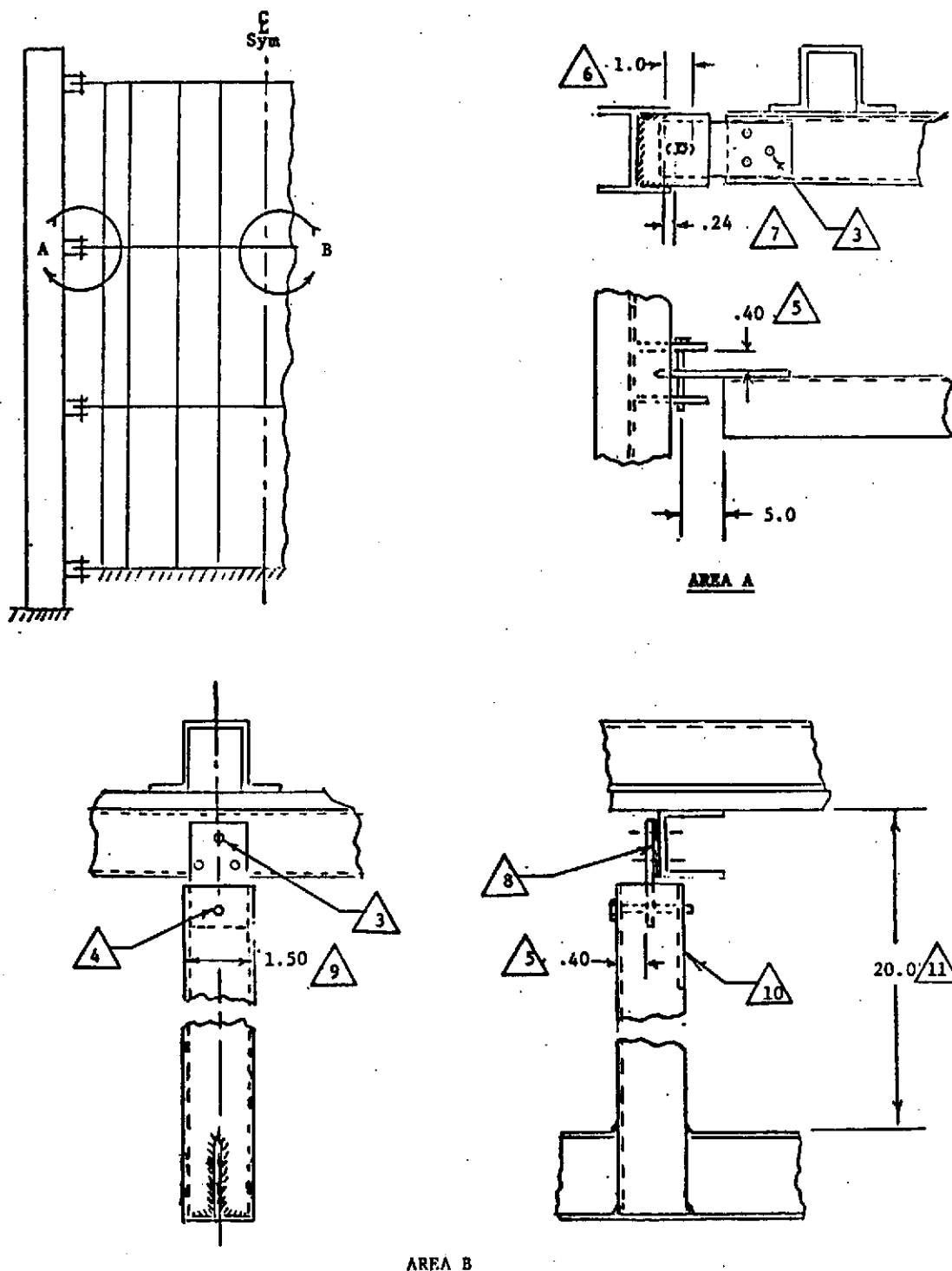

AREA A

AREA B

FIGURE B-6 NOTES:

1. Fitting concept shown in area "A" typical for fittings along both edges of compression panel at each frame. Eight fittings required.

2. Fitting concept shown in area "B" typical for compression panel centerline fittings at each frame. Four fittings required.

3. Close tolerance holes required for fastener pattern between fitting and frame interface.

4. Close tolerance hole required for connecting pin.

5. Free play required between top side of lug and clevis for vertical thermal expansion.

6. Rolling friction joint required in conjunction with close tolerance slotted hole.

7. Free play required between pin and lug slot for lateral thermal expansion.

8. Insulation pad between channel to lug interface.

9. Maximum width of centerline support frame to allow installation between heat lamp banks.

10. Plate welded to bottom of support frame for connecting pin support.

11. Minimum spacing required to allow installation of heat lamps and reflectors forward of test fixture support structure.

FIGURE B-7

STIFFNESS REQUIREMENTS OF
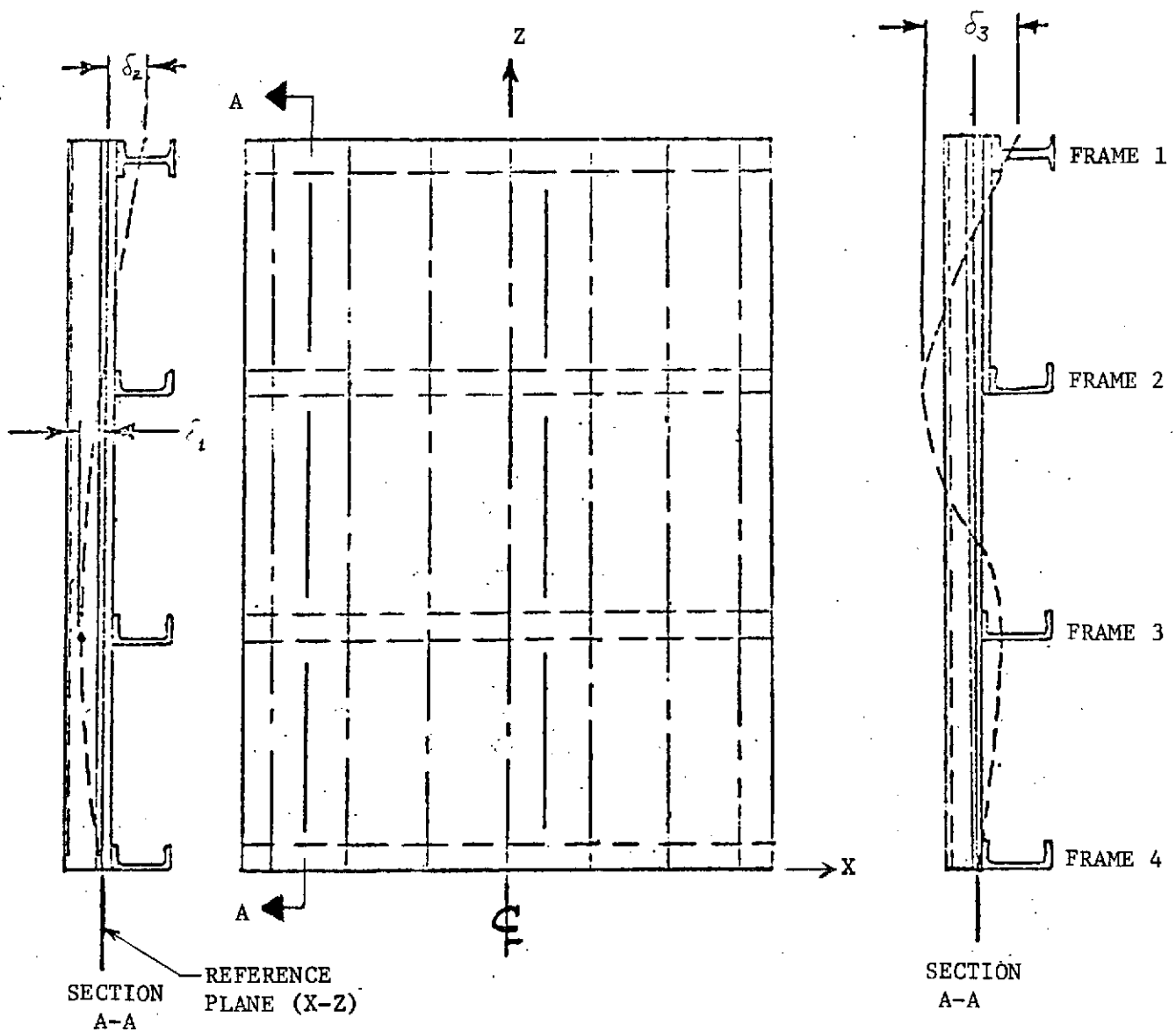
LATERAL SUPPORT STRUCTURE

FIGURE B-7 NOTES:

1. Deflection Requirements:

   a) Deflection, δ_1 or δ_2, from applied loads at any frame support point relative to plane x - z $\leq$ 0.030 in.

   b) Relative defelction, δ_3, of support points on adjacent frames from applied loads $\leq$ 0.030 in.

   c) Maximum accumulated deflection at any point shall not exceed 0.06 in. Accumulated deflection is defined as the sum of deflections from installation, alignment and application of ultimate loads.

   d) Plane x - z is defined by the intersection of skin and stringers in the unloaded position. Plane x - y remains perpendicular to the fixed head of the loading machine.

2. Relative stiffness between support points on adjacent frames will be > 200,000 lb/in.

3. Loads distribution shown in Figure B-8 has been assumed.

FIGURE B-8

LATERAL REACTIONS WHEN ULTIMATE COMPRESSIVE

LOAD IS APPLIED

LATERAL REACTIONS ALONG
PANEL VERTICAL EDGES

LATERAL REACTIONS ALONG PANEL
CENTERLINE

MCDONNELL DOUGLAS ASTRONAUTICS COMPANY - EAST